QUEEN MARY
AND WESTFIELD COLLEGE
UNIVERSITY OF LONDON

Interdisciplinary Research Centre in Biomedical Materials
Queen Mary and Westfield College
University of London

Unit for Joint Reconstruction
Institute of Orthopaedics
Robert Jones and Agnes Hunt Orthopaedic Hospital
Oswestry

The Design of a Novel Hip Resurfacing Prosthesis

Mark S Thompson, MEng, AMIM

Thesis submitted for the degree of
Doctor of Philosophy
February 2001

Abstract

Total hip replacement (THR) is one of the most successful and most frequently performed operations. For most implants the published rate of revision at 10 years is less than 10%. However the revision rates are higher for younger and more active patients who are likely to outlive their implants.

The most frequent cause of THR failure is aseptic loosening, commonly accompanied by bone loss at the implant site. THR revisions give worse functional results and fail sooner than primary THR and are complicated by this loss of bone stock.

A resurfacing hip prosthesis replaces the diseased surface layer of bone and cartilage and retains the majority of the femoral head. The stress distribution in the proximal femur is closer to that in an intact hip. A conservative resurfacing prosthesis will present the surgeon with no greater problems at revision than encountered at primary conventional THR.

Early designs of resurfacing prosthesis conserved femoral bone stock at the expense of acetabular bone. Revision rates were high and while some failures were caused by avascular necrosis and femoral neck fracture the predominant cause was acetabular loosening.

The design of a bone conserving prosthesis requires knowledge of the shape of the bony surfaces of the hip joint. A survey of the morphology of the acetabulum showed a wide variation in shape. While early resurfacing designs had hemispherical acetabular cups the bony surface is less than hemispherical. The morphology and desired range of hip motion constrain prosthesis thickness and shape.

A novel resurfacing design using a polyacetal femoral component and an UHMWPE acetabular component is proposed. This bearing combination has a lower volumetric wear rate than an equivalent Co-Cr on UHWMPE bearing. Computer modelling of the resurfacing concept showed that lower moduli materials reduced stress shielding and distributed implant-bone interface stresses more evenly. Mechanical testing of polyacetal following immersion in Ringer's solution showed substantial decreases in Young's modulus while strength was unaffected.

Morphology is not only a study of material things and of the forms of material things, but has its dynamical aspect, under which we deal with the interpretation, in terms of force, of the operations of Energy.

D'Arcy Wentworth Thompson
On Growth and Form

"Look," said Zaphod. "I'm up to here with cool, OK? I am so amazingly cool you could keep a side of meat in me for a month. I am so hip I have difficulty in seeing over my pelvis."

Douglas Adams
The Restaurant at the End of the Universe

Acknowledgements

I would like to express my gratitude to my supervisors Professor Liz Tanner and Mr Martin Northmore-Ball for the many and varied opportunities that have arisen through working on this interesting and challenging project and for their continuing guidance and advice.

At the Unit for Joint Reconstruction, Dr Jan Herman Kuiper provided much practical help and sage advice. Thanks to him along with Frank Cook, Margaret Peach, Erica Hughes, Bryan Pell and innumerable Dutch students the Unit was a stimulating and friendly place to work. Tanya Dawson, now at ORLAU, supplied the raw data for the acetabular anatomy survey.

At QMW, thanks to James Busfield and Raymond Lam for technical support and assistance on the FEA computers. John Mitchell ensured my competence on the Bionix and Vince Ford machined endless specimens. Julia Shelton provided support and a friendly ear. Professor Bill Bonfield made certain that my thinking was clear and Professor Dan Bader gave valuable academic input. Dr Mangala Patel and Professor Mike Braden helped with water uptake and diffusion. Many thanks to Carey Adams, Catherine Jones and Kirsten Lynn for tireless administrative support.

The FEA model of the human pelvis was developed by Michel Dalstra, now of the University of Aarhus, Denmark. Jenny Pickard, of Corin Medical, produced the prototype resurfacing. Steve Krikler, of Coventry Hospital, was always interested in my work and let me interview his resurfacing patients. Ben Stansfield, of the University of Strathclyde, supplied clinical gait data and Hartmut Witte, of the University of Jena, Germany, gave helpful advice on joint reaction forces.

In Oswestry Steve, Romer, Cantiones and the Oswestry Sinfonia preserved my sanity and provided a full musical life. Thanks to the inhabitants of room 205 – Sophie, Jo, Dora, John, Peter, Yak Nam and Neven – for instructing me in the subtle art of living in the East End. Friends who deserve special mention for tactfully distracting me from my work: Rani, Jane, ULCC and Velvet Chords. Love to Orla and the gang from 6 Sharon Gardens for a warm and lively home, to Angus for sharing 181 with me and to Iain, Elizabeth, Alan and Fiona for listening and encouraging.

I acknowledge the EPSRC for the core programme grant of the IRC in Biomedical Materials and the provision of my research studentship.

Abbreviations

AP	Anterior-posterior (X ray)
AVN	Avascular Necrosis
BHR	Birmingham Hip Resurfacing
BW	Body Weight
CT	Computed Tomography
DoF	Degree of Freedom
FEA	Finite Element Analysis
HA	Hydroxyapatite
HDPE	High Density Polyethylene
HIP	Hot Isostatic Pressing
ICH	Indiana Conservative Hip (resurfacing)
ICLH	Imperial College London Hospital (resurfacing)
IRC	Interdisciplinary Research Centre in Biomedical Materials
ISL	Instrumented Spatial Linkage
OA	Osteoarthrosis
PMMA	Polymethylmethacrylate
POM	Polyoxymethylene
PTFE	Polytetrafluoroethylene
RA	Rheumatoid Arthritis
RJAHOH	Robert Jones and Agnes Hunt Orthopaedic Hospital
ROM	Range of Motion
RSA	Radio Stereometric Analysis
SD	Standard Deviation
THARIES	Total Hip Articular Replacement by Internally Eccentric Shells (resurfacing)
THR	Total Hip Replacement
TPP	Thrust Plate Prosthesis
UHMWPE	Ultra High Molecular Weight Polyethylene
XLPE	Cross-Linked Polyethylene

Table of Contents

List of Figures

List of Tables

1. Introduction

The first double cup resurfacing hip replacement, made of polytetrafluoroethylene (PTFE), was implanted by Sir John Charnley (1961). The double cup replacement was a development of the Smith-Petersen interposition arthroplasty (Smith-Petersen, 1948), a single Co-Cr cup placed between the diseased surfaces of the hip joint.

The use of PTFE in hip replacement gave poor results and this may have prejudiced Charnley against the double cup concept. He went on to develop the stemmed hip replacement which has become the gold standard for hip prostheses. Resurfacing replacement became popular in the early 1970s, but poor outcomes led to its being abandoned in all but a few centres by 1980. Recently resurfacing has undergone a revival with the introduction of new materials and production techniques. Currently at least four different devices are being implanted.

Compared with conventional stemmed total hip replacement (THR) the concept of resurfacing is attractive. Only the diseased bone and cartilage at the joint surface is replaced and the sound, undiseased bone of the femoral head and neck is retained. Load is transferred to the femur proximally through the trabecular and cortical bone of the femoral neck rather than distally through a stem in the medullary canal.

The design process for a new medical device is long and complex (Yamac *et al.*, 1999). The literature on similar devices must be examined. The failures and successes of previous implants and the reasons behind them will inform and guide the design of a new device. If the device is to use new materials then these materials must be evaluated both for the function they are to perform and for their interaction with the human body.

The ability of the device to perform its function must be assessed. At the early stages of development many different designs can be evaluated with the use of computer modelling. Before clinical trials can begin, results obtained from computer simulation must be validated with the testing of prototype devices both *in vitro* and *in vivo*.

This thesis aims to present and support a proposal for a novel design of hip resurfacing. To achieve this aim the first requirement is to catalogue previous designs of resurfacing hip replacement. Design features, materials, methods of fixation and outcomes are documented for 15 different implants. Comparisons of rates of revision

and modes of failure are made between resurfacing designs and between resurfacing and conventional THR.

The resurfacing literature survey identifies the conservation of acetabular bone as an important issue. Conservation is to be achieved through a better understanding of acetabular shape. Therefore the second requirement is to measure the shape of the acetabulum. Geometric parameters of interest are defined and a study determining their values in a population of hemi-pelves is presented.

The third requirement is to compare the mechanical behaviour of a new design with other resurfacings and conventional hip replacement. Computer simulation work that investigates the effect on the bone surrounding the hip joint of different resurfacing designs is presented. The results are compared with previous work using the same model implanted with a THR.

The literature survey and computer simulations indicate that polyacetal is a suitable material for the femoral component. Therefore the fourth requirement is to support the use of this polymer in the proposed resurfacing design. A study determining the effects on the mechanical properties of polyacetal of long term exposure to the physiological environment is presented.

This thesis is divided into eight chapters. Chapter two is a survey of the literature including descriptions of the tissues and structures replaced by THR and their mechanical environment, the functions and outcomes of THR and materials suitable for use in joint replacement. Chapter three presents a survey of the literature on resurfacing hip replacement, including sections on the rationale for resurfacing, descriptions of resurfacing designs and analysis of the outcomes of resurfacing. The methods, materials, results and discussion of a study of acetabular anatomy are presented in chapter four.

Chapter five briefly introduces computer modelling and its role in biomechanics and presents results and a discussion of modelling of the effect of the proposed implant on the surrounding bone. The mechanical testing of polyacetal grades following immersion in Ringer's solution is reported in chapter six. Chapter seven discusses the proposed new design of resurfacing hip replacement and chapter eight draws together conclusions from all the studies presented. Chapter nine outlines further work to be undertaken in the development of the implant.

2. Literature Survey

2.1 Bone

The skeletal system of modern animals is the result of millions of years of natural selection. As such it represents a highly optimised solution to the problems of load transfer and distribution for locomotion and the protection of delicate vital organs. The system is also an optimised solution to the functional requirements of an individual through biological feedback mechanisms in the stages of development and in maturity. The word bone describes both the structural members of the skeleton and the material of which those members are composed.

The bones of the human skeleton are of varying shape and size, following their function in the body. The bones in the limbs are long allowing large strides to be taken and tubular to transmit the large bending and compressive forces generated. The skull, in contrast, is adapted for protecting the brain from injury and is box shaped. The bones of the middle ear are the smallest in the human body and fulfil another mechanical function, that is the transmission of sound.

2.1.1 Macro-structure with Reference to the Femur and the Coxa

There are two distinct types of bone material in the human body. Cortical, or compact, bone forms the surface layer or cortex of every bone in the body and also makes up the long shafts of load bearing bones. Where the cortex supports articulating cartilage the bone is called subchondral and consists of a thin layer of cortical bone and a layer of calcified cartilage. Cancellous, or spongy, bone is found at the end of long bones such as the femur and fills the core of others such as the pelvis and the vertebrae. It has a cellular structure made up of rods or plates (trabeculae) and varies in porosity from 30% to 90%. Together the two types of bone make a lightweight composite structure similar to the sandwich honeycomb structure used frequently in aerospace engineering. This structure is most efficient in bending and in the distribution of load. The absence of cancellous bone in a structure therefore indicates that the loads carried are parallel to the axis of the cortex. In the description following, angles and distances quoted are means for normal adult Caucasians unless otherwise stated.

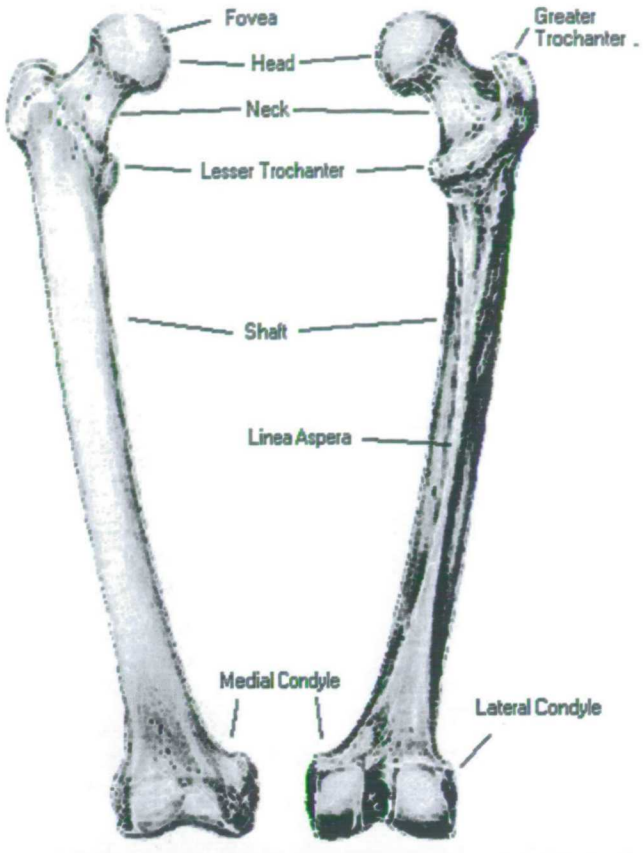

Figure 2.1.1 Anterior (left) and posterior (right) surfaces of the right human femur from Gray's Anatomy (1989).

The femur, in common with most long bones, consists of a tubular shaft (diaphysis) of cortical bone with expanded articular ends (epiphyses) containing cancellous bone (Figure 2.1.1). This demonstrates an effective use of the composite cortical/cancellous structure. The epiphyses act to "collect" loads from many different directions and transmit them to the shaft which is loaded axially. With the leg in neutral position the femoral shaft is not vertical: it is inclined posteriorly by about 5° and laterally by about 6°. The shaft itself is not straight and describes a shallow 's' curve in the sagittal plane. The femoral head is approximately spherical in shape, making up over two thirds of a sphere. A small rough fovea interrupts the postero-inferior surface and is the site of insertion of the ligamentum teres and vessels supplying the femoral head. The head is offset medially from the shaft by the femoral neck, an irregularly shaped bridge of bone between the two structures. The "axis" of the neck, a line from the geometrical centre of the head through the midpoint of the narrowest part of the neck, makes an angle with the shaft axis in the frontal plane of about 125° (Noble *et al.*, 1988; Sugano *et al.*, 1999). However, THR patients had a mean angle of 130° (Husmann *et al.*, 1997). This angle is also sex dependent reflecting the different

shapes of male and female pelves. The neck projects anteriorly from the shaft and the angle it makes in the transverse plane with the medial-lateral axis is called the femoral anteversion. This angle is highly variable: in normal hips the mean anteversion is 13° ± 7° (Reikerås *et al.*, 1983), while in THR patients the mean anteversion is significantly larger, 19° ± 9°, and in another study 24°, range 0° – 45° (Husmann *et al.*, 1997). The neck is elliptical in cross section with its major axis aligned supero-anterior to infero-posterior. With its tip approximately level with the centre of the femoral head the greater trochanter projects laterally from the proximal end of the femoral shaft. It provides attachment sites for the abductor muscles and increases their moments about the hip joint (section 2.3.4). Cancellous bone fills the femoral head and greater trochanter down to the level of the lesser trochanter. This small projection from the posterior face of the femur is the insertion for the iliopsoas muscle group. Distally the femoral shaft expands and bifurcates into two condyles, also filled with cancellous bone. These form surfaces for articulation at the knee joint.

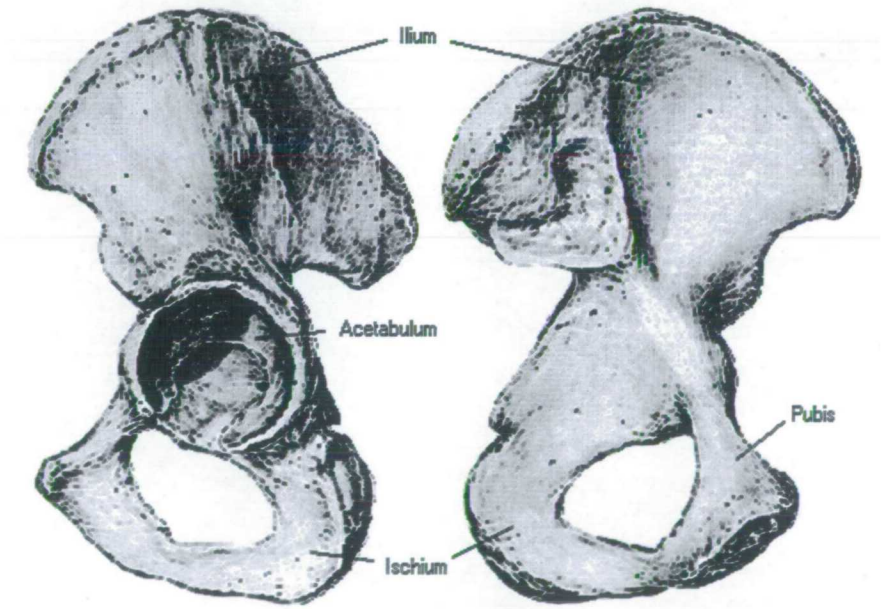

Figure 2.1.2 Lateral (left) and medial (right) surfaces of the left human coxa from Gray's Anatomy (1989).

The pelvis, made up of two coxae or innominate bones, is a thin, curved plate (Figure 2.1.2). It has a "sandwich" structure with a cortical bone shell filled with cancellous bone which is well suited for carrying bending loads. Its large surface area provides attachments for the powerful muscles articulating the hip joints and supporting the vertebral column. It has a secondary role in protecting and supporting the organs in the abdomen. The coxa is formed, in the mature adult, from the fusion of three

separate bones: the ilium, ischium and pubis. The junction between these three bones occurs at the centre of the acetabulum, the socket of the hip joint. The normal acetabulum is approximately hemispherical in shape with a large notch infero-medially. It has a raised, horse-shoe shaped (lunate) surface of subchondral bone bounding the central acetabular fossa except on the infero-medial side. The orientation of the acetabulum, usually measured unsuitably on anterior-posterior (AP) X-rays, is often described with angles of anteversion and inclination. Unfortunately there are three different definitions of these angles used variously by radiologists, surgeons and anatomists (Murray, 1993) and often little discrimination between them. The anatomist measures the θ and ϕ angles of the normal to the acetabular opening plane in a set of spherical polar coordinates oriented with the long axis of the body. The anteversion, ϕ in this system, is given as $17 \pm 6°$ (Reikerås *et al.,* 1983). The three projected angles of the vector normal to the acetabular opening plane have been measured (Witte *et al.,* 1998) giving the anteversion angle as $24.3 \pm 4.7°$, but the data are not presented so as to allow calculation of the inclination. Reynolds *et al.* (1999) measured acetabular anteversion in a group of patients and found an association between reduced anteversion (14° compared with 21° in the control group) and hip pain. They speculated that this arose from impingement of the femoral neck on the acetabular rim.

Figure 2.1.3 Trabecular structure of the proximal femur.

The orientation of the trabeculae in cancellous bone and its relative density are other features that vary macroscopically. For example the trabecular system in the femoral head is highly organised (Figure 2.1.3), with the trabeculae oriented in the directions

of maximum stress and thicker in areas of higher stress. In the cross-section shown there appear to be two arches of bone, one described as tensile, tangential to the superior cortex of the neck, and the other called compressive, inserting into the inferior cortex, also known as the calcar. Similarly the trabeculae in the dome of the acetabulum are thicker and more densely packed than elsewhere in the coxa, the dome being directly loaded by the joint force.

Modern composite design is revisiting the graphical methods used in the 19th century to simplify calculations on large pin jointed frames (Makiyama and Platts, 1996). This trajectorial theory suggests that a weight-optimised structure will have material distributed in orthogonal members following the trajectories of the principal stresses in an homogeneous structure of the same outline under the same load condition. Pauwels (1980) showed that the trabecular pattern displayed in a section of a fused human knee joint corresponded with the fringe distribution and hence with the principal stress trajectories produced in a photo-elastic model of the same shape. Trabecular orthogonality may be modified close to joint surfaces where multi-directional loading is best supported by trabeculae angled at 60° to each other (Pidaparti and Turner, 1997). Trabecular bone architecture appears to be the result of a material distribution process optimising the bone's strength to weight ratio.

The trabeculae in cancellous bone are in the form of struts or plates depending upon anatomical location. The cancellous bone structure can therefore be open or closed cell (in the sense of engineering foams), although the closed cells are usually connected by small blood vessels. Both cortical and cancellous bone are highly vascular, indicating that bone is a far from quiescent tissue, as discussed below (section 2.1.5).

2.1.2 Micro-structure

The terms cortical and cancellous bone distinguish macroscopic structures. At a microscopic scale (Figure 2.1.4) both are made up of a mixture of lamellar and woven bone. Woven bone is able to mineralise rapidly and is formed during development and following bone fracture. It has a disorganised, loose packed structure of mineralised collagen fibrils. Lamellar bone has a more organised structure where the mineralised collagen fibrils are aligned axially to form lamellae. These lamellae are grouped, in humans, into units of five to form a "rotated plywood" structure (Figure 2.1.5) with

the fibre direction changing by 30° between each ply (Wiener and Wagner, 1998). Lamellar bone exists in two main forms in humans: osteonal and circumferential. Circumferential lamellar bone is found at the endosteal and periosteal surfaces where, as its name implies, the lamellae form continuous sheets around the circumference of the bone.

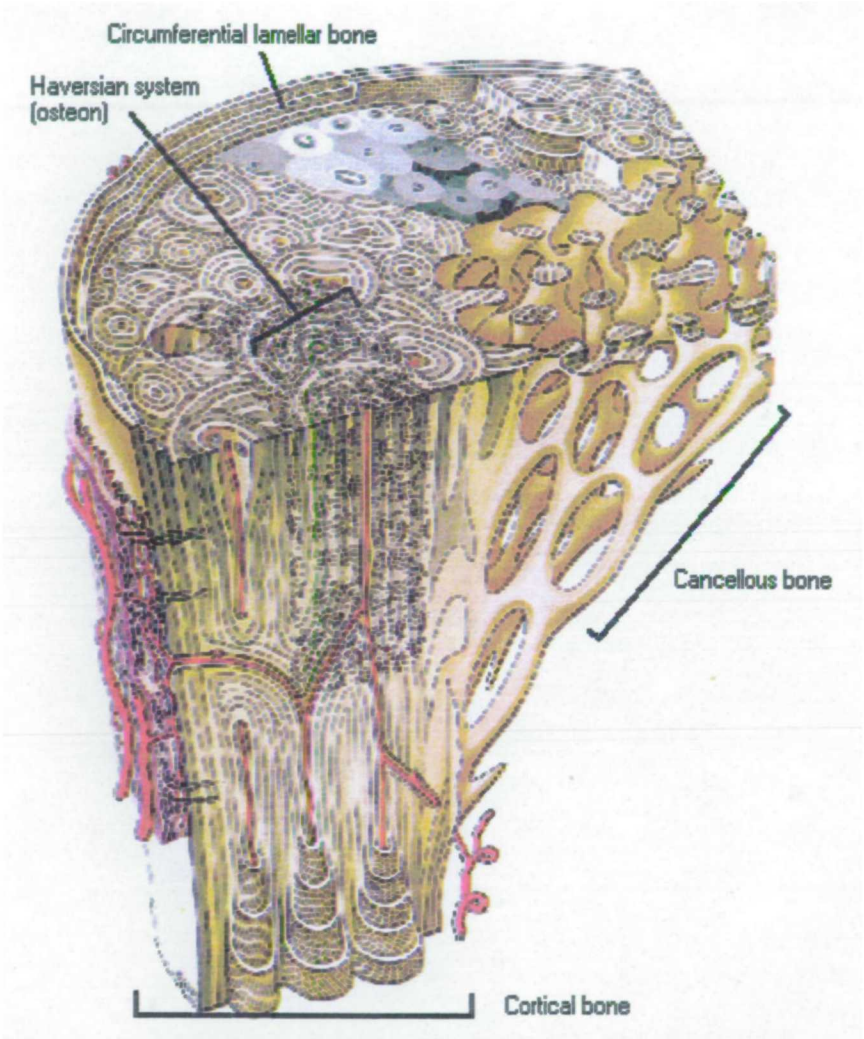

Figure 2.1.4 Microstructure of bone from Gray's Anatomy (1989).

Osteonal bone is the most interesting type of bone as it is formed both during development and also as a result of the continuous remodelling of pre-existing bone. The lamellar sheets are wrapped in seven to twenty concentric cylinders each 3 – 7 μm thick around a blood vessel (Gray's Anatomy, 1989). This cylindrical motif cancels out the asymmetry of the plywood structure producing a transversely isotropic material. The tube containing the vessel is known as an Haversian canal and the whole is called an Haversian system or osteon. Osteons, 120 – 200 μm diameter and 3 – 5 mm long, are oriented with their long axes in the main load bearing direction (axially

in a long bone like the femur). The Haversian canals are connected by transverse Volkmann's canals, also vessel bearing, but not surrounded by multiple lamellae. The representation of a transverse microradiograph in the bone section in Figure 2.1.4 shows the variation in the bone mineral density across and between osteons, older material being more heavily mineralised.

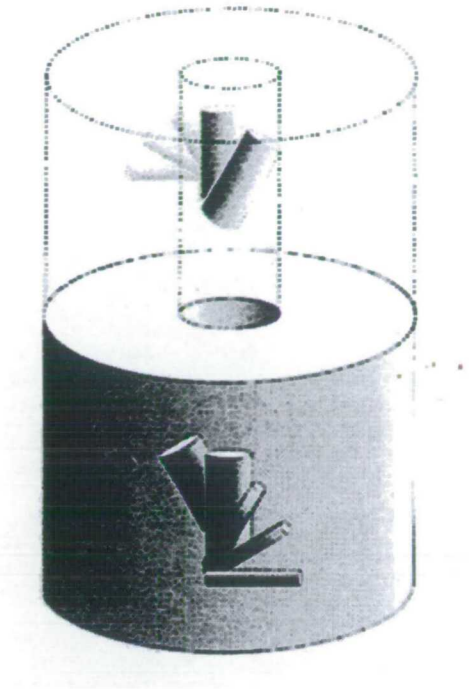

Figure 2.1.5 Osteon with rotated plywood structure proposed by Weiner and Traub (1998).

Within the lamellar matrix of bone material are small voids, or lacunae, containing osteocytes, mature bone cells. The role of osteocytes is unclear, but is thought to involve the control of turnover and maintenance of the bone matrix. The lacunae are interconnected and long osteocyte cell processes permit communication between osteocytes. There are two other main cell types in bone – the osteoblast and the osteoclast. The osteoblast is responsible for the deposition of bone matrix and its mineralisation. It is found on the surface of maturing or remodelling bone. It is hypothesised that osteocytes are osteoblasts which have been entrapped in the matrix formed around them. The osteoclast is a larger, multi-nuclear cell which is active in the removal of bone material. It is found on bone surfaces at sites of bone resorption.

2.1.3 Ultra-structure

Bone material has a composite structure with a mineral phase reinforcing an organic matrix. Cortical bone contains approximately 20% water, 45% bone mineral and 35% organic substance (Vaughan, 1975). The mineral phase is a non-stoichiometric form

of hydroxyapatite (HA), $Ca_{10}(PO_4)_6(OH)_2$. Multiple substitutions in HA may occur without affecting the hexagonal symmetry of the crystal – HA is said to be an hospitable structure. The most common substituents are carbonate, CO_3^{2-} and fluoride, F^-. Bone mineral plays an important part in the homeostasis of ionic species in blood plasma and tissue fluid by acting as an ion reservoir. HA crystals with platelet morphology and a range of sizes have been described in bone (Weiner and Price, 1986, Weiner and Wagner, 1998). Lengths ranged from 20 to 50 nm, widths from 10 to 40 nm and thicknesses from 3 to 5 nm.

The organic component of bone is mainly composed of collagen (89 wt.%) with proteoglycans and glycoproteins making up the remainder. Their relative amounts decrease as bone matures and becomes more calcified. These molecules are also found in cartilage, where their role in the mechanical behaviour of the tissue is more prominent.

Collagen is present in the human body in numerous types, but the main constituent of the organic matrix in bone is type I collagen. At the bottom of the structural hierarchy of collagen is the triple-helical molecule tropocollagen (Figure 2.1.6d) and in type I collagen all three helices are α chains. Tropocollagen molecules are gathered together in a staggered arrangement in a collagen microfibril (Figure 2.1.6c). The period of the stagger is 68 nm, although the molecules themselves are 4.4 times this length (Figure 2.1.6b). The microfibrils are in turn bundled into fibrils. The periodic arrangement of the tropocollagen molecules gives the fibrils a striated appearance (Figure 2.1.6a).

Weiner and Wagner (1998) proposed a hierarchy of structures in bone material from the Ångstrom level to the micron level. Small platelet HA crystals are arranged in parallel layers within collagen fibrils. The gaps left between adjacent tropocollagen molecules, which are arranged in three-dimensional channels within one fibril, provide a focus for the deposition of HA (Vaughan, 1975). However the crystals observed in mature bone are larger than this space. It is thought that these crystals displace surrounding tropocollagen molecules to create a "strait-jacket" effect so that the collagen matrix is pre-tensioned.

Arrays of these HA filled fibrils make up one ply in the "rotated plywood" structure outlined above. In one ply of lamellar bone the platelets in adjacent fibrils are aligned. However adjacent plies have different orientations of crystal layers. In the thinner

lamellae (in rat bone) the fibrils and crystal layers are arranged parallel to the lamellar boundaries, while in thicker lamellae the fibrils are still parallel, but the crystal layers are rotated out of the plane of the lamellar boundary.

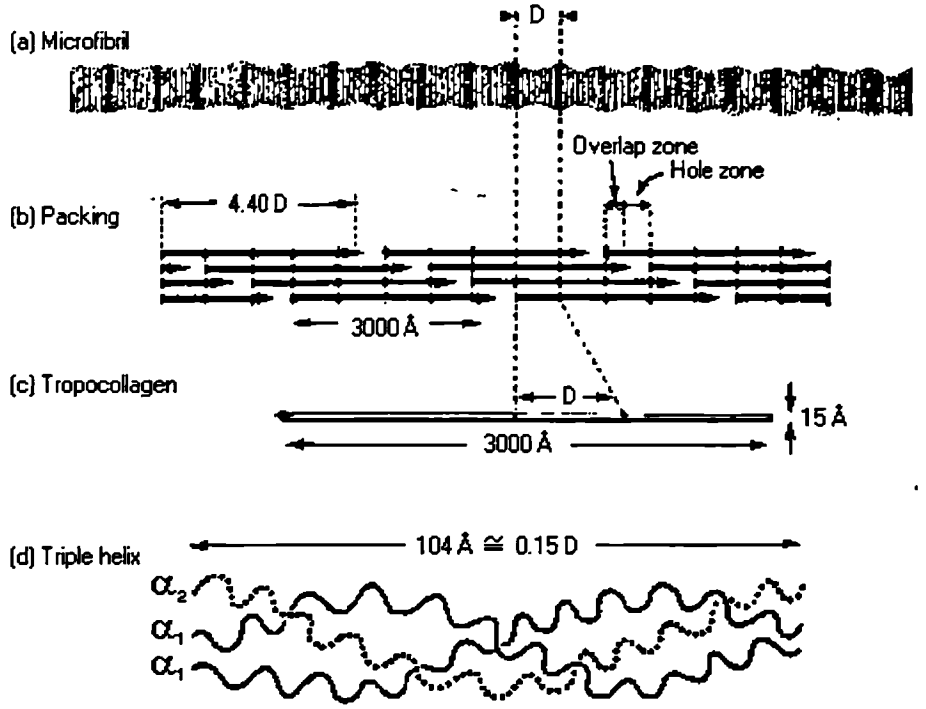

Figure 2.1.6 The strucuture of collagen from Vaughan (1975).

2.1.4 Mechanical Properties

From the outline above it is clear that the structure of bone material is highly variable according to position and function in the skeleton. The mechanical properties of this material are therefore also widely variable and any statement of them should include the anatomical origins and the sizes and orientations of the specimens tested. A further problem in a survey of reported properties is the variation in testing standards and protocols. Factors affecting results include the specimen storage and preparation conditions and the testing environment. Bone is a viscoelastic material so the strain rate also affects the measured properties (Carter and Hayes, 1976).

2.1.4.1 Cortical bone

Typically the Young's modulus of cortical bone in the longitudinal direction (parallel to the osteons) is twice that in the transverse direction. The variation of modulus with orientation does not follow the curve predicted by simple fibre reinforced composite models (Bonfield and Grynpas, 1977). The longitudinal ultimate tensile strength is

between 3 and 10 times that in the transverse direction. Longitudinal and transverse ultimate compressive strengths differ less since in compression the weak cement lines between osteons are not loaded directly. Dry bone is stiffer and stronger than wet bone. A typical stress-strain curve for wet cortical bone is shown in Figure 2.1.7.

Table 2.1.1 and Table 2.1.2 present elastic and strength data respectively from classic studies of the mechanical properties of cortical bone. In some cases data from the original papers has been supplemented by communication with the authors concerned.

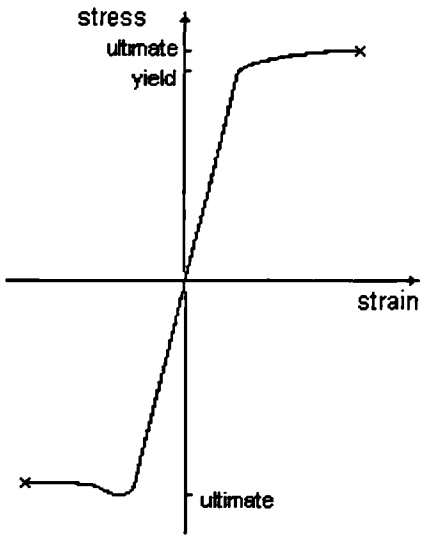

Figure 2.1.7 Stress strain characteristic of human cortical bone after Reilly and Burstein (1975).

Table 2.1.1 Elastic properties of human cortical bone (Currey, 1998). Subscripts: $_1$ – parallel to the long axis of the bone; $_2$ – radial; $_3$ – circumferential.

Author	Location and method	Tensile Modulus (GPa) Mean ± SD	Compressive Modulus (GPa) Mean ± SD	Shear Modulus (GPa)
Reilly and Burstein (1975)	Femur Mechanical Testing	$E_{11} = 17.7 \pm 3.6$, $E_{22} = 12.8 \pm 3.0$, $\nu_{12} = 0.41 \pm 0.15$, $\nu_{23} = 0.53 \pm 0.25$	$E_{11} = 18.2 \pm 0.85$ $E_{22} = 11.7 \pm 1.01$ $\nu_{12} = 0.38 \pm 0.15$, $\nu_{23} = 0.63 \pm 0.20$	$G_{12} = 3.3 \pm 0.42$ (assumed transverse isotropy)
Ashman *et al.*, 1984	Femur Ultrasound	$E_{11} = 20.0$, $E_{22} = 12.0$, $E_{33} = 13.4$ $\nu_{12} = 0.37$, $\nu_{13} = 0.35$, $\nu_{21} = 0.22$, $\nu_{31} = 0.24$, $\nu_{23} = 0.38$, $\nu_{32} = 0.42$		$G_{12} = 5.6$ $G_{13} = 6.2$ $G_{23} = 4.5$
Reilly *et al.*, 1974	Femur Mechanical Testing	$E_{11} = 17 \pm 3.15$	No significant difference from tensile.	

Table 2.1.2 Strength properties of human cortical bone (Currey, 1998). Subscripts: $_1$ – parallel to the long axis of the bone; $_2$ – radial; $_3$ – circumferential. σ_y is yield strength, σ_f is ultimate strength, ε_f is fail strain, τ_y and τ_f are shear yield and ultimate strengths.

Author	Location and method	Tensile Strengths (MPa), Fail Strain Mean ± SD	Compressive strength (MPa), Fail Strain Mean ± SD	Shear Strength (MPa) Mean ± SD
Reilly *et al.*, 1974; Reilly and Burstein, 1975	Femur Mechanical Testing	$\sigma_{y1} = 114 \pm 7.1$, $\sigma_{f1} = 133 \pm 15.6$, $\varepsilon_{f1} = 0.038 \pm 0.006$ $\sigma_{f3} = 53 \pm 10.7$, $\varepsilon_{f3} = 0.007 \pm 0.0014$	$\sigma_{f1} = 205 \pm 17.3$, $\varepsilon_{f1} = 0.019 \pm 0.003$ $\sigma_{f3} = 131 \pm 20.7$, $\varepsilon_{f3} = 0.050 \pm 0.011$	$\tau_f = 67 \pm 3.5$
Cezayirlioglu *et al.*, 1985	Femur Mechanical Testing	$\sigma_{y1} = 128 \pm 11.2$, $\sigma_{f1} = 158 \pm 8.5$, $\varepsilon_{f1} = 0.042 \pm 0.0085$	$\sigma_{y1} = 180 \pm 12.5$ $\sigma_{f1} = 213 \pm 10.1$ $\varepsilon_{f1} = 0.026 \pm 0.0056$	$\tau_y = 53 \pm 7.7$ $\tau_f = 71 \pm 7.8$

2.1.4.2 Subchondral bone

Bonfield *et al.* (1987) carried out microhardness tests comparing subchondral bone from femoral heads removed at hip replacement operations for osteoarthrosis and cadaveric femoral heads. While the microhardness did not seem to vary with load bearing function, it did vary between OA and normals and between different types of OA. The microhardness of the cadaveric subchondral bone was highest at about 40 Vickers Hardness (VH). Microhardness for the OA group varied from 21 VH to 30 VH and was lowest in the ankylosing spondylitis group at approximately 15 VH.

2.1.4.3 Cancellous bone

Cancellous bone is a cellular solid in the engineering sense and many of its basic properties can be described using an engineering analysis of foams. This analysis derives simple expressions for foam stiffness and failure stress in terms of the apparent density of the foam and the actual density, stiffness and failure stress of the bulk material. Cells are either open, with material concentrated in one dimensional interconnecting rods, or closed, with two dimensional interconnecting plates. The aspect ratio of the cells is also important – "honeycomb" materials with one cell axis appreciably longer than the other two behave differently from materials with cells having an aspect ratio closer to unity. There is good agreement between the relationships derived using these models and the experimental data (Gibson, 1985), showing a clear separation between open and closed cell bone. A representative set of mechanical properties is given in Table 2.1.3.

Table 2.1.3 Mechanical properties of human cancellous bone (Taylor, 1997) E is compressive stiffness and σ ultimate compressive strength. E_{tens} tensile stiffness; σ_{UTS} ultimate tensile strength. Subscripts: $_1$ – parallel to the long axis of the bone; $_2$ – radial; $_3$ – circumferential.

Author	Location (n)	E_{11} (MPa) Mean (range) ± SD	σ_{11} (MPa) Mean (range) ± SD	Other parameters Mean (range) ± SD
Tanner *et al.*, 1988	Male femoral heads normal (10)	110 (50 - 200)	10 (5 - 15)	
	Osteoarthritic (15)	175 (100 - 250)	15 (10 - 21)	
Ashman *et al.*, 1989	Prox. tibia (3)	1107 (340 - 3350)		E_{22} = 457 (140 – 1750) E_{33} = 346 (110 - 1230)
Linde *et al.*, 1990	Prox. tibia (5)	267 (67 - 734)		E_{22} = 84 (17 - 493) E_{33} = 83 (18 - 481)
Røhl *et al.*, 1990	Prox. tibia (7)	489 ± 331	2.2 (0.5 - 5.6)	E_{tens} = 487 ± 329 σ_{UTS} = 2.54 (0.9 - 5.38)
Deligianni *et al.*, 1991	Normal female femoral heads	100 (25 - 175)	9 (3 - 15)	
	Osteoarthritic	375 (175 - 575)	15 (10 - 20)	
Odgaarde *et al.*, 1991		232	3.2	
Dalstra *et al.*, 1993	Acetabulum	61 ± 48		E_{22} = 42 ± 29 E_{33} = 31 ± 22
Zysset *et al.*, 1994	Prox. tibia (6) Subchondral	(32 - 1116)		E_{22} = 8 - 1127 E_{33} = 3 - 226
	Epiphyseal	(102 - 1726)		
Goulet *et al.*, 1994	Various	287 (16 - 1113)	4.6 (0.5 - 14.5)	E_{22} = 123 (1 - 654) E_{33} = 173 (6 - 1524) σ_{22} = 2.5 (0.1 - 9.6) σ_{33} = 1.6 (1.11 - 2.54)

As can be seen the strength properties of cancellous bone are complex and anisotropic. However recent studies (Chang *et al.*, 1999; Keaveney *et al.*, 2000) have found that the yield strain is relatively uniform even for specimens with significant differences in volume fraction, architecture and loading direction.

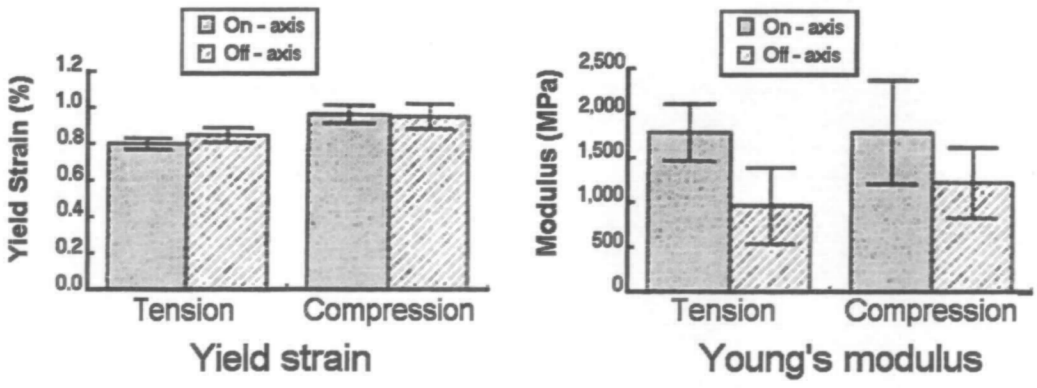

Figure 2.1.8 Trabecular bone yield strain and modulus dependence on specimen orientation in compression and tension. Off – axis specimens were offset by 30 – 40° from the principal trabecular direction. Error bars show ± 1 SD. From Chang *et al.* (1999).

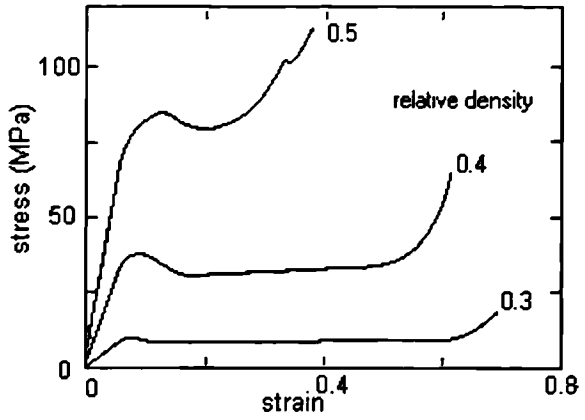

Figure 2.1.9 Compressive stress strain characteristic of cancellous bone of relative densities 0.5, 0.4 and 0.3 from Gibson (1985).

The compressive stress strain curve for cancellous bone is typical of foams. There is a short linear section characterised by the Young's modulus of the material. This is followed by a longer, nearly constant stress section that describes the buckling collapse and crushing of the cells in the material. Once full densification has occurred, the stiffness rises again (Figure 2.1.9). In tension failure occurs soon after yield.

Table 2.1.3 shows that cancellous bone properties vary widely according to the anatomical location of the specimen. This reflects the strong dependence of these properties on the volume fraction and architecture of the bone. Two techniques have been used to determine the properties of the trabecular material itself (Currey, 1998). First standard mechanical tests (tensile, bending and buckling) have been performed on isolated trabeculae. This technique using extremely small specimens is prone to size artefacts. A second approach is to develop a detailed finite element model of a cancellous bone specimen (from micro-CT scans) and compare its behaviour with that of the specimen under load. Then a value of Young's modulus can be chosen for the model that reproduces the observed deflections. More complex analysis (Niebur *et al.*, 2000) has shown that this technique may also be used to predict the specimen yield failure. Although results from both methods suggest that cancellous bone material has a lower Young's modulus than cortical bone, the values range from 1 to 14 MPa.

2.1.5 Bone Adaptation

The shapes of bones and the distribution and properties of the bone material of which they are composed are determined by a combination of evolutionary adaptation and

loading history. The loading history will affect both bone modelling in the development of the skeleton and bone remodelling in the mature adult. The relationship between load and structure was most famously stated in 1892 by Julius Wolff and is known as Wolff's law. He emphasised static loading whereas the main stimulus for bony change appears to be dynamic and he neglected hereditary effects, but his "law" survives and is much quoted in current literature. Most simply put it states that bone is laid down where needed and resorbed where not needed.

Bone remodelling is carried out by the combined action of osteoblasts and osteoclasts. In cortical bone osteoclasts first excavate a cylindrical tunnel and are followed by osteoblasts which deposit bone concentrically around a blood vessel, narrowing the channel again. The point of reversal from erosion to deposition is marked by the cement line, a layer of bone with a lower mineral content. This layer distinguishes secondary osteons, which are the product of remodelling, from primary osteons produced by modelling.

The stimuli for bone modelling and remodelling are the subject of debate. HA and wet collagen are both piezoelectric materials and it was thought that fluctuations in potential caused by mechanical strain might control the response of osteoblasts, osteoclasts and osteocytes (Vaughan, 1975). More recent research proposes that the complex intercommunicating network of osteocytes has a role in the strain related adaptive remodelling of bone (Lanyon, 1993). It is proposed that osteocytes communicate with osteoblasts and osteoclasts to coordinate the processes of bone apposition and bone resorption. The transduction of the mechanical signal is not known and candidate mechanisms include the direct deformation of the osteocytes, damage to the osteocyte processes by microfracture in the bone, the flow of fluid through lacunae or the potentials set up by such a flow of ions.

Computer models based upon a set of assumptions about the stimuli and coupling between cells similar to those outlined above (Huiskes *et al.*, 2000) produced an homeostatic trabecular architecture aligned and orthogonal to the loading direction. Two different hypotheses of the probability of osteoclast activation at a bony surface were investigated. The first assumed that micro-cracks provided the stimulation and supposed that the distribution of these was spatially random. Hence the probability of activation at all surface sites was equal. The second hypothesis assumed that osteoclasts were regulated by disuse, giving high probability of activation in disused

areas and low probability in areas of high strain. Given that disuse and microcrack activation are most likely to act concurrently Huiskes *et al.* proposed that they use the same signalling pathway. If the osteocytic network under normal loading suppresses osteoclast activation then disuse would prevent this suppression while microcracks, by "disconnecting" the canaliculi, would have a similar effect. The two hypotheses produced similar end architectures when implemented as simulations, but the disuse hypothesis, as would be expected from the coupled action of osteoblasts and osteoclasts, required fewer iterations to reach a homeostatic result.

2.2 *Morphology of the Hip Joint*

The joints between the rigid bones of the skeleton permit relative movement and force transmission. There are two main classes of joints – solid or synarthroses and cavitated or diarthroses. Synarthroses are further classified by the type of connective tissue bonding the joint and include the sutures between the bones of the skull and the symphyses between adjacent vertebrae. Diarthroses, also known as synovial joints, allow a greater range of motion. This section deals with the synovial joint between the femur and the coxa, a ball and socket joint with three angular degrees of freedom.

2.2.1 Basic Structure of a Synovial Joint

Figure 2.2.1 shows the hip joint, with synovial cavity, capsule, articular cartilage and subchondral bone. The cavity is filled with synovial fluid which at low shear rates has a high viscosity and exhibits decreased viscosity at high shear rates (Fisher, 1997).

In the hip joint the capsule thickens into ligaments that limit the extremes of motion of the joint, maintain the contact of the articulating surfaces and prevent dislocation. The acetabulum is deepened superiorly, anteriorly and posteriorly by a fibrocartilage rim called the acetabular labrum. This rim also bridges the inferior acetabular notch as the transverse acetabular ligament. Articular cartilage covers the lunate surface and the acetabular fossa is filled with a fibro-elastic fat pad. The ligament of the femoral head or ligamentum teres attaches to the fovea on the femoral head and on both sides of the acetabular notch, blending with the transverse acetabular ligament. Articular cartilage also covers the surface of the femoral head. Figure 2.2.2 shows maps of the thickness of articular cartilage on femoral and acetabular sides.

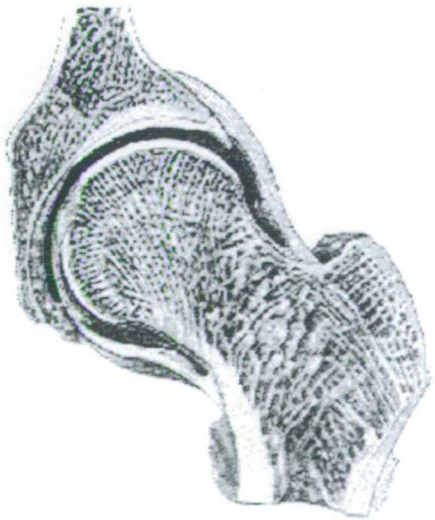

Figure 2.2.1 The hip joint from Gray's Anatomy (1989).

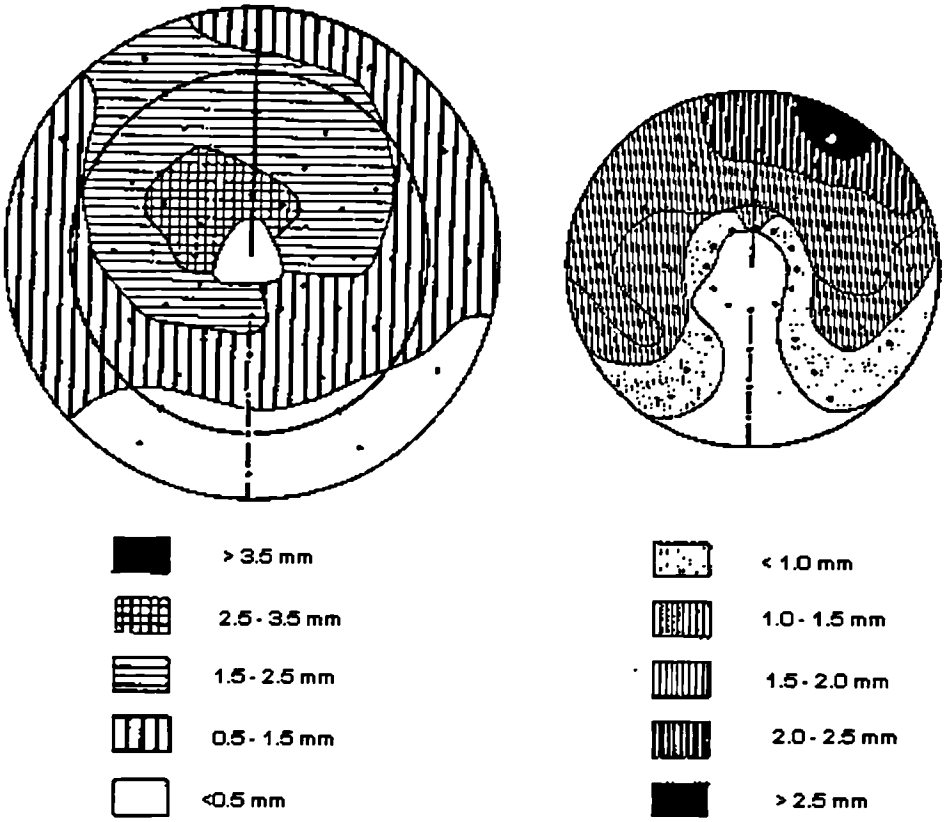

Figure 2.2.2 Thickness distribution of cartilage on the femoral head (left) and in the acetabulum from Kurrat and Oberländer (1978).

2.2.2 Incongruity and Asphericity

The femoral head articular surface is not perfectly spherical. The most nearly circular meridian is in the plane perpendicular to the neck axis (Clarke and Amstutz, 1975), while the largest radius of curvature is found superiorly. In the acetabulum ultrasound measurement of the acetabular articular surface (Rushfeldt *et al.,* 1981) showed a maximum deviation of ± 150 μm from spherical. The underlying calcified interface deviated by ± 500 μm. Another approach is to measure how incongruent the bearing is as a whole rather than the extent to which either articulating surface is not spherical. The incongruency is the degree to which the unloaded surfaces of the joint are out of contact. A study of contact area (Greenwald and O'Connor, 1971) showed a load dependence up to loads of about 50% body weight, at which complete contact was said to occur. Contact began anteriorly and posteriorly with the acetabular dome in contact only at higher loads. The variations in cartilage thickness were proposed to set up an even pressure distribution in the cartilage at the highest loads during gait. More recent studies (Eckstein *et al.,* 1997; Eisenhart-Rothe *et al.,* 1997) have described two types of contact distribution, both starting at the periphery of the lunate surface and

approaching the edge of the fossa with increasing load. A monocentric pattern is found in some hips, with contact beginning in the acetabular roof and spreading down the arms of the lunate surface. In other hips a bicentric pattern is seen with first contact on the posterior and anterior arms and spreading to the roof with increasing load. It has been suggested that the incongruity of the hip decreases with age and that a monocentric pattern of contact might be associated with the onset of cartilage degeneration and osteoarthrosis.

Lazennac *et al.* (1997) carried out a survey of the change in shape of fresh cadaveric acetabula as they were loaded in single-leg stance and double-leg stance configurations. They confirmed that a threshold force was required for congruency, estimating it to be 30% of body weight. The anterior and posterior horns of the acetabular lunate surface seemed to flex around a hinge in the acetabular roof noted by other authors. The displacements of the anterior horn were far smaller than those of the posterior horn, indicating a more rigid construction. During the transition from no load to 30% body weight the horns approached the femoral articular surface. After congruency was achieved they then began to move away again.

The incongruous nature of the hip joint is supposed to protect the cartilage from overload and to provide a mechanism for the circulation of synovial fluid for nutrition and lubrication. The contact area increases with load, so that at the highest loads the stress is evenly distributed across most of the cartilage. In a perfectly congruent hip joint the contact area could not increase with load and might even decrease with local deformation of cartilage in the dome of the acetabulum. The incongruity of the hip accords well with orthopaedic surgical experience which holds that the acetabulum is wider in the infero-medial supero-lateral than in the anterior posterior direction.

2.2.3 Geometry

While the morphology of the proximal femur has received much attention in studies of the design of stemmed hip replacement (Noble *et al.*, 1988; Rubin *et al.*, 1992; Skittides *et al.*, 1994; Sugano *et al.*, 1999), the precise shape of the acetabulum has only recently become the subject of investigation. Important parameters such as angles subtended by the articular surface edge from the centre of joint rotation have not been reported. The orientation of the acetabulum, described in section 2.1.1, and its relation in three dimensions to the orientation of the femoral neck are also not well

understood. These parameters have implications for the range of motion before impingement and for the space available for any acetabular prosthesis.

2.3 Biomechanics

Biomechanics here is used to denote the study of the mechanisms of motion and not the mechanical properties of biological materials.

2.3.1 Human Gait

Gait is described by splitting it into cycles, where a complete cycle returns the body and limbs to their starting positions and motions and thus consists of two steps (Whittle, 1991) (Figure 2.3.1). Each leg goes through two phases in a cycle – stance phase and swing phase. In walking the stance phases overlap so that there is a period of double support, whereas in running the stance phases are separated by a period of no ground contact. Heel strike occurs at the start of the stance phase and is accompanied by a transient force spike. The ground reaction force then increases to just over body weight (BW) as the body is decelerated, which with the accelerating force prior to toe-off produces a characteristic double peaked curve (Figure 2.3.2).

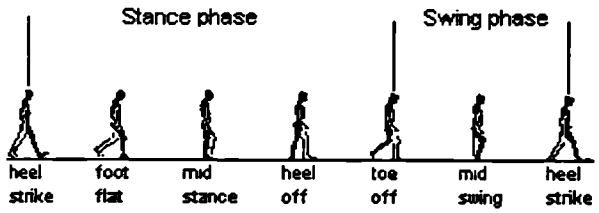

Figure 2.3.1 The phases of human gait from Whittle (1991).

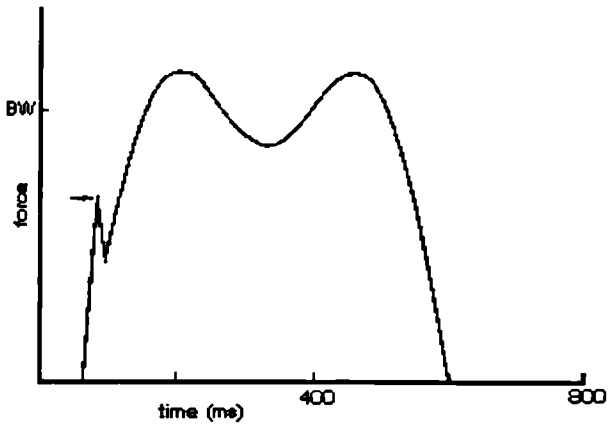

Figure 2.3.2 Ground reaction force during gait from Whittle (1991).

In common with all systems in living organisms, the means of producing motion have become optimised to give maximum output with minimum expenditure of energy. Minimising expenditure in human gait is achieved by minimising the excursion of the centre of gravity of the body, both vertically and laterally. In human gait there are six

mechanisms or determinants that accomplish this. Pelvic rotation, about the vertical axis, reduces the angle of flexion and extension at the hip needed for a given stride length, which in turn reduces the vertical movement of the hip and trunk. Pelvic rotation is produced by internal and external rotation movements at the hip joints. The second determinant is the drop of the pelvis on the side of the swing phase leg. This tilt reduces the rise of the centre of gravity at mid-stance. Tilt requires abduction and adduction motions at the hip joint and flexion of the swinging leg to avoid the ground surface. Three other determinants change the effective stance phase leg length. Knee flexion reduces the length while heel shape and forefoot flexion increase it at heel strike and toe-off respectively. The final determinant reduces the lateral motion of the centre of gravity. The adducted shape of the femur and the angulation at the knees reduce the lateral distance between the feet thus reducing the sway of the body necessary to maintain balance.

The motion of the femoral head within the acetabulum during gait is therefore complex. Flexion-extension, abduction-adduction and internal-external rotation of the femur occur simultaneously. The femoral neck is at a fixed angle to the femur, making visualisation of the effect of a particular limb movement even more difficult.

2.3.2 Range of Motion

Both soft and hard tissue limit the range of motion in a normal hip joint. The contribution that each makes in any particular direction is not reported. Hip joint motion is assessed clinically to evaluate disease and to measure the success of hip replacement. Table 2.3.1 lists ranges of motion for normal adults.

Table 2.3.1 Hip Motion in normal adults (degrees) from American Academy of Orthopedic Surgeons (1994).

Motion	Rotation mean ± SD		
	(Boone 1979)	(Roach 1991)	(Roass 1982)
Extension	12 ± 5.4	19 ± 8	9 ± 5.2
Flexion	121 ± 6.4	121 ± 13	120 ± 8.3
Abduction	41 ± 6.0	42 ± 11	39 ± 7.2
Adduction	27 ± 3.6	-	31 ± 7.3
Internal Rotation	44 ± 4.3	32 ± 8	33 ± 8.2
External Rotation	44 ± 4.8	32 ± 9	34 ± 6.8

2.3.3 Joint Forces

The forces between the femoral head and the acetabulum can be determined by two methods. In the first a ground reaction force is measured during gait and coupled with

a video analysis of gait (Paul, 1974). This analysis tracks the motion of limb segments and makes assumptions about ligament and muscle attachments and the timings of muscle action during gait to produce solutions for reaction forces at the joints. The redundancy of the structures of the limbs introduces the need for a further constraint: the forces in muscles acting at any given moment are assumed to be at an optimally low level. This assumption fails to take into account the action of antagonistic muscles, i.e. muscles which act to produce motion in opposite directions. One way of taking account of this may be to include forces in bony elements in the optimisation routine (Dobrev, 2000). Antagonistic action has been interpreted as protecting the bone from high stress levels.

In the second method an instrumented prosthesis is implanted to measure directly the loads at the joint (Rydell, 1966; Hodge *et al.,* 1989; Bergmann *et al.,* 1993; Brand *et al.,* 1994). Brand *et al.* additionally validated their instrumented prosthesis with simultaneous gait lab measurements. The gait lab method is non-invasive and much data exists for many different subjects. On the other hand the validity of its assumptions can be questioned. The instrumented prosthesis measures the real forces at the hip, but only a few subjects per study have been analysed. The data collected from these subjects may not be typical due to the pathology that led to the need for a replacement and also due to the replacement itself altering joint mechanics. Forces measured by instrumented prostheses during gait show the double peaked curve seen at the ground reaction. The directions of the largest forces have a small variation relative to the femur and their magnitudes are typically three times body weight (BW) during level walking. Faster walking and jogging can increase force magnitudes up to 5 times BW. Descending stairs places a higher load on the joint than ascending stairs, respectively 20% and 10% larger than level walking (Bergmann *et al.,* 1995). The largest forces of up to nine times BW occur if the subject stumbles.

Hip joint forces, which are measured or calculated from gait lab data in a femoral co-ordinate system, may be transformed into a pelvic co-ordinate system to assess their effect on the acetabulum. Witte *et al.* (1998) and Pedersen *et al.* (1997) calculated force vectors that varied over a relatively small area of the acetabulum. However while Pedersen *et al.* predicted smooth progression of the force direction from posterior to anterior, Witte *et al.* calculated forces pointing posteriorly at heel strike, then anteriorly at the first force maximum, posteriorly at the second maximum and

then anteriorly at toe off. Witte (2000) acknowledged that the simultaneous gait lab and instrumented prosthesis data from a single subject reported by Pedersen *et al.* is far more reliable than the gait and joint reaction force data from different subjects which he analysed.

Given that there are no muscle attachments on the femoral neck, the stress distribution here is determined by the position and direction of the joint reaction force. The force direction places the neck into slight bending. However the rest of the femur is not straightforward to analyse. There is debate about the magnitude, direction and timing of forces developed by muscles. It is contentious whether the femur is loaded in bending or in direct compression. The musculoskeletal system of the lower limb has been compared with tension compression structures such as the mast of a sailing dinghy (Ling *et al.,* 1996). The femur has a circular cross section with equal thickness of cortical bone – in bending an elliptical section with thicker cortices further away from the neutral axis would be more efficient. However Cristofolini (1997) and Taylor *et al.* (1996) have argued that the direction of bending varies sufficiently during the gait cycle that a circular cross section is still most efficient. Measuring radiographs of single leg stance has shown deflections an order of magnitude smaller than those calculated assuming a bending stress distribution, but similar to those calculated assuming a compressive stress distribution (Taylor *et al.,* 1996). This result suggests that the femur is loaded only in compression in one legged stance.

2.3.4 Muscles

Muscles and not static body weight develop the majority of the force across the hip joint during gait. Therefore it is important to understand the functional anatomy of the muscles surrounding the hip joint. Table 2.3.2 details the actions of individual muscles and Figure 2.3.3 shows the locations of the superficial muscles of the lower limb. Different parts of the same muscle may produce different motions and any particular muscle may produce motion in all three of the described degrees of freedom. A further complication is that muscles may act antagonistically during gait.

Although antagonistic action may not be related to the protection of bones from high stress levels, it is certain that muscle action reduces stress levels in the femur and the pelvis at all stages of gait (Dalstra, 1993; Duda *et al.,* 1998).

Table 2.3.2 Muscles that move the thigh.

Muscle / Group	Action
Gluteal group	
G. maximus	Extension, external rotation
G. medius	Abduction, internal rotation
G. minimus	Abduction, internal rotation
Tensor fasciae latae	Abduction, flexion, internal rotation
Obturators	External rotation
Piriformis	External rotation
Adductor group	
A. brevis	Adduction
A. longus	Adduction, flexion, internal rotation
A. magnus	Adduction, flexion (anterior portion), extension (posterior portion)
Pectineus	Flexion, adduction
Gracilis	Adduction
Iliopsoas group	
Iliacus	Flexion
Psoas major	Flexion
Biceps femoris	Adduction, extension
Semimembranosus	Adduction, extension, internal rotation
Semitendinosus	Adduction, extension, internal rotation
Sartorius	Flexion, external rotation
Rectus femoris	Flexion

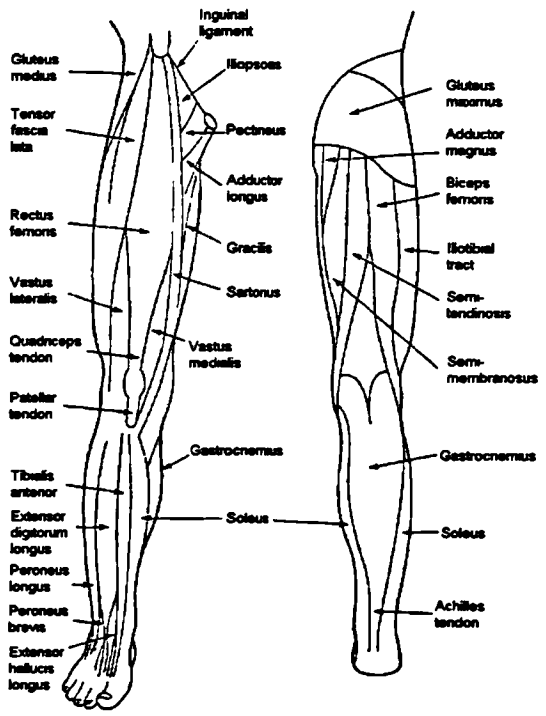

Figure 2.3.3 Superficial muscles of the right leg from Whittle (1991).

McLeish and Charnley (1970) proposed a simple model of the balance of muscle and joint forces at the hip joint. Their analysis was confined to the frontal plane but remains highly influential upon orthopaedic implant design and surgical technique. They considered force and moment equilibria about an idealised frictionless hip joint,

taking into account body weight, abductor muscle action and the joint reaction force. They found abductor muscle forces (normalised to body weight) varying between 1.0 and 1.8 and joint forces between 1.8 and 2.7. This model has also been used to show how an unfavourable skeletal morphology with a short distance between the joint centre and abductor muscle attachment can produce extremely high joint reaction forces (Eftekhar, 1993).

2.4 Diseases of Joints

This section briefly discusses the ways in which the function of the hip joint can be impaired.

2.4.1 Osteoarthrosis

The term osteoarthrosis (OA) describes the degeneration and progressive loss of normal structure and function of articular cartilage (Buckwalter and Mankin, 1997). *Osteoarthritis* implies an inflammatory disease and although inflammation frequently accompanies the disease it is not a major component. Over half of the adult population of the UK have some form of osteoarthrosis in one or more joints, with the prevalence increasing with age.

Osteoarthrosis consists of a progressive loss of articular cartilage. This may be accompanied by attempted repair of the cartilage, remodelling and sclerosis of subchondral bone and the formation of subchondral bone cysts and marginal osteophytes. A diagnosis of OA requires the presence of symptoms and signs that may include joint pain, restriction of motion and deformity. The disease occurs most frequently in the foot, knee, hip, spine and hand joints. Most commonly it develops in the absence of an identifiable cause (primary or idiopathic OA). Secondary OA may develop as a result of a joint injury or an infection. Hereditary, developmental, metabolic and neurological disorders may also be considered to cause secondary OA. Table 2.4.1 lists some known causes of joint degeneration.

Table 2.4.1 Known causes of Secondary Osteoarthrosis from Buckwalter and Mankin (1997)

Cause	presumed mechanism
Intra-articular fracture	damage to articular cartilage or incongruity of joint
High intensity impact loading	damage to articular cartilage or subchondral bone
Ligament injuries	instability of joint
Developmental and hereditary dysplasia	abnormal shape of joint or articular cartilage
Aseptic necrosis	collapse of articular surface and incongruity of joint
Paget's disease	distortion or incongruity of joint due to remodelling
Infection of joint	destruction of articular cartilage
Haemophilia	multiple joint haemorrhages
Neuropathic arthropathy (including diabetes)	loss of proprioception and joint sensation - increased impact loading, joint instability, fracture

The age of onset of secondary OA depends upon the underlying cause and so it may develop in children and young adults as well as in the elderly. In contrast there is a strong association between prevalence of primary OA and increasing age. However OA cannot be seen as "normal wear and tear" because the changes observed in

articular cartilage from older individuals differ from those seen in people who have osteoarthrosis. There are no simple relationships between joint use, aging and joint degeneration.

The earliest signs of OA visible from the articular surface are localised areas of fibrillation of the superficial layers of cartilage. As the disease progresses more of the surface becomes involved and the small defects deepen into clefts. Fissures eventually reach down to the subchondral bone and material is torn from the fibrillated cartilage tips. Cartilage is lost progressively leaving dense and often necrotic eburnated bone.

Patterns of cartilage degeneration in primary OA for both acetabulum and femoral head have been identified (Byers *et al.,* 1970). A distinction can be drawn between patterns of progressive and non-progressive changes. Non-progressive changes are speculated to occur in non-loadbearing areas.

2.4.2 Rheumatoid Arthritis

Rheumatoid arthritis is an immunological disorder of unknown cause, but with an inherited component, which culminates in the release of enzymes that can destroy articular cartilage and bone surrounding the affected joint. The disease affects 5% of women and 2% of men in the UK, but of these only 25% will go on to develop severe symptoms and loss of function. Juvenile rheumatoid arthritis affects children and teenagers, but resolves with no permanent damage except in rare cases. Osteoarthrosis can also be secondary to the damage to cartilage caused by rheumatoid arthritis (RA).

2.4.3 Ankylosing Spondylitis

Another inflammatory disorder, ankylosing spondylitis involves the ossification of ligaments at their attachments sites close to the affected joint. This leads to loss of motion which can be complete in severe cases. Although the joints affected are principally the sacro-iliac and those of the lumbar spine, the hip and knee joints are often involved. The disease has an incidence of 0.5% in men and 0.05% in women with onset in late teens and early twenties.

2.4.4 Avascular Necrosis

Bone is a living tissue and therefore requires a good blood supply. If the blood supply to an area of bone is disrupted the osteocytes in the bone die, hence avascular necrosis (AVN). Cell death is followed by attempts by the surrounding living tissue to remodel

the bone material. However with no osteocytic co-ordination of the actions of osteoblasts and osteoclasts this results in the mechanical collapse of the dead bone. AVN occurs in areas with particularly vulnerable blood supplies such as the femoral head and scaphoid bone. AVN, now known as osteonecrosis, is associated with steroidal drug treatment and alcohol abuse.

The ligamentum teres contains blood vessels but in the adult the main supply for the femoral head is via an arterial ring around the base of the femoral neck, near the attachment of the fibrous capsule (Gray's Anatomy, 1989). This ring is formed principally by the femoral circumflex arteries. Ascending branches from this ring pass up along the femoral neck surface and penetrate the femoral head (Figure 2.4.1) (American Academy of Orthopaedic Surgeons, 1997). These vessels are normally disrupted during the division of the capsule prior to dislocation of the hip in a conventional hip replacement operation. If the femoral head is retained, as in a resurfacing operation, the blood supply to this region may be severely compromised.

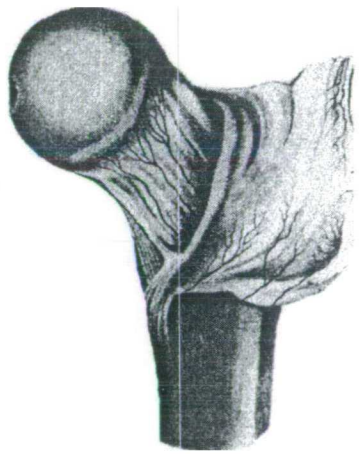

Figure 2.4.1 The ascending arteries on the anterior surface of the femoral neck from American Academy of Orthopedic Surgeons, 1997.

2.5 Hip Replacement

2.5.1 History of Hip Replacement

The treatment of hip disorders has evolved continuously since the early nineteenth century. Surgical treatment for arthropathy in the Victorian era involved the excision of the diseased portions of cartilage and bone, a technique which usually resulted in the fibrous union of the joint. A recognition that the loss of mobility in the joint was due to fibrous or bony adhesion of the articulating surfaces lead to the concept of the interposition arthroplasty. This procedure separated the articulating surfaces by a layer of material. Opinion as to the types of materials suitable to use as spacers differed (Black and Sholtes, 1982). Some favoured materials of biological origin, for example flaps of fascia lata, periosteum and pig bladder, while others attempted to implant sheets of more durable materials such as zinc, gold and rubber. The exponents of gold interposition arthroplasty included Sir Robert Jones of Liverpool (Eftekhar, 1978). Gluck writing in 1890 reports the use of an ivory prosthesis which he cemented in place with plaster of Paris (Eftekhar, 1978).

Smith-Petersen, working in the early decades of the twentieth century, introduced an anatomical surgical approach that provided exposure of the acetabulum and femoral head without massive trauma to the patient (Smith-Petersen, 1948). The encapsulation of a glass fragment in a wound by a membrane and liquid similar to that of a synovial capsule led him to use a glass hemisphere as an interposition arthroplasty. His rationale was that the glass would encourage the repair of the damaged cartilage surfaces, moulding them into shape, and could then be removed. Unfortunately the glass frequently broke and he experimented with a range of other materials, including celluloid and Bakelite, before settling on Vitallium, a Co-Cr-Mo alloy introduced for dental applications in 1929. By 1938 the Smith-Petersen arthroplasty was no longer a temporary mould for the repair of the cartilage, but a permanent substitute articulation.

The origin of total hip replacement (THR), in which both femoral and acetabular sides of the joint are replaced, is usually associated with Philip Wiles (Eftekhar, 1978). In 1938 he performed six replacements at the Middlesex Hospital, London. He used stainless steel components fixed on the acetabular side by screws and on the femoral side by a bolt down the femoral neck which was screwed to the lateral femoral cortex.

Other early THRs were attempted in Boston by Coutts and in New York by Haboush, who implanted one Co-Cr prosthesis fixed with self-curing polymethylmethacrylate (PMMA) (Eftekhar, 1978). The short stemmed Judet PMMA femoral head replacement was in widespread use in 1948 (Judet and Judet, 1950). This implant and a subsequent design using nylon showed that plastics could be tolerated, at least in the short term, in the human body. The 1950s saw the appearance of the stemmed metal femoral component which was designed to be inserted into the medullary canal. The Austin Moore and Thompson hemi-replacements are examples of this type.

From the 1950s on, THRs can be split into two groups by their type of articulation: metal-on-metal and metal-on-polymer. Metal-on-metal designers include McKee, Watson-Farrar, Ring, Scales and Müller. Many of these early implants were adaptations of the Thompson and Moore hemi-replacements. Changes in design following clinical experience eliminated many undesirable features. These are discussed in more detail in the relevant sections below. Some of the designs are illustrated in Figure 2.5.1.

The history of the metal-on-polymer articulation in THR is dominated by the achievements of Charnley (1961), (1963). His research into the lubrication of animal joints led him to the development of a Low Friction Arthroplasty. After attempts using polytetrafluoroethylene (PTFE) as the bearing material he introduced high density polyethylene (HDPE) and established the use of bone "cement" (PMMA) in THR. His implants differed radically from the preceding ones in the small size of the replacement femoral head. He developed the surgical techniques, instrumentation and theatre design and procedures for THR. The success of his implant is partly due to his insistence on training at Wrightington all those surgeons who wanted to use his implant.

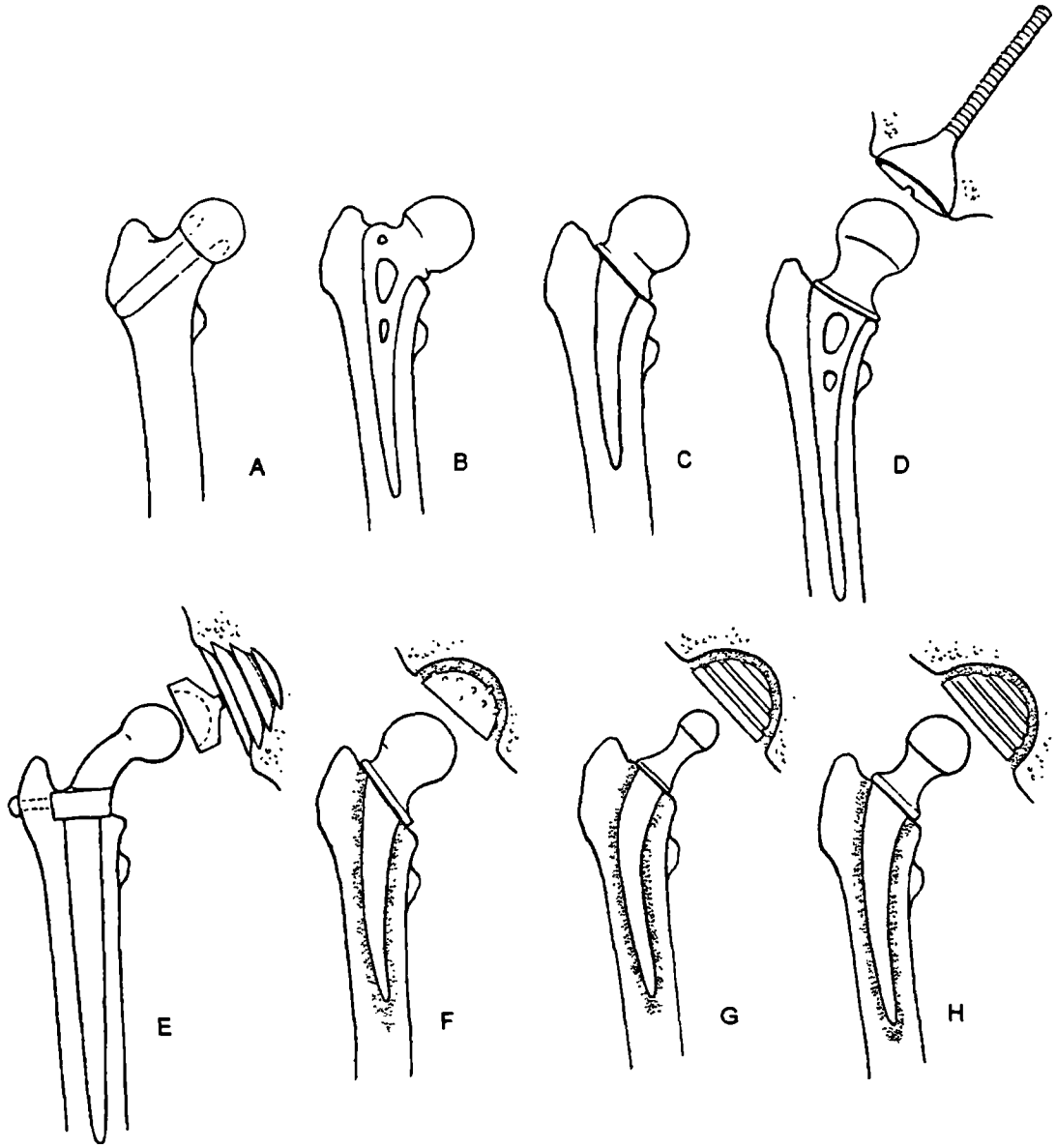

Figure 2.5.1 Types of hip replacement. A Judet, B Moore, C Thompson, D Ring, E Sivash, F McKee-Farrar, G Charnley, H Müller from Eftekhar (1993).

2.5.2 Total Hip Replacement

There are many types of modern total hip replacement, differing in detailed shape, head size, fixation method and bearing materials. However the basic shapes of the components are common and essentially unchanged from the components implanted 40 years ago.

The femoral component of a THR has an intramedullary stem, a neck and an articulating head. The intramedullary stem provides stability and load transfer to the femur. The neck of the implant is angled with the stem and chosen to be of a length to reproduce as nearly as possible the mechanics of a normal hip. The head is spherical and highly polished. Many modern THRs are modular so that head size and stem and

sometimes neck length may be chosen independently. The acetabular component is an hemispherical, or slightly shallower, cup.

The success (in terms both of implant sales and clinical outcomes) of any particular combination of features often seems a matter of fortune rather than design. The Swedish hip register (Malchau *et al.*, 2000) gives an overview of the Swedish market for THR between 1979 and 1998 (see Table 2.5.1).

Table 2.5.1 Numbers of commonly used primary THR implants in Sweden 1979 – 1998 from Malchau *et al.* (2000).

Implant	1979-1987	1988-1998
Cemented		
Charnley	19,298	29,363
Lubinus SP II	860	24,404
Lubinus IP	14,374	3,286
Scan hip collar	1,391	5,077
Exeter polished all poly		5,862
Exeter polished (mixed cup)	2,298	2,822
Lubinus SP I	3,302	1,034
Exeter polished (metal backed)		4,122
Müller straight	1,996	2,062
Exeter matte	3,694	0
Brunswik	2,158	57
Stanmore	1,500	592
Christiansen	1,939	
Others (373 implants)	6,825	20,295
Uncemented		
PCA	564	666
Romanus Bi-metric		569
Securefit / Omnifit		412
CLS Spottorno	6	362
Lord	311	
ABG HA / ABG		303
Harris-Galante	80	146
Others (116 implants)	668	1,471
Hybrids (total)	328	4,918

Increasingly the products of any one orthopaedic device manufacturer are designed to cater for the prejudices of as many surgeons as possible. There are few companies who will stand by one system of implants and defend the theory behind their function. Thus the debates over the theory behind the practice of total hip replacement are between individual surgeons and their followers.

2.5.3 Load Bearing, Load Transmission and Motion

Three primary functions that THR must fulfil are load bearing across the hip joint, load transmission to the bones surrounding the hip joint and relative motion at the joint itself.

The total hip replacement must be capable of bearing cyclic loads of three to four times BW with occasional peak loads of up to nine times BW (Bergmann *et al.*, 1993). In a year the number of cycles ranges from 0.5 to 3×10^6 depending upon the age and activity of the subject (Wallbridge and Dowson, 1982). This has implications for the fatigue resistance (crack nucleation and propagation resistance) of the materials used (section 2.6) and the shape of the implant. Sharp corners and other stress concentrations must be avoided. The Ring THR, which enjoyed initial clinical success, was modified to accept bone ingrowth mesh on its proximal surfaces (Wilson *et al.*, 1992). The stress concentrating effects of sharp recesses machined into the stem were compounded by the welding of the mesh into the weld intolerant, notch sensitive titanium alloy. Following high fracture rates these implants were recalled. Superalloy technology and good engineering design should have eliminated completely fatigue failure of the stem of the femoral component. However fracture of ceramic femoral heads is still a concern. While catastrophic fatigue fracture of polymer components is rare,fatigue may play a major role in the wear of the articulating surface.

A second function that the THR must fulfil is the transmission of the load across the hip joint into the musculoskeletal system. In distributing load to bone the design must take into account the remodelling behaviour of bone. The prosthesis must not produce stresses higher than the static or dynamic yield strength of bone – a strength which varies with bone material density (section 2.1.4). Remodelling of bone caused by the changed stress distribution in the implanted femur and acetabulum must not compromise the mechanical stability of the implants. Areas that resorb due to unloading after implantation must not be involved in the maintenance of the prosthesis' position.

The debate about load distribution in THR has been focused on the femoral component. Particular attention has been paid to calcar loading. This is the point of insertion of one of the trabecular systems of the femoral head into the medial femoral cortex. Collars on the medial side of the implant are supposed to load the calcar, but whether this is achieved in cemented hips or even if it is desirable is questionable (Forester and Draper, 1997). Bone cement is inappropriately named because it acts as a grout and thus its role is not so much in cementing as in load distribution. It fills the irregular cavity around the implant so that load transmission can take place over a wider area. The low elastic modulus of PMMA (section 2.6.3.3) reduces the overall

stiffness of the implant-cement construct. If the stiffness of the construct is closer to that of the bone then the stress in the surrounding bone is more evenly distributed. The stiffness of metals routinely used in joint replacement is up to ten times higher than cortical bone. The tapering of the distal stem is another subject of controversy, some implants having double (e.g. Exeter) and some single tapers (e.g. Charnley).

Uncemented femoral components are designed to "fit and fill" the proximal femoral canal (Noble *et al.*, 1988). In practice the irregular shape of this space and a finite number of implant sizes mean that the component is supported initially by bone only in a few small areas. The bone material in these areas is likely to be loaded above its elastic limit and so fail, leading to the migration of the implant (Taylor, 1997). Increasing numbers of custom-made femoral stems are being implanted with the aim of improving the initial fit of the implant. However it is questionable whether the vast increase in cost of this operation is reflected in improved clinical outcomes (Plath *et al.*, 2000).

Transmission of load to the pelvis by the acetabular component has been studied in detail (Dalstra, 1993). A finite element analysis of the implanted pelvis showed that stresses in distant bone were affected very little by changes in the acetabular component. However stresses in subchondral bone and in the polyethylene (PE) of the implant depended strongly upon the stiffness of the implant. A stiff cup/cement combination keeps implant stresses low. However stiff cups increase the stresses in the bone and cement at the periphery and stress shield the dome of the acetabulum. Load transmission is closely linked with the fixation of the components to bone (section 2.5.4).

A third function of THR is to provide an adequate range of motion. The ratio of the femoral neck diameter to the diameter of the bearing surface defines a limit to the range of motion (using a hemispherical acetabular component (Figure 2.5.2)). This range can be increased by increasing the femoral head diameter, by decreasing the neck diameter or by reducing the subtended angle of the acetabular component (Freeman, 1986). Impingement between the cup and the femoral neck is given as one of the reasons for failure of the early metal-on-metal THR designs (Amstutz and Grigoris, 1996).

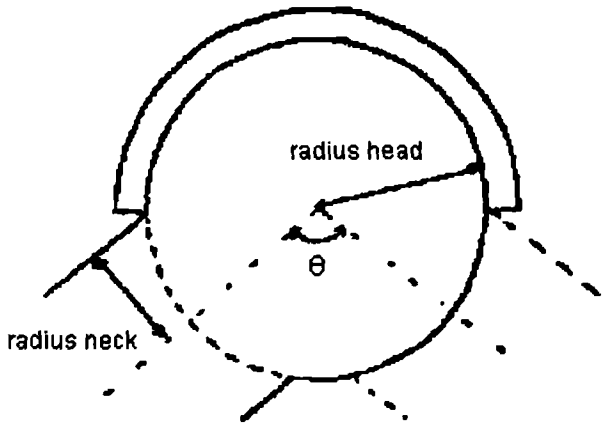

Figure 2.5.2 Parameters determining the range of motion in a hemispherical joint. $\theta = 2 \cos^{-1}$ (radius neck/radius head).

2.5.4 Fixation

The mechanical stability of THR in the body depends upon the method by which the implants are fixed to bone. Loose prostheses are associated with pain and have to be revised, so the provision and maintenance of fixation are essential. Methods of fixation include the use of PMMA bone cement, screw threads and bone ongrowth or ingrowth surfaces.

Polymethylmethacrylate is used on both femoral and acetabular sides with pressurisation. Pressurisation is relatively easy to obtain inside the femoral canal. Techniques for acetabular pressurisation have also been developed (New, 1997), but this is more difficult. Pressurisation is used to drive the setting cement into the trabecular spaces of cancellous bone. Cement is not adhesive and fixes by mechanical interlock, that is the interdigitation of cement into bone. Bone cement polymerisation is an exothermic reaction. The heat given off can raise the local temperature to 56° C, sufficient to kill bone cells close to the cement (Toksvig-Larsen *et al.,* 1992). The resorption of this necrotic bone may lead to some initial migration (section 2.5.6). Bone cement is also a brittle and low strength material and so has to be used in sufficient thickness to prevent fracture.

Threaded screws may be used for acetabular fixation. Some acetabular designs have used screw threads on their external surface. These have some good early results in combination with bone ingrowth fixation (Loupasis *et al.,* 1997) but longer term results are much poorer (Simank *et al.,* 1997). Bone is a viscoelastic material, so the stress that a screw thread initially places bone under will relax over time. Therefore screw fixation should be presumed to provide short term stability only.

Bone ingrowth fixation is achieved by a surface up to or into which bone will grow. Bony ingrowth will only occur with relative motions of less than 150 μm between the implant and bone (Pilliar *et al.*, 1986). This means that the implants must have an initial stability and maintain it while bone ingrowth occurs. Initial or primary stability may be achieved by screw fixation, or by an interference fit. Bone ingrowth has been compared to fracture healing in which limited straining of the fracture callus is used to promote bone growth. This analogy is used in advocating early mobilisation of patients with ingrowth fixated implants.

Interference or press fit can be used as the main fixation system for a prosthesis. This type of fixation is limited to patients who place very low demands on their prosthesis. The argument against it is similar to the one stated above for uncemented implants: that initially stress transfer between implant and bone takes place over only a few small areas. The same considerations as in screw fixation of the viscoelasticity of bone apply, so that the "pre-stress" generated by an interference fit will eventually be relaxed. Press fit has the further drawback that the primary stability will not be reinforced by secondary bone ingrowth fixation.

The different fixation methods have differing clinical outcomes. Kobayashi *et al.* (1997a) compared press fit, HA coated and cemented versions of the same femoral component. They found increased early migration and lower survival rates for smooth or ridged press fit than for cemented and HA coated prostheses.

2.5.5 Bearing Design and Tribology

One of the main functions of a THR is to allow motion at the hip joint. This implies the existence of bearing surfaces that can slide relative to one another and transmit load. The science of the behaviour of such surfaces is tribology. There are four bearing combinations in current use for THR: metal-on-metal, metal-on-polymer, ceramic-on-polymer and ceramic-on-ceramic. These can be thought of in two groups – hard-on-hard and hard-on-soft – with separate design issues.

The first THRs used metal-on-metal bearings. Pairs of components were lapped together, machining technology not being accurate enough to produce surfaces with the required tolerances. This process frequently resulted in an equatorial bearing pair, in which contact took place over a large portion of the bearing surface and large torques were produced by friction at large radii. . Highly congruent bearings

of hard materials are prone to seize under load and early failed THRs sometimes had to be hammered apart at revision. If the congruency of the bearing is reduced so that the contact half-width is reduced ι, polar bearing is produced and the frictional torques are much lower, but contact stresses are increased. Modern hard-on-hard bearings are designed with differing surface radii that give a clearance of between 50 and 150 μm, ensuring polar bearing (Semlitsch *et al.,* 1994). Some ceramic-on-ceramic manufacturers pair the femoral and acetabular components at the factory to obtain the required clearances, but the processing technology exists to produce each separately (Murray, 1998).

The wear behaviour of metal-on-metal bearings depends critically on the initial clearance between the two bearing surfaces (Semlitsch *et al.,* 1994). Small initial clearances (<10 μm) are undesirable for the reasons stated above. With the optimum clearance (between 25 μm and 100 μm), the implant at first shows a higher wear rate, 10 - 20 μm (Streicher *et al.,* 1990) or 0.20 – 0.80 mm^3 per million cycles (Chan *et al.,* 1999). After a "wear in" period of approximately one year (Täger, 1994) this rate decreases to a stable minimum of 2 – 4 μm or 0.07 – 0.11 mm^3 per million cycles. With too large a clearance (> 200 μm) the high "wear in" rate continues for the lifetime of the implant. The wear rate is speculated to depend upon the effective radius of the contact area, which depends inversely on the clearance (Chan *et al.,* 1996). Ceramic-on-ceramic bearings wear at an even lower rate than metal-on-metal – 0.004 – 0.014 mm^3 per million cycles depending upon the ceramic (Clarke *et al.,* 2000).

Charnley introduced the metal-on-polyethylene articulation. He was concerned with producing a low friction bearing pair and famously demonstrated the superiority of his implant over metal-on-metal bearings with the pendulum friction test. He reduced the size of the femoral head to reduce the moment arm of the friction at the bearing surfaces. Theoretical analysis of the tribology of metal-on-polymer articulations predicts mixed lubrication conditions (Fisher and Dowson, 1991). The fluid film thickness with elastohydrodynamic lubrication is smaller than some of the asperities on the polymer surface, so boundary lubrication must play a part.

The wear of hard materials on polyethylene has been extensively studied (Unsworth, 1991). One of the most important factors is the surface roughness of the hard

counterface, with dramatic increases in wear for small increases in roughness. Simple wear theory characterises a bearing pair with a wear coefficient so that wear is proportional to load and sliding distance. A study of 200 retrieved acetabular sockets (Hall *et al.,* 1998) showed that components with smaller femoral heads and hence smaller sliding distances had lower volumetric wear rates. However the scatter was considerable indicating that other factors such as patient activity were equally important.

The sliding velocity (high velocities lead to frictional heating and higher wear) and contact stresses (especially if of a similar magnitude to the elastic limit of the soft bearing material) also affect the wear rate. However increasing sliding velocity sufficiently for the bearing to enter the hydrodynamic regime will of course markedly reduce the wear rate. The lubricant used has a dramatic effect on the wear rate – Besong *et al.* (1999) reported that the UHMWPE wear rate was 14 times larger with deionised water as a lubricant than with 25% bovine serum. Average rates of penetration of Charnley prostheses range from 0.07 to 0.15 mm/year which correspond to volumetric wear rates of 25 – 60 mm^3/year (Fisher and Dowson, 1991). Revised sockets showed up to 0.51 mm/year penetration.

Attempts have been made to produce a bearing couple that operates in the fluid film lubrication regime using layered polyurethane with graded stiffnesses on a metal backing (Bigsby *et al.,* 1998). With a zirconia ceramic femoral component the wear volumes measured were negligible, but there were problems with the debonding of the polyurethane from the metal (section 2.6.3).

2.5.6 Failure of Total Hip Replacement

The definition of failure of THR is variable and depends upon the purpose of the study for which failure is defined. Most commonly "failure" is used to mean the re-operation and removal of one or both components of the THR. Since operation dates depend upon waiting lists and the persistence and tolerance of pain of the patient a second definition of failure may be used. A hip score with input from both patient and clinician gives an indication of the success of the implant. Failure can be defined as the fall of this rating below some threshold value. A third definition, which may or may not be included within the second, is radiographic failure. This occurs if the position of the components as measured on an X-ray has changed by a prescribed

amount, or if radiolucent lines of prescribed width and extent are apparent. However radiographic failure may not be accompanied by any symptoms. Unless otherwise stated the first definition of failure may be assumed to apply in this discussion.

Hip replacements are revised to relieve pain and improve function. Pain is associated with the mechanical instability of the implants giving rise to large motions relative to bone during use. This instability or looseness may have arisen for a variety of reasons. The first is the most familiar to the engineer – the fracture of the implant itself, but this is comparatively rare in modern prostheses and the solution may be found in better designs and stronger, more fatigue resistant materials. However, bone cement may be considered to be an implant material as well and if it is used in too thin a mantle it will fracture. Thicknesses of the cement mantle below 6 mm on the acetabular side and 2 mm on the femoral side have been shown to correlate with aseptic loosening (Massoud *et al.*, 1997; Joshi *et al.*, 1998).

A second engineering failure concerns the wear of bearing surfaces. Wear through of an 8 mm thick PE acetabular component at mean wear rates (0.07 – 0.15 mm/year (Dowson, 1992)) would take several decades (failure would probably be a secondary complication to this long before wear through occurred). However with the interposition of some hard particle, e.g. barium from radiopaque bone cement, or the scratching of the metal bearing surface, wear can be rapid.

Loosening can be caused exclusively by the infection of the joint. This is termed sepsis and occurs soon after the surgical procedure. Sepsis accounted for 7.2% of all revisions in Sweden between 1979 and 1996 and rates have been greatly reduced following the introduction of clean air operating theatres and antibiotic impregnated cement (Malchau *et al.*, 1998).

The majority of hip replacements (> 80%) fail following aseptic loosening of the components (Malchau *et al.*, 1993). This is a catch-all term for loosening that is not caused by infection. Theories that attempt to explain the cause of aseptic loosening with a single mechanism therefore over simplify the problem. The various factors responsible are often separated into mechanical and biological groups. However, there is a close relationship between these two groups: mechanical loosening must have a biological element and vice-versa.

The early failure of joint replacements can be predicted from the radiological findings at 2 years postoperatively (Freeman and Plante-Bordeneuve, 1994; Ryd *et al.,* 1995; Krismer *et al.,* 1996; Kobayashi *et al.,* 1997a). Implants that migrate rapidly in the first 2 years continue to migrate rapidly and fail early. Migration can be divided into three phases (Taylor and Tanner, 1996) – initial, stable steady state and rapid to failure. Some migration in the postoperative period is expected when mechanically and thermally damaged bone is resorbed and the implant settles. With stable steady state migration the balance between fatigue damage of bone and repair of that damage is maintained. Once the rate of fatigue damage to bone exceeds the repair rate, damage accumulates and the implant begins to migrate more rapidly. Various mechanisms identified as causes of aseptic loosening are then active and aggravate the loosening process. These are thought to be secondary to the primary event of fatigue and migration (Mjöberg, 1994). Many of the mechanisms for bone fatigue failure are also mechanisms for cement failure. Cement failure may be a primary event (Massoud *et al.,* 1997) that upsets the balance between bone fatigue and bone repair rates.

Rates of damage may exceed rates of repair for a variety of reasons. Stress concentrations (and concomitant stress shielding) in bone may arise from bad design, poor positioning of the components or poor cementing. The bone may have reduced strength and ability to repair itself due to disease or age. The implant designers may not have taken into account all the forces that act between implant and bone. For example, the torsional moment of up to 5.4% BW m during fast walking that Bergmann *et al.* (1993) measured around the stems of femoral components was not considered in implants of the time. The implant may be subject to loads it was not intended to bear. Impingement between the femoral neck and the acetabular component may occur in active individuals and also in patients in whom the components have not been well positioned. Friction at the articulating surfaces places additional torsional forces on the components. However it is accepted that these frictional forces are well resisted by the implant fixation surfaces (Clarke *et al.,* 1991; Adler *et al.,* 1992; Curtis *et al.,* 1992) and are not a factor in loosening (Mai *et al.,* 1996).

Friction at the bearing surfaces also produces heating. Bergmann *et al.* (2000) found a maximum temperature of 43.1° C inside the head of their instrumented implant. There was considerable variation between patients and a finite element study indicated that

the volume and properties of the synovial fluid and the perfusion rates in surrounding tissue were the most important factors. Temperatures raised above 45° C for bone and 42 – 43° C for soft tissue are thought to be damaging. Therefore frictional heating may play a role in aseptic loosening.

There is wide scope for many different secondary processes once initial loosening has taken place. The observations that these theories have to explain are accelerated loosening, generalised and local bone resorption and inflammation. Histological findings must also be accounted for, including increased macrophage and giant cell activity and the ubiquitous presence of wear debris. These observations are common to all types of implant and all bearing material combinations. The most popular theory currently is that wear debris induces a tissue reaction. Once the accumulation of particulate wear debris (usually PE) passes a threshold (10^{10} particles/g wet tissue (Kobayashi *et al.,* 1997b)) an inflammatory response is triggered in which bone is actively resorbed. A second, competing theory is that of osteocyte death caused by fluid motion and pressure in the caniculae (Aspenberg and van der Vis, 1998a). The micromotion of the implant relative to the bone results in a pumping action, pushing fluid (and with it wear debris) into the bone. The death of the osteocytes results in the resorption of the bone. Animal experiments attempting to replicate particle induced osteolysis appear to show that particles in the absence of micromotion merely diminish osteoblastic activity (Aspenberg and van der Vis, 1998b). Osteoclastic action independent of osteocytic control (i.e. without some osteoblastic activation) is only found in the resorption of necrotic bone and therefore Aspenberg and van der Vis suggest that this is the process occurring.

McGee *et al.* (1997) state that "polyethylene particles ... induce a tissue response that precedes aseptic loosening". They offer circumstantial retrieval evidence and cite an *in vitro* study that found increased levels of a marker for bone resorption (prostoglandin 2, PGE_2) in macrophages cultured with UHMWPE particles 0.5-4.0 μm at high (8×10^7 particles cm^{-3}) and even higher levels of PGE_2 in cultures with Ti alloy particles. However they admit that "initial stability and the degree of bone apposition to an implant are important in determining the effects of wear". Whether micromotion at the interface is the *cause* through fluid pressure oscillation of bone resorption or whether it simply allows ingress of wear particles seems to be immaterial. Wear particles are clearly a secondary problem to that of initial stability,

as is demonstrated by the predictive value of initial migration. Instead of attempts to ever increase the wear resistance of UHMWPE, more effective and fruitful research will address the primary problem of achieving good initial stability.

Revision of THR for aseptic loosening of the femoral component occurs later than for loosening of the acetabular component (Morscher, 1992). The reasons for the vulnerability of the acetabular component are uncertain. Acetabular components have undergone fewer modifications and less emphasis has been placed on their development. The area of fixation of an acetabular component is smaller than that available for a femoral component. Assuming a constant rate of loss of fixation (Mai *et al.,* 1996) the acetabular component will loosen first. The acetabular fixation interface is closer to the articulating surfaces and so wear debris (or pumped joint fluid) may have easier access (Black and Sholtes, 1982).

2.5.7 Revision of Hip Replacement

The revision of THR is a complex and time-consuming operation. The bone resorbing processes associated with loosening implants reduce the quality and quantity of bone available for fixing new devices. Revision of one component may inevitably mean the removal of the other, however well fixed. While cement extraction is a painstaking task a well fixed bone ingrowth implant is even more difficult to remove without causing damage to the bone stock (Wilson *et al.,* 1992).

Revision of THR will become more and more common as life expectancy increases and candidates for THR become younger and younger. The challenge is the conservation of bone stock. Young patients can expect multiple revisions and if every loosening destroys more and more bone then eventually conventional hip replacement becomes impossible. Conservation of bone stock can be effected in two ways. The first is to reduce the bone loss during loosening. This means understanding the processes of loosening and attempting to design implants and operative techniques that eliminate the causes – wear particles, fluid pressure etc. Early detection of loosening and early operation would also reduce bone loss. Early revision, sometimes in asymptomatic patients, is practised only at specialist orthopaedic centres (Wroblewski *et al.,* 1999). The second way to conserve bone is to ensure that the quantity of bone removed at the primary replacement operation is as small as possible. At each subsequent operation bone removal will be incremental. This approach must

also include the reduction of the scale of bone loss during loosening, otherwise there may be no gain over other less conservative operations. This second method is the subject of this thesis and will be treated more extensively in the sections below.

2.5.8 Alternatives to Total Hip Replacement

While THR is a very successful operation, it is not indicated in every case of hip joint disease. Techniques descended from the early methods of excision arthroplasty still have a place in the surgical armamentarium. Arthrodesis involves the removal of cartilage and the setting of the hip joint as if it were a bony fracture. Although all movement at the hip is lost relief of pain is gained and walking can still be possible. In an osteotomy the femur or the pelvis is cut in one or more places and the sections displaced and rotated. This might bring into use undamaged sections of articular cartilage or produce a more favourable mechanical situation for muscles about the joint. A recent study of this technique indicated a 67% survival rate at 12 years in young (mean age 38) patients (D'Souza *et al.*, 1998).

Autologous chondrocyte culture and reimplantation is the use of a patient's own healthy cartilage cell population to fill in defects in the cartilage surface. While the technique is not suitable for use in extensive erosions its current limited use in repairing small defects in the knee has shown high clinical success rates at 2 – 9 years (Peterson *et al.*, 2000). Biopsy specimens from the repair sites showed hyaline-like tissue containing collage type II as opposed to fibro-cartilage which is commonly found in untreated lesions. Although currently experimental and with limited indications, this approach of regenerating rather than replacing tissue is clearly the future of the treatment of joint disease.

2.6 *Materials for Joint Replacement*

2.6.1 Biomaterials

A material must fulfil two requirements before it can be used successfully in the human body (Williams, 1992). The first requirement is that it be capable of carrying out its prescribed function (e.g. load bearing, sound transmission) in the physiological environment. The material must also exhibit biocompatibility. This is a complex requirement that the interactions between the material and its biological environment must not prejudice its prescribed function. Problems of incompatibility arise because of the crudeness of the artificial model of living tissue, both biologically and mechanically.

The three functions of load bearing, load transmission between implant and supporting tissue and motion define the requirements for materials used in joint replacement. The loads on a hip replacement during level walking are of the order of 3 kN (Bergmann *et al.*, 1993). This will produce stresses of 30 MPa when applied axially to a typical THR femoral neck, with a cross sectional area of 100 mm^2. However the loading is usually applied in bending so stresses may be much higher. While there are many materials that can withstand this magnitude static stress, there are few biocompatible ones that can survive a 20 year life with up to 3×10^6 cycles per year (Wallbridge and Dowson, 1982). Load transmission to the surrounding bone defines the strength requirements for the interfaces between the implant and living tissue. The strength of the implant-bone interface is dependent upon the tissue reaction to the implant material, discussed below. Material stiffnesses similar to those of bone (section 2.1) are required to distribute load evenly across the interface. Joint replacement requires bearing materials that have low wear and friction. The wear resistance of a bearing pair is determined by many different mechanical properties, since wear proceeds by various mechanisms.

The physiological environment is aggressive and the body is well equipped to defend itself against foreign objects. This suggests that only the most inert materials are suitable for use in implants, however no material is completely inert, that is eliciting no response at all from the body. A bioactive material interacts beneficially with the surrounding tissue. Long term biocompatibility may be divided into issues of material degradation and host response. Corrosion of metals is the most obvious form of

degradation, but polymers and ceramics also change due to attack by chemical and biological agents within the body.

The host response is the most complex part of the implant-tissue interaction. Responses occur both local to the implant and remotely (systemic effects). The local host response to an implant can be considered a modification to the normal wound healing process (Williams, 1992), which consists of two overlapping phases. The first phase is inflammation, when cells are attracted to the site of the injury, damaged tissue and dead cells are removed and foreign bodies such as microbes are attacked by the immune system. Repair, the second phase, begins with the re-vascularisation of the wound area, then continuity is re-established by the laying down of new connective tissue. An implant within the wound site will prolong inflammation and, in the worst case, will act as a persistent source of irritation. With a perfectly inert material the inflammation, though prolonged, would resolve and the implant would become encapsulated by a thin fibrous layer.

Degradation products may also provoke local responses. Corrosion products of metals and polymer degradation products may interfere with local cell activity. Particulate debris will exacerbate the inflammatory response caused by the implant. The products of implant material degradation, particularly if soluble, can enter the blood stream and so affect many organs and tissues throughout the body, the systemic effect of an implant. Metal ions may be excreted leaving no residue or they may accumulate in certain tissues. There is concern that the accumulation of metal ions in various organs may cause cancer, although evidence of reduced incidence rates in joint replacement patients has been documented (Lewold *et al.,* 1996; Visuri *et al.,* 1996; Paavolainen *et al.,* 1999). Hypersensitivity to metals in implant alloys has been demonstrated in patients with loose THR (Merritt and Brown, 1996). Exposure to methylmethacrylate monomer from the curing bone cement in sufficient quantities can cause a rapid and potentially fatal loss of blood pressure.

2.6.2 Metals

Metals and their alloys readily meet strength, toughness and fatigue resistance design criteria for load bearing. They can be hardened and surface finishes with low roughness and high tolerance can be achieved. However in the aggressive physiological environment most metals will corrode and those that do not, such as

gold and platinum, are too soft for structural use. Therefore metals that are in a passive corrosion regime are used so that the corrosion rate is small enough not to endanger mechanical function or provoke adverse biological reactions. Passivation is achieved by the build up of a layer of oxide on the metal surface. There are three metal alloys in current use and their mechanical properties are listed in Table 2.6.1.

Table 2.6.1 Mechanical properties of metals and alloys used in implants. σ_Y is 0.2% offset yield strength, σ_{UTS} is ultimate tensile strength, % EL is % elongation to fracture, E is Young's Modulus from 1. Pilliar and Weatherly (1986), 2. Smith (1995), 3. Howatson *et al.* (1994), 4. Fraker (1992).

Metal Alloy	σ_Y (MPa)	σ_{UTS} (MPa)	% EL	E (GPa)	Reference
Stainless Steel					
316L annealed	170	480	40	190	ASTM F138 (1986)
316L cold-worked	310	655	28	200[4]	ASTM F138 (1986)
Ortron 90	810	1150	15		[1]
Duplex (2205)	550	800	25		[2]
Cobalt Chrome					
cast Co-Cr-Mo	450	655	8	248[4]	ASTM F75 (1982)
Wrought Co-Cr-W-Ni	310	860	30	242[4]	ASTM F90 (1982)
Wrought Co-Ni-Cr-Mo soln. annealed	241-448	793-1000	50	228[4]	ASTM F562 (1984)
cold worked	1586	1793	8		ASTM F562 (1984)
Titanium					
c.p.	100-225	240-370		120	[3]
Ti-6Al-4V	800-900	900-1000		115	[3]

2.6.2.1 Stainless steels

Low cost and ease of fabrication make stainless steel an attractive implant material. In stainless steels chromium (in concentrations of at least 12 wt. %) is responsible for forming the surface oxide layer that prevents corrosion. Molybdenum increases resistance to pitting corrosion and the carbon content is decreased to prevent intergranular corrosion at grain boundary carbides. Nickel is used to stabilise the austenitic (fcc) phase at room temperature and is balanced by the chromium which stabilises the ferritic (bcc) phase (Table 2.6.2). 316L steel is prone to crevice and pitting corrosion and it is now only used for temporary implants (6 – 12 months). The corrosion and mechanical properties of Ortron 90, the austenitic stainless steel used in the manufacture of the Charnley implant, are enhanced by the addition of nitrogen and niobium.

Table 2.6.2 Composition of stainless steels used in joint replacement from 1. Pilliar and Weatherly (1986).

	Element (wt.%)										
Alloy	C	Mn	P	S	Si	Cr	Ni	Mo	N_2	Nb	Fe
316L (ASTM F138)	0.03 max	2.0 max	0.025 max	0.01 max	0.75 max	17.0 to 19.0	13.0 to 15.5	2.0 to 3 0	-	-	balance
Ortron 90[1]	0.05	3.7	0.017	0.003	0.19	21.4	9.3	2.7	0.39	0.28	balance

The mechanical properties depend upon the extent of work hardening and fatigue strengths follow the Hall-Petch equation. Austenitic steels are preferred to ferritic steels which are particularly susceptible to grain coarsening, linked with fatigue failure of implants.

2.6.2.2 Cobalt alloys

Cobalt chromium was first used as the alloy Vitallium® in dental applications and was adopted in the 1930s by Smith-Petersen for his interposition arthroplasty. Cobalt alloys have since been used widely in other fields, including aerospace and turbines and, although now largely replaced in these applications by nickel superalloys, their properties are well established (Sullivan *et al.*, 1970). Hardening of the fcc cobalt matrix occurs mainly as a result of carbides (chromium, titanium) and intermetallic precipitation (aluminium, nickel, titanium), but solid solution strengthening also contributes (tantalum, niobium, tungsten). Corrosion resistance is obtained by the addition of chromium, molybdenum, tungsten and aluminium (Table 2.6.3).

Table 2.6.3 Composition of cobalt base alloys used in joint replacement from Kohn and Ducheyne (1992).

	Element (wt.%)											
Alloy	Cr	Mo	Ni	Fe	C	Si	Mn	P	S	W	Ti	Co
Cast Co-Cr-Mo (ASTM F75 (1982))	27.0 to 30.0	5.0 to 7.0	1.0 max	0.75 max	0.35 max	1.0 max	1.0 max	-	-	-	-	Balance
Wrought Co-Cr-Mo (ASTM F 90 (1982))	19.0 to 21.0	-	9.0 to 11.0	3.0 max	0.05 to 0.15	0.40 max	1.0 to 2.0	0.04 max	0.03 max	14.0 to 16.0	-	Balance
Wrought Co-Ni-Cr-Mo (ASTM F562 (1984))	19.0 to 21.0	9.0 to 10.5	33.0 to 37.0	1.0 max	0.02 5 max	0.15 max	0.15 max	0.015 max	0.01 max	-	1.0 max	Balance

Thermal processing of the as-cast alloy is important. As-cast material is inhomogeneous and large grained, both of which result in poor mechanical and corrosion properties. The alloy is heat treated and aged to allow the controlled

precipitation of carbides and intermetallics. Wrought cobalt chrome alloys have a finer grained structure with a fine carbide distribution. This gives them superior corrosion resistance and mechanical properties to as-cast and solution annealed alloys. Hot isostatic pressing (HIP) increases the fatigue strength of the alloy by eliminating porosity and grain boundary carbides. This is important because *in vivo* failure of Co-Cr-Mo stems is linked with fatigue crack initiation at casting defects (Kohn and Ducheyne, 1992).

A Cobalt nickel alloy is also as used as an implant material. The alloy is called MP35N, MP standing for multiphase, since the cobalt matrix is present in both fcc and hcp phases. The transformation from fcc to hcp is achieved by work hardening.

2.6.2.3 Titanium

Titanium is used both in commercially pure (c.p.) form, as a coating, and alloyed with 6 wt.% aluminium and 4 wt.% vanadium for load bearing applications. Other Ti alloys with sufficient strength and corrosion resistance are available, but are not used commonly. Thermal and thermomechanical treatments determine the relative quantities of α (hcp) and β (bcc) phases, yielding a wide variety of microstructures and mechanical properties. Oxygen, carbon, nitrogen and hydrogen are all highly soluble at room temperature and if not controlled at all processing stages will embrittle the alloy. Table 2.6.4 shows the composition limits for c.p. Ti and Ti-6Al-4V.

Table 2.6.4 Composition of commercially pure (c.p.) Ti and Ti-6Al-4V from Kohn and Ducheyne, (1992).

	Element (wt.%)							
Alloy	**N_2**	**C**	**H_2**	**Fe**	**O_2**	**Al**	**V**	**Ti**
c.p. Ti (ASTM F67 (1983))	0.03 max	0.10 max	0.0125 max	0.20 max	0.18 max	-	-	balance
Ti-6Al-4V (ASTM F136 (1984))	0.05 max	0.08 max	0.012 max	0.25 max	0.13 max	5.50 to 6.50	3.50 to 4.50	balance

ASTM F136 recommends a fine (3-10 μm) equiaxed α grain structure with a dispersion of β for surgical implants. Lamellar microstructures may also be used for implant material and may be refined by ageing treatments. The fatigue properties of titanium alloys are extremely sensitive to microstructure, with conflicting requirements for resistance to crack propagation and to crack nucleation (Pilliar and Weatherly, 1986). However high cycle fatigue life is controlled by crack nucleation

for which the optimum microstructure is that of fine equiaxed α grains with a well dispersed β phase.

C.p. Titanium, as used in dental implants, is the material around which the theory of osseointegration developed. The term was coined by Brånemark in 1977 (Albrektsson *et al.,* 1998) to describe intimate bone to implant contact on an histological level. A loaded implant that has at least 50% average surface area contact with bone and, at its passage through cortical bone, 90% surface area contact, may be defined as osseointegrated. Implants of c.p. Ti showed better osseointegration than implants of Co-Cr, stainless steel and even Ti-6Al-4V. This may be because of the high dielectric constant of TiO_2 which makes up the protective surface layer. A high dielectric constant is supposed to inhibit the movement of cells to the implant surface and so promote a positive biological response (Kohn and Ducheyne, 1992).

2.6.2.4 Corrosion

Corrosion is a problem not only because loss or degradation of material will affect mechanical function, but also because the products of corrosion will affect the local and systemic biocompatibility of the implant. All the metals and alloys mentioned so far possess passivating oxide layers, however, passive films do not prevent corrosion completely.

Pitting and crevice corrosion may take place at defects in the passive layer or at sharp discontinuities in the surface profile, particularly in 316L stainless steel. Pitting and crevice corrosion do not occur with titanium and cobalt based alloys. Ti-6Al-4V has been shown to have superior resistance to the combined effects of mechanical fatigue and electrochemical reaction compared to 316L and Co-Cr alloys (Fraker, 1992). In fretting corrosion the passive layers of two metal surfaces in contact are broken down mechanically by oscillatory relative motion. The hard metal oxide debris then acts as an abrasive third body increasing the wear of the surfaces and allowing rapid corrosion of the unprotected metal. Titanium has the ability to reform its oxide layer extremely quickly, whereas Co-Cr repassivates only after the release of a large amount of dissolution product.

The galvanic corrosion of pairs of dissimilar implant metals is determined by the difference in rest potential in the physiological environment. While thermodynamically these reactions may be possible, their speed depends upon the

kinetics of the anodic and cathodic reactions and the ratio of the surface areas of the implants involved. Dissimilar metals are often used within the same device with apparent disregard for galvanic effects. Kawalec *et al.* (1995) carried out short term fretting corrosion tests on combinations of Ti-6Al-4V and CoCr. The titanium alloy was damaged less when fretted in a mixed metal combination. Unfortunately the large volume of wear debris produced obscured any galvanic effects. Table 2.6.5 shows the relative potentials of some common implant materials.

Table 2.6.5 Anodic back series of implant metals and alloys in equine serum versus standard carbon electrode (SCE). From Fraker (1992).

Metal or alloy	Ti	Ta	Au	Cr-Ni-Mo	Cr	Cr-Co-Mo	316L stainless	Ag	Co
Potential vs SCE (V)	3.5	1.65	1.0	0.88	0.75	0.65 - 0.75	0.48	0.11	-0.35

Even if all the above forms of corrosion are prevented, slow dissolution of metals still occurs with the surfaces in their passive state. Using metals as implant materials therefore raises several serious questions including what material is released, how much is released, what effect it has on biological reactions, how much is excreted, what the site of any accumulation is and the biological effects of such accumulation. Experiments attempting to answer these questions by measuring levels of ions in blood serum or urine are confounded by the unknown role that these ions play in metabolism.

2.6.2.5 Wear mechanisms

Wear can take place between two similar metal surfaces by abrasion and by adhesion. In abrasive wear a hard third body or a hard component within the metal ploughs material from the opposite surface. Adhesive wear occurs when the raised stresses local to an asperity disrupt the surface oxide layer to produce a cold weld to the opposing surface. Subsequent movement fractures the asperity and material is transferred from one surface to the other. The process hardens the metal of the asperity which may then produce abrasive wear.

In spite of its rapid repassivation, titanium has poor wear characteristics because of the low resistance to abrasion of the oxide layer. This fails by spalling, producing hard TiO_2 particles, third bodies for further abrasive wear. The Beuchel-Pappas range of joint replacements are all coated with titanium nitride (TiN) which is claimed to reduce the wear rate on UHMWPE to two thirds of that of Co-Cr (Pappas *et al.*,

1995). Versions of the 3M Capital THR with a TiN coated modular head had a higher loosening rate than those with an uncoated Co-Cr modular head, although this difference was not statistically significant (Massoud *et al.*, 1997).

The wear of cobalt chrome alloy bearing pairs has been the subject of recent controversy. The effects of processing and bulk properties on the wear properties of the bearing were at issue. Unfortunately the metallurgical questions were not central to the debate and while laboratory wear tests showed that one type of processing produced a combined femoral and acetabular linear wear rate of 6 μm per annum (Corin, 1998) there was no proper comparison with other processing routes. McMinn (1997) speculated that carbides play a central role in Co-Cr on Co-Cr bearing and that the majority of contact took place carbide to carbide. Wear tests comparing high Carbon wrought, low Carbon wrought and as-cast Co-Cr (Chan *et al.*, 1999) showed significant differences in wear rate only during an initial "wear in" phase. Low C material had significantly larger initial wear rates than as-cast and high C material. There was no significant difference between high C and as-cast alloy. Steady state differences in wear rates were not significant. Surface roughness and bearing clearance were shown to be far more important factors. Differences in wear rates seen previously between alloy grades may have arisen from the lower surface roughness of the finer grains and carbide precipitates in wrought material (Chan *et al.*, 1996).

In metal on polymer bearing systems the wear rate may be increased rapidly by the scratching of the metallic surface (McNie *et al.*, 1998). Scratching on metal surfaces raises two lips on either side of a trough. Finite element studies of the contact between a scratch lip and a polymer surface (McNie *et al.*, 1998) show that the ratio of the lip height to its width is critical in determining the magnitude and location of the plastic strain in the polymer surface. These factors in turn determine the severity of the wear.

2.6.3 Polymers

Polymers can fulfil two of the three requirements of joint replacement materials, providing load distribution and articulating surfaces. For load bearing applications such as THR femoral stems they are generally used in conjunction with metals as they have stiffnesses much lower than bone. However a polymer (e.g. PMMA) which can be moulded to the contours of bone and harden *in situ* will provide a good even load distribution. Polymer bearing counterfaces have low friction and follow the traditional

engineering design of using a hard material for the convex component bearing upon a concave component of less hard material.

2.6.3.1 Polyethylene

Polyethylene was first produced in low density form by ICI in 1939 and High Density Polyethylene (HDPE) was introduced in the 1950s (Dowson, 1992). Charnley began the use of HDPE as an implant material in the early 1960s (Charnley, 1963).

Polyethylene has a simple $(C_2H_2)_n$ structure with no side groups. This structure and the mobility of the chain allow a high degree of crystallinity, the ratio of crystalline to amorphous regions in the material. HDPE has a lower degree of branching than Low Density PE (LDPE) producing more efficient packing and hence higher crystallinity and density. Ultra High Molecular Weight PE (UHMWPE) although of lower density and crystallinity than HDPE has much larger mean relative molecular weight, ranging from 1 to 4 × 10^6 $gmol^{-1}$ (Kohn and Ducheyne, 1992). Increases in the degree of crystallinity increase stiffness and yield strength, but decrease toughness, while increasing molecular weight improves tensile and impact strengths. Table 2.6.6 compares the properties of LDPE, HDPE and UHMWPE.

Table 2.6.6 Physical and mechanical properties of polyethylene. MW is molecular weight, UTS is ultimate tensile strength and %EL percentage elongation to fracture from Kohn and Ducheyne (1992) and RS data sheet (1992).

Property	LDPE	HDPE	UHMWPE
MW / $gmol^{-1}$	3 to 4 × 10^3	5 × 10^5	1 to 4 × 10^6
Density / Mgm^{-3}	0.90 to 0.93	0.92 to 0.97	0.93 to 0.94
Modulus / MPa	96 to 260	410 to 1240	70 to 490
Yield strength / MPa	-	-	21 to 25
UTS / MPa	4 to 16	21 to 40	37 to 46
% EL	90 to 800	20 to 100	200 to 525
Hardness / Shore D	-	-	64 to 67

The manufacturing method used for UHMWPE determines the properties and homogeneity of the material. There are three distinct methods (Li and Burstein, 1994). In direct compression moulding (DCM) UHMWPE powder is placed in a mould and heated under pressure to consolidate it and form the final shape of the device. Secondly, the UHMWPE powder may be ram extruded into cylindrical bar stock, which can then be machined to the final shape. The third method is to mould large sheets of UHMWPE, which are then machined to the implant shape. The homogeneity of the material from each process is determined by the uniformity of the processing conditions across a material batch and across each component. DCM produces

consistent components, but the material properties vary from the surface to the interior. Ram extrusion produces components that have uniform material properties, but those properties vary between components machined from different parts of the bar stock (Lewis, 1997). Moulded sheet machining may be seen as an attempt to compromise between these two extremes.

Many different grades of UHMWPE are used for the production of implants. The Hoechst numbering system assigns a four digit GUR code to each grade, e.g. GUR 1120. The leading figure one indicates that this is medical grade polymer. The second digit is one for a polymer containing calcium stearate and zero otherwise. The third digit indicates the molecular weight: 2 for lower (~4 million $gmol^{-1}$) and 5 for higher (~ 6 million $gmol^{-1}$). The final digit is always zero.

UHMWPE is used for acetabular cups and cup liners and the tibial trays of knee replacements. The most critical properties are wear and creep resistance although fatigue and environmental resistance are also important. Wear of UHMWPE occurs through abrasion and adhesion mechanisms. Adhesive wear results in the accumulation of a transfer layer of polyethylene on the hard counter bearing surface. This is a well accepted mechanism for polymer wear industrially. However in laboratory wear tests of hip replacements transfer layers have been observed with distilled water but not with serum lubrication so this mechanism may not operate *in vivo* (Bigsby *et al.,* 1997). Abrasive wear in joint replacement is produced by damaged metal surfaces or by hard third body particles. The third body may be a particle of bone cement or a fragment of bone and will abrade the bearing surfaces directly. The roughening of the hard counterface by the third body will increase the long term wear rate. Wear may also be increased by the deterioration of the mechanical properties of the subsurface layer of the polymer through oxidation (Li and Burstein, 1994).

Although polyethylene in bulk elicits little tissue reaction, polyethylene particulate debris resulting from wear processes has been linked with a more severe reaction (section 2.5.6).

The wear behaviour of UHMWPE is complex. During wear testing molecules in the surface of the polymer orient preferentially with the direction of the principal stress component (Wang *et al.,* 1997). This orientation is a form of strain hardening and it

reduces the wear rates observed in a linear (single direction) test. However a concomitant effect of orientation is strain softening in the perpendicular direction. In a biaxial wear test the strain softened direction is loaded by a secondary stress and surface rupture results. UHMWPE with increased cross linking between molecules (which are therefore less able to change orientation) shows increased wear in linear tests and reduced wear in biaxial tests. Dramatic reductions in wear rates in hip simulator wear studies (McKellop *et al.*, 1999) with cross linked UHMWPE have also been demonstrated. However a concomitant effect of cross linking is the stiffening of the polymer which, in the case of a scratched metallic opposing bearing, will increase the rate of wear.

Cross linking in UHMWPE can be achieved by gamma irradiation or by addition of peroxide to UHMWPE powder before direct compression moulding (McKellop *et al.*, 1999). Radiation exposure has a detrimental effect on the mechanical properties of the polymer. McKellop suggests 10 MRad is the optimal radiation dose for achieving saturated cross linking without reducing strength, elongation and stiffness values below the ASTM (F648-96) standard for medical UHMWPE. The remelting of bar stock following radiation cross linking has been shown to reduce the surface oxidation which may occur due to free radicals remaining in the material following radiation (McKellop *et al.*, 1999).

Gamma irradiation became the industry standard technique for UHMWPE sterilisation in spite of the well documented effects of radiation on polymers. Birkinshaw *et al.* (1988) studied the effects in UHMWPE of irradiation in air and showed increases in crystallinity, ultimate tensile strength and reduction in elongation at break for doses of 10 MRad. They proposed a mechanism involving the production of metastable groups containing oxygen at the initial radiation event. These groups, on ageing, decompose to carbonyl groups resulting in chain scission and cross linking. Baker *et al.* (1999) showed that irradiation in air produced material with reduced fatigue crack propagation resistance compared with material irradiated in an inert atmosphere and untreated material.

Carbon fibre reinforcement (CFR) of UHMWPE increases the strength, stiffness and creep resistance of the material. The wear rate using alumina on CFR polymer is supposed to be much reduced (Scheller *et al.*, 1999), but this is controversial. The

biological response to particulate reinforced polymer is similar to the response to unreinforced polymer (Rushton and Rae, 1984).

Enhanced UHMWPE (DuPont tradename "Hylamer") has increased crystallinity without a reduction in molecular weight. In the laboratory it has demonstrated increased yield strength, hardness and greater resistance to creep, crack growth and oxidation. However in clinical use acetabular components made from Hylamer have performed only slightly better (Sychterz *et al.,* 1998) and in one study less well (Graeter and Nevins, 1998) than conventional UHMWPE. Another study (Collier *et al.,* 1998) has suggested that, while fresh Hylamer may have similar or even superior wear properties to UHMWPE, its mechanical properties are more quickly degraded by oxidative attack, resulting in poorer long term performance.

2.6.3.2 Polyacetal

Polyacetal, also known as polyoxymethylene (POM) has the general formula $(OCH_2)_n$. Delrin® is the trade name for the polyacetal homopolymer marketed by Du Pont. Its linear backbone structure is similar to that of polyethylene. However the shorter backbone (C-O) bond allows closer packing of the molecules, giving a harder polymer with a higher melting temperature. Other properties which arise from this structure are increased toughness, resistance to chemical attack and resistance to fatigue and creep. The copolymer form of polyacetal has slightly superior resistance to "unzipping" to monomer (formaldehyde), but its mechanical properties are inferior to those of the homopolymer. The second monomer in polyacetal co-polymer is generally a cyclic ether, for example ethylene oxide (Brydson, 1993). Table 2.6.7 compares the properties of Delrin homo-polymer with co-polymers from two different sources.

Table 2.6.7 Selected properties of polyacetal from http://www.dupont.com; RS data sheet (1992); Chanda and Roy (1998); Brydson (1995).

Property	Delrin 111P	Copolymer	BASF copolymer
Yield strength / MPa	72	58	60-69.9
% elongation to fracture	40	23-35	
Tensile modulus / GPa	3 10	2.5	2.8
Density / Mgm^{-3}	1 42	1.41	
Hardness / Rockwell R	120	80	
% water absorption: 24 hr	0 4	0.22	0.22
Equilibrium	0 9	0.8	
Notch impact strength / kJm^{-2}	11-13	9	9
Melting temperature / °C	175	163	157

The fatigue limit for polyacetal is approximately 30 MPa at 10^7 cycles tested at 100% relative humidity and 25°C (Brydson, 1993). Although the moisture content does not appear to affect this value the presence of notches has a profound effect.

Gamma irradiation of polyacetal results in a severe deterioration of mechanical properties and, with sufficiently high doses, the loss of physical integrity of the material. A maximum level of 1.5 Mrad is recommended (Skeins and Williams, 1983).

Polyacetal has been used in several different joint replacements and also in heart valve replacements. The stem of the Isoelastic RM total hip replacement had a tapered titanium core surrounded by a polyacetal sheath, designed to reduce stress shielding of the femur by creating a composite stem with a structural stiffness similar to the femoral shaft (Morscher and Dick, 1983). The clinical outcome of this design was poor, with a 10% revision rate at a mean follow up of 8 years (Niininmaki *et al.*, 1994), but this was not linked to adverse reactions to polyacetal, but to the cementless fixation and large diameter neck of the femoral component. In the Christiansen THR, a four-component implant, polyacetal homopolymer was used for the trunnion liner and for the acetabular cup, which articulated against a cobalt-chromium femoral head. The implantation of this prosthesis was discontinued after high aseptic loosening rates were reported (Ahnfelt *et al.*, 1990). The large quantities of wear debris from both polyacetal components were supposed to have caused an unusually powerful synovial reaction that actively broke down bone tissue. However, from work measuring wear rates in retrieved implants, Mathiesen *et al.* (1986) concluded that the large volume of wear debris and increased friction were sufficient explanation for the high rates of aseptic loosening. Polyacetal homopolymer has also been used for nearly thirty years

as the occluder disc of the Björk-Shiley Delrin® (BSD) heart valve. Characterisation of retrieved material from both BSD heart valves and from the Christiansen hip has been carried out to determine the long term stability of polyacetal in the body (McKellop *et al.,* 1996). FTIR, viscometry and chromatography of controls and implants retrieved after up to 20 years all indicated that no systematic degradation of polyacetal took place under exposure to body fluids. In particular no evidence was found in the Christiansen hip retrievals of a reduction in wear resistance due to degradation of the polyacetal.

In 1980 Freeman began to implant a series of total knee replacements using polyacetal femoral components (Bradley *et al.,* 1993). The use of polyacetal was justified by reduced stress shielding due to its lower stiffness, absence of metal ion release, low cost, radiolucency and lower wear rates bearing on UHMWPE compared with Co-Cr. Following conventional engineering practice, the harder, stiffer material was used for the convex bearing. The outcomes of a clinical comparison between all-plastic and identically shaped metal-on-plastic knee replacements were confounded by fixation and sterilisation issues (Moore *et al.,* 1998). However no knee replacements failed because of fracture or wear of the Delrin femoral component.

The reduced wear rates cited by Bradley *et al.* (1993) were produced by McKellop *et al.* (1993) who used a hip simulator to compare the wear rates of polyacetal copolymer (Hoechst) and Co-Cr on UHMWPE. The polyacetal component studied was a 41 mm diameter sphere and the Co-Cr comparison was a 41 mm diameter femoral head surface replacement component. Both were articulating against UHMWPE cups machined from the same sample and sterilised at the same time. The all polymer bearing showed reduced frictional torque and reduced UHMWPE wear. The total wear volume of the all-polymer bearing, that is wear of both polymers, was 23% less than the UHMWPE wear volume of the metal on polymer bearing.

2.6.3.3 Bone cements

The main functions of bone cement are to stabilise a prosthesis by filling the gap between it and bone and to transmit loads from the prosthesis to bone (Kohn and Ducheyne, 1992). Polymethylmethacrylate (PMMA) has been used as a bone cement for nearly 40 years with little change in its composition and structure. PMMA is prepared in the operating theatre from powdered polymer containing an initiator

catalyst and liquid monomer containing an activator. Polymerisation is initiated on mixing these components and proceeds by an exothermic free radical reaction. Barium or zirconium sulphate is usually added to the polymer powder to render the cement X-ray opaque and antibiotic is commonly added to reduce the risk of infection. Control of the exothermic polymerisation reaction is essential to prevent thermal damage to the bone. The thermal expansion and contraction of the polymer itself must also be limited to maintain good contact with the surrounding bone and implant surfaces. Acute exposure to high levels of monomer at operation is known to be dangerous, but there is also concern about chronic exposure to low levels of unreacted monomer leaching from the bone cement (Borzacchiello *et al.*, 1998).

Mixing is carried out under vacuum to prevent the entrapment of air bubbles that would weaken the cement. However, significant porosity is always present in set material produced by polymerisation shrinkage. The mechanical properties of PMMA (Table 2.6.8) are determined by a range of physical factors – the powder size distribution, ratio of powder to liquid and molecular weight – and by the mixing technique.

Table 2.6.8 Mechanical properties of PMMA. UTS is ultimate tensile strength, UCS is ultimate compressive strength from Kohn and Ducheyne (1992) and Black (1988).

Property	Range
Tensile modulus / GPa	1.6 to 2.6
UTS / MPa	24 to 48
% elongation to fracture	5 to 10
UCS / MPa	77 to 92

The porosity of the set material, the presence of particles of barium sulphate and the roughness of the bone-cement interface all provide sites for crack initiation in bone cement. PMMA is a brittle material and stronger in compression than in tension. Fatigue failure may therefore be seen as the main mechanical problem. However definitive studies determining the critical flaw size and stress intensity where the governing stage of fatigue changes from crack initiation to propagation have yet to be carried out.

2.6.3.4 Other Polymers

Polyurethane (PU) has been considered for use as an acetabular cup lining material (Bigsby *et al.*, 1998). Hip simulator wear tests showed that a "soft lining" concept using layers of PU with graded moduli in a metal shell could produce fluid film

lubrication with lower wear rates than UHMWPE cups. There were some problems with debonding of the PU from the substrate. More recent work (Smith *et al.*, 2000) has confirmed that the lubrication regime in PU compliant bearings is closer to full fluid film than in conventional UHMWPE bearings. Smith *et al.* reported PU wear rates of 12.0 ± 3.6 mm^3 per million cycles compared with UHMWPE wear rates of 48.2 ± 3.7 mm^3 per million cycles when paired against 28 mm CoCr femoral heads. Creep of the material may be a problem since penetration gives rise to the "pinching" of the femoral component which starves the bearing surfaces of lubricant. Earlier work on PU degradation (Blamey *et al.*, 1991) showed that an aliphatic PU provided the best resistance to degradation of its properties and maintained fluid film lubrication after four month's immersion in Ringer's solution.

2.6.4 Ceramics and Glasses

The inherent chemical stability of ceramics and glasses due to the oxidised state of their component elements makes them attractive materials for use in the physiological environment (Kohn and Ducheyne, 1992). Engineering ceramics are extremely hard and may be polished to produce high tolerance low wear bearing surfaces. Ceramics and glasses can also display bioactive properties that produce positive tissue responses. The main disadvantage of monolithic ceramics used for load bearing is their brittleness. The strength of the ceramic is determined by the size of the largest flaw. For adequate toughness and strength, grain sizes must be of the order of 1 μm and processing of the ceramic must be carefully controlled to limit defects (Kohn and Ducheyne, 1992). Defects arise from agglomeration of powder before sintering, from contaminants, from residual stresses generated during sintering and cooling and from damage due to contact stresses during handling. Engineering ceramics are stiffer than metals, so the problem of stress distribution at the implant-bone interface is increased. Representative properties of some ceramic implant materials are presented in Table 2.6.9.

Table 2.6.9 Physical and mechanical properties of ceramic implant materials ρ is density, E is Young's modulus, UCS is ultimate compressive strength, UTS is ultimate tensile strength, flex is flexural strength from Kohn and Ducheyne (1992).

Property	Ceramic				
	Bioactive glass ceramics	Hydroxyapatite (0.1 - 3% porosity)	SiAlON (0% porosity)	Alumina (0% porosity)	Zirconia (0% porosity, stabilised)
ρ / Mgm^{-3}	2.8	3.05 to 3.15	3.2 to 3.9	3.93 to 3.95	4.9 to 5.56
E / GPa	-	7 to 13	280 to 320	380 to 400	150 to 190
UCS / MPa	500	350 to 450	400 to 1000	4000 to 5000	1750
UTS / MPa	-	38 to 48	-	350	-
flex / MPa	100 to 150	100 to 120	-	400 to 560	150 to 700

Alumina has been used as an implant material for nearly 30 years (Sedel, 1992), most commonly for modular femoral heads. The low surface roughness and wettability produce lower clinical wear rates (< 0.1 mm/year) with an UHMWPE counterface than metal bearings (Willmann, 1997). As discussed in section 2.6.2.5 scratches in metals have lips that stand proud of the rest of the surface, however, scratches in ceramic surfaces remain flush. Also the defects in a ceramic surface are all recessed, while metal surface defects tend to protrude so mean ceramic on UHMWPE wear rates are lower than metal on UHMWPE. Clinical wear rates of alumina on alumina are even lower (5 μm/year). Ceramic on ceramic hip wear simulator studies have produced rates 20 times smaller. This discrepancy is suggested to be due to separation of the bearing surfaces during the swing phase of gait (Nevelos *et al.*, 2000). While brittle fracture of the material is perceived to be its main disadvantage, in a survey of over 1.5 million ceramic heads only 0.02% had been revised for fracture, while septic and aseptic loosening together accounted for 11% (Willmann, 1997). Sedel has been a great advocate of the use of ceramic on ceramic bearings. He reported a 94.6% survival rate at 10 years for alumina on alumina hip replacements in patients younger than 50 (Sedel *et al.*, 1990).

Zirconia is another engineering ceramic used for orthopaedic applications. Modular femoral heads made from zirconia are available for use with UHMWPE cups (Willmann, 1998). Zirconia exists in three different crystal structures – monoclinic at low temperatures, tetragonal at intermediate and cubic at high temperatures. The transformation from tetragonal to monoclinic phases is martensitic and volume increasing and is used to toughen the ceramic. The addition of yttria (Y_2O_3) broadens the tetragonal phase field allowing sintering in the tetragonal field to produce tetragonal zirconia polycrystal (TZP). With sufficiently small grain size these

tetragonal crystals will self-constrain from transformation, becoming meta-stable at low temperatures. Stress concentrations, such as at a crack tip, will induce the martensitic transformation and the accompanying volume change will impose a crack closing stress, toughening the material. Unfortunately catastrophic wear rates in ring-on-disc tests have been widely reported (Früh *et al.*, 1997) for TZP articulating against itself or against alumina. This is speculated to be due to cracking in the surface following tetragonal – monoclinic transformation induced by frictional heating.

Silicon aluminium oxynitride (SiAlON) is an extremely versatile engineering ceramic with alloying type behaviour. A range of solid solutions of Al_2O_3 in the basic Si_3N_4 structure are possible, allowing fine control of the mechanical properties of the ceramic. These include outstanding hardness and wear resistance. SiAlON has been used in a femoral resurfacing type hip replacement canine trial (Clarke *et al.*, 1979), articulating on an UHMWPE acetabular component. The wear properties of SiAlON on UHMWPE were similar to those of stainless steel on UHMWPE. While macro-keying of bone and implant took place, a fibrous layer separated the implant from the bone. This raised doubts about the biocompatibility of the material. There are no further reports of the use of this ceramic.

Alumina, zirconia and SiAlON may be characterised as bioinert ceramics. Bioactive ceramics include calcium phosphate ceramics such as hydroxyapatite (HA), the synthetic analogue of bone mineral, and glasses and glass ceramics such as Bioglass® and AW glass ceramic. Their main applications in joint replacement are as coatings or as components of a composite. AW glass ceramic has however been successfully used as a bone graft material for iliac crest and spinal defects (Yamamuro *et al.*, 1988).

Hydroxyapatite (HA), $Ca_{10}(PO_4)_6(OH)_2$, is used as a biomaterial from the expectation that better tissue bonding will occur to a material similar to the mineral phase of bone. Bone contains non-stoichiometric forms of HA. Multiple substitutions occur in bone mineral as discussed in section 2.1.3. Non-stoichiometry may also result from the processing method used for synthetic HA. HA coatings are made by several different routes, all of which affect the phase and microstructure of the calcium phosphate ceramic produced.

The bioactive properties of HA, Bioglass® and AW glass ceramic stem from the ion exchange reactions that take place at their surfaces in the physiological environment. This ion exchange leads to the nucleation of carbonate substituted HA crystallites. These may then be incorporated into an ordered collagen matrix and form mineralised bone (Kohn and Ducheyne, 1992). This reaction critically depends upon the composition of the materials. Small variations in composition may produce changes of an order of magnitude in solubility and therefore in biological response.

Ceramic coatings may be used on the femoral components of joint replacements to enhance their wear properties. Coatings investigated include diamond like carbon which is vapour deposited onto the metal substrate (Kohn and Ducheyne, 1992). Coatings may improve wear rates, but can only be deposited in a limited thickness. Wear through of the coating may occur rendering it ineffective or even aggravating wear by delamination and production of third body particles (Harman *et al.*, 1997). One risk of carbon coatings on metal is that of increasing the susceptibility to corrosion of the substrate. Stainless steel coated with carbon demonstrates increased corrosion at defects or cracks in the coating layer (Pilliar and Weatherly, 1986).

2.6.5 Composites

The use of composite materials in joint replacement fulfils two of the three functional roles defined above: load bearing and load transmission. The particular advantage of composites in joint replacement is the ability to tailor the properties of the material to the application.

Load bearing composites may be produced with similar stiffnesses to bone. Another possibility is variation of stiffness through the material allowing the use of a design with an optimised stiffness distribution (Kuiper, 1993). The matrices of composite biomaterials are typically thermoplastic polymers and the properties of some common materials are given in Table 2.6.10. Polysulfone is chemically stable and does not degrade or cross link when exposed to radiation, steam sterilisation and oxidative environments. The benzene rings within the polymer chain allow dissipation of energy without loss of structural integrity, giving the material good fracture resistance (Kohn and Ducheyne, 1992). Polyetheretherketone (PEEK) is likewise chemically stable, but not as tough and fracture resistant. UHMWPE has far inferior strengths to these two materials and is included for comparison.

Table 2.6.10 Properties of composite matrix materials. ρ is density, σ_Y is yield stress, E is Young's Modulus, % EL is % elongation to fracture, σ_{flex} is flexural strength. From Kohn and Ducheyne (1992).

Property	Polysulfone	PEEK	UHMWPE
ρ (Mgm^{-3})	1.3	1.3	0.9
σ_Y tensile (MPa)	70	92	20
σ_Y comp. (MPa)	96	118	15
E (GPa)	2.5	3.6	0.6
% EL	50 to 100	50	200 to 525
σ_{flex} (MPa)	106	170	13

Reinforcing fibres investigated for use in biocomposites include carbon-graphite and polyamide, known as Kevlar, (Table 2.6.11).

Table 2.6.11 Properties of composite fibre materials. E_1 is Young's Modulus parallel to fibre axis, E_2 is Young's Modulus perpendicular to fibre direction, UTS is ultimate tensile strength. From Kohn and Ducheyne (1992).

Property	Carbon type I	Carbon type II	Kevlar
Diam. (μm)	7 to 100	8 to 9	12
E_1 (GPa)	390	250	125
E_2 (GPa)	12	20	-
UTS (MPa)	2200	2700	2800 to 3600

As mentioned above the main use of bioactive ceramics other than as coatings is in bioactive composite materials. The bioactive ceramics are not strong enough for structural use and so are incorporated into a material that is strong, but bioinert.

HAPEX™ is one such composite of HA and HDPE developed for bone replacement by Bonfield *et al.* (1980). HAPEX™, with an HA volume fraction of 40%, is in clinical use in orbital floor implants and middle ear bone replacements, both minor load-bearing applications (Tanner *et al.*, 1994; Dornhoffer, 1998). The material has demonstrated high bioactivity *in vitro* supporting the proliferation and differentiation of human osteoblasts with the HA particles providing favourable sites for cell attachment (Huang *et al.*, 1997). Huang *et al.* also reported that the mechanical properties do not deteriorate after up to three months immersion in a simulated physiological environment. The mechanical properties have been extensively characterised (Table 2.6.12). Guild and Bonfield (1998) carried out FEA of particle matrix interactions at high strain to investigate failure mode dependence on HA volume fraction. PE shear yielding was found to be dominant at low HA volume fractions and interface debonding dominant at volume fractions above 40%. This points to the need for altered interface properties to achieve useful strength at the high volume fractions required to approach cortical bone stiffness. Study of the fatigue

properties of HAPEX™ (Ton That *et al.*, 2000a; Ton That *et al.*, 2000b) showed that in uniaxial fatigue stress levels of 25% of the ultimate tensile and shear strengths were resisted for over 1 million cycles. Biaxial fatigue showed appreciable lowering of fatigue life at higher stresses, but the combination of 25% tensile and 25% shear strength was still resisted for over 1 million cycles.

Table 2.6.12 Selected mechanical properties of HAPEX (40% vol. HA). (Wang *et al.*, 1998a; Wang *et al.*, 1998b; Ton That *et al.*, 2000a; Ton That *et al.*, 2000b)

Property	HAPEX (21° C, air)	HAPEX (37° C, saline)
Tensile Young's modulus (GPa)	4.29 ± 0.17	3.76 ± 0.11
Shear modulus (GPa)	1.180 ± 0.074	1.19 ± 0.13
Tensile strength (MPa)	20.67 ± 1.56	17.39 ± 0.44
Shear strength (MPa)		19.13 ± 0.37
Tensile failure strain (%)	2.6 ± 0.4	0.8 ± 0.1

3. Hip Resurfacing

The tremendous success of the Charnley low friction arthroplasty focused attention on the development of the stemmed total hip replacement. The concept of hip resurfacing, with which Charnley briefly experimented (Charnley, 1961) has never achieved such widespread acceptance despite its obvious attractions. His rejection of the idea in favour of a stemmed replacement was due to the necrosis of the bone of the femoral head under the resurfacing. However subsequent experience with the acetabular cup of the first low friction arthroplasty showed that polytetrafluoroethylene (PTFE), of which both his prosthetic cups were made, was a poor implant material (Charnley, 1963). The evolution of hip arthroplasty from the Smith-Petersen cup would seem to point naturally in the direction of surface replacement and the arguments for resurfacing are at first glance compelling. However, attempts at resurfacings have been sporadic and the implants have not been widely adopted. This section will catalogue the designs and outcomes of resurfacing since Charnley and attempt to show why resurfacing has so far failed to achieve a place alongside conventional THR in the orthopaedic armamentarium.

3.1 Rationale for Resurfacing

The basic concept of resurfacing focuses on the conservation of the bone of the femoral head and neck. In conventional THR this bone is resected and the medullary canal broached. A resurfacing aims to remove only the diseased surfaces of the femoral head and acetabulum and replace them with artificial materials. This is achieved with the "double cup" design. The femoral component is a cup placed over the top of the re-shaped femoral head. Its internal surface provides fixation and its external surface bears upon the internal surface of the acetabular component. The acetabular component is a cup inserted into the reamed acetabulum, relying upon its external surface for fixation.

The theoretical advantages of resurfacing hip replacement over conventional replacement are easy to appreciate:

- A smaller amount of a superior, self-repairing structural material, bone, is removed.

- The loading of the proximal femur is closer to that in the normal, unreplaced hip and therefore bone resorption related to stress shielding and concentration should be reduced.
- At revision a conservative resurfacing replaced hip should retain all of the options open to the surgeon at a primary hip replacement operation.

As candidates for hip arthroplasty become yet younger and thus must expect more and more revision operations it is becoming more important to conserve bone at every operation. This conservation will compensate for bone loss during the loosening process and help to increase the success of the revision replacement.

A further advantage claimed for resurfacing is shortened operating times. This reduces the risks of medical complications such as deep vein thrombosis (DVT) and embolism and a smaller volume of blood will be lost by the patient. The risk of infection is also reduced and the intact medullary canal is unlikely to be involved.

3.2 Early Design of Resurfacing Arthroplasties 1951 - 1976

The first double cup hip replacement was that of Charnley in 1951 (Charnley, 1961). Both femoral and acetabular components were made of polytetrafluoroethylene (PTFE) (Figure 3.2.1). Internally the femoral component was cone shaped and press fitted onto the reamed femoral head. The acetabular component was also a press fit. Unfortunately the PTFE wore quickly and the wear debris provoked an inflammatory response which resorbed bone at the bone-implant interface, loosening the implant.

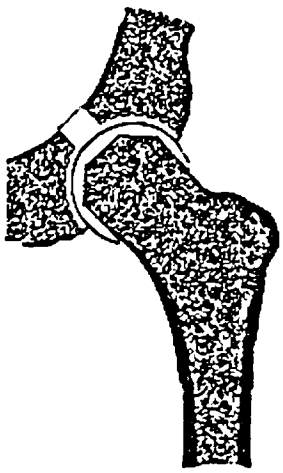

Figure 3.2.1 The original Charnley PTFE cup arthroplasty from Charnley (1961).

Charles Townley began a series of hemiarthroplasties in 1952 using a Co-Cr-Mo (Black and Sholtes, 1982) femoral cup with a long curved intramedullary stem (Townley, 1982) (Figure 3.2.2). The Total Articular Replacement Arthroplasty (TARA) developed from this and was designed to correct the perceived failings of the Smith-Petersen arthroplasty. The "at risk" portion of the proximal femoral head was excised and replaced, stable and immobile fixation prevented the relative motion of the implant and the femoral head and a large load bearing interface was provided to distribute stress evenly to the femoral neck. Internally the cup was a flat-topped cylinder and the component was much thicker in the polar direction, at 11 mm, than equatorially. The outer surface made 5/8 of a sphere and the centrally placed stem bent distally through an angle of 140°. A ceramic version of the femoral component appeared later (Townley, 1995) but no further clinical or materials data were published. The femoral component was first used as part of a total arthroplasty in 1960.

The acetabular component and cement were polyurethane, though this material was not satisfactory and in 1977 PMMA cement was used for fixation and the acetabular component became high density polyethylene (HDPE). The component's surfaces were eccentric, providing thicker material superiorly. It had a brim to give stability and the option of additional screw fixation. Holes through the body of the cup allowed the surface to be lubricated by blood from the acetabulum in the period before the formation of a pseudocapsule.

Townley used reamers and other instrumentation of sizes specific to each of the 8 sizes of implant. However, the femoral head was not reamed, but the trial femoral implant was used as an osteotome to shape the head into a cylinder. Trial acetabular components were also used and a reduction attempted with both trials in place. In the event of excessive soft tissue tension, bone was removed from the top of the resected femur in preference to deeper reaming of the acetabulum. The acetabular component was to be positioned at 45° to the vertical and its brim was to fit flush with the acetabular margin. Portions of the acetabular component exposed by gaps in the acetabular rim were trimmed to prevent impingement.

Townley noted a gender difference in the ratio of diameters of the femoral head to the neck and the thickness of the acetabular wall. Males have small head-to-neck ratios and thick acetabular walls and females have large head-to-neck ratios and thin

acetabular walls. Thus more femoral bone can be removed in females and more acetabular bone in males. In total resurfacing he suggested that the femoral component diameter must always be smaller than the diameter of the head it was replacing to prevent excessive acetabular reaming.

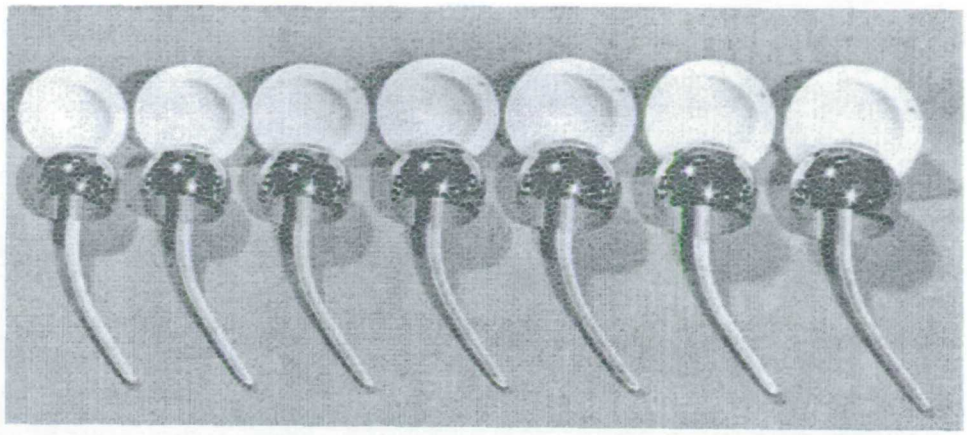

Figure 3.2.2 TARA hip prosthesis from Townley (1982).

Müller in 1968 implanted a double cup prosthesis in a short series of patients (Freeman, 1978a). Both components were made of a Co-Cr alloy and were not cemented. The revision rate was unacceptably high and the procedure was abandoned. However, Müller demonstrated that conversion to arthrodesis was possible at revision of double cup arthroplasty. Some of these arthroplasties were still functioning in 1978, although no further reports of the implant have been made.

The next attempt at a double cup arthroplasty design was made in 1970 by Gerard (Gerard, 1978). The acetabular component was free to slide and rotate between the reamed acetabulum and the femoral component and so acted as an interposition arthroplasty (Figure 3.2.3). It was concentric and over hemispherical and initially made from Co-Cr, but was then changed to UHMWPE to decrease the coefficient of friction. The UHMWPE articulating directly on bone produced large amounts of wear debris and subsequent resorption of bone, so the final design had a Co-Cr shell lined with 4.5 mm thick UHMWPE. The femoral component, which was press fitted onto the reamed femoral head, had an outer surface that comprised 2/3 of a sphere. Around the neck opening it had a non-load bearing skirt. The internal shape was cylindrical, capped with a hemisphere concentric to the surface. Gerard reamed the femoral head along the neck axis. He emphasised the importance of conserving the blood supply to the head by using a lateral approach and an anterosuperior capsulotomy.

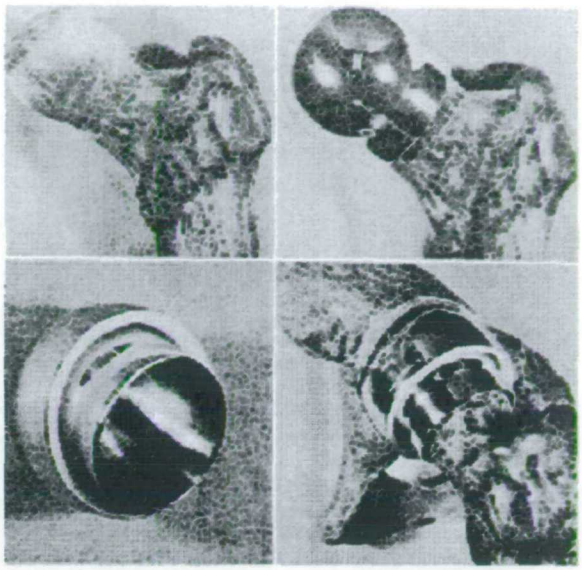

Figure 3.2.3 Gerard resurfacing prosthesis from Gerard (1978).

The first cemented double cup arthroplasties (Freeman, 1978a) were implanted independently by Trentani in Bologna and Furuya in Tokyo in 1971. The Paltrinieri-Trentani surface replacement (Figure 3.2.4) was intended as an additional alternative procedure for younger patients (Trentani and Vaccarino, 1982). The femoral component of 1 mm thick polished stainless steel was 2/3 spherical and had a 4 mm long load bearing skirt. This was to reduce the risk of femoral neck fracture by providing a "stress shield" for the femoral head-neck junction. It also stiffened the thin component against flaring at the rim and enhanced the normal stressing of the medial calcar. Coarse concentric grooves on the inside of the component enhanced cement fixation. The UHMWPE acetabular component was concentric and had 5 mm thick walls. It had 3 mm deep circumferential grooves for cement fixation, one of which contained a radiographic marker wire. The head was reduced to a chamfered cylinder of the same diameter as the femoral neck, with its axis parallel to the medial trabecular system. Trentani advocated the use of a saw rather than a cylindrical reamer to avoid damage to the cortex of the neck.

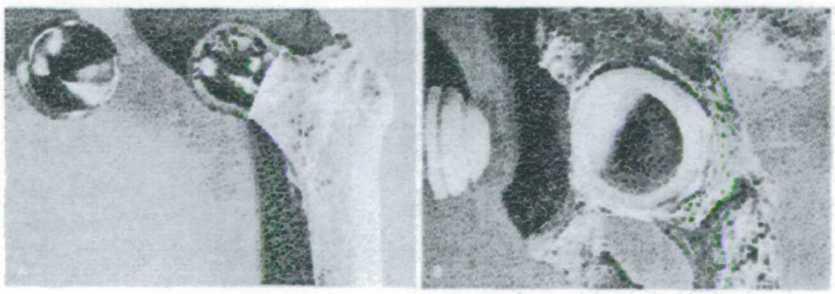

Figure 3.2.4 Paltrinieri – Trentani resurfacing from Trentani and Vaccarino (1982).

The resurfacing designed by Furuya *et al.* (1978) went through a succession of changes. When first implanted in 1971, the femoral component was a press fit hemisphere of HDPE, articulating against a hemispherical stainless steel acetabular component, fixed by cement. The third design reversed the femoral and acetabular component materials and the final implant appears to be a ceramic-on-ceramic articulation, although the actual material used is not reported (Figure 3.2.5).

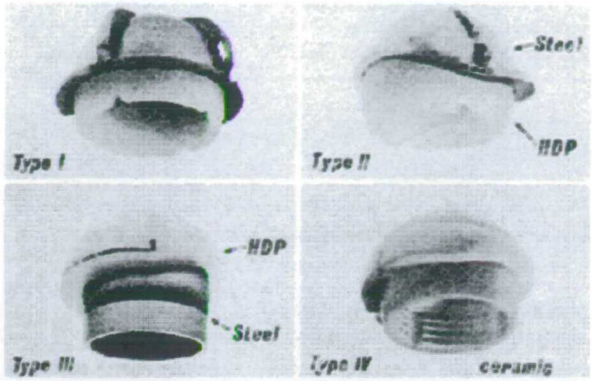

Figure 3.2.5 Furuya resurfacing from Furuya *et al.* (1978).

Another design which began by using HDPE on the femoral side and stainless steel for the acetabular component was the Imperial College London Hospital prosthesis (ICLH), first implanted in 1972 (Freeman *et al.,* 1975). A high loosening rate prompted a change in design and in 1974 the acetabular component was changed to HDPE and less than hemispherical, subtending an arc of 168°. The inner and outer surfaces were axially coincident and the outer surface was grooved for cement fixation. The Co-Cr femoral component was more than hemispherical and internally was a chamfered cylinder. Like the TARA prosthesis, it was much thinner equatorially than at the pole, having a polar thickness of 10.5 mm, but was designed for cemented fixation (Freeman *et al.,* 1978) (Figure 3.2.6). The preparation of the femoral head was carried out with a Tuke saw, not a reamer, to avoid damage to the neck cortex. Freeman emphasised the alignment of the axis of the prepared cylinder with the medial trabecular system and not with the femoral neck (Freeman, 1978b). However the medial edge of the prepared head was to be flush with the medial cortex of the neck. A large diameter femoral head was used at the expense of acetabular reaming. There were only three different sizes of prosthesis, but "phantom" prostheses were used for a trial reduction to enable correct positioning. The trochanteric osteotomy which was used for the first design of prosthesis was discontinued in 1974. Use of the ICLH implant was abandoned in 1987 (Cotella *et al.,* 1990).

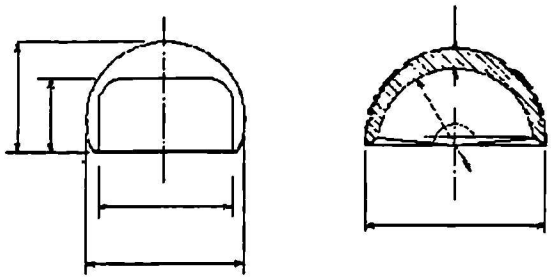

Figure 3.2.6 ICLH resurfacing from Freeman *et al.* (1978).

Nishio (1978) and colleagues began a series of surface replacements in Japan in 1972 to address concerns about the long term efficacy of THR in patients under 60 years old. The prosthesis was specifically designed with an 80° range of motion. The report unfortunately fails to mention the metal used for the femoral and acetabular components, although it notes that at first the articulation was metal-on-metal, but later the acetabular component was lined with PE (Figure 3.2.7). Both components were uncemented, although 3 bone screws were used for additional fixation of the acetabular component. The femoral component was cylindrical with a hemispherical cap of uniform thickness. A trochanteric osteotomy was used to provide sufficient exposure of the joint.

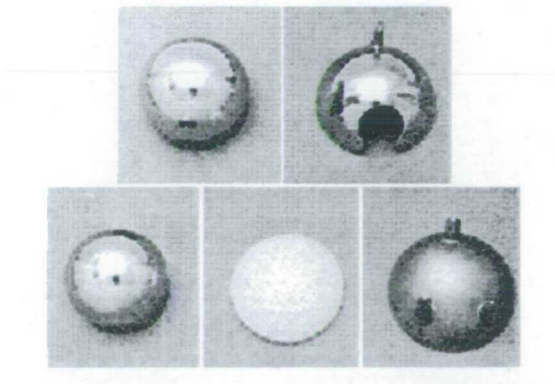

Figure 3.2.7 Nishio resurfacing from Nishio (1978).

The Indiana Conservative Hip (ICH) (Figure 3.2.8), developed by Eicher and Capello (Capello *et al.,* 1978), was first implanted in 1973. The design was a response to the loosening and fracture of femoral components in THR and the expansion of the indications for THR to include younger patients. Between 1975 and 1980 the prosthesis evolved on both femoral and acetabular sides (Capello *et al.,* 1982a). The Co-Cr femoral component, over-hemispherical and with slightly eccentric surfaces, was reduced in thickness from 3 – 4 mm to 1.5 mm. In its final form the interior was porous coated to enhance cement fixation and a central stud was provided for

positioning. On the acetabular side a grooved Ti backing was added to the HDPE cup to distribute the loads more evenly and to minimise cement deformation. The inner and outer surfaces became concentric allowing a reduction in overall thickness of the implant, to 5 – 6 mm thick. The acetabular component was reduced from 1 mm over hemispheric to 3 mm under a hemisphere and a section removed medially to reduce the risk of impingement and to allow for clearance of the psoas tendon.

X-ray templates for the components were used to determine the size of implant required. However, the authors found that the anterior-posterior dimension of the acetabulum was the constraining factor and not the supero-lateral infero-medial dimension which is visible on a standard frontal (AP) plane X-ray. The surgical approach used changed from trans-trochanteric to posterior. Simple aligning guides were used and acetabular and femoral reamers specific to the six component sizes were produced. The subchondral bone in the superior aspect of the acetabulum was considered to be of structural importance and therefore reamed as little as possible. Multiple drill holes were made for cement fixation and PMMA spacers used to ensure uniform thickness of cement and to prevent "bottoming-out". Trial components for both sides were used to check correct positioning in a trial reduction. The femoral component was placed in 5° of valgus relative to the neck and the acetabular component set at 45° to the vertical, with the anteversion as near anatomic as possible. Protection of the femoral head blood supply to prevent avascularity was considered of vital importance.

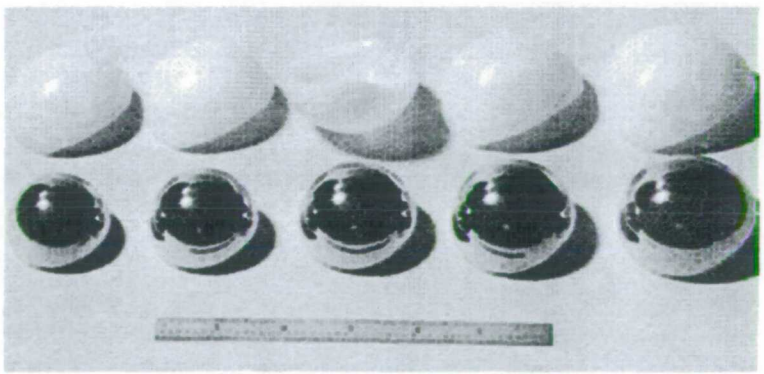

Figure 3.2.8 ICH resurfacing from Capello *et al.* (1982a).

Another Japanese double cup arthroplasty, first implanted in 1974, was designed by Seisuke Tanaka (1978), who wished to reduce the amount of bone cement used in order to decrease the number of complications involving hypotension, hypoxemia, alveolar bleeding and cardiac arrest. He was also concerned about fracture of the

femur and femoral component, loosening of the intramedullary stem, high rates of infection and the difficulty of removal and revision of THR. The over hemispherical femoral component was press-fit and made of stainless steel of 3 mm uniform thickness (Figure 3.2.9). It came in three sizes, with articulating surface diameters of 38 – 44 mm. On the acetabular side, the HDPE component surfaces, which were both hemispherical, were eccentric with a greater thickness of material in the supero-lateral weight bearing portion. The acetabular component had grooves for cement fixation and was available in four sizes. The surgical procedure was similar to that described by Aufranc (1962) and Harris (1967) for cup arthroplasty.

Figure 3.2.9 Tanaka resurfacing from Tanaka (1978).

The problem of revision of stemmed THR also concerned Heinz Wagner (Wagner, 1978). However he considered that the main difficulty with stemmed prostheses was stress shielding of the proximal femur which, through bone resorption, would lead inevitably to their failure. His resurfacing arthroplasty design (Figure 3.2.10) aimed to encase as little bone as possible to avoid avascular necrosis and to make the components as thin as possible for minimal bone removal. The femoral component was designed to be stiff and to load the femur in a physiological manner, with load transference by direct and not shear stresses at the implant bone interface. It was slightlyover-hemispherical,concentric and made from 3 mm thick Co-Cr-Mo alloy or alumina ceramic, with a polar hole for the expulsion of air, blood and excess cement during fixation. The concentric hemispherical acetabular component was made from 4 mm thick UHMWPE, making it compliant so that it would follow the deformations of the acetabulum during weight bearing. Radial and circumferential grooves were provided for cement fixation and a clearance gap of 0.1 mm between the articulating surfaces allowed ingress of joint fluid. The prosthesis was available in three sizes with articulating surface diameters of 42, 46 and 50 mm.

Wagner used an anterior approach and underlined the need for preservation of the retinacular vessels, particularly on the posterior surface of the femoral neck. The acetabulum was reamed to accept as large an implant as possible while preserving subchondral bone superiorly to prevent excessive reaming of the femoral head. The component was positioned at 45° to the vertical with 25° of anterversion. The acetabular component was cemented in place before reaming of the femoral head began, but trial femoral implants were used to check positioning.

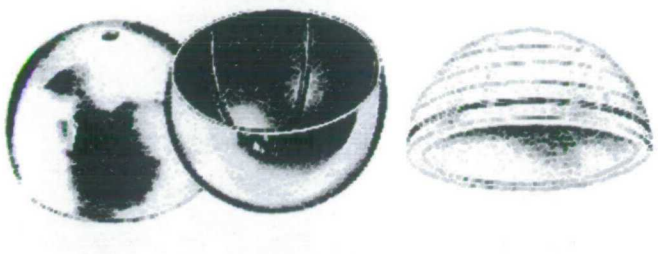

Figure 3.2.10 Wagner resurfacing from Aesculap sales brochure (1980).

The THARIES (Total Hip Articular Replacement by Internal Eccentric Shells) hip resurfacing arthroplasty, developed in UCLA by Harlan Amstutz *et al.*, was first implanted in 1975 (Amstutz *et al.*, 1978). Both femoral and acetabular components were eponymously eccentric, providing the thickest material (femoral 2.5 mm, acetabular 4 mm) on the supero-lateral aspect of the articulation (Figure 3.2.11). The UHMWPE acetabular component was 3 mm under a hemisphere and after 1981 had a Co-Cr backing, itself plasma-spray coated with Co-Cr beads. A trimmable rim was added to provide cement pressurisation and pre-polymerised PMMA spacers used on both acetabular and femoral sides to obtain uniform cement thickness. The design evolved further and a chamfered cylinder design fixed by bone ingrowth was later adopted (Amstutz *et al.*, 1988). The femoral component was over hemispheric and the eccentricity also provided more load bearing surface on the superior wall (used in abduction). The interior of the cast Co-Cr-Mo alloy cup was a chamfered cylinder, with broad cement fixation grooves in the top surface and around the periphery. There were six diameters of articulating surface ranging from 36 to 54 mm and several combinations of femoral and acetabular sizes available for each one.

The principle of the THARIES design was to resect nonviable bone while removing as little femoral head and neck as was consistent with fixation (Amstutz *et al.*, 1986), thus saving bone stock for anticipated revision or conversion to conventional hip arthroplasty. In some early cases the preservation of the femoral bone stock was at the

expense of excessive acetabular reaming. The procedure was intended for younger patients. Complex instrumentation was developed to obtain consistent and reproducible reaming of the femoral head. The designers advocated a small trochanteric osteotomy to provide optimal exposure and hypotensive anaesthesia to obtain a dry field for PMMA fixation. Reaming of the femoral head was performed before the resection of the dome of the head and an integral stop prevented damage to the neck Lavage of the prepared head and removal of subchondral cysts were considered important in ensuring bone viability and mechanical strength

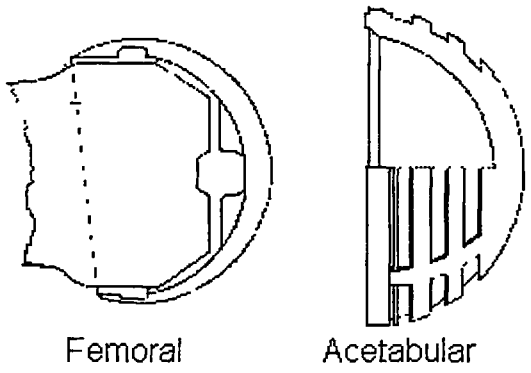

Figure 3.2.11 THARIES resurfacing (showing eccentricity of femoral component) from Zimmer sales brochure (1978).

A ceramic-on-ceramic resurfacing arthroplasty was introduced in 1976 by Salzer *et al* (1978) (Figure 3.2.12). No cement was used and fixation was achieved with the press fit of a conical prosthesis onto a tapered bone. The bone was then expected to grow into the grooves on the implants within a few weeks. The prosthesis was available in three sizes – external acetabular diameters of 60, 56 and 52 mm with corresponding femoral internal diameters of 39, 36 and 33 mm. The acetabular component had three fixation pegs and appears to have a hemispherical articulating surface. The femoral head was over hemispherical and had annular grooves on the tapered cylindrical interior. The pegs of the acetabular component located in holes drilled in the reamed acetabulum. The femoral head was shaped to a tapered cylinder and the femoral component twisted down onto it.

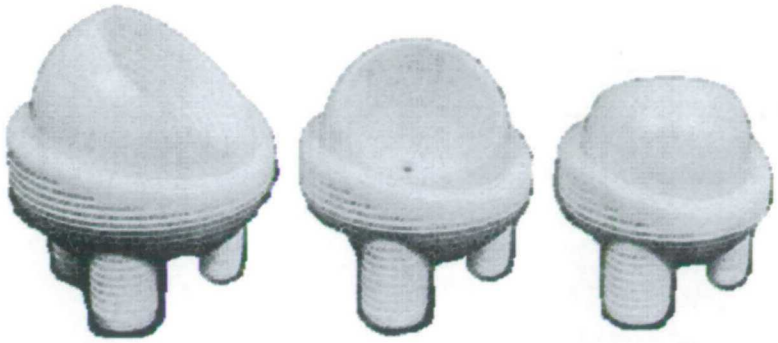

Figure 3.2.12 Salzer alumina on alumina resurfacing from Salzer *et al.* (1978).

Even by the mid 1970's it was obvious that the clinical outcomes of resurfacing were not fulfilling their designers' high expectations. Fewer and fewer were implanted and no new designs appeared until the 1990's. Improvements in metals machining technology and new surface treatments as well as technical advances in the operating theatre have brought about a resurgence of interest in the concept.

3.3 Modern Design of Resurfacing Arthroplasties 1990 - 2000

Although the Beuchel-Pappas resurfacing implant has been used in several centres since 1991, there have been no reports in the literature of its design and few of its implantation. The prosthesis is part of a system of hip replacements comprising conventional stemmed THR, bipolar implants as well as resurfacing replacements. The resurfacing has a TiN coated Ti alloy femoral component with a porous coating internally and a short central stem Figure 3.3.1. The PVD TiN coating is said to reduce UHMWPE wear and eliminate metallic wear debris (Endotec data sheet, 1990). The femoral component is 1 mm thick, has an internal porous coat and is a press fit. The acetabular component has a 1 mm thick Ti alloy backing with porous coating and a 3 mm thick UHMWPE lining. The contour of the edge mimics that of the normal acetabular rim, with a medial cut out and "anatomical" flares. The backing has holes for screw fixation. The acetabular component is positioned at 30° to the vertical and with variable anteversion. Trial components are used for component fit, but not for trial reductions. The prosthesis is available in 11 sizes with articulating surface diameters ranging from 36.5 mm to 52.5 mm.

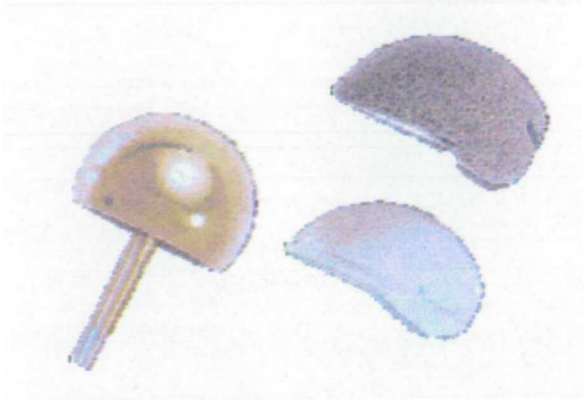

Figure 3.3.1 Beuchel-Pappas resurfacing from Endotec sales brochure (1990).

Interest in metal-on-metal resurfacing was renewed in 1991 with the implantation of two designs – those of Wagner and Wagner (1996) and McMinn *et al.* (1996). The new Wagner prosthesis sought to reduce the amount of wear debris produced by replacing the UHMWPE articulating surface with metal. The resurfacing has a bilayer design, using rough blasted Ti for osseointegration on the fixation surfaces and forged Co-Cr-Mo for the articulating surfaces (Figure 3.3.2). There are sharp radial and annular fins on the acetabular component to resist rotation and tilting with a central peg for positioning. Initial stability is provided by a snap fastener mechanism and may be supplemented with two peripheral pins. The internal and external surfaces are apparently concentric, but the articulating surface is considerably less than a hemisphere. The femoral component has an articulating surface only slightly over hemispherical and fixation surface appears to be hemispherical. A threaded screw-on design was abandoned after difficulties with insertion. The implant has four sizes of articulating surface ranging from 38 to 50 mm in diameter.

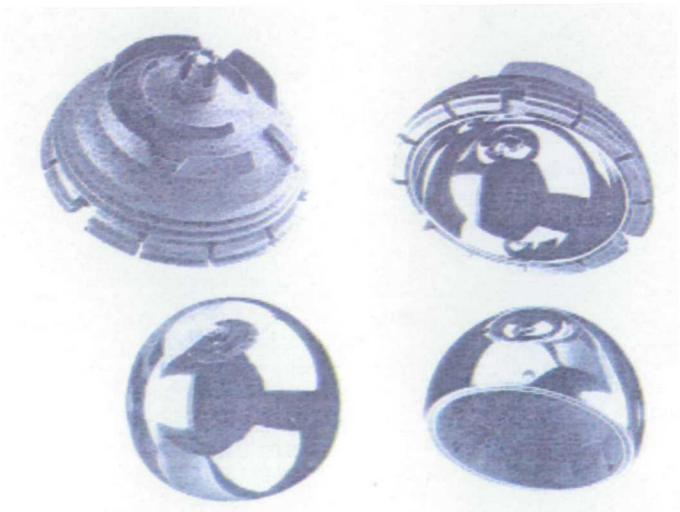

Figure 3.3.2 Wagner metal-on-metal resurfacing from Wagner and Wagner (1996).

The McMinn prosthesis underwent several changes in fixation from its first implantation in 1991 up to the finalised hybrid design of 1994. Thin components, low wear debris production and the use of materials with a proven clinical history were considered to be essential to the design. Surgical technique and instrumentation were developed alongside the design to prevent femoral neck notching and varus placement of the femoral component. The Co-Cr alloy and its casting and treatment were as similar as possible to the alloy used in the Ring prosthesis, which has a 60% survival rate at 21 years (Bryant *et al.*, 1991).

The first design was press fit on both acetabular and femoral sides, with supero-lateral fins on the acetabular component for axial and rotational stability (Figure 3.3.3). This design was modified with an hydroxyapatite (HA) coating on both sides, but then the fixation method was changed to cement and the fins and peg on the acetabular component fixation surface were removed. The final design uses cement on the femoral side and HA coating on the acetabular side and peripheral splines for rotational stability. The femoral component articulating surface is 2/3 of a sphere and the fixation surface is a flat-topped, chamfered cylinder. A short, central stem ensures correct alignment and bridges the head/neck junction. Unusually the acetabular component has an ellipsoid fixation surface, being of a slightly larger radius at its geometrical equator than at its pole. This gives a tight peripheral jam fit in the hemispherically reamed acetabulum and the central peg locates in a drill hole. The articulating surface subtends 160°, allowing a good range of motion before impingement.

There are now two resurfacings which share the McMinn pedigree. The main difference is that the Birmingham Hip Resurfacing (BHR) uses cast Co-Cr identical to that in the Ring prosthesis while the Cormet 2000 uses cast Co-Cr which has been heat treated. The femoral components remain identical in shape, but the acetabular components differ substantially. The Cormet 2000 retains the ellipsoidal fixation surface and central peg of the McMinn, but the BHR has abandoned the peg and returned the outer shape of the component to hemispherical. The BHR also uses a novel method of introduction and impaction into the acetabulum.

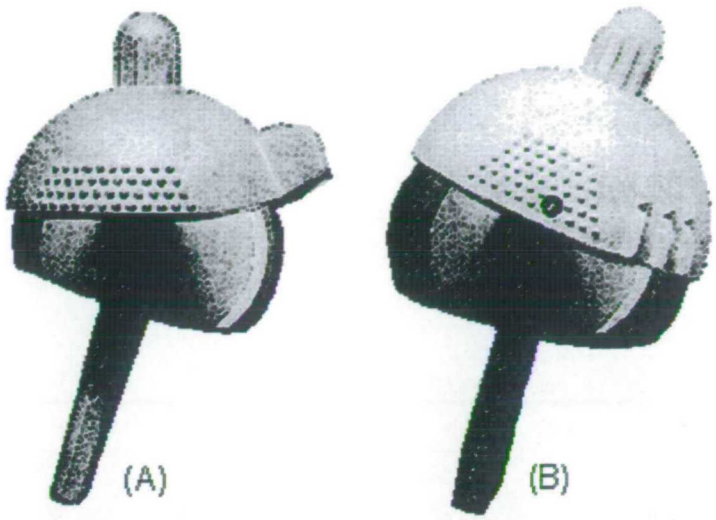

Figure 3.3.3 McMinn metal-on-metal resurfacing showing early finned design (A) and current hybrid design (B) from McMinn (1996).

Amstutz *et al.* (1998a) began trials of a metal-on-metal resurfacing device in 1996, following a short pilot series with McMinn and new Wagner devices. The new Amstutz resurfacing, "Conserve plus" (Figure 3.3.4), has bone ingrowth fixation on the acetabular side and is designed for an initial interference fit. The cemented femoral component is identical to the THARIES chamfered cylinder design except for a short central stem and improved sphericity and surface finish. The resurfacing is designed to minimise wear and optimise fixation. Amstutz hypothesises that the metallic wear debris produced by a metal-on-metal articulation is better tolerated by peri-prosthetic tissues than PE debris. The designers prefer a posterior approach, but it is suggested that the best exposure is the one the surgeon knows best. A trochanteric osteotomy is suggested only for use in heavy patients or those with severely contracted hips.

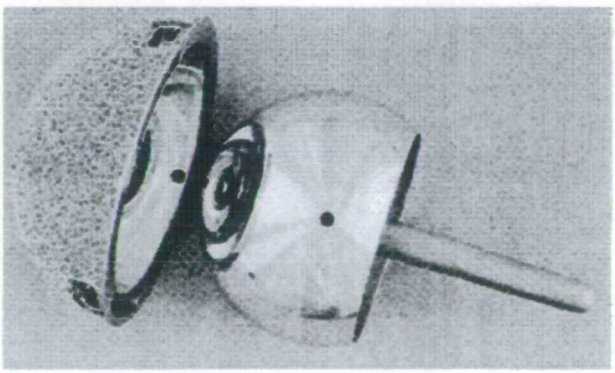

Figure 3.3.4 Conserve Plus metal-on-metal resurfacing from Amstutz *et al.* (1998b).

The details of shape, materials, fixation and thickness of the designs reported in this chapter are summarised in Table 3.3.1.

Table 3.3.1 Designs of resurfacings (see text for references). Abbreviations: w/o is without, s/l is supero-lateral.

	Femoral Component						Acetabular Component							
Implant version	*External shape*	*Internal shape*	*Materials*	*Fixation*	*Features*	*Thickness*	*External shape*	*Internal shape*	*Materials*	*Fixation*	*Features*	*Thickness*	*No. of sizes*	*Comment*
Beuchel-Pappas 1990	over hemi-spheric	hemi-spheric	Ti , TiN coating	porous ingrowth	short stem - 5cm	max 3mm	hemi-sphere with lugs and cut away	hemi-sphere (mimic acetab shape)	UHMWPE liner in Ti with TiN coat shell	porous ingrowth	anatomic shape, snap fit liner	PE 1-3mm, Ti 1mm	11 femoral	compatible with other Endotec hips
Conserve Plus 1998	over hemi-spheric	chamfered cylinder	Co-Cr	cemented	short stem		under hemi-spheric	subtends 170°	Co-Cr	porous ingrowth			2 mm incre-ments	
Furuya 1971	over hemi-spheric		HDPE	press fit			hemisphere + flanges	hemisphere	stainless steel	cemented			3 sizes	other designs w/o outcomes
Gerard 1970	over hemi-spheric	cylinder capped with hemi-sphere	Co-Cr	press fit	Luck cup with skirt	? 3mm	smooth, over hemi-spheric	concentric	Co-Cr	free to move against acetabulum	Aufranc cup	? 3mm	4 sizes	motion at two sites to prevent protrusio
Gerard 1972	over hemi-spheric	cylinder capped with hemi-sphere	Co-Cr	press fit	Luck cup with skirt	? 3mm	smooth, over hemi-spheric	concentric	PE	free to move against acetabulum	Aufranc cup	? 3mm		massive PE/ bone wear
Gerard 1975	over hemi-spheric	cylinder capped with hemi-sphere	Co-Cr	press fit	skirt now 4mm long	? 3mm	smooth, over hemi-spheric	concentric	Co-Cr with PE liner	free to move against acetabulum	shape avoids entrap-ment	liner 4.5mm thick		no cement
ICH 1973, (ICH 1975)	over hemi-spheric	hemi-spheric	Co-Cr	cemented	small central stud	? 3mm, (1.5mm)	1mm over hemi-spheric	hemi-spheric with medial cut out	UHMWPE	cemented		? 6mm	5 sizes	
ICH 1981	over hemi-spheric	hemi-spheric	Co-Cr + beaded coat	cemented	small central stud	1.5mm	3mm under hemi-spheric	hemi-spheric with medial cut out	UHMWPE liner with Ti backing	cemented		5-6mm	6 sizes	early design w/o metal back
ICI H 1972	over hemi-spheric	cylindrical	PE	cemented		not stated, no picture	hemi-spherical	hemi-spherical	stainless steel	cemented (2mm layer)		not stated	not stated	

	Femoral Component						Acetabular Component							
Implant version	*External shape*	*Internal shape*	*Materials*	*Fixation*	*Features*	*Thickness*	*External shape*	*Internal shape*	*Materials*	*Fixation*	*Features*	*Thickness*	*No. of sizes*	*Comment*
ICLH 1974	over hemi-spheric	flat-topped cylinder	Co-Cr	cemented		max 10.5 mm, min 3 mm	hemi-spherical	subtends 168 °	HDPE	cemented	annular grooves	max 6.5 mm, min 4mm	3 sizes	
ICLH 1980	over hemi-spheric	flat-topped cylinder	Co-Cr, ceramic (very few)	cemented		unchanged	under hemi-spherical	subtends 140 °	HDPE	interference fit	3 pegs	max 10 mm	3 sizes	
McMinn 1991	over hemi-spheric	chamfered cylinder	Co-Cr-Mo (as Ring)	press fit	stem	smallest size 6mm	?hemi-spherical	?subtends 140 °	Co-Cr-Mo (as Ring)	interference fit	s/l fins, central peg	4mm		acetab based on Freeman SLF cup
McMinn 1992 #1	over hemi-spheric	chamfered cylinder	Co-Cr-Mo (as Ring)	press fit + HA coat	stem		?hemi-spherical	?subtends 140 °	Co-Cr-Mo (as Ring)	interference fit + HA coat	s/l fins, central peg			acetab based on Freeman SLF cup
McMinn 1992 #2	over hemi-spheric	chamfered cylinder	Co-Cr-Mo (as Ring)	cemented	stem		?hemi-spherical	?subtends 140 °	Co-Cr-Mo (as Ring)	cemented	shallow keying pits			
McMinn 1994	over hemi-spheric	chamfered cylinder	Co-Cr-Mo (as Ring)	cemented	stem 64-70mm	min 3.75 mm, max 8mm +/- 2mm	hemi-ellipsoidal	subtends 160 °	Co-Cr-Mo (as Ring)	interference fit + HA coat	central peg + peripheral splines		4 sizes	acetab peripheral jam fit
B'ham Hip Re-surfacing	over hemi-spheric	chamfered cylinder	Co-Cr-Mo (as Ring)	cemented	stem 64-70mm					porous ingrowth + HA				
Cormet 2000	over hemi-spheric	chamfered cylinder	Co-Cr-Mo (HIP + soln treated)	cemented	stem 64-70mm		hemi-ellipsoidal	subtends 160 °	Co-Cr-Mo (HIP + soln treated)					
Nishio 1972	over hemi-spheric	uniform thickness	metal	press fit	skirt at opening	?2mm	hemi-spherical	hemi-spherical	metal	cementless, 3 screws		?3mm	not stated	
Nishio 1975	over hemi-spheric	uniform thickness	metal	press fit	skirt at opening	?2mm	hemi-spherical	hemi-spherical	metal + PE liner	cementless, 3 screws		?6mm	not stated	
Paltrinieri -Trentani 1971	2 3 spherical + 4mm skirt	uniform thickness + fixation groove	18/8 stainless steel	cement		1mm	hemi-spherical	hemi-spherical	RCH 1000 HDPE	cemented	2mm deep circular grooves	4mm	not stated	

	Femoral Component						Acetabular Component							
Implant version	*External shape*	*Internal shape*	*Materials*	*Fixation*	*Features*	*Thickness*	*External shape*	*Internal shape*	*Materials*	*Fixation*	*Features*	*Thickness*	*No of sizes*	*Comment*
Salzer 1976	over hemi-spheric	conical	Alumina (Rosenthal Technik)	screw on	fixation grooves	?5mm	hemi-spherical	hemi-spherical	alumina (Rosen-thal Technik)	interferenc e fit of pegs	3 large fixation pegs	?5mm - total implant is 10mm	3 sizes	
Tanaka 1974	over hemi-spheric	uniform thickness	Stainless steel	press fit	concentric	2mm	hemi-spherical	hemi-spherical	HDPE	cemented	eccentric	laterally 9mm, medially 4mm	4 acetab, 3 femoral	acetab reamed deep
TARA 1977	over hemi-spheric	cylinder, thick at pole	Co-Cr-Mo OR ceramic (1995)	cemented	valgus curved stem (long)	max 11mm	brimmed hemi-sphere		HDPE	cemented + screw	blood lubrication holes, eccentric	not stated	8 matched	
THARIES 1975	over hemi-spheric	flattened sphere - cross fixation groove	Co-Cr-Mo cast	cemented	eccentric	max 2mm	grooved and ribbed	1mm over hemi-spheric	HDPE	Cemented	Trimmable rim, eccentric	max 4mm	7 femoral, each fits 3 acetab	
THARIES 1981	over hemi-spheric	flattened sphere - cross fixation groove	Co-Cr-Mo cast	cemented	eccentric	max 2mm	plasma sprayed Co-Cr-Mo beads	3mm under hemi-spheric	UHMWPE + Co-Cr-Mo backing	Cemented	Trimmable rim, eccentric	max 4mm	8 femoral, each fits 3 acetab	
Wagner 1968	over hemi-spheric	roughened, constant thickness	Co-Cr-Mo cast OR Alumina	cemented	hole for extrusion of excess cement	3mm	hemi-sphere	hemi-sphere	HDPE	Cemented	Fixation grooves	4mm	4 or 5 sizes	
Wagner 1996 design A	over hemi-spheric	chamfered cylinder (?)	Co-Cr-Mo + Ti bilayer	ingrowth - roughened Ti	screw thread for 1o fixation	?	under hemi-spherical	under hemi-spherical	Co-Cr-Mo + Ti bilayer	Ingrowth – roughened Ti	Anti-rotation fins	?	4 sizes	
Wagner 1996 design B	over hemi-spheric	chamfered cylinder (?)	Co-Cr-Mo + Ti bilayer	ingrowth - roughened Ti	press fit	?	under hemi-spherical	under hemi-spherical	Co-Cr-Mo + Ti bilayer	ingrowth - roughened Ti	Anti-rotation fins	?	4 sizes	

3.4 Outcomes of Resurfacing

Comparing the outcomes of different implants is difficult even with good data and well-defined outcome criteria. Long term follow-ups of large groups of patients are required to provide reliable comparisons between prostheses: according to Malchau *et al.* (1993) 19,180 patients in a five year study would be needed for an 80% power comparison between the Charnley and the C.A.D. prostheses. Although the outcomes of resurfacings differ more than the outcomes of those two implants studies with similar orders of magnitude of patient numbers and follow-up times would be required to achieve the same power. A further issue in assessing resurfacing outcomes is the quality of the data reported.

In order for a report to be comparable with the rest of the literature it must include certain basic information. The group of hips followed must be well defined and any exclusions justified. The age, aetiology and sex distributions in the followed groups should be reported. Accurate matching of patient groups is required to reduce the possibility of differences in populations obscuring the effects of different implant designs. The details of the implant design should also be clear: what materials and what forms of fixation are used. The operating technique and level of experience of the implanting surgeons have a strong effect on outcome thus should also be reported.

The best measure for comparison is survivorship. This is a statistical analysis that predicts the probability of a prosthesis being in place at any given time after implantation. Many of the resurfacing designs listed above have been reported once only and data have often been presented either in misleading or incomplete forms. Without the full original data set it is impossible to carry out survivorship analysis. Therefore this study utilises reported rates of revision (calculated from numbers of revisions at mean follow-up times) and reported modes of failure as parameters for comparison.

Inaccuracy in this study may arise from many causes. The rate of revision may be expected to increase with time after implantation. The parameter used here for comparison, the revision rate at one mean time after operation, is therefore not strictly characteristic of an implant. Patient demographics and indications vary and the effect of this relative to that of implant design is unknown. Designs and indications may be changed in mid-series. Other errors arise from the overlap of patient groups between

consecutive reports and from incomplete recording of data (including losses to follow-up and deaths). Some patient groups have been reported twice or three times at the same mean follow-up. Obvious repetitions have been eliminated. Some resurfacing revisions have been recorded without modes of failure; these lead to further loss of reliability in comparison. The remainder of this section will present graphs of the failure modes and rates of revision and a brief analysis of follow-up reports. Some resurfacings have been omitted from detailed numerical comparison because of insufficient data.

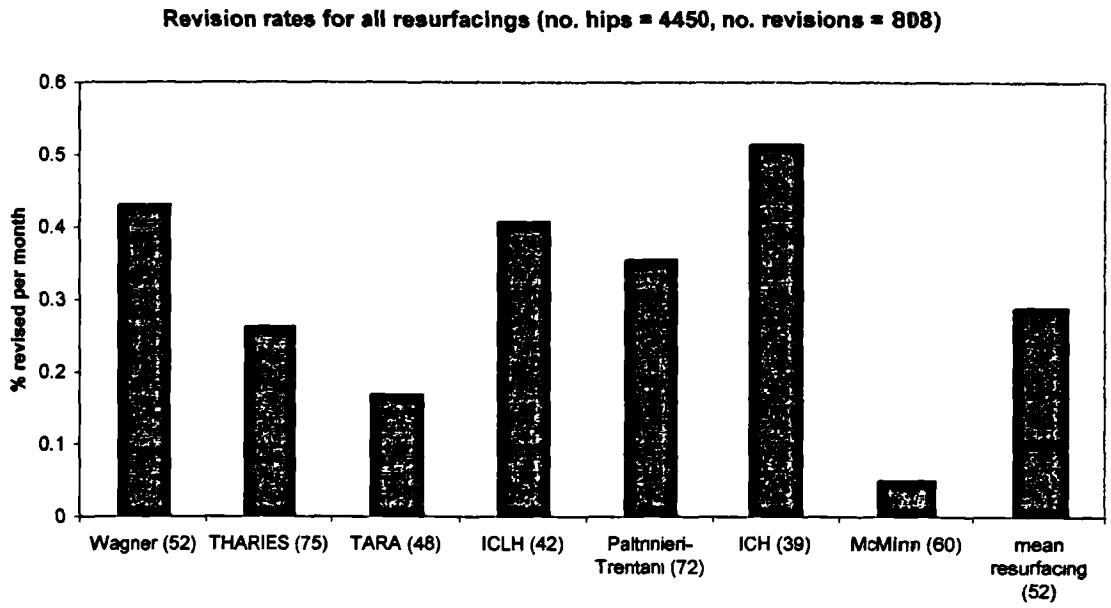

Figure 3.4.1 Failure rates (% revised per month) for selected resurfacings. Mean follow-up times (months) for each resurfacing in brackets.

Figure 3.4.1 compares the revision rates of different designs of resurfacing. Comment will be made on the relative performances in the more detailed discussions below. However it is worth noting that a 95% survival rate at 10 years is equivalent to a mean revision rate of 0.042 % per month.

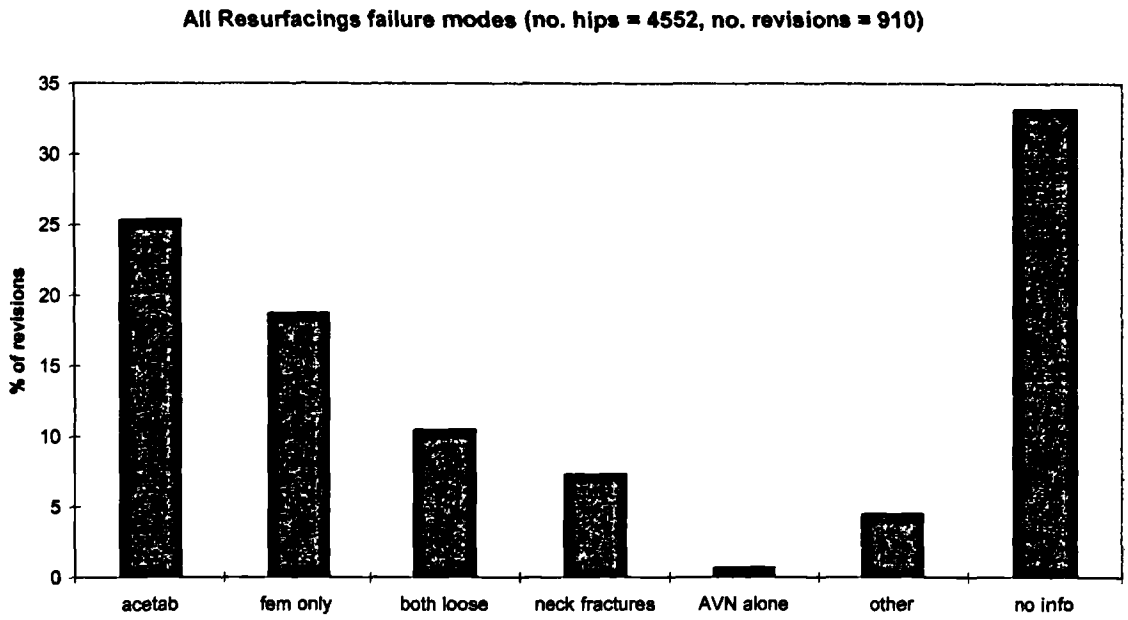

Figure 3.4.2 Failure modes for selected resurfacing designs: acetab is acetabular loosening only; fem only is femoral loosening only; both loose is both acetabular and femoral loosening; neck fracture includes that complicated by necrosis; AVN alone is avascular necrosis with no other complication and other is other failures including sepsis and component fracture.

Figure 3.4.2 shows the modes of failure of all resurfacings included in the analysis below. The distinction between necrosis occurring as a result of neck fracture and fracture caused by necrosis is difficult to make, so these groups were combined. The size of the group of hips for which no mode of failure information was recorded (no info) reduces the validity of the following discussion which can only consider reported failures.

It is interesting that avascular necrosis and neck fractures together are less important than other modes of failure. Following Charnley (1961), one of the main arguments against resurfacing has been that enclosing the femoral head will provoke necrosis. In intact hips the femoral head is prone to necrosis as a result of its largely distal blood supply. The predominant recorded cause for revision is acetabular loosening. Unfortunately the uncertainty produced by unreported reasons for revision is too large to make a more general statement.

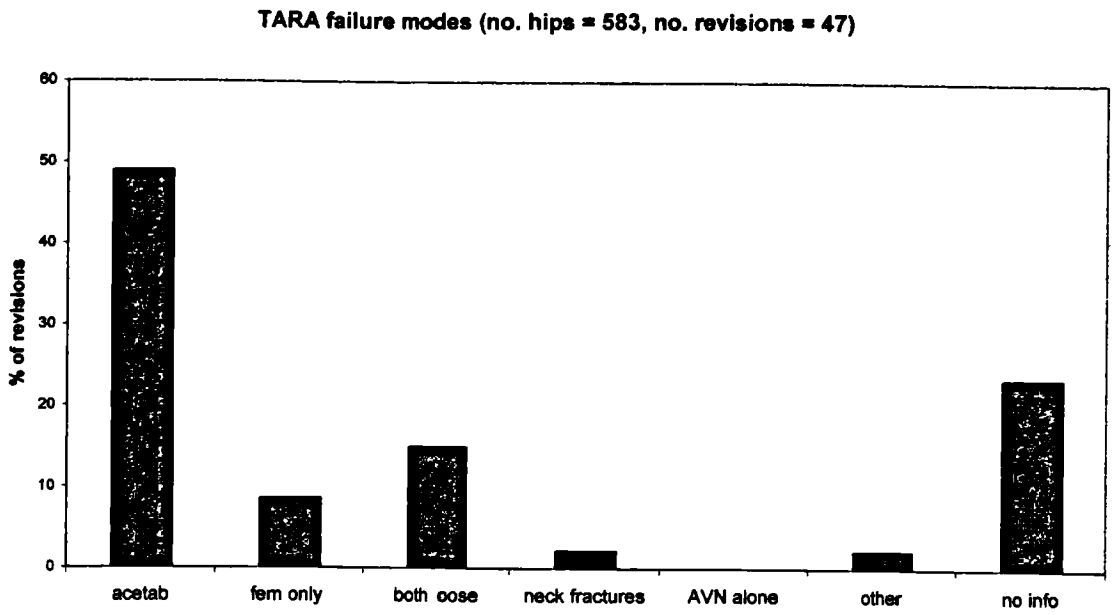

Figure 3.4.3 Failure modes for the TARA resurfacing. Data from Townley, 1982; Head, 1984; Mallory *et al.*, 1984; de Waal Malefijt and Huiskes, 1993; Mesko *et al.*, 1994.

The mean age of patients implanted with the TARA prosthesis was 55 years and the revision rate at the mean follow-up time of 48 months was 0.17 % per month. Risk factors reported for early loosening were male gender, lower age and poor placement of the acetabular component resulting in neck impingement. Figure 3.4.3 shows acetabular loosening was the major problem. Delays in bringing patients in for revision operations led to osteolytic enlargement of the acetabulum. These problems may be linked with the thinness of the acetabular component. The instruction in the original report to drill holes through the component so that blood would lubricate the articulating surface seems to have been wisely ignored. The long curved stem seems to have reduced the rate of neck fractures compared with other resurfacings.

There were insufficient data on the Gerard double cup (Gerard, 1978; van Raay *et al.*, 1993) to make any revision rate comparisons. The first version of this implant demonstrated the folly of an HDPE-bone articulation which lead to rapid wear. Varus placement of the femoral component was considered to produce rapid resorption of the femoral head. Some implants were revised for acetabular protrusion. Defective attachment of the HDPE liner to the acetabular cup was blamed for the initial high rate of failure. Longer term follow-up (van Raay *et al.*, 1993) linked the design with high wear rates and impingement leading to massive femoral head bone resorption and necrosis.

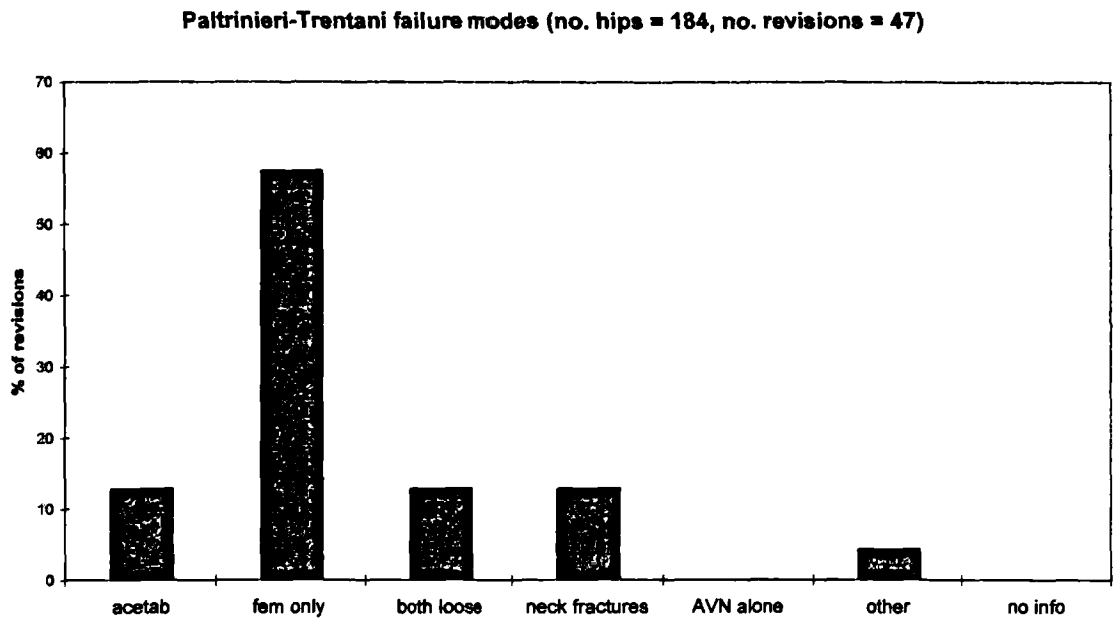

Figure 3.4.4 Failure modes for the Paltrinieri - Trentani resurfacing. Data from Trentani and Vaccarino, 1978; Trentani and Vaccarino, 1981a; Trentani and Vaccarino, 1981b; Trentani and Vaccarino, 1982.

Although the Paltrinieri-Trentani resurfacing is shown to have a high revision rate (0.35 % per month) in Figure 3.4.1 this is offset in comparison with other resurfacings by the long mean follow-up time of 72 months. However the mean age of patients is 56, which is comparatively high. The high rate of femoral loosening shown by Figure 3.4.4 should not be attributed to necrosis. Revised heads were demonstrated to be viable by pre-operative injection of tetracycline and examination under UV light (Trentani and Vaccarino, 1978). An initial varus tilt was thought to be a risk factor for early loosening. Loosening of the femoral component was associated with an increasing tilt to varus and progressive damage to the bone of the head and neck. This was resorbed and replaced with fibrous tissue. The assertion that the skirt of the femoral component provided beneficial "stress shielding of the head neck junction" appears to be contradicted by the high rate of femoral and neck fracture failures.

The size of the patient group implanted with Furuya resurfacings (13 hips) is too small for any firm conclusions. However it is significant that 6 of the 7 failures were due to acetabular loosening. This may be connected with the author's emphasis on reaming the acetabulum "as deeply as possible" to prevent loosening (Furuya *et al.*, 1978)

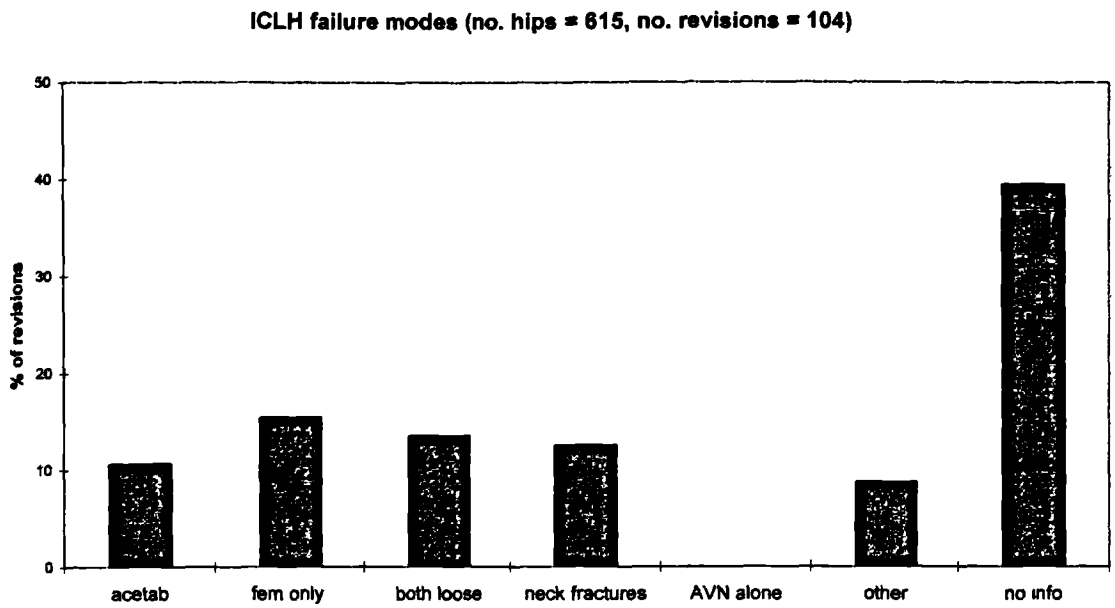

Figure 3.4.5 Failure modes for the ICLH resurfacing. Data from Freeman *et al.*, 1975; Freeman and Brown, 1978; Freeman *et al.*, 1978; Freeman and Bradley 1981; Freeman and Bradley 1982; Jolley *et al.*, 1982; Murray and Meter, 1982; Bradley and Freeman, 1983; Freeman and Bradley, 1983; Herberts *et al.*, 1983; Reigstad 1986; Bradley *et al.*, 1987; Cotella *et al.*, 1990.

Early results of the first ICLH implants demonstrated the inadvisability of using a soft material as the convex component of the bearing pair. The surprisingly high rate of neck fractures shown in Figure 3.4.5 may be due in part to the use of trochanteric osteotomy. However this technique was discontinued early in the experience with the implant (Freeman *et al.*, 1978). Other authors (Jolley *et al.*, 1982) suggest that the femoral component was difficult to position correctly in the recommended valgus angle and scoring of the femoral neck frequently occurred. The question of necrosis has been studied (Bradley *et al.*, 1987; Cotella *et al.*, 1990), but histological examination failed to prove that wide scale bone death in the femoral head occurred as a primary event following resurfacing. Impingement caused loosening of the acetabular cup where it protruded superiorly beyond the bony rim of the acetabulum. As a result of this observation the acetabular component was reduced from hemispherical.

Thin HDPE and thin acetabular cement produced stress concentrations and consequently more wear debris. ICLH revision material was included in the study by Kobayashi *et al.* (1997b) of wear particulate levels in tissue around loosened implants. No differences in particle size or morphology were seen between ICLH and Charnley debris (Yamac, 1999). While particle number densities were similar, the ICLH hips

had come to revision earlier. The mean follow-up of 42 months and mean age of 56 years and the high revision rate (0.41 % per month) suggest that the ICLH implant did not perform well in comparison with other resurfacings.

The Nishio resurfacing (Nishio *et al.*, 1978) frequently changed design. 67 hips were reported with a mean follow-up of 36 months. Three hips had been revised, two for acetabular loosening and one for varus tilting of the femoral component.

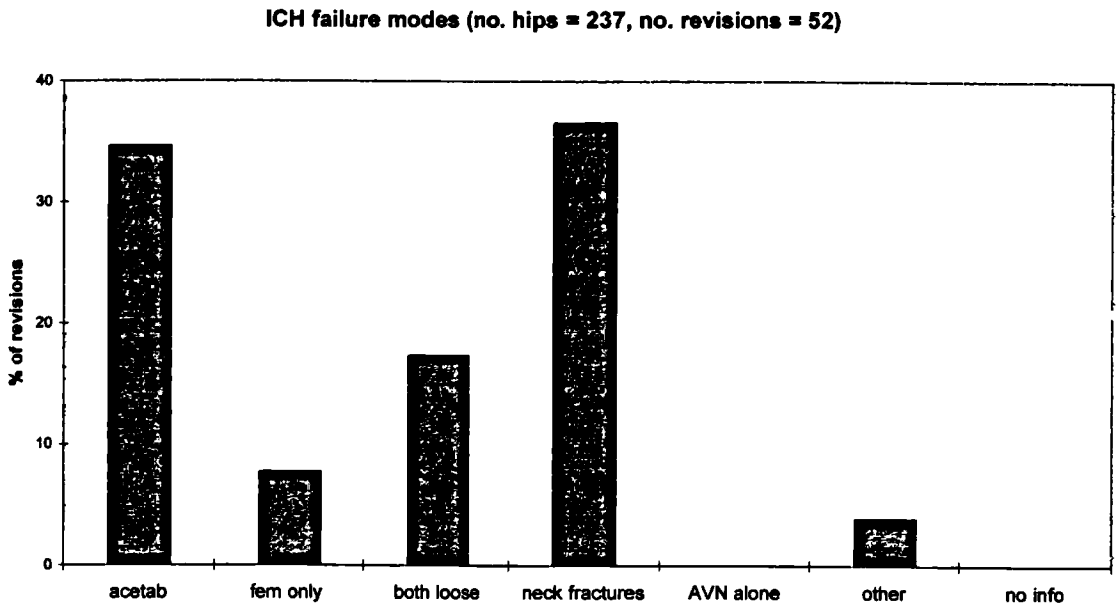

Figure 3.4.6 Failure modes for the ICH resurfacing. Data from Capello *et al.*, 1978; Capello and Trancik, 1981; Bogoch *et al.*, 1982; Capello *et al.*, 1982a; Capello *et al.*, 1982b; Murray and Meter, 1982; Capello *et al.*, 1984; Ritter and Gioe, 1986.

The ICH resurfacing shows the highest revision rate (0.51 % per month) for the shortest mean follow-up times (39 months). The mean age of ICH patients was 52 and neck fractures were the prevalent mode of failure (Figure 3.4.6). Initial reports (Capello *et al.*, 1978) suggested that this was due to stress concentrations caused by operative scoring and the shape of the component at the implant - femoral neck junction. An abductor limp was suspected to aggravate these stress concentrations. Many of these neck fractures were accompanied by necrosis of the femoral head. The lack of signs of a biological inflammatory response in the tissue of three heads was held to show necrosis as a primary event after resurfacing (Bogoch *et al.*, 1982).

Metal backing of the acetabular socket was introduced (Capello and Trancik, 1981), but acetabular loosening remained the chief concern (Capello *et al.*, 1984). The complete coverage of the acetabular component and medially rather than superiorly

directed reaming to preserve subchondral bone were advocated to reduce acetabular loosening. Large head-to-neck ratios were associated with faster loosening. This was presumably related to the correspondingly greater amount of reaming for large acetabular components. The risk of impingement is lowered with increasing head-neck ratio. The last report (Ritter and Gioe, 1986) recorded that the ease of femoral revision was outweighed by the difficulty of revising an enlarged acetabulum with poor bone quality.

Tanaka (1978) reported only 37 hips, none of which had been revised at a mean follow-up of 2 years. He did not cement the femoral side believing that the heat of polymerisation was a major cause of necrosis. Deep reaming of the acetabulum to accommodate the large components was advocated.

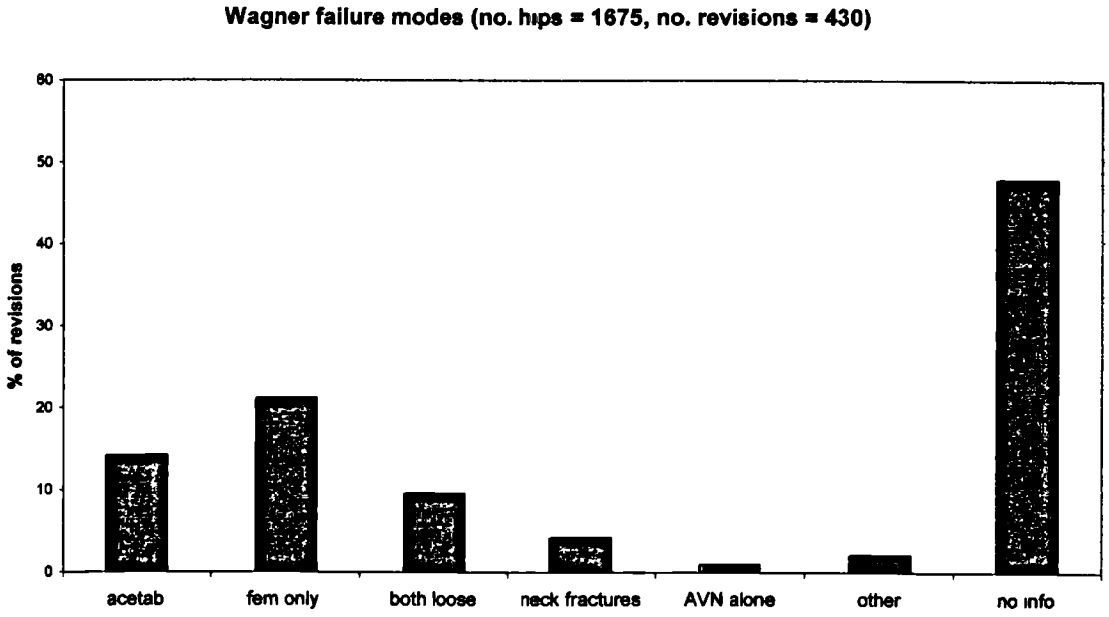

Figure 3.4.7 Failure modes for the Wagner resurfacing. Data from Wagner, 1978; Head, 1981a; Head, 1981b; Wagner, 1981; Boettcher *et al.*, 1982; Capello 1982b; Grujic *et al.*, 1982; Head, 1982; Bell *et al.*, 1985; Strens, 1986; Abrahamsson *et al.*, 1987; Arajärvi and Santavirta, 1987; Ahnfelt *et al.*, 1990; Howie *et al.*, 1990a; Howie *et al.*, 1990b; Wiadrowski *et al.*, 1991; Howie *et al.*, 1992; Franzén *et al.*, 1993; Howie *et al.*, 1993.

The high failure rate (0.43 % per month) and mean follow-up time of 52 months make the Wagner implant less successful than the average resurfacing. However the mean age of the patients was 47, which may account for this poorer performance. The reason for the very high number of unrecorded modes of failure is the inclusion of data from the Swedish hip register (Ahnfelt *et al.*, 1990).

The high levels of femoral failure (Figure 3.4.7) sparked a debate over AVN. Trochanteric osteotomy and the spherical internal shape of the femoral component were implicated as risk factors in a comparison study with TARA (Head, 1981). However AVN as a primary event was concluded not to be a likely outcome of resurfacing (Howie *et al.,* 1993). Necrosis did occur at the bone-cement interface, caused by abrasion and local circulation interference, but this was not to be confused with extensive AVN. However a recent communication (Furlong, 1998) compared Wagner resurfacing with traumatic dislocation of the hip which is prone to necrosis even following successful reduction.

The valgus placement advocated by Wagner was suspected of causing neck fracture due to the notching of the superior lateral neck cortex (Boettcher *et al.,* 1982). However two researchers found no difference between varus and valgus angle in susceptibility to loosening (Grujic *et al.,* 1982; Abrahamsson *et al.,* 1987). Boettcher also reported the severe weakening of the acetabulum by over-reaming and the difficulty of acetabular revision caused by loss of bone stock. High acetabular failure rates have been linked with the thinness of the HDPE component which increased peak stresses in the component itself and in the cement-bone interface (Bell *et al.,* 1985). This lead to PMMA fracture and large quantities of wear debris. The metal backing of the acetabular component was shown to improve the survival of the Wagner implant (Franzén *et al.,* 1993). The role of impingement between the femoral neck and the periphery of the acetabular component has been assessed (Wiadrowski *et al.,* 1991). Impingement can cause failure through shear stresses at the bone-implant interface and also by massive PE wear. 92 out of 109 revised Wagner implants showed evidence of impingement, with similar wear patterns in well-fixed and loose components suggesting impingement was a cause rather than an effect of loosening. PE wear debris was found more than 20 mm from well fixed Wagner femoral component interfaces (Howie *et al.,* 1990b) and bone resorption was seen to occur before macroscopic loosening.

Follow-up analysis and two dimensional finite element models of the resurfaced femur were combined by Strens (1986). He suggested that the thin flexible acetabular component and thin bone cement set up tensile stresses at the cement-bone interface, leading to micro-motion and loosening. The stress distibution in the proximal resurfaced femur was not physiological, with concentrations at the rim and shielding

of the centre. He introduced the concept of secondary stability to describe the progression of micromotion after initial interface loosening. Poor secondary stability was in his view integral to the resurfacing concept. This sensitivity to interface loosening rather than a higher initial incidence of loosening was held to account for the poor performance of resurfacing in comparison with conventional THR (Huiskes *et al.*, 1990). The varus tilting mechanism of femoral loosening was also modelled, showing the likely failure of the cement-bone interface in tension or shear. Once the cement-bone interface fails bone loss can proceed rapidly through micro-motion and fluid pumping.

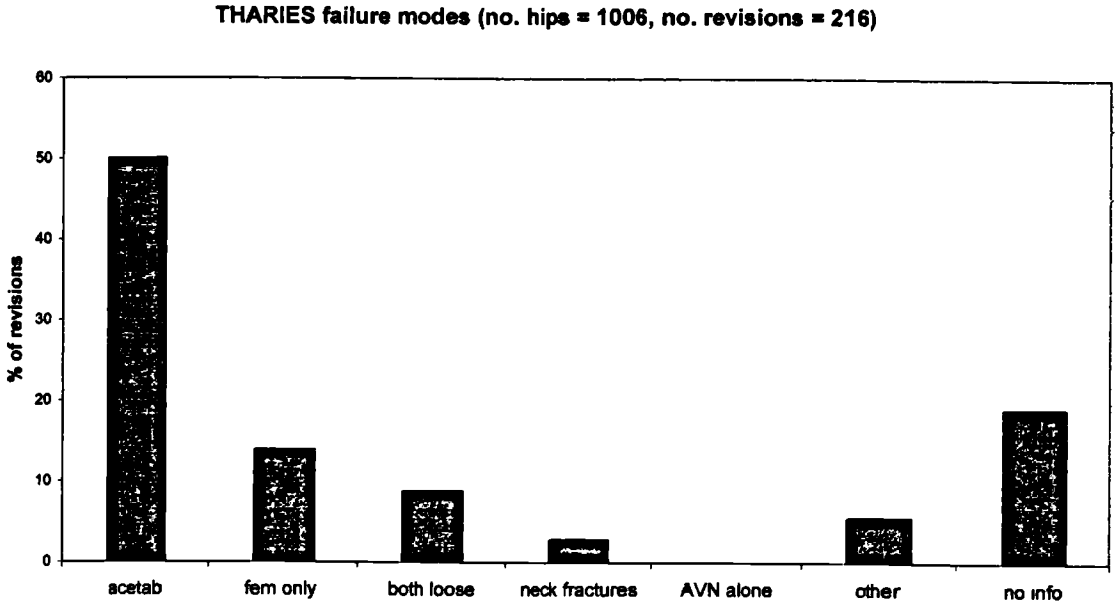

Figure 3.4.8 Failure modes for the THARIES resurfacing. Data from Amstutz *et al.*, 1978; Amstutz *et al.*, 1981a; Amstutz *et al.*, 1981b; Bassett *et al.*, 1982; Boettcher *et al.*, 1982; Jolley *et al.*, 1982; Murray and Meter, 1982; Amstutz, 1983; Ma *et al.*, 1983; Amstutz *et al.*, 1984; Amstutz *et al.*, 1986; Kim *et al.*, 1987; Mai *et al.*, 1996.

The combination of a mean age of 50 years, a mean follow-up 75 months and a relatively low revision rate (0.26 % per month) make THARIES one of the most successful early resurfacings. The main cause of revisions has been acetabular loosening (Figure 3.4.8). The number of hips with no record of their mode of failure is small.

The early THARIES aim of minimal femoral reaming (Amstutz *et al.*, 1978) was soon altered to conserve acetabular bone. The first failures were due to incomplete coverage of the acetabular component and its impingement on the femoral neck. Poor femoral positioning and poor cementation technique (Amstutz *et al.*, 1981a) were also

blamed. Loosening of the femoral component was accompanied by tilting to varus. Despite carefully designed instruments to aid the positioning of the femoral component, scoring of the neck and femoral positioning were reported (Jolley *et al.*, 1982). The reaming of the acetabulum was also felt to be excessive, although the most common failure in this particular series was femoral loosening.

Concern about the frictional torque of the large diameter resurfacing bearing lead to two investigations. The first (Ma *et al.*, 1983) measured frictional torque on implants with constant loading in bovine serum. This group found that the frictional torque increased with increasing size of head. Other factors such as local deformation and stiffness affected the friction which produced a maximum torque of 3.2 Nm. This value is not large enough for static failure, but may cause fatigue failure of fixation. The second study (Mai *et al.*, 1996) compared the survivorship of large, medium and small implants. Large implants lasted significantly longer than small and medium sized ones. The loosening mechanism was proposed to have a constant rate per area of fixation surface. Large implants, having larger fixation surfaces, took longer to loosen.

The change to metal backed UHMWPE acetabular components did produce an improvement in the survivorship of the THARIES implant (Kim *et al.*, 1987). With improved acetabular survival, later femoral loosening became more frequent (Mai *et al.*, 1996).

Salzer (1978) reported 16 ceramic-on-ceramic implantations at a follow-up range of 8 to 28 months. Four of these hips had loosened by 7 months, two of these because of malpositioned femoral components. The thickness required to make a strong enough ceramic implant and its high stiffness relative to bone were suggested to be contributing factors.

While no reports have been made of the definitive Beuchel Pappas resurfacing, there has been a report of a resurfacing of similar design using Co-Cr instead of Ti. It was fixed by bone ingrowth into a porous Co-Cr coat and bone screws (Beuchel *et al.*, 1994). Large osteolytic regions were observed in the pelvis at short (24-60 months) follow-up times. These were particularly concentrated around the fixation screws. The screws and screw holes may have provided wear debris with easy access to the trabecular spaces in the pelvis, thus causing the lesions. However the only apparent

modification made to the final resurfacing was to change the material to titanium and to coat the femoral component with titanium nitride for lower wear.

The metal-on-metal resurfacing designed by Wagner was reported at a mean follow-up of 20 months (Wagner and Wagner, 1996). Of 35 hips implanted, five had been revised. Three of these were femoral loosenings due to the screw on thread design which was discontinued and there was one acetabular loosening and one femoral neck fracture. Independently Schamlzried *et al.* (1996) reported 4 Wagner metal-on-metal hips with no revisions at a mean follow-up time of 16 months.

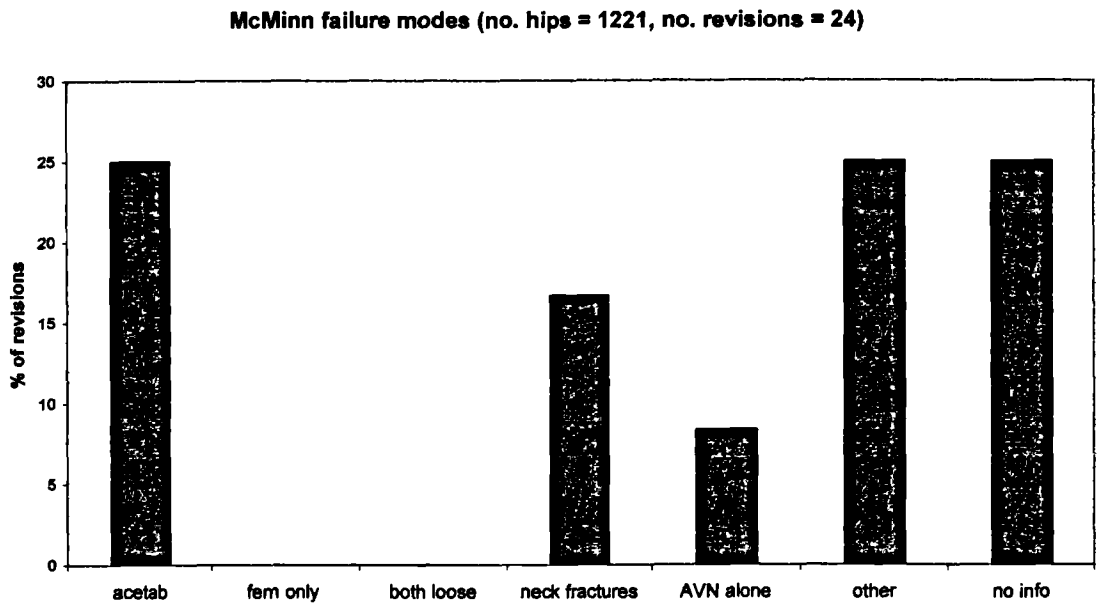

Figure 3.4.9 Failure modes for the McMinn and Birmingham Hip Resurfacing. Data from McMinn *et al*, 1996; Schamlzried *et al.*, 1996; McMinn *et al.*, 2000.

The McMinn resurfacing has a rate of revision of 0.049% per month at a mean follow-up time of 60 months. The data from McMinn *et al.*, 1996 and Schmalzried *et al.*, 1996 include 136 hips from the trial period when the fixation system for the implant was being developed. The mean age of these patients was 47 years. The 70 pilot press-fit implants performed badly with six revisions for aseptic loosening by 50 months. Three of the 43 all cemented implants were revised for acetabular loosening following cement mantle fracture at 33 months. There were no revisions reported for the all HA coated implants.

Both the McMinn and BHR hybrid implants were reported in McMinn *et al.*, 2000. The mean age of patients was 53. The first 294 hips in the series were implanted with the McMinn resurfacing. There were five revisions: two for infection, two for

acetabular loosening and one for femoral head collapse in a patient with pre-existing AVN. The remainding 791 patients in the series were implanted with the BHR. There were also five revisions in this group, four for femoral neck fractures and one for femoral head collapse in a patient with pre-existing AVN. The cumulative survival of the McMinn and BHR hybrid implants at 5-6 years was 98%. Mean migration, measured on standard clinical X-rays, was 0.015 mm/year for the acetabular component and 0.031 mm/year for the femoral component. However this implies total migration at 6 years of at most 0.19 mm, which is at the limits of stereoscopic X-ray (RSA) accuracy (Yuan, 1999) and far beyond that possible with conventional X-rays. This result is therefore meaningless. A more useful figure would be the mean migration of all those components that showed measurable migration. Unfortunately the commercial aspects of the promotion of the BHR indicate that until clinical outcomes and migration rates are reported in a peer reviewed journal, preferably by a surgeon not involved with the implant design, the data should be treated with some caution.

Schmalzried *et al.* (1996) reported progressive acetabular radiolucency in a large proportion of a small all-cemented McMinn series. The average age was 42 years and there had been one revision due to bad initial acetabular fixation in sclerotic bone. The femoral component was difficult to position accurately without the use of a pinned centring guide.

Due to the controversy over changes in the materials and manufacturing of the McMinn hip AEA Harwell carried out a wear test of a Cormet 2000 hip on their hip wear simulator (Corin, 1998). After 1.5×10^6 cycles they measured 2 μm cumulative linear wear on the femoral and 4.5 μm on the acetabular component. This compares favourably with similar tests on the Metasul hip articulation.

The Conserve Plus resurfacing has no published long term follow-up, although no postoperative complications were reported for 60 implanted hips at an unspecified follow-up time (Amstutz *et al.*, 1998a).

3.5 Summary of Outcomes

The resurfacing outcomes catalogued above seem to fall into three distinct categories. The resurfacings with the most rapid failures form the first category with large numbers of revisions due to femoral loosening or femoral neck fracture. These reports

emphasise the conservation of the femoral neck vessels and generally report a majority of failures on the femoral side. Included in this lower level of outcome are the "copy-cat" resurfacings introduced in the early 1970's. These seem to have had little engineering input in their design and often lose sight of the aim of resurfacing – conservation of bone – in their desire to implement a new technique. However three of the more widely reported resurfacings (Paltrinieri-Trentani, ICLH, Wagner) also show early failure on the femoral side.

The second outcome category is characterised by failure initiated predominantly on the acetabular side. With careful femoral head shaping technique and accurate positioning of the femoral component the most vulnerable part of the prosthesis becomes the acetabular component. Failure occurs at longer times after implantation than the first level of outcome, but still with rapidity and bone loss. Both the TARA and the THARIES implants have later acetabular loosening as their main mode of failure. The main physical difference between these implants and the Paltrinieri-Trentani, ICLH and Wagner implants is the number of different implant sizes available: the more successful implants had eight sizes, whereas the ICLH and Wagner had four or fewer. In other respects – fixation, shape and materials – the two groups are similar.

In comparison failures in stemmed THR occur later and with less bone destruction, due to the intrinsic stability of the stem in the medullary canal. Although the later resurfacing components lasted longer, the problems presented at revision may have been more complex than the quicker failing implants. Compensating for bone loss is much more difficult on the acetabular side than on the femoral side.

The early results of modern metal-on-metal resurfacings fall into a third category. Taken at face value they are encouraging. The low migration rates of the BHR predict good long-term outcomes. However the early reports of previous resurfacing designers were equally confident of long term success.

3.6 Problems in Resurfacing Design

The initial focus of resurfacing was conservation of the femoral head. Many of the reports of resurfacings have commented on how deeply the acetabulum must be reamed to accommodate the large components. Later authors have appreciated this and attempted to design resurfacings that conserve both acetabular and femoral bone

stock. However the femoral head cannot be reduced below a certain size before the hip range of motion is significantly limited and impingement is a certainty in all directions of movement.

The challenge of designing a femoral component for resurfacing is in providing a reasonable solution to the problems of stress distribution and stability. These are problems of designing the bone-implant interface. Since revision to THR or even to another conservative hip replacement (section 3.7) does not depend critically upon the retention of the femoral neck there is a wide scope for innovation and also a wide margin for error. The design space is physically and conceptually large.

The acetabular component on the other hand presents a more difficult task. Not only must the design provide a good solution to the problem of the bone-implant interface, it is also constrained by very demanding physical limits if it is to conserve bone. Conservation of bone is more critical on the acetabular side than on the femoral side simply because there is less bone initially. Conservation is of primary importance for the success of any subsequent revision operations (as outlined in section 3.1). If the resurfacing is to be truly conservative it must present the surgeon with an acetabulum that can be treated "as a primary" at revision. All the other design features – fixation, load distribution and bearing design – must follow from this.

Conservation means limiting the removal of bone to the minimum necessary. It means shaping the implant to the bone, rather than shaping the bone to the implant. In order to achieve this it is first necessary to know what is the shape of the bone. Review of the literature and requests for help from anatomists (Eckstein, 1998; Parkin, 1998) have shown that the morphology of the acetabulum is little known. In particular studies linking its gross physical form with its function are scarce. Although the problems of incongruity, distribution of subchondral bone and cartilage thickness have been investigated (Greenwald and O'Connor, 1971; Eckstein *et al.,* 1997; Eisenhart-Rothe *et al.,* 1997; Lazennac *et al.,* 1997) the data required are more basic. They include the solid subtended angles of the articular and subchondral surfaces at the centre of rotation of the hip joint. Measurement of these angles however requires that the centre of rotation of the joint be known and since this is defined by the articular surface itself extensive information is needed.

It is also necessary to understand what are the aims of acetabular bone removal and how the process of reaming changes and moves the shape of the acetabulum. A conservative reaming operation has been defined as follows (Northmore-Ball, 1998):

- Ream medially with small diameter reamer until the true acetabular floor or fossa is just grazed.
- Increase reamer diameter incrementally until the subchondral bone anteriorly and posteriorly is just grazed.
- Ream with this diameter reamer in a supero-medial direction until the subchondral bone in the supero-lateral acetabulum is grazed.

The preceding survey of outcomes shows that, in the past, resurfacings failed due to loosening of the acetabular component. This view is supported by surgeons who used the implants (Freeman, 1998). Modern resurfacings seem to behave differently although long-term results are still not known. However, given the neglect of the acetabular component in hip replacement in general, it is reasonable to conclude that improving acetabular component design is fundamental to the improvement of resurfacings.

3.7 Other Conservative Hip Replacements

Resurfacing is not the only solution to the problem of replacing the hip joint in a conservative fashion. The Thrust Plate Prosthesis (TPP), designed by Jacob and Huggler, is one such implant (Bereiter *et al.*, 1991). The femoral head is partially resected perpendicular to the neck axis and the plate of the prosthesis is bolted to this platform (Figure 3.7.1). The bolt passes down the neck and is secured to the lateral femoral cortex. The diameter of the femoral articulating surface is not constrained to be as large as the femoral head diameter and so an acetabular component similar to that of conventional THR may be used. The thrust plate itself is porous Ti coated for bone ingrowth fixation. The Co-Cr bolt provides initial stability. Modular femoral heads allow a variety of articulations including metal-on-metal.

The thrust plate relies upon the bolt through the lateral cortex to prevent relative motion at the flat implant-bone interface while bone ingrowth occurs. The pre-stress created by tightening the bolt at operation will help to keep a compressive stress distribution in the femoral neck, minimising interfacial shear and tensile stresses and

thus relative motion. However as discussed earlier in section 2.1.4, bone is a viscoelastic material and will creep under constant stress. Ingrowth must be complete before the pre-stress is relaxed, or the implant will become unstable. Substantial bending and torsion moments were measured in instrumented conventional prostheses by Bergmann *et al.* (1993).

Short term follow-up results have been reported: with a mean age of 52, five out of 78 hips had been revised within two years of operation. However three of these were for sepsis and 42 of the other hips had at least a five year follow-up (Bereiter *et al.*, 1991).

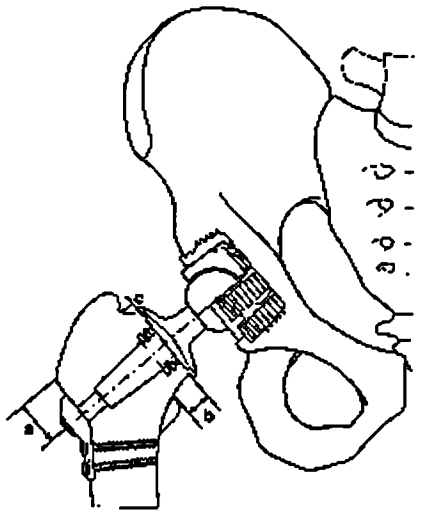

Figure 3.7.1 The Thrust Plate Prosthesis from Allopro technical data sheet (1997).

Munting, working in Belgium, reported the implantation of a similar design (Munting and Verhelpen, 1995; Munting *et al.*, 1997). A bolt down the femoral neck to the lateral cortex and porous Ti bone ingrowth are employed as in the TPP. However the plate of the TPP is replaced with a curved surface interrupted by four lamellae designed to anchor the implant in the cancellous bone of the proximal femur. At a mean follow-up of 5.8 years there have been 8 revisions for technical errors out of a total of 48 implanted hips (0.24% revised per month). Six of these were revised for varus positioning of the implant and 2 for partial seating on bone. The mean patient age was 36.

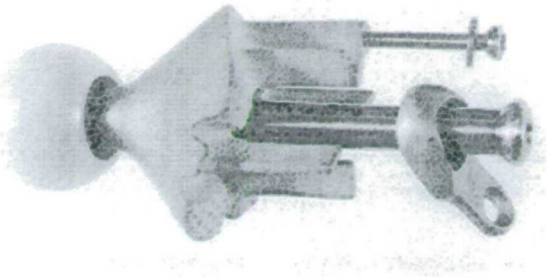

Figure 3.7.2 Munting stemless femoral implant from Munting and Verhelpen (1995).

A Swedish conservative prosthesis inspired by Brånemark's work on osseointegration was described by Albrektsson *et al.* (1998). The Gothenburg Osseointegrated hip arthroplasty echoes the design of the Brånemark dental implants. A large threaded c.p. Ti barrel is inserted down the femoral neck and a smaller bolt passes through it and into the lateral femoral cortex. At 4 – 5 years follow-up five out of ten implants in the pilot trial are in place. One patient has died, and four were revised. The authors suggested that placement of the implant centrally in the neck rather than nearer to the calcar caused the failures. RSA of implants placed near to the calcar showed "minimal" migration at five years follow-up.

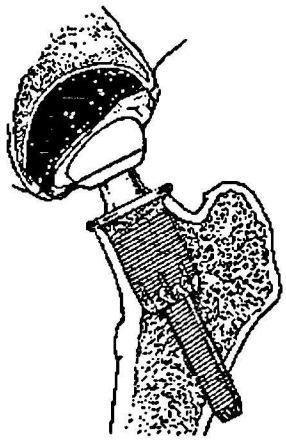

Figure 3.7.3 The Gothenburg osseointegrated hip arthroplasty from Albrektsson *et al.* (1998).

4. Anatomical Survey of the Acetabulum

4.1 Introduction

In order to shape the implant to the bone (section 3.6) the shape of the bone needs to be known accurately. The shape of the proximal femur is much studied and detailed information (Clark *et al.*, 1987; Noble *et al.*, 1988; Husmann *et al.*, 1997; Sugano *et al.*, 1999) on offsets, neck-shaft angles and retro- and ante-version is available. These extensive data are the result of the recent emphasis on femoral stem fixation, with the resulting drive to produce an uncemented stem that accurately fits and fills the femoral canal. However, the more difficult question of the shape of the acetabulum is much less studied. Given the importance of the acetabulum to the design of a resurfacing, a project to characterise its morphology was undertaken.

The first difficulty was to decide which parameters were important. Consideration of the effect of an acetabular implant upon range of motion (Figure 4.1.1) shows the importance of the subtended angle. This angle (with the head-to-neck ratio) defines the angle through which the implanted hip can move. In fact a whole set of angles is required to characterise the irregular shape of the natural acetabulum. They apply a constraint upon the thickness of the implant: the smaller the subtended angle the thicker the component can be made without removing more bone for a given range of motion.

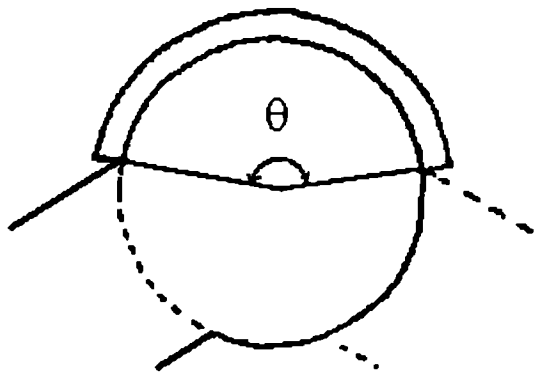

Figure 4.1.1 The subtended angle (θ) and its effect on range of motion.

Anatomical parameters can be obtained directly from measurements of cadavers, or indirectly from analysis of images or scans of the body. Two types of images of the pelvis – plane X-rays and Computed Tomography (CT) scans – were available.

Although plane-X rays of a large population group were easily obtainable they were immediately discounted. Without information about the relative orientation of the patient and the X-ray source and the magnification it is impossible to extract meaningful three dimensional measurements. The CT scans at the Robert Jones and Agnes Hunt Orthopaedic Hospital (RJAHOH) were stored as hard copies and digitally on 8" floppy disks. The small size of the hard copy pictures proved difficult to measure and the digital information was in a proprietary file format on disks usable only in a CT scanner which had been replaced. For reasons of patient confidentiality CT and X ray data may not be transferred outside hospital limits and so digital data from modern CT scanners elsewhere in Britain could not be used. Therefore the option of direct measurement of cadavers was explored.

Obtaining human material was the most difficult part of the project. The Anatomy Laboratory at the RJAHOH was reluctant to allow the cadavers used for teaching purposes to be dissected down to expose the acetabula. A planned collaboration with Mitutoyo Co-ordinate Measuring Machines in Leeds, who had helped to carry out a survey of the morphology of the proximal humerus (Roberts *et al.,* 1991), was abandoned due to the difficulty in obtaining material. The problem seemed to be solved when the Anatomy Laboratory of Munich University, who have studied the acetabular subchondral plate and cartilage thickness in detail, offered access to up to 80 cadavers in Munich.

An electronic digitiser (Polhemus' "Fastrak") which determined the position and orientation (6 DoF) of a receiver in 3D space to 0.7 mm could be used to gather data points. However, preliminary tests demonstrated that the stainless steel tables upon which cadavers are stored interfered with its operation. To take advantage of the Munich offer it was planned to build an Instrumented Spatial Linkage (ISL) and use it as a substitute digitiser. ISLs use mechanical joints and potentiometers to determine the co-ordinates of a point in space.

However, in the course of asking for help in making an ISL, Dr. Tanya Dawson, of the University of Liverpool, offered the use of data sets from dried human pelves, scanned using a laser surface scanner. This technique uses the reflected light from a laser line scanned across a solid surface to build up a 3D computer image. These data removed the need for any actual measurement, allowing concentration on the extraction and analysis of suitable parameters.

4.2 Materials

There were 18 hemipelves altogether, of which 8 were female, 9 male and one was of undetermined gender. The most common estimated age range at death was 25-35 years, with the oldest range 41-67 and the youngest 16+. The bones came from two archaeological sites in Gloucester (periods 43-410 AD and 1066-1500 AD) and one came from the Pathology Laboratory in the RJAHOH. Table 4.2.1 contains information on the subjects and the condition of the bones. Heights estimated from the length of the femur ranged from 1.49 m to 1.81 m with a mean of 1.62 m. There were 12 right and 6 left hemipelves, including one right and left pair. None of the hemipelves showed signs of degenerative joint disease, although many were broken, the most common sites being the pubic ramus and the anterior horn of the acetabular rim. The scanned hemipelvis data files were in ASCII format and consisted of a list of nodal co-ordinates and a list of triangular element connectivities.

Table 4.2.1 Biographical data and condition of hemipelves. PS pubic symphysis, IT ischial tuberosity, ASIS anterior superior iliac spine, PSIS posterior superior iliac spine, AH anterior horn of acetabular rim.

Period	Subject	Side	Estimated			Condition
			Sex	Age at death	Height	
43 – 410 AD	1	R	F	17-25	1.54	complete
	2	R	M	41-67	1.81	PS, IT and AH missing
	3	L	F	17-25	-	PS missing
	4	R	F	25-35	1.49	complete
	5a	R	F	25-35	1.61	PS and AH missing
	5b	L		pair of 5a		ASIS and PSIS missing
	6	L	M	17-25	1.60	complete
	7	L	?M	<16	-	complete
	8	R	M	17-25	1.72	complete
	9	R	?M	17-25	-	ASIS and PS missing
	10	R	M	25-35	1.65	complete
	11	R	F	25-35	1.58	complete
1066 - 1500 AD	12	R	?F	25-35	1.57	complete
	13	R	?M	35-45	1.65	PS and AH missing
	14	L	F	25-35	1.52	complete
	15	R	M	25-35	1.77	PS and AH missing
	16	R	M	25-35	1.60	complete
modern	17	L	-	-	-	complete

4.3 Method

Using a routine written in Basic the files were converted to an ASCII format that MENTAT, the solid modeller pre-processor for MARC (MARC Analysis Corporation, Palo Alto, CA, USA) could read. Once loaded and displayed in the solid modeller the nodes and elements on the acetabular articular surface were picked and output as a separate file. The co-ordinate data from this file were extracted using

another Basic routine and saved as a Matlab executable file. A short Matlab routine (Appendix A) was implemented to fit a sphere to the nodal co-ordinate data in the acetabular shell. The mean position vector of the set of nodal co-ordinates and its magnitude were used as first approximations for the centre co-ordinates and radius. The routine then used an iterative Newtonian method to reach a better approximation, minimising the square of the distance from the sphere's surface to the data set nodes. The best-fit sphere centre co-ordinates, radius and maximum, mean and standard deviation of the error were output.

Eight approximately equidistant points on the acetabular rim were picked at anterior, posterior, superior and inferior locations and the quarter points between these (Figure 4.3.1). In five hemipelves the anterior horn of the acetabular rim was broken so no point was picked in this region. The superior, posterior and inferior (points 3, 5 and 7) points were used to define the acetabular opening plane except in three pelves where the rim was damaged at the inferior position (point 7). The angles between the rim-centre vectors and the opening plane normal were calculated. The subtended angle in any plane through the centre of rotation is the sum of two of these angles. Therefore four different subtended angles were calculated. Table 4.3.1 shows the relationship between the rim points, bony landmarks, the directions in which the subtended angles were measured and anatomical directions.

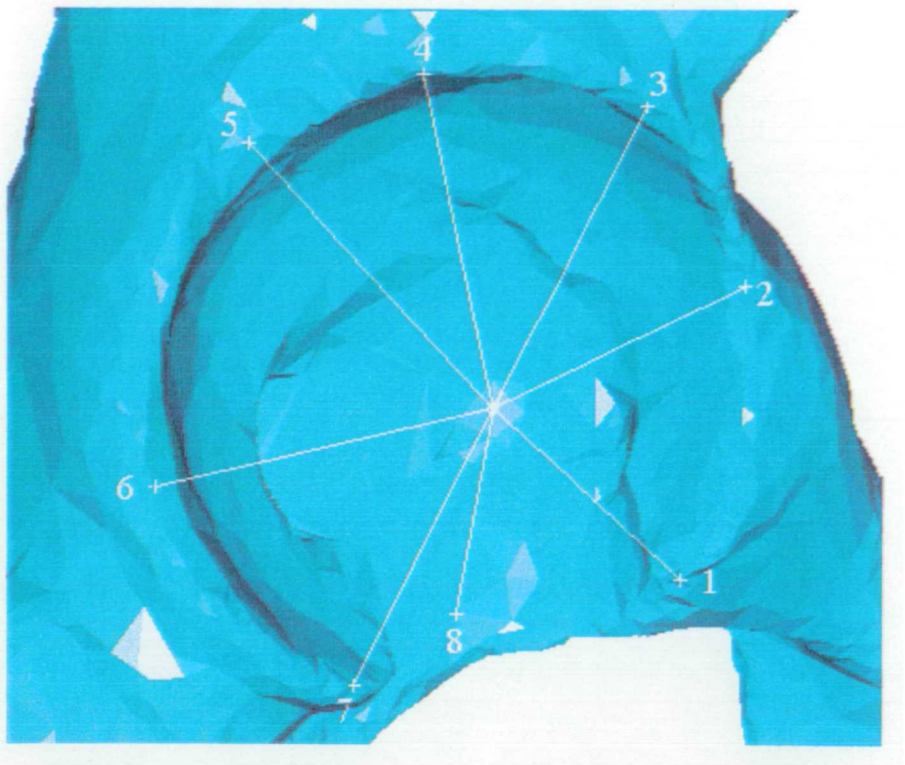

Figure 4.3.1 Locations of points on acetabular rim, showing rim-centre vectors (1 = anterior, 3 = superior, 5 = posterior, 7 = inferior).

Table 4.3.1 Subtended angle directions

Rim points	Landmarks	Approximate anatomical direction
1 and 5	Anterior horn of lunate surface	Anterior – posterior
2 and 6	-	Supero-anterior – infero posterior
3 and 7	Anterior iliac crest and posterior horn of lunate surface	Superior – inferior
4 and 8	Acetabular notch	Infero-anterior – supero-posterior

The next step was to simulate the conservative reaming of an acetabulum and then re-calculate the subtended angles. In a conservative reaming operation the acetabulum is first deepened medially to the "true floor", increasing the reamer size until the anterior and posterior rim are just grazed. The reamer is then pushed superiorly until the most lateral portion of the rim is just grazed. This operation was simulated by selecting one node on the floor and one on the rim and moving the best fit sphere centre medially and superiorly until its surface contained those points.

The angles between rim-centre vectors and the opening plane normal could then be re-calculated for the reamed acetabulum and a theoretical maximum removed bone volume calculated. This simulation was not performed on the three hemipelves which did not have acetabular floors.

4.4 Results

4.4.1 Sphere fitting

The diameters of the spheres fitted to the acetabula ranged from 43.7 mm to 58.2 mm. The overall mean diameter was 50.9 mm, with a standard deviation (SD) of 3.6 mm. The mean diameter of the male acetabula was 52.9 mm (SD 1.7 mm), of the female 49.0 mm (SD 1.45 mm) and this difference was significant ($p < 0.05$). These figures are compared with published data (Clarke and Amstutz, 1975; Noble *et al.*, 1988; Sugano *et al.*, 1999) in Figure 4.4.1. There was a 2 mm difference in diameter between the left and right acetabula of the only paired bones, but there was no significant difference between right and left acetabula groups. The mean diameter of the Norman period (1066 – 1500 AD) acetabula was 3 mm larger than that of the Roman period (43 – 410 AD), however the difference was not significant. The group mean of the mean deviation from each fitted sphere was 0.6 mm and the group mean of the maximum deviation was 3 mm, while the maximum deviation for any acetabulum was 6 mm. The location and magnitude of each nodal deviation was not plotted. However visualising the set of nodes to which the sphere was fitted together with the best-fit sphere allowed qualitative assessment of the size and region of the deviations. In general the anterior and posterior regions of the articular surface lay just within the sphere, while the superior part of the surface lay outside.

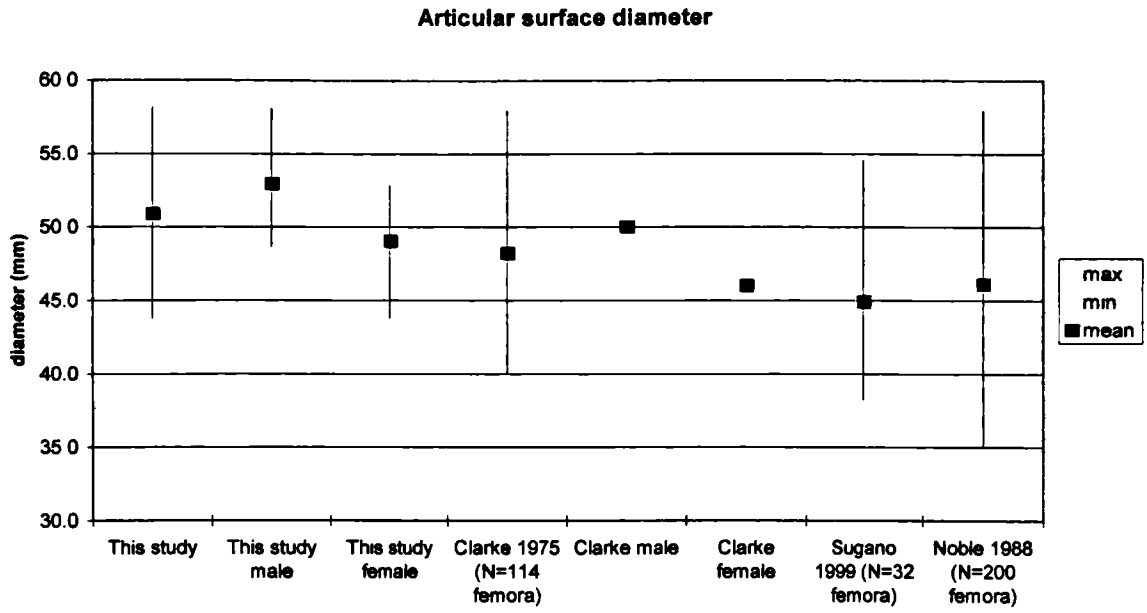

Figure 4.4.1 Acetabula diameters and gender differences compared with the literature.

The acetabular diameter plotted against the estimated height in Figure 4.4.2 shows a strong correlation (R^2 = 0.5994). The estimated height is calculated from the maximum length of long bones using a regression formula reported by Trotter and Peterson (1970).

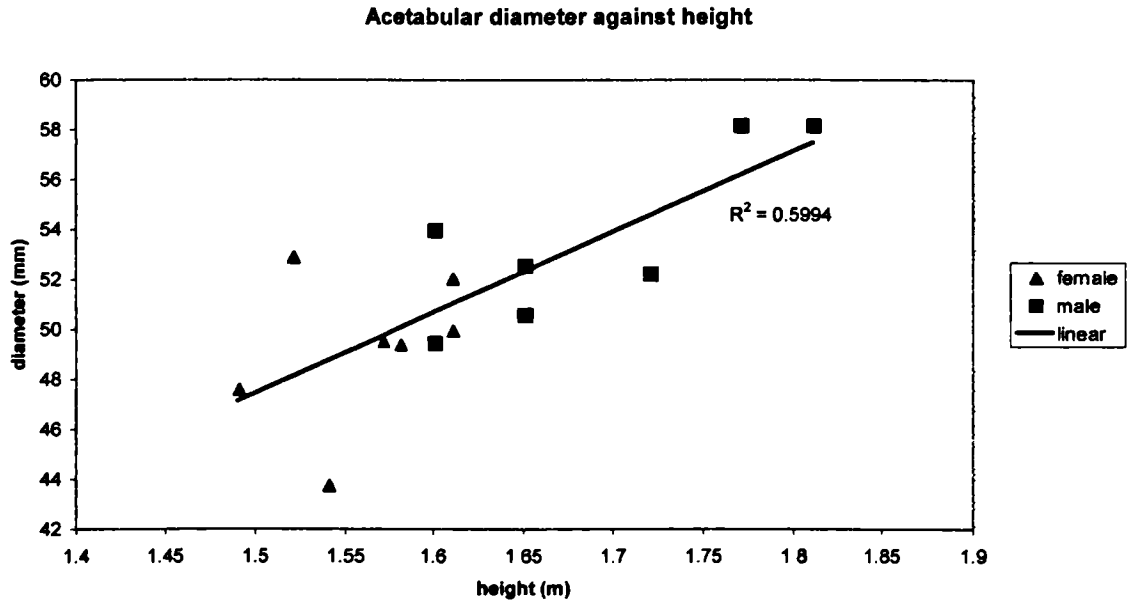

Figure 4.4.2 Estimated height plotted against acetabular diameter showing least square fit.

A separate plot of male and female diameters against height shows a stronger relation between male diameter and height than female diameter and height. However the

small size of the sample groups (seven and seven respectively) prevents any firm conclusions from being drawn.

4.4.2 Subtended Angles

The mean subtended angles in each of four directions – anterior to posterior, supero-anterior to infero-posterior, superior to inferior and infero-anterior to supero-posterior – are presented in Figure 4.4.3. The error bars represent one standard deviation of the distribution. The only subtended angles in the data series larger than 180° are in the superior – inferior direction, the maximum being 188°. One acetabulum has a supero-anterior – infero-posterior angle of 180° but the remaining acetabula have substantially smaller angles in this direction. The minimum subtended angle, 128°, is in the infero-anterior – supero-posterior direction of the acetabulum of a male subject of above average height. The mean subtended angle for each acetabulum, a measure of its depth, ranges from 145° to 173°, with a mean of 158°.

Also shown in Figure 4.4.3 are the differences between the male and female groups. Males have slightly larger subtended angles and hence deeper acetabula than females although the difference is not significant. In males the acetabular notch is slightly deeper and hence the inferior-superior angle is smaller. The gender difference is largest in the superior – inferior direction (difference of 6.7°) but this is still less than a single standard deviation (7.7°). The mean subtended angle showed no correlation with the estimated height or with estimated age at death.

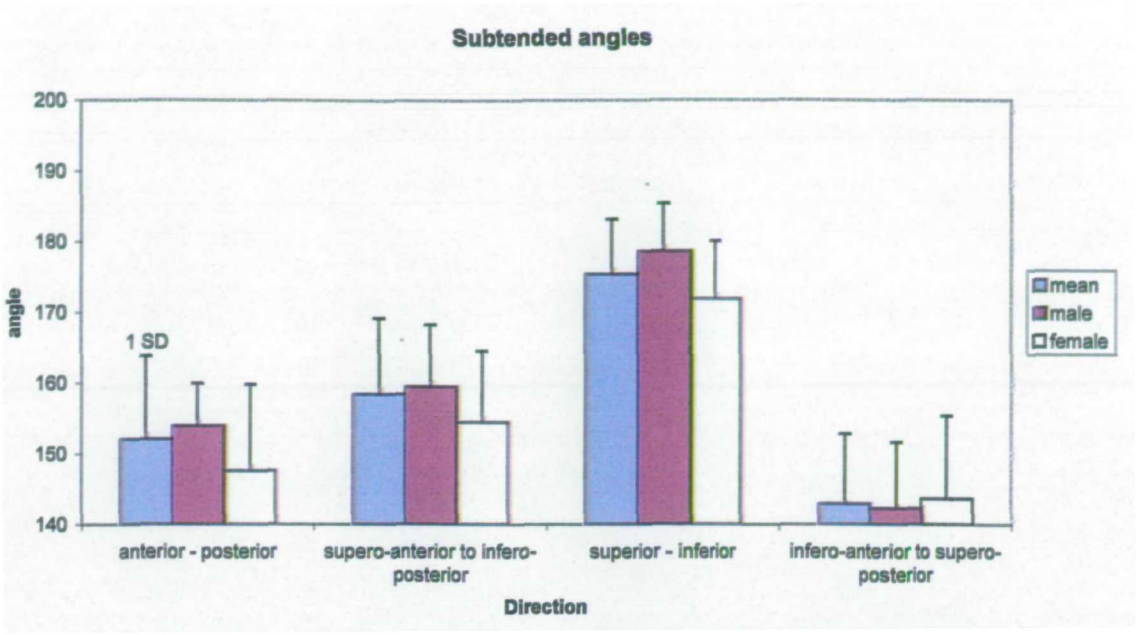

Figure 4.4.3 Acetabular subtended angles in four directions. Overall mean and mean male and female compared. Error bars show one standard deviation.

4.4.3 Reaming Simulation

The mean distance moved medially and superiorly by the centre of the sphere during the simulated reaming operation was 3.6 mm (1.2 mm – 5.4 mm). Figure 4.4.4 shows that the subtended angles in each direction were increased by approximately 10°. The mean estimated bone volume removed was 7,400 mm^3 (2,200 – 14,400 mm^3). The gender differences for the reamed acetabula were similar to those before reaming.

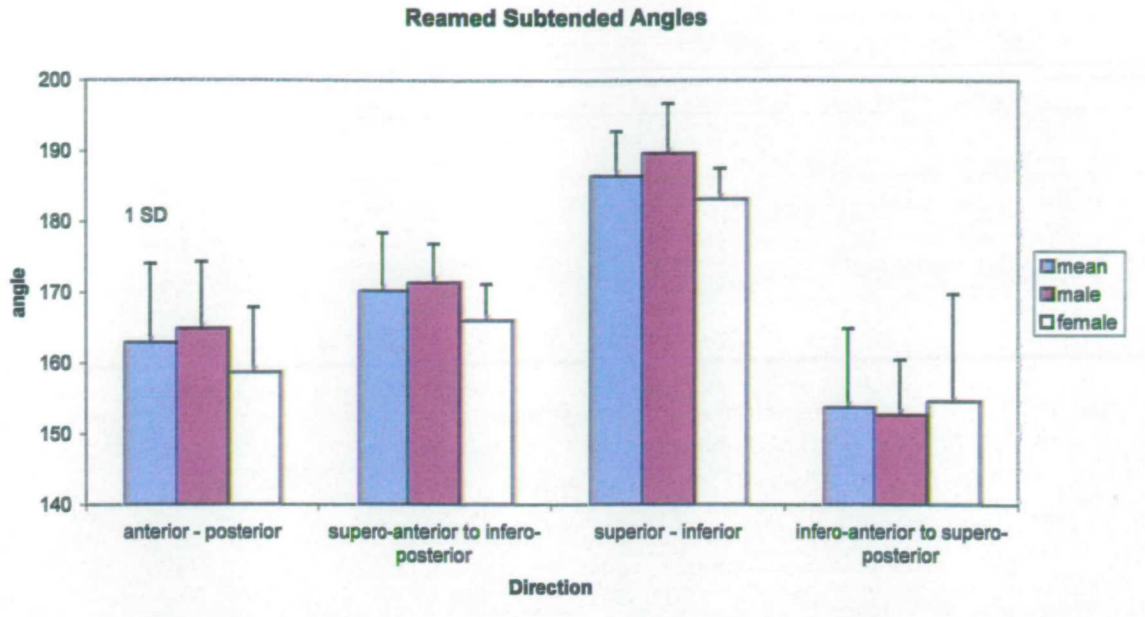

Figure 4.4.4 Acetabular subtended angles in four directions after simulated reaming. Error bars show one standard deviation.

4.5 Discussion

4.5.1 Sphere Fitting

The sphere fitting results show that the semi-lunate surface of the acetabulum lies on an extremely close approximation to the surface of a sphere. Rushfeldt *et al.* (1981) reported a 500 μm maximum deviation from spherical of the acetabular subchondral bone. The locations of these deviations were idiosyncratic. They only measured two specimens, aged 62 and 49 years, both of which showed signs of degenerative joint disease. It is speculated that hips become more spherical with age and congruency is associated with joint disease (Eisenhart-Rothe *et al.*, 1997), so the larger deviations in the younger healthy population presented here are to be expected. The largest maximum deviations noted are likely to be associated with nodes peripheral to the articular surface that were mistakenly not eliminated from the model. The acetabulum previously has been reported to be ovoid with a slightly reduced anterior-posterior axis and increased superior-inferior axis (Greenwald and O'Connor, 1971; Eckstein *et al.*, 1997; Eisenhart-Rothe *et al.*, 1997). However these authors have all studied the cartilage surface and not the subchondral bone which was studied in this case.

The range of sizes and difference between genders corresponds well with the literature on femoral head sizes if an intervening 2 – 3 mm thickness of cartilage is

taken into account. This correspondence also helps to confirm the sexing of the hemipelves, which in archaeological remains is subject to some uncertainty. Lack of significance in the differences between groups of acetabula such as that between the Norman and Roman groups may only reflect the small sizes of the sample groups.

4.5.2 Subtended Angles

The subtended angles measured provide new information on the morphology of the acetabulum. The first point to note is the large variation in acetabular depth. The mean acetabular subtended angle is 158° with a range of 28°. This variation may be seen as part of a spectrum that begins with acetabula so shallow that the hip is unstable (congenital dislocation of the hip). A second point is that some subtended angles are larger than 180°. These largest angles are exclusively in the superior – inferior direction. These angles limit the ad- and abductive motion of the femur. The rim points were chosen to lie near maxima on the acetabular rim, ensuring that the subtended angles measured are the maximum for the acetabulum. The small anterior – posterior subtended angle reflects the large range of motion in the flexion – extension plane. The lowest subtended angle, that measured between the supero-posterior quadrant and the acetabular notch would be larger *in vivo* due to the presence of the transverse acetabular ligament.

It is interesting that Rushfeldt *et al.* (1981) suggest that the centre of the best-fit sphere to the acetabular cartilage surface lies medially and anteriorly to that of the best fit sphere to the subchondral bone. The consequence of this and of the larger subtended angles would appear to be the curtailment of the range of motion of the femur. However it is important to note that the largest angular motions possible include a large component of rotation about the axis of the femoral neck which is limited solely by the acetabular ligaments and musculature.

No measure of the portion of a sphere that the acetabular surface occupies has been documented before. The measure proposed here, the subtended angle, is imperfect. First it is a discrete measure, taken in four directions between eight points across the acetabular rim. The points were chosen carefully to reflect similar positioning with respect to landmarks such as the iliac crest and the anterior and posterior horns of the lunate surface. The smoothness of the rim prevents the error from variation in relative position from rising above 1°. Secondly the opening plane normal is defined by three

of the rim points and is therefore an arbitrary direction. By using subtended angles as a measure, rather than the individual rim-centre vector to normal angles, the variation introduced by the opening plane normal should be eliminated.

The hemipelves studied here are those of modern *homo sapiens* (Aiello and Dean, 1990) and although differences in lifestyle may have an impact on their morphology the hemipelves are comparable with present day populations. It is important to note that hip replacement candidates include people with a wide diversity of lifestyles. The correspondence between measured acetabular diameter and published values of femoral head diameter helps to confirm the validity of this comparison.

The main sites of damage to the hemipelves were the pubic ramus and the anterior horn of the acetabular rim. Three bony landmarks were always available to provide adequate orientation. In five cases the anterior horn of the rim was absent and no rim point 1 could be assigned therefore no anterior – posterior subtended angle was calculated, increasing the uncertainty in the value of this angle.

The simulated reaming operation may be taken as a guide to the change of shape the acetabulum undergoes at hip replacement. The points in the floor and on the rim that define the simulated reaming operation are arbitrarily chosen. The simulation is unrepeatable and unreproducible. However the uniform increase of the mean subtended angles in all directions by 10°, leaving a cavity that is still less than hemispherical, is an important result.

The observation made by Townley (1981) that males have thicker acetabular walls and smaller head-to-neck ratios and females have thinner acetabular walls and larger head-to-neck ratios is interesting when related to the gender differences reported in this study. Small head-to-neck ratios in males will further reduce the range of motion already limited by large subtended angles, while large head-to-neck ratios will further increase range of motion in females. The different orientation of the acetabulum and femoral neck in males and females, not considered in this study, may account for these apparent discrepancies, although Reikerås *et al.* (1983) in a study using CT scans found no gender difference for anteversion of the femoral neck and acetabulum.

4.5.3 Implications for Resurfacing Design

The parameters measured in this survey affect the shape and thickness of a conservative resurfacing both directly and indirectly. First the acetabular subtended

angle has a direct effect upon the subtended angle of the acetabular component. Acetabular cups which overhang the acetabular rim are associated with impingement, early loosening and increased wear (Cotella *et al.*, 1990; Wiadrowski *et al.*, 1991). The fixation surface of the resurfacing acetabular cup therefore must conform to the subtended angles of the reamed acetabular rim.

The subtended angle of the bearing surface of the acetabular component should reflect the subtended angles of the unreamed acetabulum if the component is not to restrict range of motion or give rise to impingement. Several resurfacing designers reduced the subtended angle of the acetabular component following early experience with their implants (Amstutz *et al.*, 1981a; Capello and Trancik, 1981). The ICLH resurfacing acetabular component was first reduced from 180° to 168° and then to 140° (Cotella *et al.*, 1990).

The diameter of the bearing surface of the resurfacing prosthesis must not exceed that of the original cartilage bearing surface. If it were larger then more acetabular bone would have to be reamed than necessary to insert the implant. An increased bearing surface diameter would also decrease the available thickness for the acetabular component, leading to material strength and fatigue problems. The lower limit on the bearing surface diameter is determined by the thickness of the femoral neck. If the ratio of the bearing surface to the femoral neck diameter is reduced too far the range of motion of the hip will again be restricted and impingement will occur.

Thus the subtended angles of the reamed and unreamed acetabulum lie at the top of a long chain of related design decisions. The challenge of designing a new conservative resurfacing hip prosthesis will be to address the problem of the large variability in shape of the acetabulum.

5. Finite Element Analysis of a Novel Resurfacing Prosthesis

Finite Element Analysis (FEA) has applications throughout engineering. The biharmonic equation ($\nabla^4\phi = 0$) describes the spatial variation of a range of quantities including stresses and fluid and heat flows. Analytical solutions to the biharmonic equation exist for a few special cases, for example for the stress field around a circular hole in an infinite plate under uniaxial loading. In general, however, an alternative method for determining the solutions is required. FEA is a numerical technique which is used during the engineering design process to predict stress and strain distributions in components during use. This chapter provides a brief description of the basic concepts of FEA before presenting an FEA study of the resurfacing concept.

5.1 FEA basic theory

FEA splits the component to be analysed into a number of elements of finite size. Within each element, in stress analysis, the displacement field is assumed to vary in a particular way. These variations, which are expressed with arbitrary constants, are then used to derive expressions for strains and hence stresses within each element. The total strain energy for an element can then be deduced, also in terms of these arbitrary constants. Further, the work done by external loads on the element can be calculated from the displacements of the points at which the loading is applied. Summing the strain energies for all elements and the work done gives the total potential energy for the component. The best choice of arbitrary constants in the displacement field variations minimises the total potential energy. FEA needs computers to carry out the large matrix operations involved in this minimisation problem.

In preparing a problem for FEA, the first step is to define the volumes and surfaces of the components to be analysed. Well-defined components may be modelled using engineering design software packages such as IDEAS, but irregular anatomical shapes must be imported from imaging software. Meshing, that is defining the elements, can then proceed with varying degrees of user control depending upon the irregularity of the volume shape. Meshing the irregularly shaped components frequently encountered in biomechanics is awkward and time consuming.

The choice of element size depends upon the size of the smallest detail to be modelled and the local stress gradient. The mesh is specified by a list of spatial co-ordinates

defining the nodes and a list of nodal connectivities defining the elements. Different types of elements are available. The most appropriate element type depends upon the kind of problem and the capabilities of the FEA code to be used.

With the geometry of the problem described, the next step is to ascribe material properties to the elements and to prescribe boundary conditions. Boundary conditions place constraints upon the Degrees of Freedom (DoF) at nodes. In three dimensions there are a maximum of six DoFs (translation along and rotation about each of the three axes) at each node. Finally the loading conditions are defined and the model is ready for the analysis program.

FEA can produce large quantities of data describing the loaded state of the model. These can be displayed as contoured plots of stress or strain variables superimposed on the elements of the model. While these plots are useful in determining areas of stress concentration and maximum stresses in a model they can be misleading. Artefacts arise from the discretisation of complex anatomical geometry so frequently the maximum stresses have no relevance to the real situation. Analysing the statistical distribution of stress and strain magnitudes gives a description of the overall response to loading and allows meaningful comparisons between different models (Murphy *et al.*, 2000).

5.2 Role of FEA in Biomechanics

As discussed in section 2.5.6 one theory of aseptic loosening (Taylor and Tanner, 1996) unifies the three successive stages of migration and relates them to the fatigue failure of trabeculae in the cancellous bone adjacent to a prosthesis. The initial postoperative stress distribution in the cancellous bone surrounding an implant can be determined by FEA. Comparing the magnitudes of these stresses with reported ultimate strengths and fatigue and creep thresholds allows a prediction of relative rates of migration for different prostheses and fixation systems. A comparison of four different fixation systems used on the same prosthesis produced results that correlated well with clinically observed migration rates (Taylor *et al.*, 1995). Migration rates have been shown to be predictive of late aseptic loosening (Freeman and Plante-Bordeneuve, 1994; Kärrholm *et al.*, 1994).

5.3 Aims of this analysis

Resurfacing has a poor clinical history (section 3.4) therefore careful analysis of the concept is necessary. FEA can be used to determine stress and strain levels in the bone surrounding an implant which are predictive of the subsequent migration and long-term clinical outcome of an implant. There is only one published three dimensional FEA study of the resurfacing concept (Watanabe *et al.*, 2000) which deals solely with the femoral component at three instants in the gait cycle. In addition FEA must be used to investigate the contact behaviour of the proposed polyacetal on UHMWPE implant which is too compliant for the use of simple Hertzian analysis.

The studies presented here have four aims:

- to compare the resurfacing concept with conventional THR and the intact hip joint.
- to compare the novel design presented in chapter 7 with resurfacing prostheses in clinical use.
- to investigate the contact behaviour of a large diameter compliant bearing.
- to investigate the potential for acetabular fixation by bone ingrowth.

5.4 Models

All the analyses were carried out using a three dimensional model of the human hemi-pelvis developed and reported by Dalstra (1993). The model is shown in Figure 5.4.1. Dalstra used quantitative Computer Tomography (CT) to image the left pelvic bone of an 89 year old male in 4 mm thick slices. These slices provided the template for an FE mesh and additionally gave information on the thickness of the cortical shell and the apparent density of the cancellous bone. Each solid element representing cancellous bone was assigned material properties corresponding to the apparent density of the same region on the CT image according to relationships derived in Dalstra's previous work. Similarly the membrane elements representing cortical bone were assigned thicknesses according to the measurements from the CT image. Cortical thicknesses ranged from 0.96 to 2.06 mm.

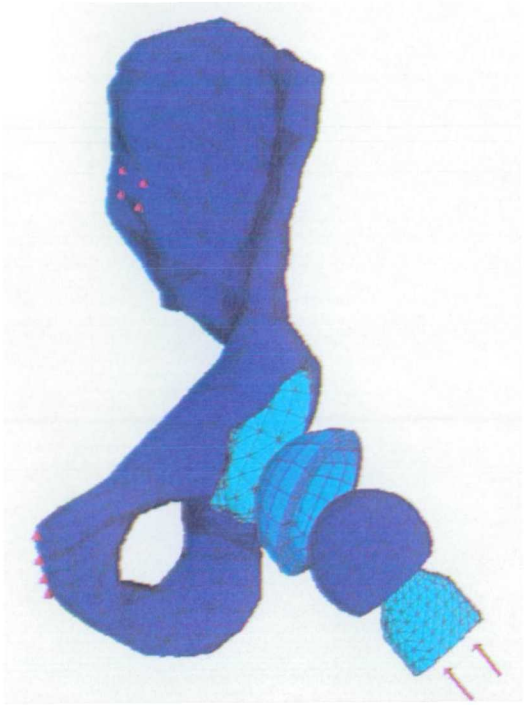

Figure 5.4.1 Exploded view of the implanted pelvis model used in the analysis. The red arrows represent joint force loading and the red triangles the built-in nodes at the symphysis pubis and the auricular surface of the sacro-iliac joint.

Table 5.4.1 Material properties assigned in the FE model. E is Young's Modulus, ν Poisson's ratio.

Material	E	ν
Cancellous bone	1.3 MPa – 1.6 GPa	0.2
Subchondral cortex	2 GPa	0.3
Cortical bone	17 GPa	0.3
UHMWPE	0.5 GPa	0.3
Polyacetal	2.7 GPa	0.3
Co-Cr alloy	228 GPa	0.3
Femoral neck	114 MPa	0.2
In-growing bone	114 MPa	0.2

The model of the pelvis was developed for the MARC FEA solver and subsequently translated by New (1997) for use with ANSYS software. The original MARC version was no longer available so the ANSYS model was translated to be used in ABAQUS™ (version 5.8, Hibbitt, Karlsson & Sorensen Inc.), the software available at the IRC. Owing to differences in material and element property assignments in the different codes it was necessary to group both sets of properties leading to a lower resolution in their spatial distribution than in Dalstra's original model.

The membrane elements used in this and in Dalstra's original model to represent cortical bone have no out-of-plane stiffness. Although the cortex might provide some

bending stiffness the use of shell elements (with out-of-plane stiffness) alters the behaviour of the model substantially. This would make the comparison of the novel implant with Dalstra's work impossible.

Models of the femoral and acetabular components were developed and meshed using the IDEAS software package. The geometry of these components was based upon that of the components of the prosthesis proposed in chapter 7. In order to fit the reverse of the acetabular component to the pelvis model it was necessary to import a section of the pelvis mesh into IDEAS and generate surface and volume information to define the volume between the basic component shape and the subchondral bone. This volume could then be meshed.

The femoral component was loaded via a cylindrical portion of bone representing the bone of the femoral head and neck. Following the validation study carried out on the pelvic model by Dalstra (1993), the pelvis was constrained by "built-in" nodes on the auricular surface at the sacro-iliac joint and at the pubic symphysis.

The contact between the acetabular and femoral components and between the un-bonded acetabular component and the subchondral bone was modelled using elements automatically generated by ABAQUS. ABAQUS uses a master-slave contact model. The "small sliding" approximation was used in which the nodes on the slave surface are constrained not to penetrate a local tangent plane to the master surface. This assumes that each slave node will interact with the same local area of master surface throughout the analysis. A friction coefficient of 0.2 was used for both CoCr and polyacetal on UHMWPE. This value is at the higher end of the range of reported values (McKellop *et al.*, 1981), but the friction was simply to stabilise the femoral head in the acetabular cup to allow load to be transmitted.

5.5 Loading

The model was loaded with the joint reaction force via the femoral component and with 22 muscle forces at the nodes corresponding to their attachments on the pelvis. Five load cases representing the stance phase of gait were considered (Figure 5.5.1). The sizes of the joint reaction forces and applied muscle forces are given in Table 5.5.1.

Table 5.5.1 Hip joint reaction and muscle forces in Newtons for the five load cases during the stance phase of gait.

	Load case				
Force	1	2	3	4	5
Hip joint reaction	2158	1876	1651	1180	187
Gluteus maximus	930	167	377	456	491
Gluteus medius	1053	1474	1509	1412	982
Gluteus minimus	140	263	228	175	123
Tensor fasciae latae	132	88	158	149	88
Iliacus	0	0	228	307	27
Psoas	0	316	175	88	175
Gracilis	0	0	0	88	158
Sartorius	88	0	0	35	158
Semimembranosus	368	333	368	421	298
Semitendinosus	140	105	246	316	368
Biceps femoris longus	202	88	70	123	114
Adductor longus	88	0	0	88	158
Adductor magnus	0	0	0	132	263
Adductor brevis	114	0	0	0	202
Obturator externus	0	0	0	123	167
Obturator internus	123	0	61	61	149
Pectineus	0	175	96	0	149
Piriformis	175	0	0	0	0
Quadratus femoris	96	0	0	88	184
Superior gemellus	88	123	79	0	0
Inferior gemellus	0	0	0	0	140
Rectus femoris	123	0	0	0	175

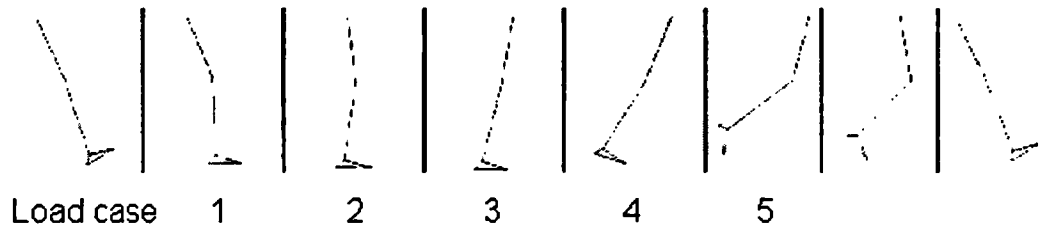

Figure 5.5.1 Phases of gait represented by the five load cases analysed from New (1997).

The directions of the muscle forces were calculated from three dimensional insertion and attachment data (Dostal and Andrews, 1981) taking into account the anterior-posterior motion of the femur during gait. The magnitudes of muscle forces were based on EMG data from Crowninshield and Brand (1981). These forces were identical to those used by Dalstra (1993). The magnitudes of the hip joint reaction force were identical to those used by Dalstra. However following a discussion on the "BIOMCH-L" newsgroup the directions of the reaction force were altered.

Dalstra took into account only the anterior-posterior motion of the femur relative to the pelvis when transforming from the femoral Co-ordinate System (CS) in which the joint reaction forces were measured (Bergmann *et al.*, 1993) into a pelvic CS. The

forces used in his model point anteriorly throughout the gait cycle, moving anteriorly from heel-strike to toe-off. The relative motion between femur and pelvis was measured on a different subject from that reported by Bergmann. Pedersen *et al.* (1997) reported gait lab measurements, validated by instrumented prosthesis data taken from the same subject, of the direction of the joint reaction force in a pelvic CS. They calculated a force that pointed posteriorly throughout the gait cycle, but still moving anteriorly during the stance phase. Witte *et al.* (1997), using data from the Bergmann instrumented prosthesis and their own gait lab data, reported a far more complex pattern of motion of the joint reaction force relative to the pelvis. However Witte (2000) suggested that the most reliable data were those reported by Pedersen. Finally data calculated by the usual inverse dynamics process from gait lab measurements (Stansfield, 2000) and transformed into a pelvic CS showed the joint reaction force pointing posteriorly at heel strike, moving anteriorly through vertical and pointing anteriorly at toe off.

The relative displacements between load cases of the joint reaction forces used in these analyses were identical to those used by Dalstra. However, all the forces were rotated posteriorly by approximately 20 degrees so that the direction at heel strike was 20 degrees posterior to vertical in the sagittal plane following the data from Stansfield (2000).

5.6 Analysis Methods

The Finite Element Analysis carried out in the course of this project may be divided into three studies, summarised in Table 5.6.1.

The first study looked at the contact behaviour of large diameter bearings, comparing polyacetal on UHMWPE with CoCr on UHMWPE. The components were "implanted" in the pelvis and loaded with the joint reaction and muscle forces listed in Table 5.5.1. Differences between the two bearings were assessed by comparing contact pressures and areas. The contact behaviour of an implanted CoCr on CoCr resurfacing proved too difficult to model, but fortunately this combination is susceptible to the Hertzian analytical solution for contact stresses and areas (Jin *et al.*, 1997). For all of the implant combinations investigated the bearing surface diameter was 48 mm with a radial clearance between femoral and acetabular components of 0.24 mm. The contact analyses were carried out in two steps: first contact was

established between the femoral and acetabular components by imposing a displacement boundary condition on the femoral component. In the second step this displacement condition was released and the loading applied. This method avoids the unconstrained motion that occurs when loaded contact surfaces "miss" each other.

The second study investigated the influence of implant materials on the stress and strain levels and distribution in the surrounding bone. In contact analyses the femoral component material was polyacetal or CoCr and the acetabular component UHMWPE. All components were assumed to be fully bonded. Due to modelling difficulties with contact between CoCr components, for CoCr on CoCr analyses only the acetabular component was included. The joint reaction force was applied to a node at the centre of the sphere defined by the acetabular component, which was linked to all the nodes on the bearing surface by rigid one-dimensional elements. Tensile stresses that do not occur in real contact were set up but their magnitudes were small.

In the third study a further set of analyses compared the stress and strain distributions in surrounding bone for different acetabular materials with fully de-bonded acetabular components. Contact surfaces were defined between the acetabular cup and the subchondral bone. A press-fit fixation was simulated using the ABAQUS ADJUST command, which moves the nodes of the slave surface (acetabular cup) until they are exactly in contact with the master surface (subchondral bone) before the analysis begins. This analysis was carried out with both UHMWPE and CoCr acetabular components with coefficients of friction of both μ = 0.1 and 0.5 at the fixation surfaces. Loading was applied as previously via the node at the centre of the acetabular sphere, but only load case 1 was investigated. The potential for bone ingrowth fixation was assessed by monitoring the tangential and normal motion between the contact nodes.

Table 5.6.1 Analyses carried out. μ is the coefficient of friction for implant bearing surfaces in studies 1 and 2, and for the fixation surfaces in study 3.

Study	Variable	Values	Load cases	Output
1 (resurfacing contact)	Femoral component material	Polyacetal; CoCr (μ = 0.2)	1, 2, 3, 4, 5	Contact area, pressure
2 (stress, strain: bone, implant)	Femoral component material	Polyacetal; CoCr	1, 2, 3, 4, 5	Strain statistics
	Acetabular component material	UHMWPE; CoCr	1, 2, 3, 4, 5	Strain statistics
3 (as 2 plus micromotion)	Fixation	"press-fit" μ = 0.1; μ = 0.5; CoCr; UHMWPE	1	Motion of contact nodes

5.7 FE results

The pictures displaying contour maps of finite element models are shown from two viewpoints. The first displays the lateral side of the pelvis, the superior axis pointing up the page and the anterior axis pointing to the left. In the second, used to show the medial aspect of the pelvis, the superior axis again points up the page, but the anterior axis points to the right.

5.7.1 Contact behaviour

The results characterising the contact behaviour in the loaded hip implanted with CoCr and polyacetal on UHMWPE resurfacings are shown in Tables 5.7.1 and 5.7.2.

Table 5.7.1 Contact results for polyacetal on UHMWPE. Contact area estimated from number of nodes in contact. Area of contact patch also estimated in ABAQUS Post. Edge refers to length of acetabular cup edge involved in contact.

Polyacetal on UHMWPE	Load case 1	Load case 2	Load case 3	Load case 4	Load case 5
Contact area / mm^2	1017	888	990	780	197
Number of contact squares	248	231	224	210	113
Edge / mm	49	45	56	49	15
Max gap / mm	0.88	0.94	1.26	1.20	0.72
Max contact stress / MPa	6.45	6.10	5.81	5.54	2.56
Mean contact stress / MPa	2.57	2.47	1.94	1.77	1.03

Table 5.7.2 Contact results for CoCr on UHMWPE. Contact area estimated from number of nodes in contact. Area of contact patch also estimated in ABAQUS Post. Edge refers to length of acetabular cup edge involved in contact.

CoCr on UHMWPE	Load case 1	Load case 2	Load case 3	Load case 4	Load case 5
Contact area / mm^2	1065	956	909	726	183
Number of contact squares	238	218	221	205	103
Edge / mm	49	45	52	45	15
Max gap / mm	0.94	1.00	1.26	1.20	0.72
Max Contact stress / MPa	7.37	6.70	6.48	6.38	2.64
Mean Contact stress / MPa	2.47	2.32	2.11	1.07	1.09

The contact areas are calculated assuming each contact node is associated with an equal portion of the contact surface. The contact area is also estimated by counting elements in contact on the post-processor display. The largest contact areas and pressures are associated with the highest hip joint reaction force in load case 1. The

largest distortion of the contact surfaces occurs in load case 3 where the maximum contact gap is 1.26 mm. There are no consistent differences in contact gap between the polyacetal and CoCr on UHMWPE implants. The largest number of elements on the edge of the acetabular component in contact occurs in load case 3. This number of elements, 15, corresponds to a distance along the edge of approximately 56 mm, compared to the total circumference of 149 mm.

The greatest difference between the polyacetal and CoCr on UHMWPE results is in the size of the peak contact pressure and is only sizeable in load case 1. The polyacetal component however shows higher mean contact pressures in load cases 1, 2 and 4. The polyacetal also shows a more non-linear relationship between applied load and contact area, with the contact area rising from load case 2 to load case 3 while the joint reaction force is decreased.

Figures 5.7.1 and 5.7.2 map contact area and the gap between the surfaces for polyacetal and CoCr on UHMWPE respectively. The contour scales are different for each plot, but the dark blue area always represents zero gap i.e. contact.

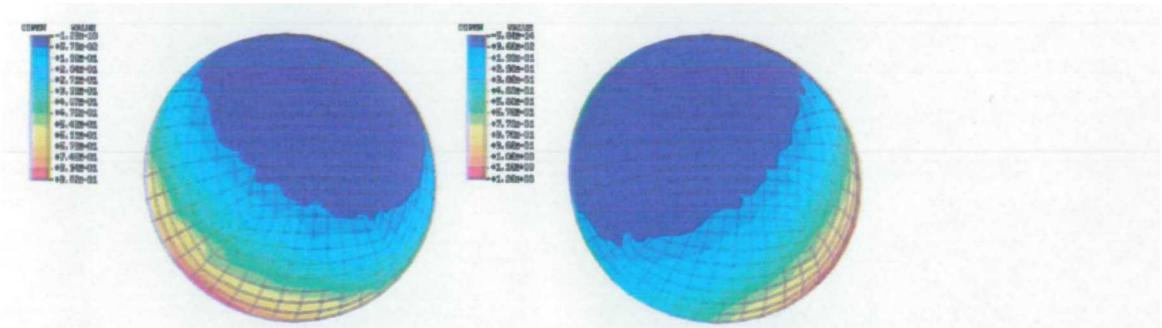

Figure 5.7.1 Contact gap between polyacetal and UHMWPE components, load cases 1 (left) and 3 (right). Blue indicates contact, red the largest gap.

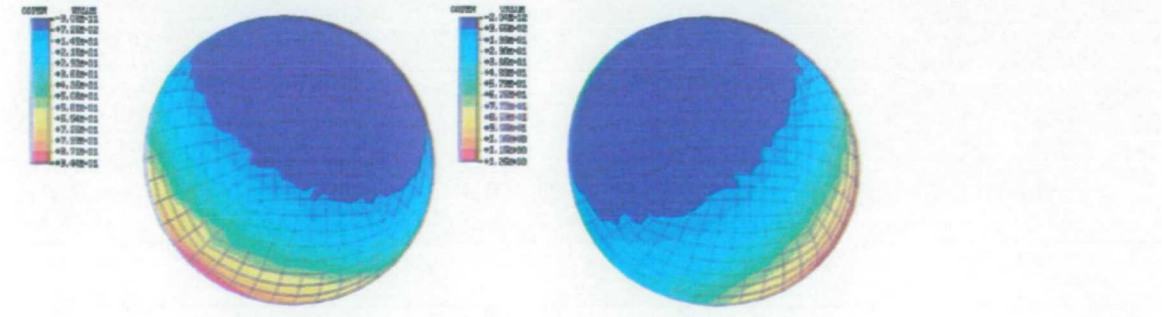

Figure 5.7.2 Contact gap between CoCr on UHMWPE components, load cases 1 (left) and 3 (right). Blue indicates contact, red the largest gap.

5.7.2 Periacetabular cancellous bone

Histograms of the distribution of maximum principal strain in the cancellous bone immediately surrounding the implant were plotted for all analyses. These frequency distributions are summarised in bar graphs. An example frequency distribution plot is also included. The frequency distribution was used to calculate the percentage of periacetabular cancellous bone element integration points with compressive strains larger than 0.010 or tensile strains larger than 0.008, the compressive and tensile yield strains found by Chang *et al.* (2000) in their study on bovine trabecular bone. These two percentages were summed to give the total percentage at risk of yielding. The upper quartile value of the von Mises stress was calculated for comparison with these strain-based values.

A representative plot of the frequency distribution of strain in the periacetabular cancellous bone is shown in Figure 5.7.3. The frequency curve is normalised with respect to its maximum and is shown together with a cumulative frequency curve.

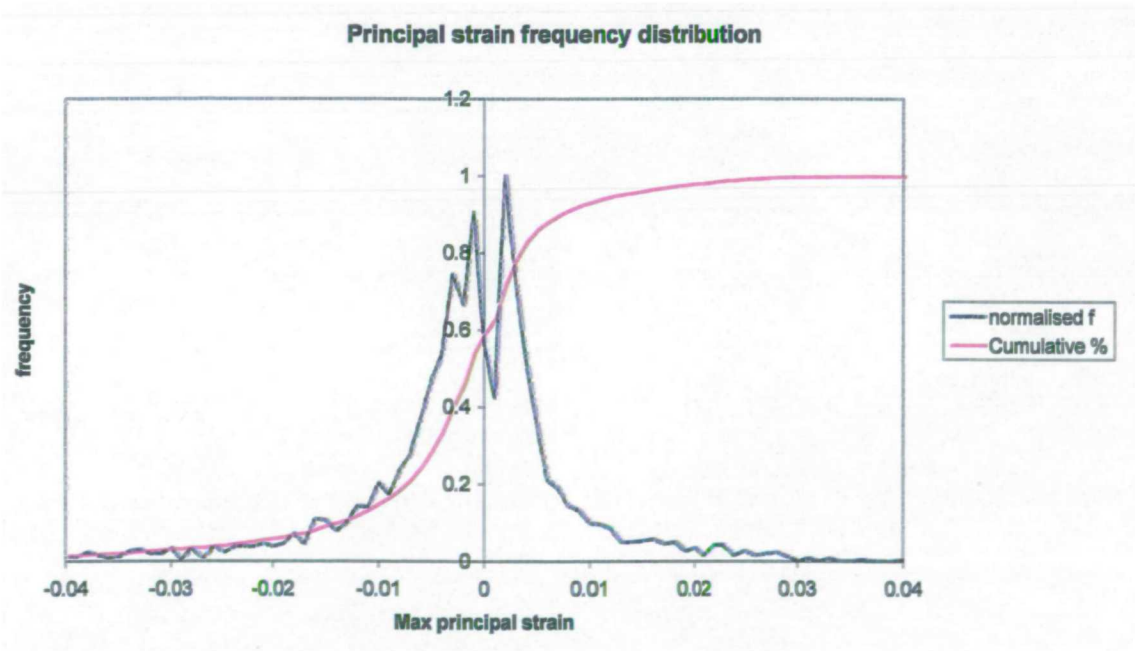

Figure 5.7.3 Periacetabular principal strain frequency distribution. Polyacetal on PE, load case3.

Figures 5.7.4 and 5.7.5 compare the percentages of integration points at risk of compressive and tensile failure respectively in polyacetal and CoCr on UHMWPE and CoCr on CoCr. The upper quartile von Mises stresses for all three material combinations are plotted in Figure 5.7.6. These graphs use the abbreviation POM (polyoxymethylene) as an alternative to polyacetal.

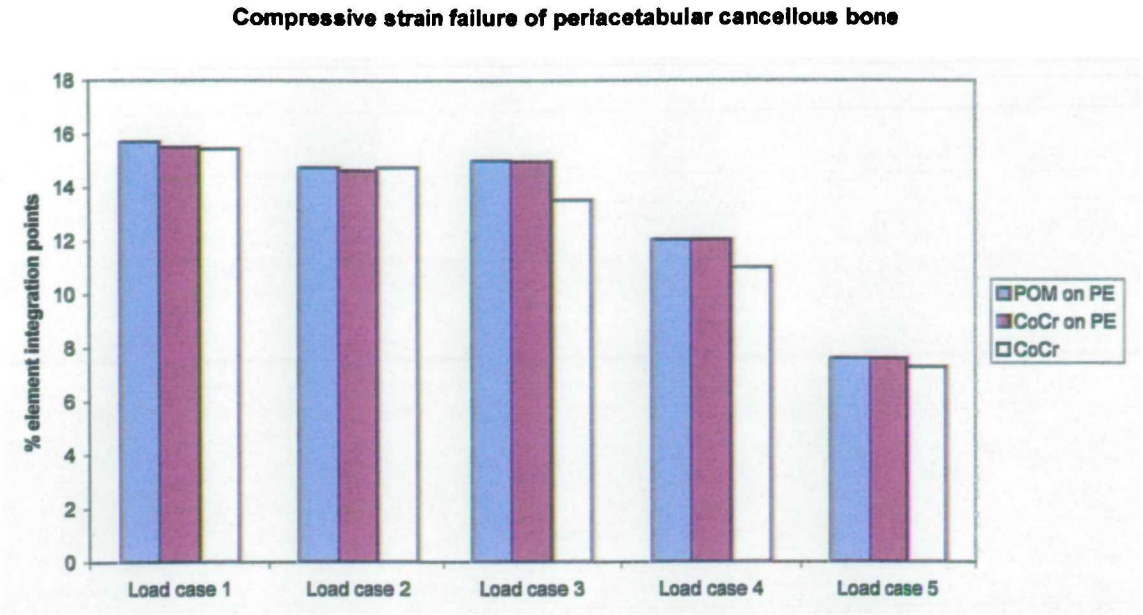

Figure 5.7.4 Percentage of element integration points with maximum principal strains less than -0.010.

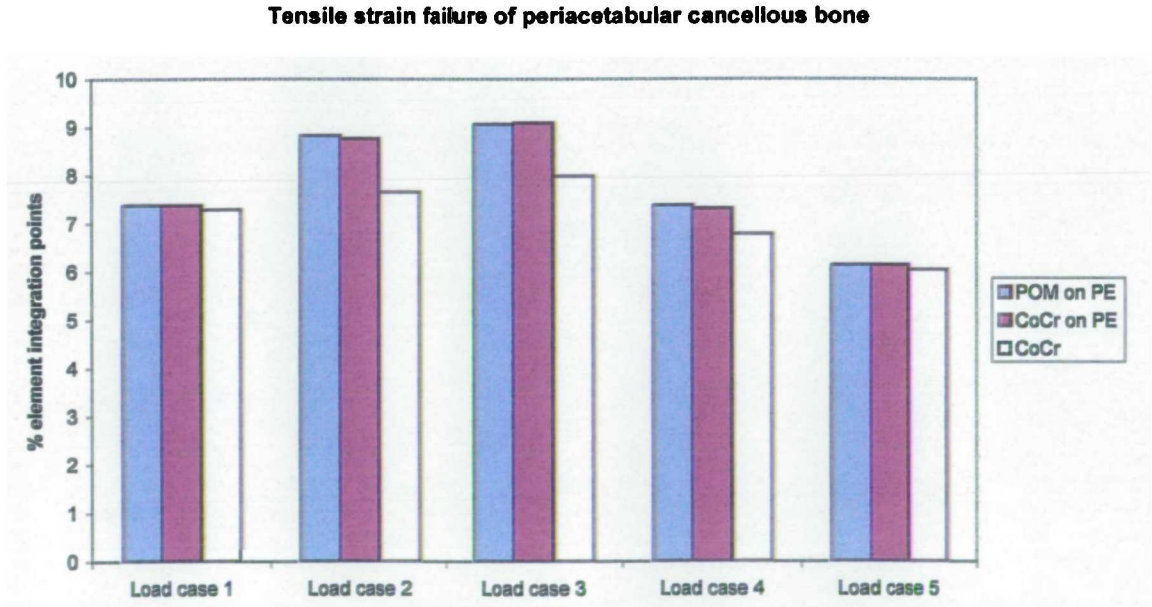

Figure 5.7.5 Percentage of element integration points with maximum principal strains greater than 0.008.

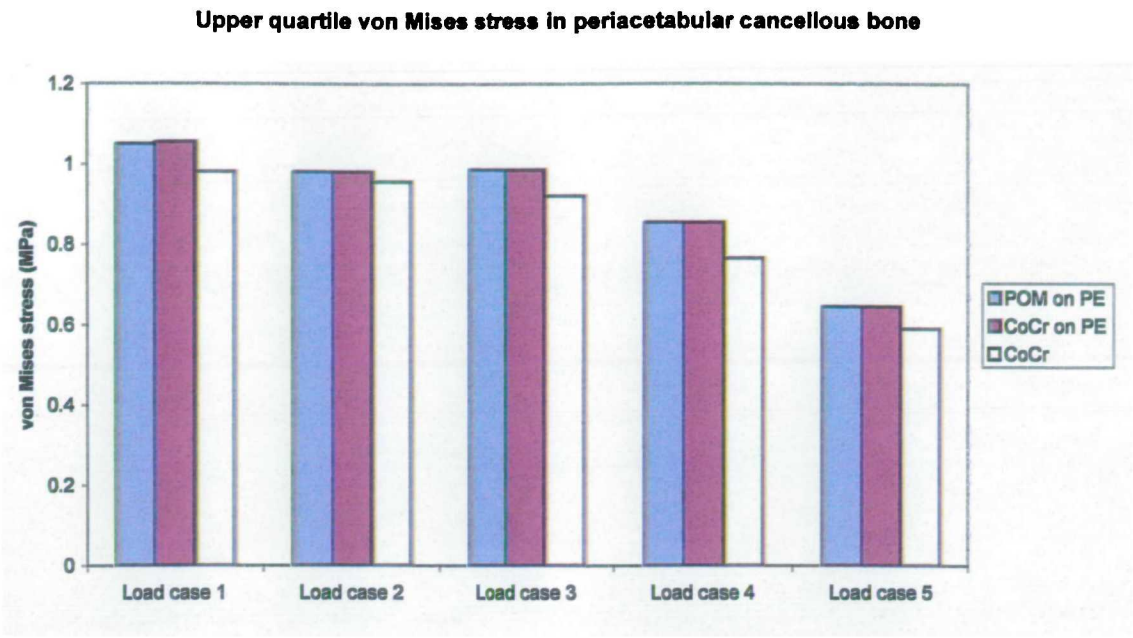

Figure 5.7.6 Upper quartile von Mises stress (MPa) in periacetabular cancellous bone.

The first and most obvious point to note is that the effect of different implant materials on the strains and stresses in the elements considered is small compared with the effect of the different joint reaction and muscle forces between different load cases. The percentage of element integration points with compressive strains larger than 0.010 (Figure 5.7.4) decreases from load case 1 to 5, while the corresponding graph of tensile strains larger than 0.008 (Figure 5.7.5) increases from load case 1 to 3 then decreases to load case 5. The percentages exceeding the compressive strain limit are greater than those exceeding the tensile limit throughout the gait cycle. There is also a smaller variation over the gait cycle in the tensile than in the compressive graph. The upper quartile von Mises stress graph (Figure 5.7.6) shows a similar trend to the compressive strain distribution and the joint reaction force, which also falls continuously over the gait cycle. However the comparison between the large fall in reaction force between load case 4 and 5 and the much smaller fall in the levels of strain failure and stresses shows that muscle forces also have a strong effect.

The CoCr acetabular cup model tends to have fewer integration points with strains outside the range $-0.010 < \varepsilon < 0.008$ over the whole gait cycle. The upper quartile von Mises stress for the CoCr acetabular cup is consistently lower than that for the other two implant combinations.

5.7.3 Peak von Mises stresses

The peak von Mises stresses in all model components are presented in this section. The graph of peak von Mises stress in the cortical bone (Figure 5.7.7) shows lower or equal stress peaks with the CoCr acetabular component. The highest peak stresses are in load cases 3 and 4 while load case 5 shows higher peak stresses than load case 1.

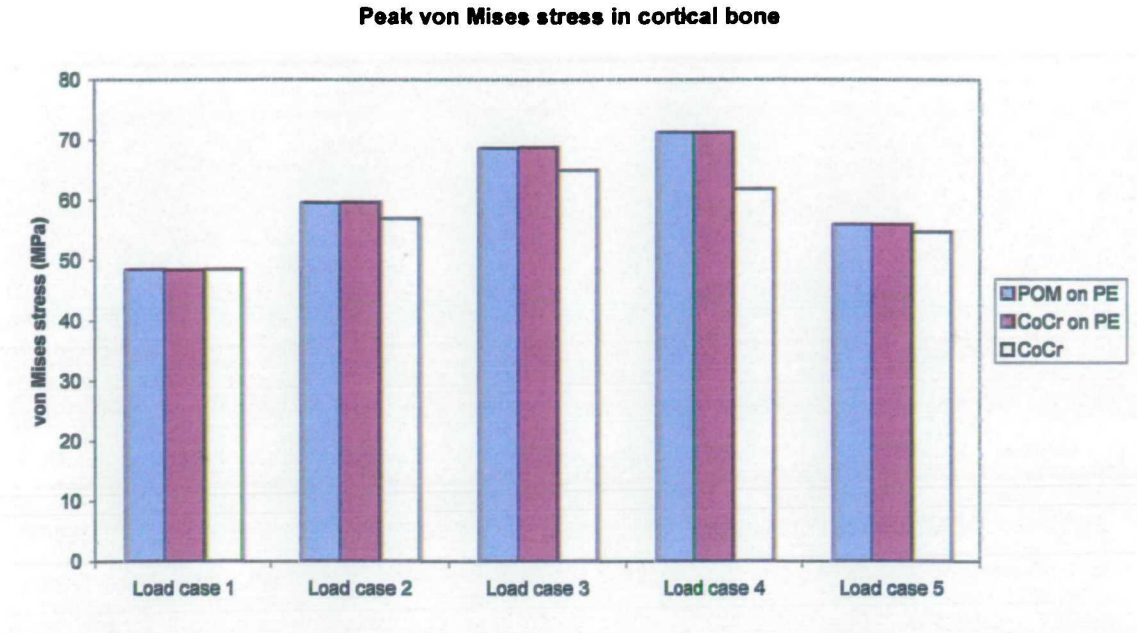

Figure 5.7.7 Peak von Mises stress (MPa) in cortical bone.

The contour plot of von Mises stress in the cortical bone (Figure 5.7.8) in the CoCr acetabular component analysis under load case 1 shows a similar stress distribution to the other implant material combinations. The highest stresses are in the region of the anterior inferior iliac spine and around the posterior inferior iliac spine. Three other areas experience stresses above 30 MPa (green in the contour plot): a small area on the medial iliac surface immediately superior to the sacro-iliac joint; a band running approximately inferior-superior from the acetabular rim on the lateral iliac surface; and the cortical bone at the superior acetabular rim.

The cortical bone stress condition under load case 4 for polyacetal on UHMWPE is illustrated in Figure 5.7.9. The peak stresses are higher, but distributed in a similar pattern to those in Figure 5.7.8 (the colour scale used in the plots is identical, but the peak stresses are different). There is little variation with different implant material combinations.

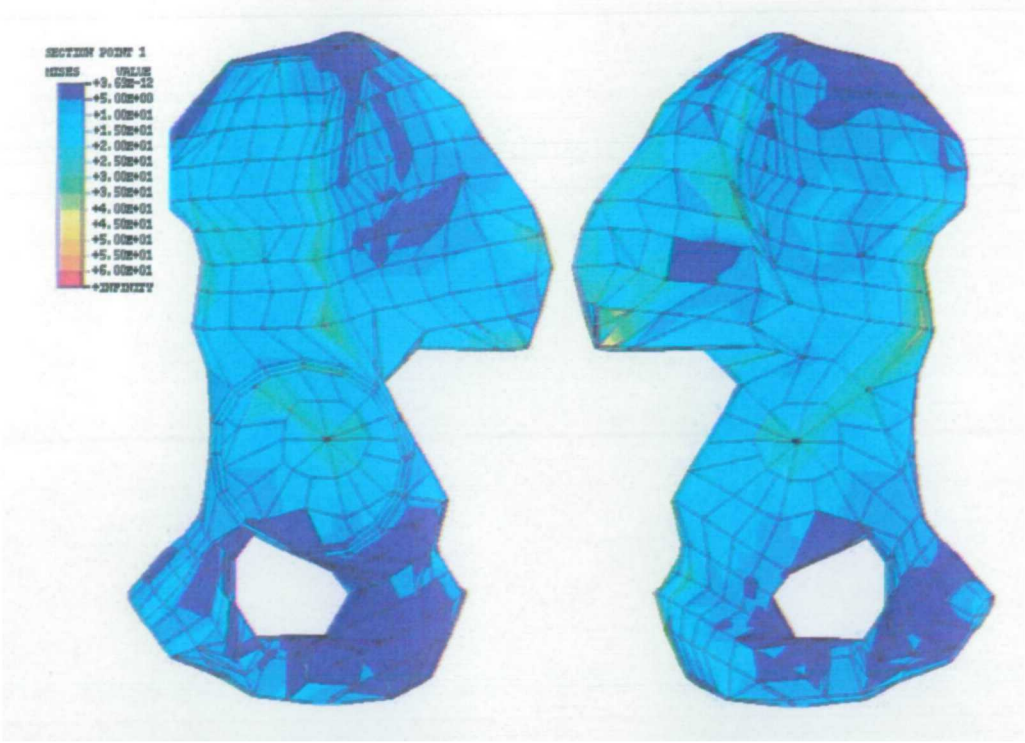

Figure 5.7.8 von Mises stress, CoCr acetabular component, load case 1. Lateral and medial aspects of cortical membrane elements.

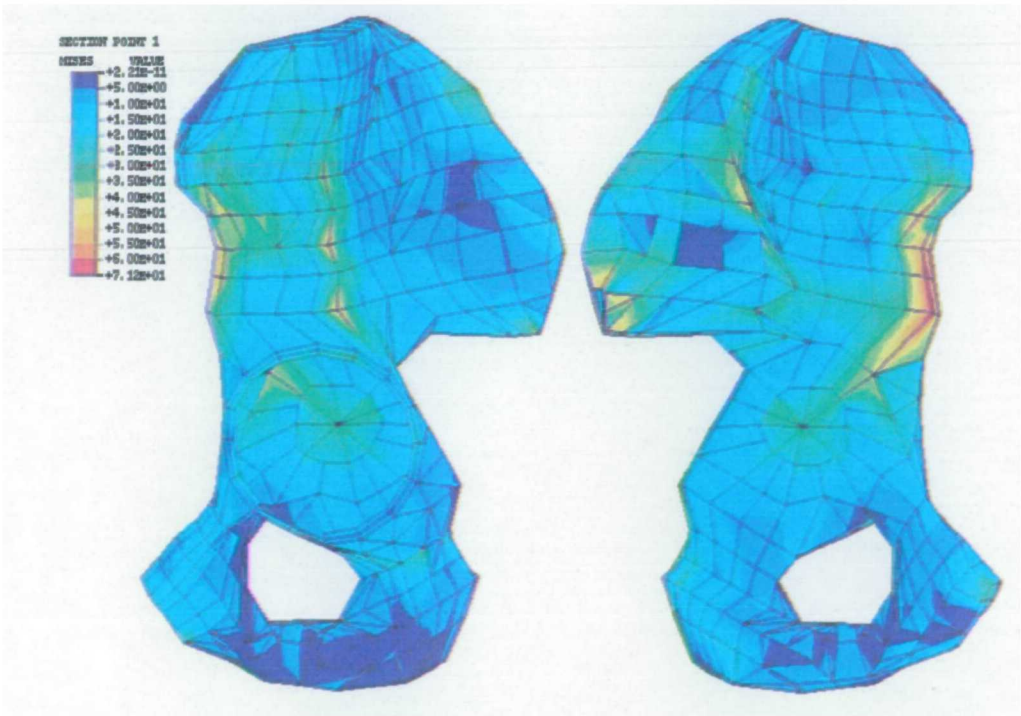

Figure 5.7.9 von Mises stress, polyacetal on UHMWPE, load case 4. Lateral and medial aspects of cortical membrane elements.

The peak von Mises stresses in periacetabular cancellous bone (Figure 5.7.10) follow a different pattern to that of the upper quartile values presented in Figure 5.7.6. The peak stresses are highest in load case 3 and there are no differences between CoCr and

polyacetal on UHMWPE combinations. The CoCr acetabular component produced the highest peak stresses in load cases 2, 3 and 5.

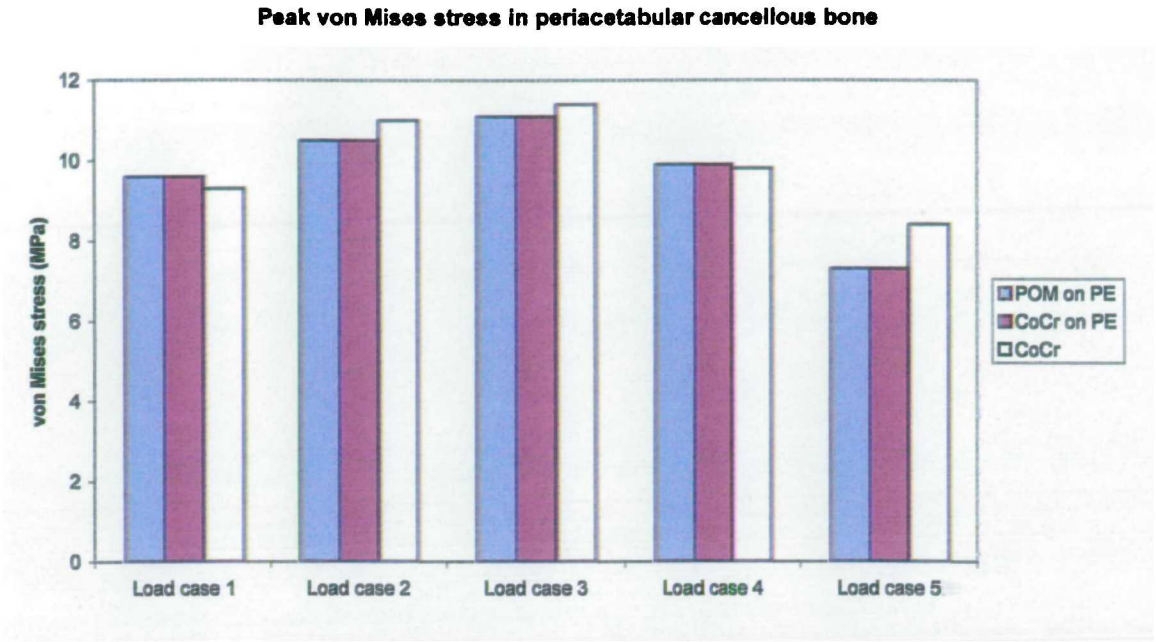

Figure 5.7.10 Peak von Mises stresses (MPa) in periacetabular cancellous bone.

The peak stresses found when all elements representing cancellous bone are considered (Figure 5.7.11) demonstrate the need for careful interpretation of FEA results. The highest stresses were found in load case 5, but visualisation of the element with the highest stresses showed that the element was badly warped. The principal stress direction in load case 5 was also the direction in which this geometry had the greatest effect in distorting the element's behaviour.

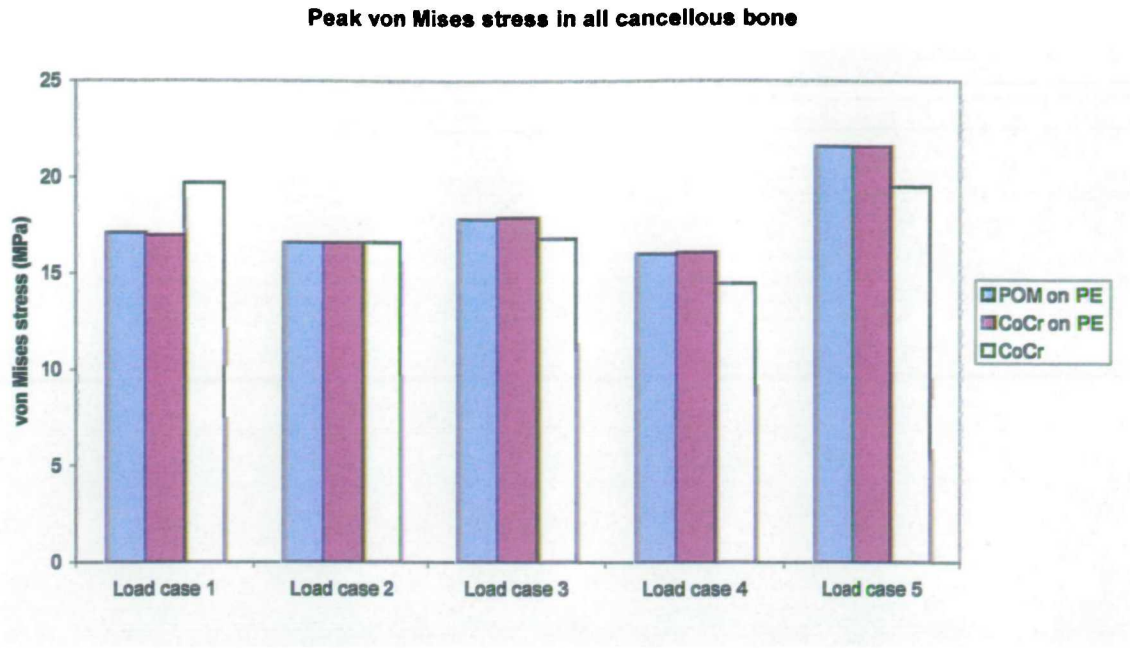

Figure 5.7.11 Peak von Mises stresses (MPa) in all cancellous bone.

Figure 5.7.12 shows the von Mises distribution in the cancellous bone for load case 3 in the CoCr on UHMWPE model. As the graphs in Figures 5.7.10 and 5.7.11 indicate there is no consistent difference between implant material combinations. The stress distributions in other load cases do not follow markedly different patterns.

Figure 5.7.12 von Mises stresses, CoCr on UHMWPE, load case 3. Lateral and medial aspects of solid cancellous elements.

The peak stresses in subchondral bone (Figure 5.7.13) are highest in load case 3. The differences between polyacetal on UHMWPE and CoCr on UHMWPE are small and the CoCr acetabular cup shows the highest stresses in all load cases except 2.

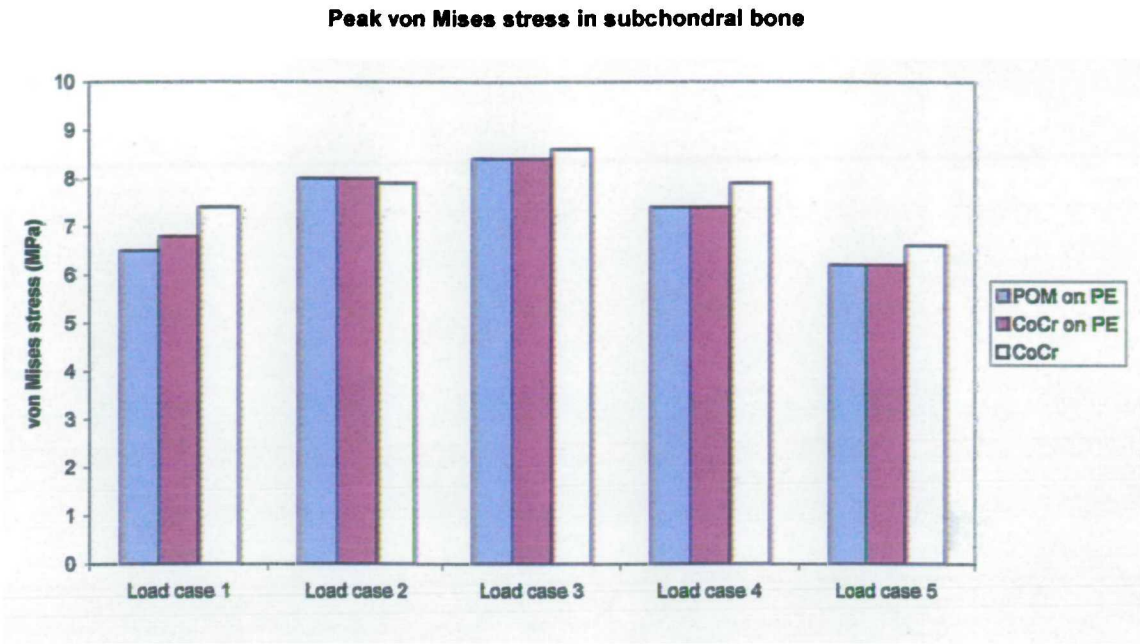

Figure 5.7.13 Peak von Mises stress (MPa) in subchondral bone.

The von Mises stress distributions in the subchondral bone show differences between implant material combinations and between load cases. Both load cases 1 and 3 with the CoCr acetabular component (Figure 5.7.16) show marked stress shielding of the bone. The areas of dark and light blue are more extensive than in either the CoCr on UHMWPE (Figure 5.7.15) or polyacetal on UHMWPE (Figure 5.7.14). In all of the material combinations and load cases the largest stresses occur in a narrow band on the supero-posterior quadrant of the acetabular rim and in a smaller patch on the anterior rim. In the CoCr acetabular component the area of slightly lower stress (green – yellow) in the acetabular dome is absent.

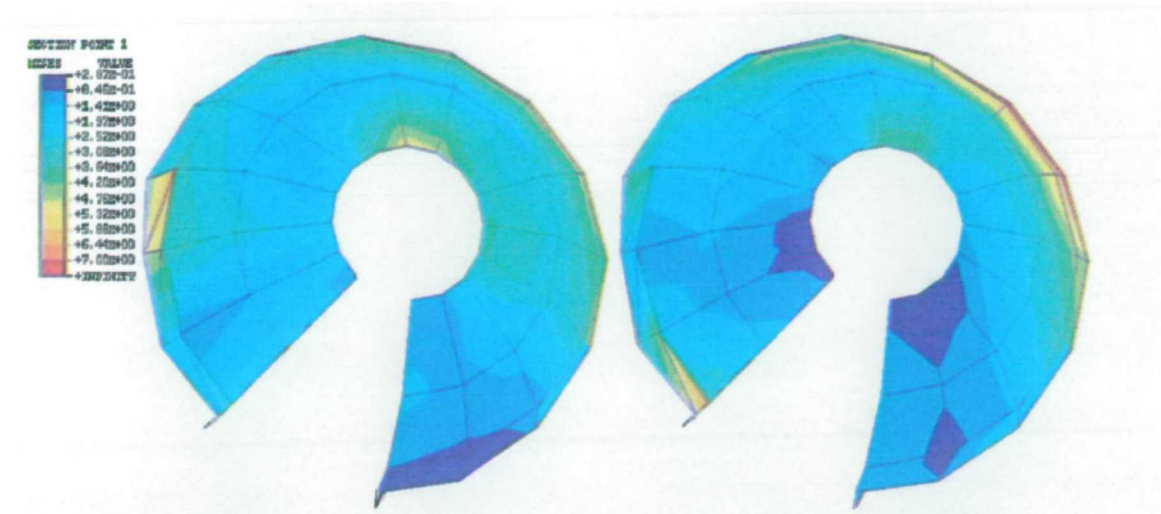

Figure 5.7.14 von Mises stress, load cases 1 (left) and 3 (right). Polyacetal on UHMWPE, subchondral bone.

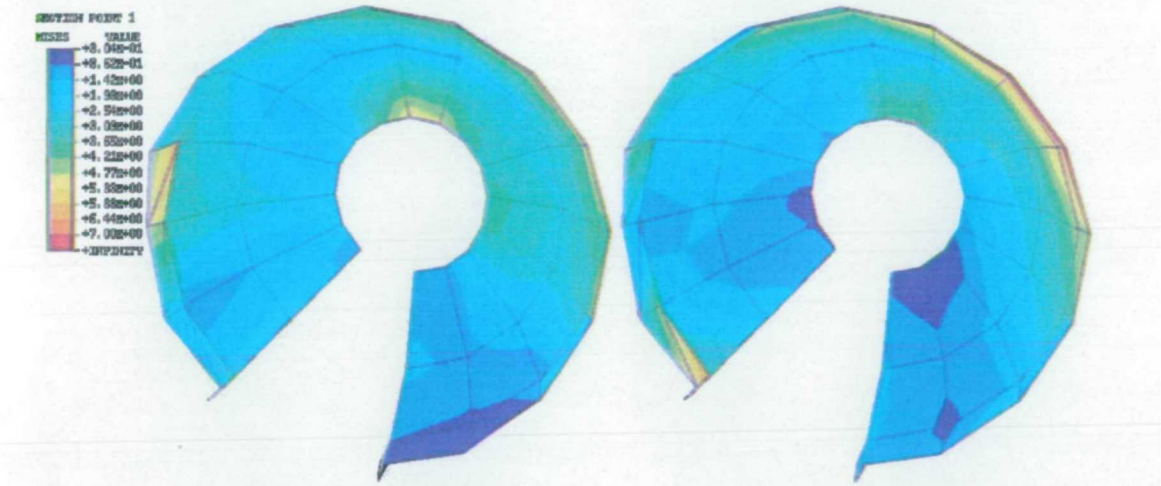

Figure 5.7.15 von Mises stress, load cases 1 (left) and 3 (right). CoCr on UHMWPE, subchondral bone.

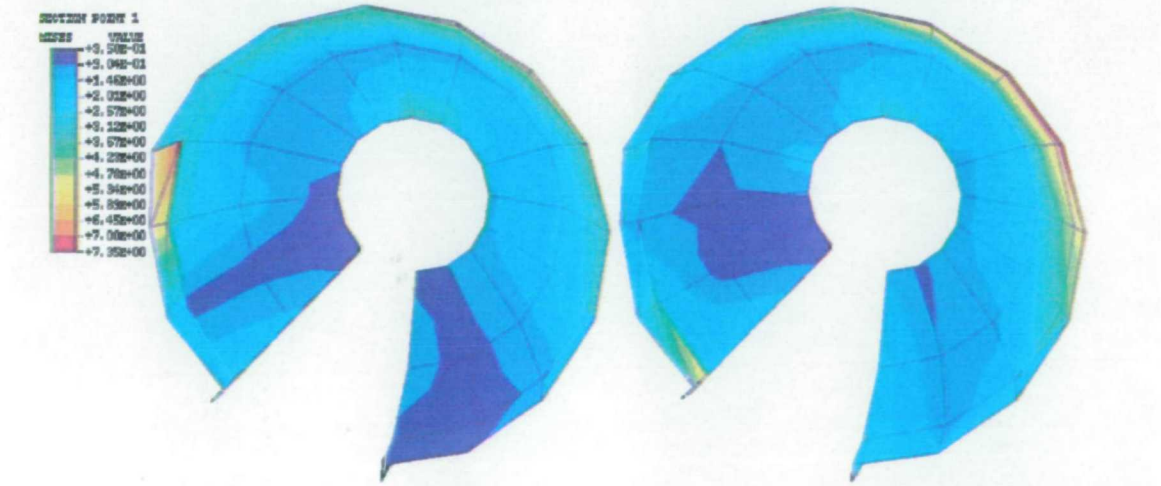

Figure 5.7.16 von Mises stress, load cases 1 (left) and 3 (right). CoCr acetabular component, subchondral bone.

The stress distributions in the polyacetal and CoCr on UHMWPE implanted hips in load case 1 most closely resemble the distributions described by Dalstra in subchondral bone of intact hips, although in Dalstra's pictures the concentrations are more anterior due to the rotation of the joint reaction force in this study (the reaction force magnitude and all muscle forces are identical). The subchondral bone in Dalstra's implanted model is largely stress-shielded unlike the subchondral bone in any of the implanted hips in this study. However the peak stresses are of similar magnitudes (6 – 8 MPa) to those found in this study.

The direction of the loading has a large influence on the von Mises stress distribution in the subchondral bone. Load case 1 (left Figure 5.7.14 and 5.7.15) shows much more loading of the acetabular dome than load case 3 for both UHMWPE acetabular cup models. However with a CoCr acetabular cup (Figure 5.7.16) the bone experiences similar amounts of stress shielding in both load cases. The change in reaction force direction shifts the area of peak stresses posteriorly around the acetabular rim.

Figure 5.7.17 shows a decrease in the peak von Mises stresses in the in-growing bone from load cases 1 to 5. While in load case 1 peak stresses in all three analyses are similar, in all other load cases the CoCr acetabular cup produces the highest peak stress. The peak stresses in CoCr and polyacetal on UHMWPE analyses are similar in all load cases.

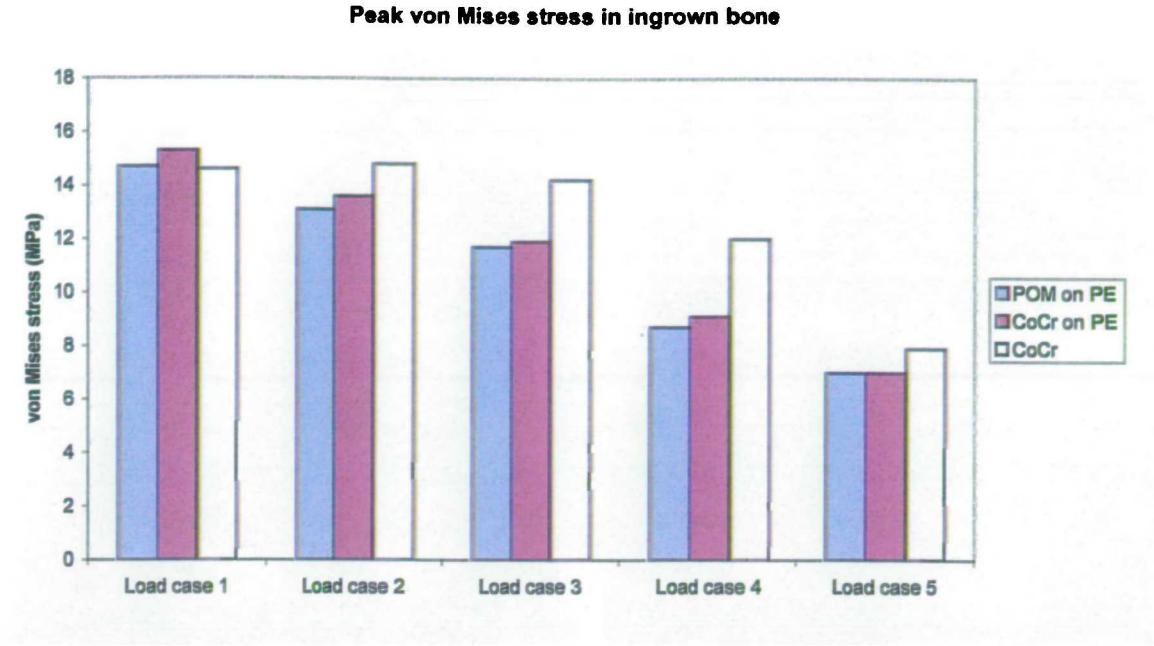

Figure 5.7.17 Peak von Mises stresses (MPa) in in-growing bone.

Figures 5.7.18 to 5.7.21 present contour plots of the in-growing bone. The highest stresses in load case 1 of all three implant material combinations are in a patch around the locus of the joint reaction force. In load cases 3, 4 and 5 the highest stresses, seen in the CoCr acetabular component analyses, are at the posterior edge of the acetabular rim.

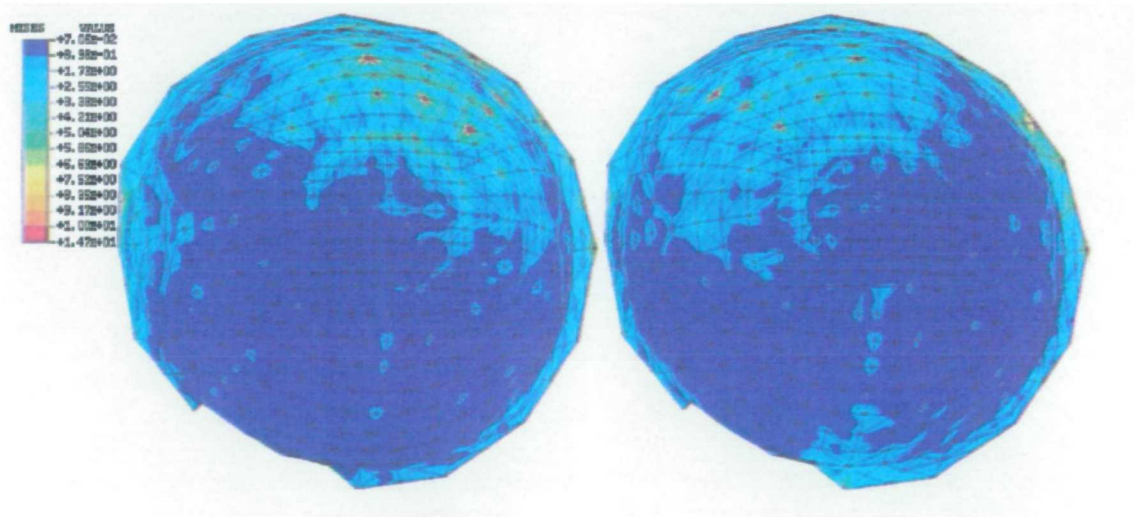

Figure 5.7.18 von Mises stress, polyacetal on UHMWPE, load cases 1 (left) and 3 (right). Ingrowing bone.

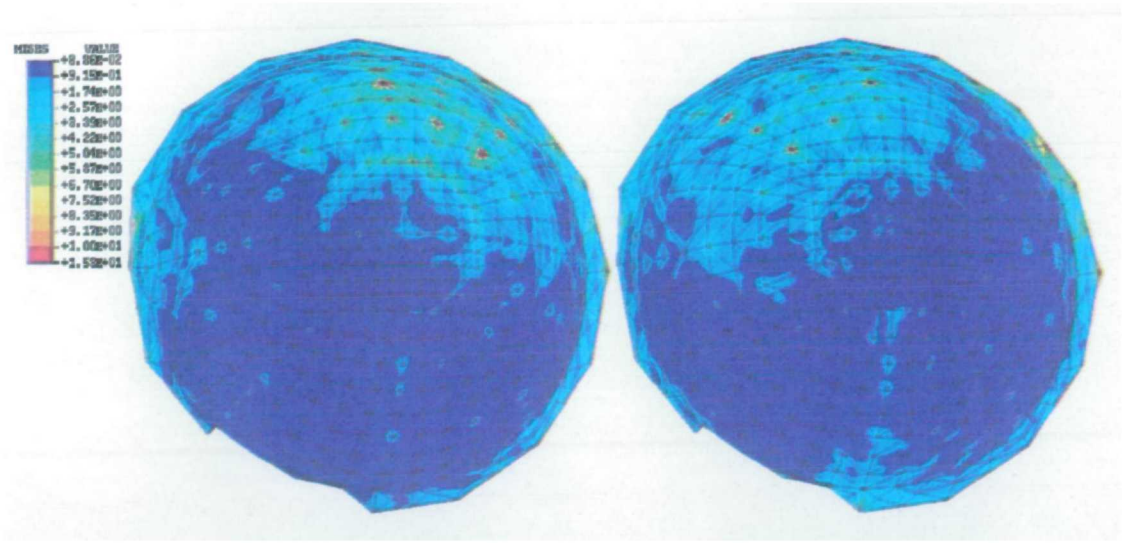

Figure 5.7.19 von Mises stress, CoCr on UHMWPE, load cases 1 (left) and 3 (right). Ingrowing bone.

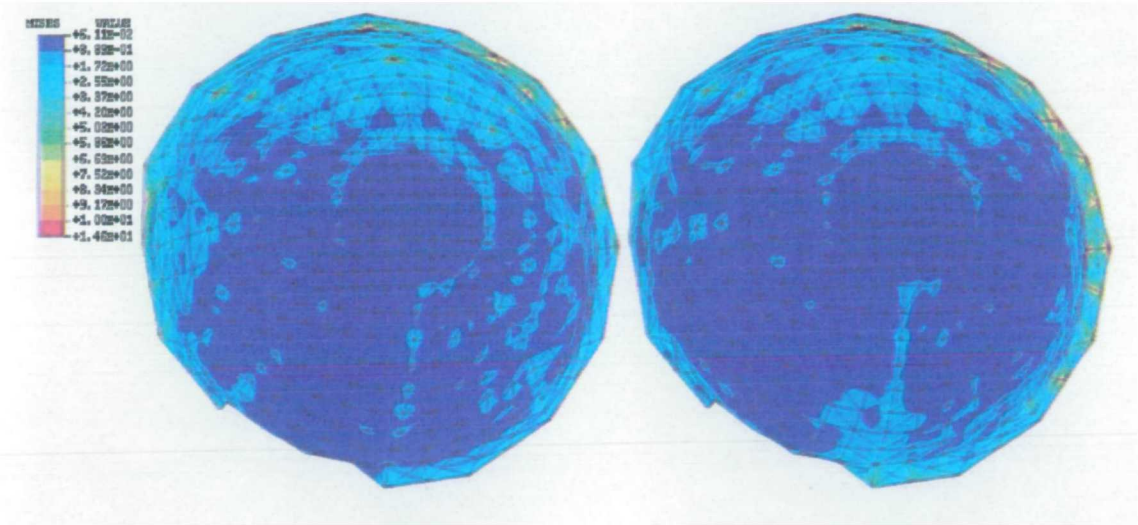

Figure 5.7.20 von Mises stress, CoCr acetabular component, load cases 1 (left), and 3 (right). Ingrowing bone.

The peak von Mises stresses in the CoCr femoral component (Figure 5.7.21) are higher than those in the polyacetal component except in load case 5.

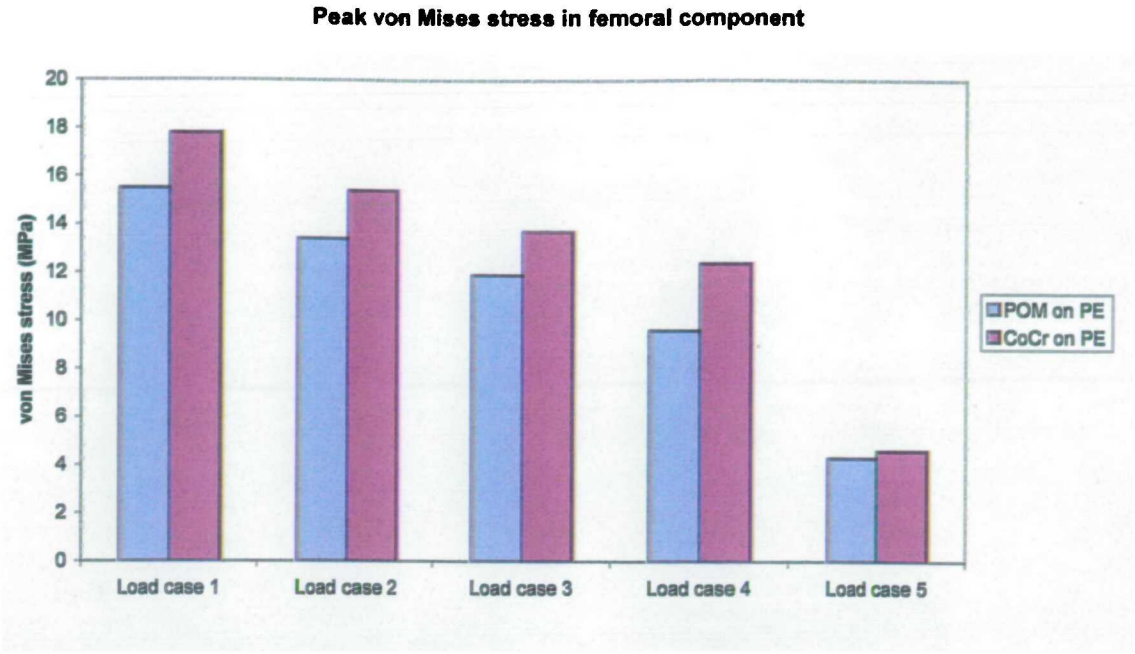

Figure 5.7.21 Peak von Mises stresses (MPa) in femoral component.

Figure 5.7.22 shows a contour plot of a polyacetal femoral component for load cases 1 and 5. Load case 1 shows the stress concentration at the rim of the component (15 MPa).

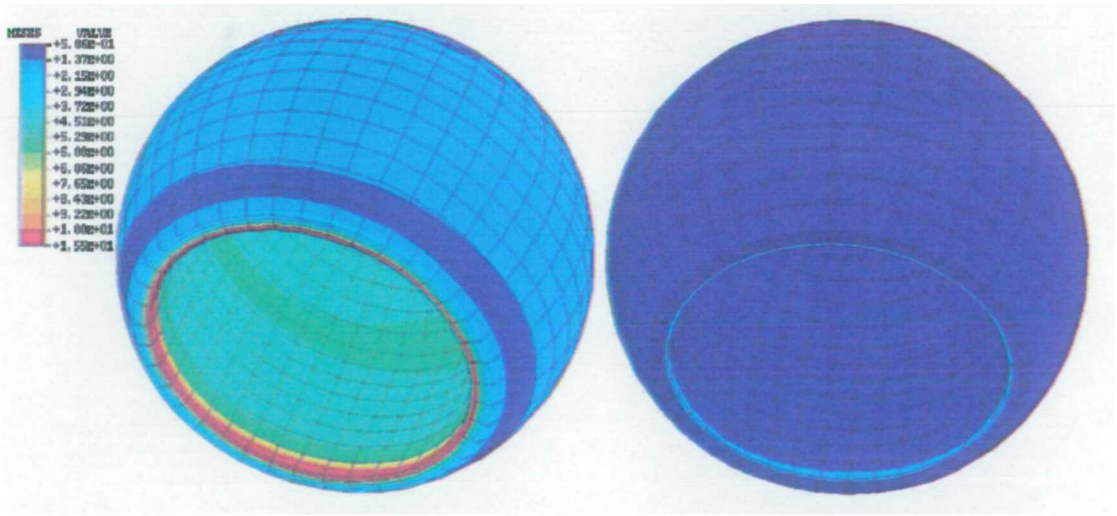

Figure 5.7.22 von Mises stresses, POM on UHMWPE, load cases 1 (left), and 5 (right). Femoral component.

The peak von Mises stresses in the acetabular component (Figure 5.7.23) are highest in load case 1 and decrease to load case 5. There is no consistent pattern of difference between implant material combinations, although the stresses in the CoCr on UHWMPE analysis are highest in load cases 1, 2 and 4 and those in the CoCr acetabular cup analysis are highest in load cases 3 and 5.

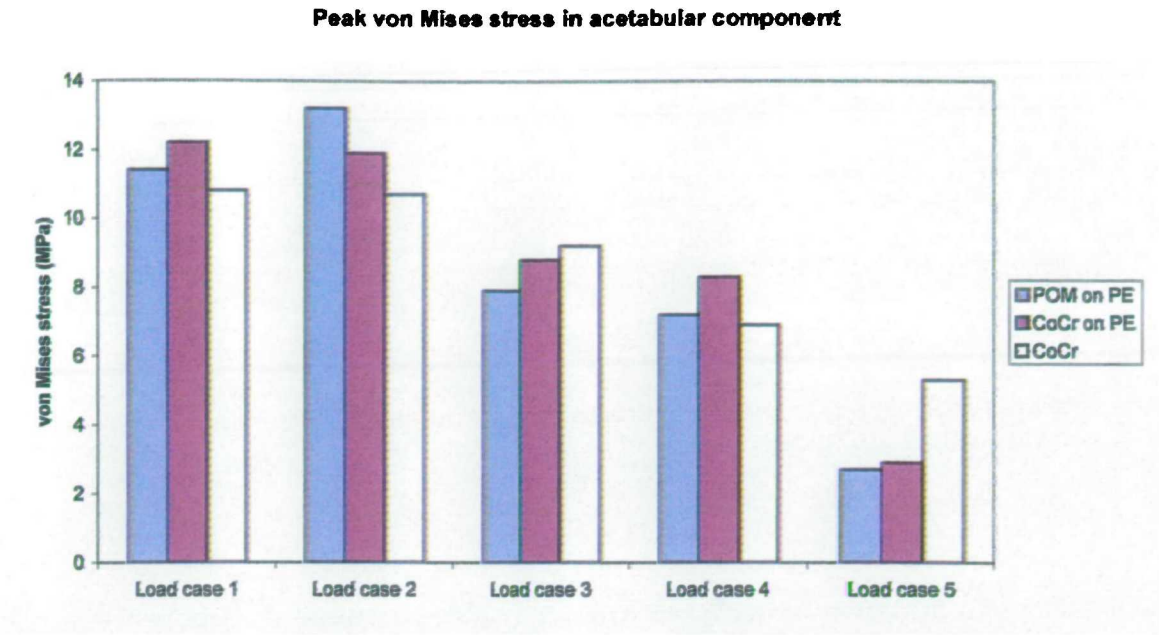

Figure 5.7.23 Peak von Mises stresses (MPa) in acetabular component.

The contour plots of the von Mises distribution in the acetabular components however show large differences between implant material combinations. The articulation surfaces of the two cups in the contact studies (polyacetal on UHWMPE and CoCr on UHMWPE) show a blotchy pattern due to the discretisation of the spherical surfaces (Figures 5.7.24 and 5.7.25), while the CoCr cup is loaded as if with a perfect rigid match to the cup surface and shows a smoother distribution (Figure 5.7.26). The stresses around the rim of the cups are indicative of the load transfer to the surrounding bone. The CoCr cup shows large areas of high stress at the superior rim edge suggesting that most of the load is transferred directly to the cortical bone at this point. The two UHMWPE cups show much lower stresses at the rim suggesting that the load is transferred over a larger area to the subchondral and cancellous bone in the acetabulum. The higher periacetabular cancellous bone stresses found in the two contact studies confirm this view.

The rotation of the joint reaction force between load cases 1 and 5 is clearly demonstrated in all the plots and in the two contact studies the stress distribution in load case 5 mimics the shape of the intact acetabular lunate surface.

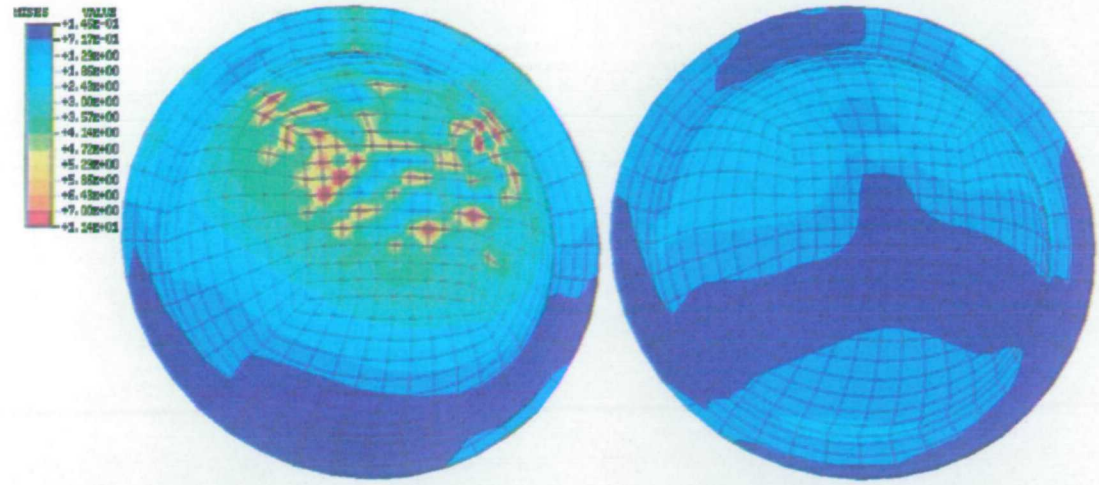

Figure 5.7.24 von Mises stresses, POM on UHMWPE, load cases 1 (left) and 5 (right). Acetabular cup.

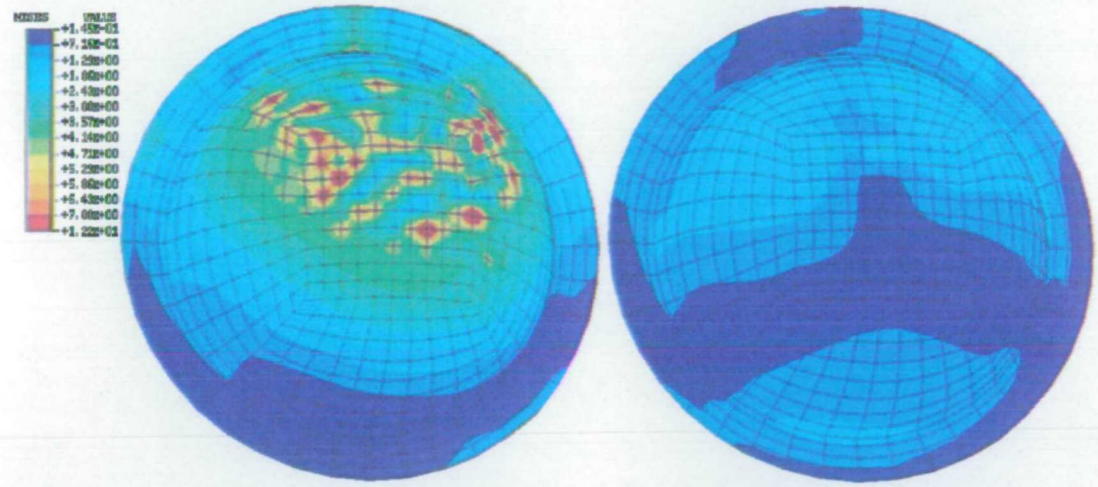

Figure 5.7.25 von Mises stresses, CoCr on UHMWPE, load cases 1 (left)and 5 (right). Acetabular cup.

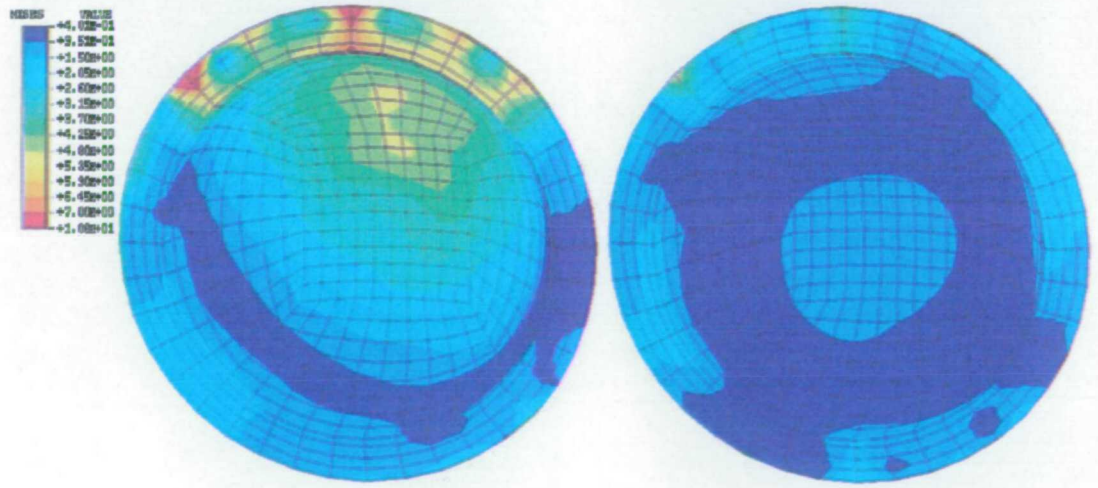

Figure 5.7.26 von Mises stresses, CoCr acetabular component, load cases 1 (left) and 5 (right). Acetabular component.

5.7.4 Fixation assessment

This section presents the results of studies investigating the effect of fixation of the acetabular component on the stress and strain distributions in the surrounding bone. All of the parameters reported for the previous studies are included as well as the normal and tangential relative motions at the cup – bone interface.

Table 5.7.3 Relative implant – bone motion. % < 100 μm gap is the percentage of contact nodes with interface gaps smaller than 100 μm. % < 40 μm tangential is the percentage of contact nodes with interface tangential motion smaller than 40 μm. μ is the friction coefficient.

Interface motions	UHMWPE μ = 0.1	UHMWPE μ = 0.5	CoCr μ = 0.1	CoCr μ = 0.5
Max tangential (μm)	450	310	430	300
Max gap (μm)	220	130	210	130
% < 100 μm gap	93.42	98.64	94.10	98.19
% < 40 μm tangential	1.13	13.38	0.45	10.88

The locations of the maximum and minimum tangential motions at the cup – bone interface are displayed in the contour plots in Figures 5.7.27 and 5.7.28. The normal or gap motions are displayed in Figure 5.7.29. These plots are for the CoCr cup with a friction coefficient of 0.1, but the distribution patterns are representative of other material and friction coefficient combinations. The total tangential motion reported in Table 5.7.3 is simply the square root of the sum of the squares of the two orthogonal slip magnitudes plotted in Figures 5.7.27 and 5.7.28. The maximum tangential motion is in the infero-posterior quadrant of the acetabulum while the maximum normal motion is in the infero-anterior quadrant of the acetabulum. Changing the implant-bone interface friction coefficient has a much greater effect on both normal and tangential micromotion than does implant material.

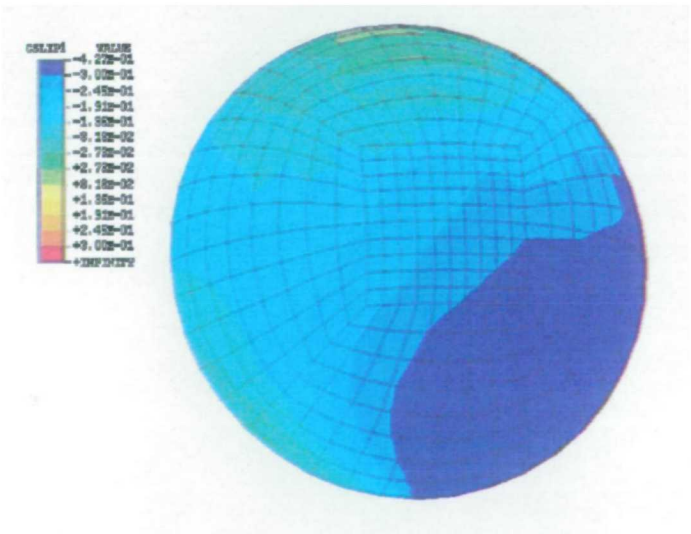

Figure 5.7.27 CoCr cup, low friction. Tangential relative motion at the contact surface (first slip direction). Green areas are static, dark blue indicates largest motion.

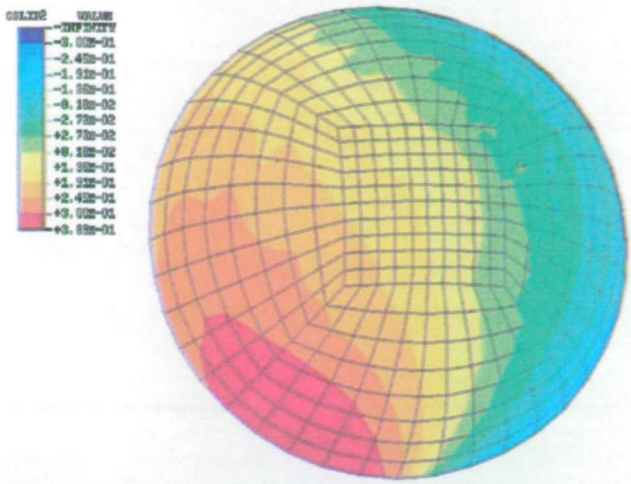

Figure 5.7.28 CoCr cup, low friction. Tangential relative motion at the contact surface (second slip direction). Green areas are static, red indicates largest motion.

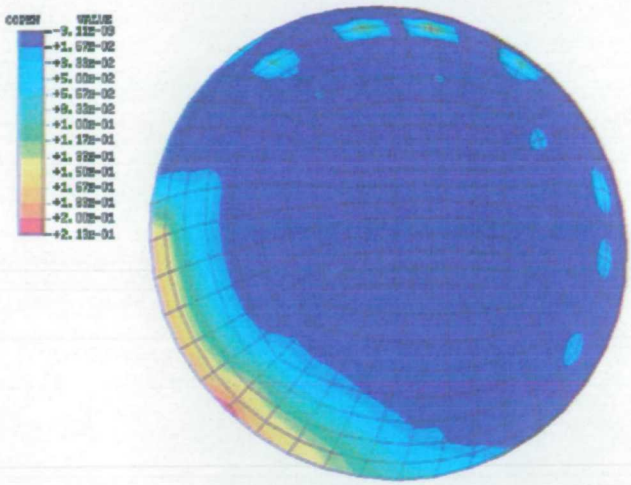

Figure 5.7.29 CoCr cup, low friction. Contact gap magnitude. Red is largest gap, blue indicates intimate contact.

Table 5.7.4 Stress and strain results for fixation studies. % ε < -0.010 and % ε > 0.008 are the percentages of integration points in periacetabular cancellous bone elements with strains outside the –0.010 < ε < 0.008 limits. % at risk is the sum of these two values. Mises 75% is the upper quartile value of von Mises stress in the periacetabular cancellous bone. μ is the friction coefficient. Peak σ are the peak von Mises stresses reported by model component.

	UHMWPE μ = 0.1	UHMWPE μ = 0.5	CoCr μ = 0.1	CoCr μ = 0.5
% ε < -0.010	17.4	16.2	17.6	16.2
% ε > 0.008	7.3	6.8	7.2	6.8
% at risk	24.7	23.0	24.8	23.0
Mises 75%	1.15	1.09	1.16	1.09
Peak σ / MPa				
Cortical	48.4	47.7	48.4	47.5
Cancellous	16.7	13.1	16.6	13.0
Subchondral	7.9	6.2	7.9	6.3
Acetabular cup	7.9	7.5	11.9	11.2
Peak contact σ / MPa	3.7	2.9	4.7	3.7

All four un-bonded scenarios analysed show larger percentages of compressive strains below -0.010 than the corresponding fully bonded analyses (Table 5.7.4). The

percentages are lower in the de-bonded models with a higher friction coefficient. There are smaller differences in percentages of tensile strains exceeding 0.008, but the high friction de-bonded cups show the lowest of these, with very little difference apparent due to implant material.

Peak von Mises stresses are similar to those found for load case 1 with fully bonded interfaces except for those in the subchondral bone, where the stresses are higher in the de-bonded cases.

The plot of the von Mises stress distribution in the subchondral bone under a CoCr acetabular cup (Figure 5.7.30) is similar to that with an UHMWPE cup with the same friction coefficient. There is an area of higher stress near the centre of the acetabulum which is less marked in the plot of the fully bonded situation (Figure 5.7.16), but in other respects the distributions are similar. The distribution patterns in the analyses using a friction coefficient of 0.5 with both UHMWPE and CoCr cups are similar, although the stress magnitudes are lower.

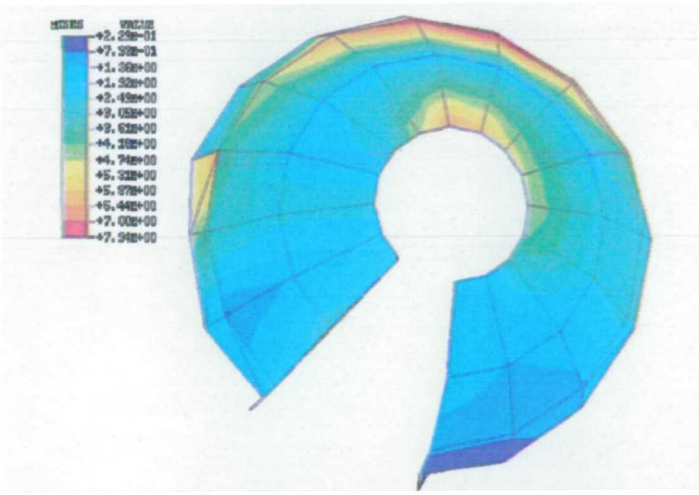

Figure 5.7.30 CoCr cup, low friction. Von Mises stresses in subchondral bone.

5.8 Discussion

5.8.1 Bearing behaviour

The contact pressures, areas and gaps for a polyacetal on UHMWPE resurfacing are not significantly different from those calculated for a CoCr on UHMWPE resurfacing. Such differences as are apparent are not consistent over the five load cases considered.

In contact analyses of conventional hip replacement Mantell *et al.* (1998) found contact stresses of between 6.0 and 11.4 MPa depending upon clearance between

articular surfaces, femoral head size and fixation conditions. Thus contact stresses in a polyacetal on UHMWPE resurfacing are of a similar magnitude to those in conventional THR.

Hodge *et al.* (1989) recorded contact pressures *in vivo* with an instrumented hemi-prosthesis of up to 18.0 MPa with peak values decreasing to 9.7 MPa three years postoperatively. The conditions between the head of a hemi-arthroplasty and intact acetabular cartilage may be closer to those in an intact hip than those between the surfaces of a total implant. However these data indicate that the hip joint is able to tolerate far higher pressures in the joint fluid than will be produced with any resurfacing implant.

Jin *et al.* (1997) predicted contact half-widths of 3 – 4 mm for radial clearances similar to those achieved in metal-on-metal resurfacing (50 – 100 μm). This implies contact areas of less than a tenth of those found in polyacetal and CoCr on UHMWPE.

The rim of the acetabular cup was significantly involved in the contact behaviour of both CoCr and polyacetal on UHWMPE resurfacings. Any study of the tribology of these resurfacing implants must take into account this reduction in contact area. Special attention must be paid to the design of the rim of resurfacing acetabular components.

5.8.2 Periacetabular cancellous bone

The CoCr acetabular cup consistently showed slightly lower percentages of strains outside the -0.010 to 0.008 range as well as lower von Mises stress levels in cancellous bone close to the acetabulum. This result can be attributed to a shift in the load transfer pattern, with a stiffer acetabular component more of the load is transferred directly to cortical bone. Except in load case 5, there is little difference in peak von Mises stresses between the models.

The implication of these results is that an acetabular cup made from CoCr will migrate and loosen less rapidly than one made from UHMWPE. However the FE model assumes that there is perfect bonding between the acetabular cups and the subchondral bone at the acetabular rim allowing direct transfer of the load from the cup to the cortical bone. In practice perfect bonding will not be achieved and so more load will be transferred to cancellous bone from the acetabular cup. The four analyses

performed to investigate the motions at the interfaces of completely de-bonded acetabular cups showed that the percentages of cancellous bone strained outside the -0.010 to 0.008 range and the levels of the von Mises stresses with a CoCr cup were higher or equal than those with an UHMWPE cup. The higher levels of compressive strain failure than in fully bonded analyses indicate that the load is transferred mainly to cancellous bone.

If up to 25% of all cancellous bone volume were to fail on first loading of a resurfacing implant, as is predicted by this model, then the implant would clearly not be suitable for clinical use. However CoCr acetabular resurfacing components are in clinical use and do not suffer catastrophic failure or even fast migration. Although some resurfacing patients are placed on a restricted load bearing regime post-operatively resisted muscle contraction exercises have been shown to produce as high a joint contact pressure as early post-operative walking (Hodge *et al.,* 1989). Therefore the model and the failure criteria used have overestimated the amount of cancellous bone failure, this may be due to badly shaped elements.

Taylor *et al.* (1995) and New (1997) both used stress based criteria to predict the failure of cancellous bone and hence the likely migration rate of an implant. However both used ultimate stresses calculated from linear regression relationships between the cancellous bone stiffness and strength. These are therefore effectively strain-based criteria. The isotropic asymmetric failure strains found by Chang *et al.* (2000) supersede these earlier regression relations and allow a more accurate method of determining bone failure. Keyak and Rossi (2000) compared nine stress and strain based failure theories in their model of femoral fracture. All the failure criteria predicted fracture loads that correlated significantly ($p \leq 0.001$) with experimentally measured loads. However they found that strain based criteria were not the most robust at predicting bulk fracture. They attributed this to the complex triaxial stress state and the presence of cortical bone in their model in contrast with the simple biaxial conditions in trabecular bone test specimens.

The patterns of von Mises stress distribution in the cancellous bone in the acetabular region are similar to those found by Dalstra (1993) in a model of the pelvis implanted with a conventional THR. Given that the majority of the reaction force load is transferred to the cortical bone in both Dalstra's model and in the models presented here this is not surprising.

5.8.3 Peak von Mises stresses

The peak von Mises stresses in the rest of the model also did not differentiate the CoCr on UHMWPE from the polyacetal on UHMWPE implant. However there were differences in stress magnitudes and distributions between these two implants and the CoCr acetabular cup implant. Peak stresses in cortical bone in the CoCr acetabular cup model were higher than peak stresses in the other two models for all load cases except the first for which they were equal. The stress distributions in the cortical bone are similar to those found by Dalstra (1993). The largest areas of peak stress in Dalstra's implanted model of the pelvis were on the lateral face in the region of the sciatic notch, while in the present models the highest stresses were found near the anterior inferor iliac spine. Dalstra found higher stresses in the cortex of the pubis bone than those reported in this study at all stages during the gait cycle. This is probably due to the slightly different hip joint reaction force direction used, calculated from the gait data of Stansfield (2000). The maximum stress predicted, 71.2 MPa, is below reported values of cortical bone ultimate strength (section 2.1.4), but may exceed fatigue strengths which are reported between 40 and 80 MPa at 10^7 cycles (Currey, 1998). However bone responds to overload by remodelling to reduce stresses and with approximately 10^6 cycles expected per year for a THR patient (Wallbridge and Dowson, 1982) these fatigue strengths correspond to a 10-year fatigue life, giving ample time for remodelling to occur.

The peak stresses in the cancellous bone of the whole model do not show any consistent differences between implant material and surprisingly predict the highest peak stress for the case with the smallest joint reaction force. However the stress distributions in the cancellous bone under the acetabular subchondral bone were visibly altered both by changes to the direction of the joint reaction force and in the implant material. The patch of higher stresses in this bone followed the posterior to anterior sweep of the joint reaction force. The effect of implant material has been discussed in the previous section. The location of the peak stress was similar to that in the implanted Dalstra model. Unfortunately Dalstra did not report the magnitudes of peak stresses in the cancellous bone in his model. The peak magnitudes found in the current models (up to 20 MPa) are rather high and may be due to distorted elements.

The subchondral bone showed the most interesting changes in stress magnitude and distribution between load cases and implant materials. The stress shielding effect of

the CoCr acetabular component on the dome of the acetabulum is clear from the comparison of contour plots. The substantially lower joint reaction forces in the later stages of the gait cycle produce stress peaks of similar magnitude to those in the earlier stages, but concentrated in a smaller area. This shows that these later stages of gait are as important in the design of an implant as those at the joint reaction force maxima.

The peak stresses in the layer of ingrowing bone between the acetabular cup and the subchondral bone showed a pattern that was more obviously related to the magnitude of the joint reaction force. The effect of the CoCr acetabular component was to increase the stress concentrations in this bone, mainly at the acetabular rim, in the later stages of the gait cycle.

Load case 3 produced some of the highest peak stresses found in the study. The gluteus medius muscle force is at its peak in this load case. Although the joint force is not at a maximum it produces the highest levels of tensile strain failure in the periacetabular cancellous bone. The direction of the joint force in this load case is near vertical. Latour and Brattain (2000) recently showed that the most severe test of a femoral component's performance was in the later stages of gait rather than at the moment of peak joint reaction force.

The material of the femoral component had an effect only on the peak stresses in the component itself and in the underlying cancellous bone. The polyacetal component, as expected, produced less stress shielding of this bone and reduced stress concentrations at the rim where most of the load was transferred. The maximum stresses recorded in the polyacetal femoral component was 15.5 MPa, while a fatigue limit for polyacetal was 30 MPa measured at 10^7 cycles in water at 23°C and 30 Hz (Brydson, 1993). In their study of a CoCr femoral resurfacing component, Watanabe *et al.* (2000) found stress shielding and stress concentrations of up to 170 MPa at the rim of the component.

The results for the acetabular component did not show consistent differences in peak stresses between different implant material combinations. This may be due to the lack of smoothness of load transfer over the contact patch. The maximum stress of 13.2 MPa occurs on the bearing surface at the contact patches. The stresses here are high due to the non-smooth contact surfaces, but 13.2 MPa is well within the static failure

limit for UHMWPE. Some fatigue softening may occur (Krzypow and Rimnac, 2000), but the compressive stresses found at the surface are less damaging than tensile stresses.

The distribution of stress on the rim of the acetabular cups did show differences between implant material combinations. The CoCr cup showed stress concentrations on the superior rim which neither of the UHMWPE cups displayed. This confirms that the CoCr cup transferred most of the joint reaction force directly to cortical bone, whereas the UHMWPE cups distributed the load more evenly producing higher stresses and strains in the periacetabular cancellous bone. *In vivo* perfect implant-cortex bonding is unlikely to occur, but it is likely that a stiff cup would load cortical bone rather than periacetabular cancellous bone. However it is not clear whether cortical based load transfer would be preferable to load transfer to the cancellous bone in the long term. Stress shielding of the acetabular cancellous bone would result in its gradual resorption which would complicate revision to cemented conventional THR.

5.8.4 Fixation assessment

The effect of bone-implant interface friction on both normal and tangential micromotions is much larger than that of implant material. This suggests that until the real friction coefficient at the interface is measured precisely models investigating interface micromotions using FEA will not provide useful solutions. However it is expected that rougher interfaces with higher friction coefficients will give rise to lower stresses due to a greater portion of load being transferred across the interface by shear. Spears *et al.* (2000) used a friction coefficient of 0.5 in their model of acetabular bone implant micromotions while New (1997) used a value of 0.25. Taylor *et al.* (1995) used femoral stem friction coefficients varying from 0 to 0.4 and found no further reductions in cancellous bone stresses by increasing μ above 0.3.

While the study reported here only measured the micromotion that occurred between an unloaded state and one loaded state, Spears *et al.* (2000) investigated relative and absolute motion throughout the gait cycle. They reported a combination of literature values that suggested that ingrowth would occur at a particular point along the bone-implant interface if:

i) there was less than 40 μm relative tangential motion

ii) the bone-implant gap decreased to less than 100 μm during the gait cycle

iii) the bone-implant gap did not increase beyond 500 μm at any point during the gait cycle.

Using these criteria for the single case investigated here suggests that the tangential motion will prevent ingrowth occurring in up to 90% of the interface area with high friction and up to 99% with low friction. The criteria concerning maximum normal or gap motion are far less strict for this single case, but may be more important for the rest of the gait cycle.

Spears *et al.* (2000) predicted bony ingrowth only over a relatively small area of the interface along the posterior rim of the acetabulum. This conflicts with the finding in this study that tangential micromotions are largest in the infero-posterior quadrant of the interface. However this result again must be considered in the context of motion over the whole gait cycle for proper comparison.

5.8.5 Limitations

The model presented here did not include an elastic-plastic model of bone failure. The badly shaped elements in the model would have failed prematurely producing large inaccuracies. Therefore this model does not simulate the change in load transfer that would occur due to the failure of the over-strained elements. Hence these results also underestimate the volume of cancellous bone at risk.

Many of the shortcomings of this analysis have been attributed to poor element shape. The analysis could have been carried out with an FE model developed especially for this purpose which would have provided more accurate and reproducible results. However the development of an FE model of the pelvis is a lengthy and involved process. Secondly comparisons with the published results of the model (Dalstra, 1993) are beneficial.

While Dalstra validated the original FE model of the pelvis by mechanical testing of the strain gauged cadaveric pelvis on which it was based (Dalstra, 1993), the model implanted with a resurfacing replacement reported in this chapter has not been validated by mechanical testing. Exact validation of the resurfacing model with the original pelvis is impossible without access to the original specimen. However the distributions and magnitudes of the stresses and strains found using the resurfacing model are sufficiently similar to those reported by Dalstra for the pelvis implanted

with a conventional hip replacement that further validation is not considered essential, although it would be beneficial and increase confidence in the model.

5.9 Conclusions

In comparison with the results of FE studies of conventional THR and the intact hip joint the model presented performed well. The patterns of stress and strain distribution in bone around the acetabular prosthesis and their magnitudes were similar to those previously reported (Dalstra, 1993). The model suggests that the acetabular component of the novel implant design presented in this thesis will perform less well, migrating faster and requiring revision earlier than resurfacing implants in current clinical use. However this prediction is based upon a model which hugely overestimates cancellous bone failure in the implanted pelvis. Further, the stiffer CoCr cup transfers load directly to the cortical bone at the superior acetabular rim, which may lead to poor acetabular cancellous bone quality at subsequent revision procedures. Further work is required to be able to accurately model the effect of over- or under-load on the acetabulum.

The polyacetal femoral component reduced stress shielding and stress concentrations on the bone of the femoral head and neck remnant and so would be expected to migrate more slowly and have a better long-term outcome than a CoCr femoral component.

At the contact surfaces the stresses found were comparable with those in simulations of conventional THR. Contact took place over a large area and was frequently affected by the implant rim.

The most severe test for the performance of acetabular components appears to be not at the moment of peak joint reaction force but shortly after mid-stance.

The micromotions between press-fitted acetabular components and bone were largest in the infero-posterior quadrant of the acetabulum and would prevent bone ingrowth from occurring over 90% of the interface. The tangential motions were more effective than normal motions in preventing ingrowth. Therefore the use of fixation pegs or fins preventing this motion is necessary for bone ingrowth fixation to be viable in this prosthesis.

6. Mechanical Testing of polyacetal

6.1 Introduction

While polyacetal is a well known engineering polymer and has been used previously in orthopaedic implants, there is little data on the effect of long-term exposure to the physiological environment on its mechanical properties. The aims of this study were twofold: to characterise the static mechanical properties of polyacetal before and after one and six months immersion in Ringer's solution and to use these properties to differentiate between homo-polymer and co-polymer grades.

6.2 Materials

Five samples of polyacetal sheet extrusion were obtained and machined to standard tensile testing specimens (Figure 6.2.1). The polyacetal samples obtained were: co-polymer from BASF ("Ultraform" or "Pomalux"), homo- and co-polymers ("Ertacetal") from DSM and homo- ("Delrin") and co-polymers from Du Pont. None of the polymer samples obtained was "medical grade". However the sample of BASF co-polymer was identical to material supplied to Corin Medical for the manufacture of orthopaedic instrument handles except for the more stringent lot control applied to the medical material. All of the polymers were unpigmented and unfilled.

Flat dumb-bell specimens were machined from the polyacetal sheet with dimensions given by BS 2782:3 (1976) and shown in Figure 6.2.1.

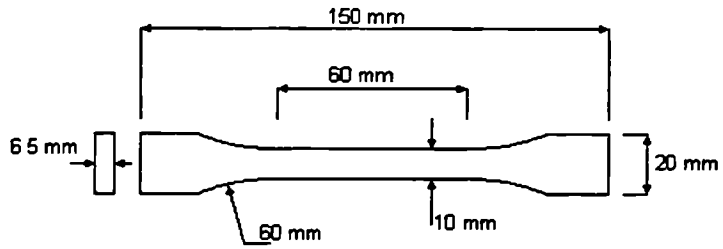

Figure 6.2.1 Polymer mechanical test specimen (BS 2782:3, 1976).

6.3 Method

The test specimens were divided into three groups, the first to be tested immediately, the second after one month's soaking in Ringer's solution and the third after six months soaking. There were five specimens of each polymer grade per group.

The specimens were soaked in half strength Ringer's solution at 37°C. The solution was obtained by dissolving BDH Ringer's solution tablets in de-ionised water. Full strength Ringer's solution typically has a composition of: 111 mMol NaCl, 1.9 mMol KCl, 1.1 mMol $CaCl_2$, 2.4 mMol $NaHCO_3$, 0.8 mMol NaH_2PO_4.

Static tensile testing was undertaken on an MTS Bionix 858 with a 25 kN axial load cell. An environmental chamber which sprayed the specimens with physiological saline at 37°C was used. Specimen strain was calculated from cross head displacement using a geometric correction factor (Appendix A) as waterproof extensometers were not available. The cross head speed was 1 mm s^{-1} and data were recorded at 0.05 mm intervals. Manually operated immersible stainless steel specimen grips were used. The action of tightening the grips placed the specimens under axial compressive loads of up to 700 N.

The specimens were weighed before and after soaking. Young's moduli were calculated from data over the first 0.8 mm displacement. Nominal stress and strain were recorded at failure. Considere's criterion (appendix B) was used to calculate the true stress (load / instantaneous cross sectional area) at which necking of the specimen began and this stress was compared with the maximum true stress to assess plastic instability. The significance of changes to properties following immersion in Ringer's solution was tested using two tailed t-tests assuming unequal variances.

6.4 Results

All the specimens fractured and the fracture surfaces were perpendicular to the axis of loading. The fracture surfaces were rough and the regions around the fracture were more opaque than the rest of the material.

A typical group of stress strain curves is shown in Figure 6.4.1. The shape of the curves and the scatter are similar in all groups.

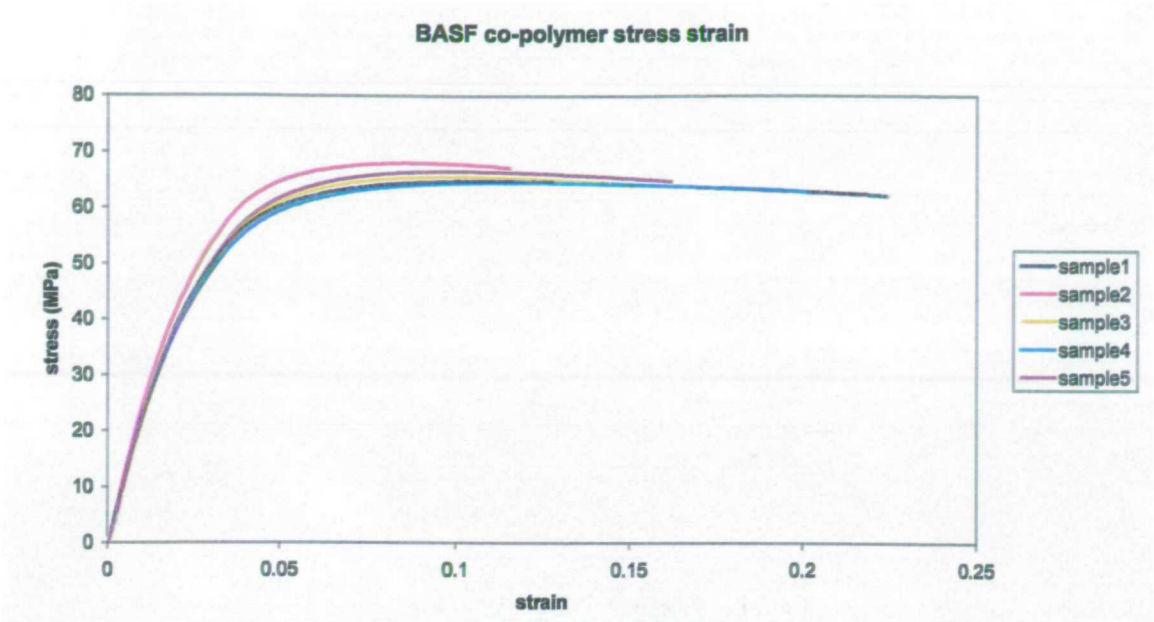

Figure 6.4.1 Stress strain curves for as received BASF co-polymer.

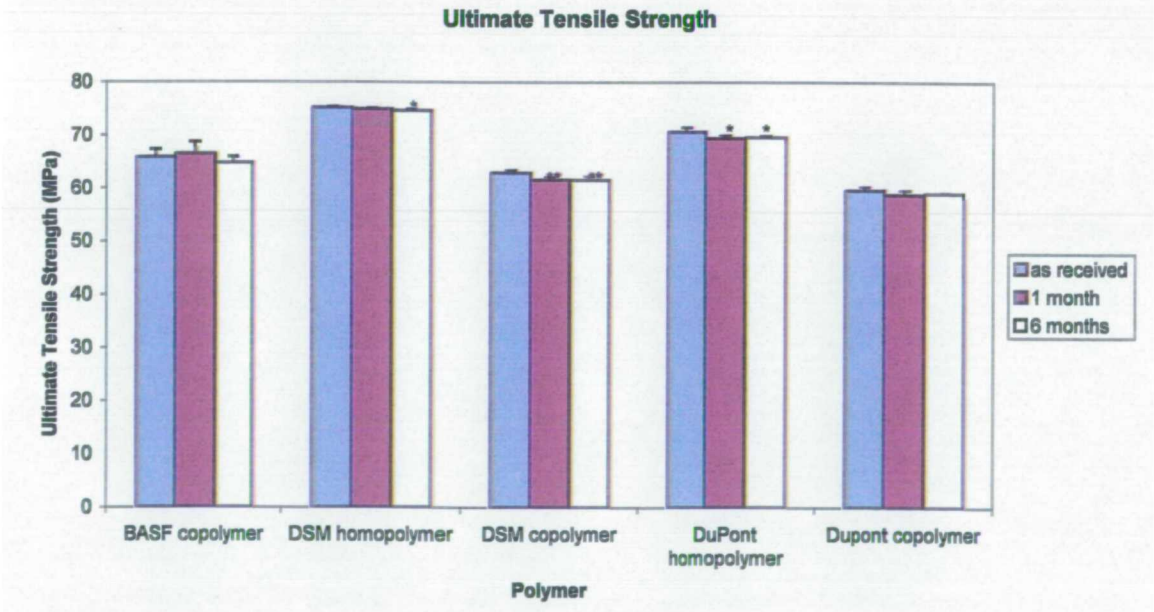

Figure 6.4.2 Ultimate tensile strength of polyacetal as received and after 1 and 6 months immersion in Ringer's solution. Significant differences with the as received group are indicated * $p < 0.05$ and ** $p < 0.01$. Error bars show one standard deviation.

The ultimate tensile strengths of all polymer grades were slightly decreased by immersion in Ringer's solution (Figure 6.4.2). In five cases the decrease after immersion for one or six months was statistically significant with $p < 0.05$ including two with $p < 0.01$. However the decreases are so small that in practice they may be neglected. There were no significant differences between tensile strengths after one

and after six months immersion. The homo-polymer grades showed the highest strengths while the BASF co-polymer showed the greatest variability in strength.

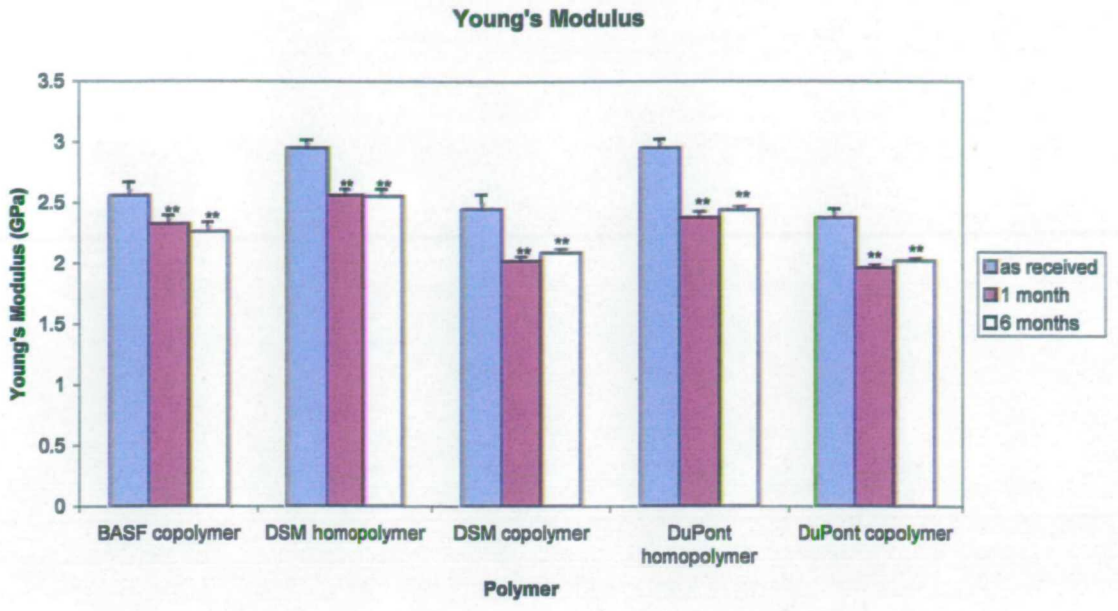

Figure 6.4.3 Young's modulus of polyacetal as received and after 1 and 6 months immersion in Ringer's solution. Significant differences with the as received group are indicated * $p < 0.05$ and ** $p < 0.01$. Error bars show one standard deviation.

The Young's modulus decreased significantly ($p < 0.01$) by between 9 and 20 % in all polymer grades after immersion in Ringer's solution (Figure 6.4.3). The homo-polymers showed the highest stiffnesses before and after immersion, but the DuPont homo-polymer showed the largest percentage decrease (19.5 %). The BASF co-polymer showed the smallest reduction in stiffness. There were small, but significant ($p < 0.05$), increases in stiffness between one month and six months' immersion for the DSM co-polymer and both DuPont homo- and co-polymer.

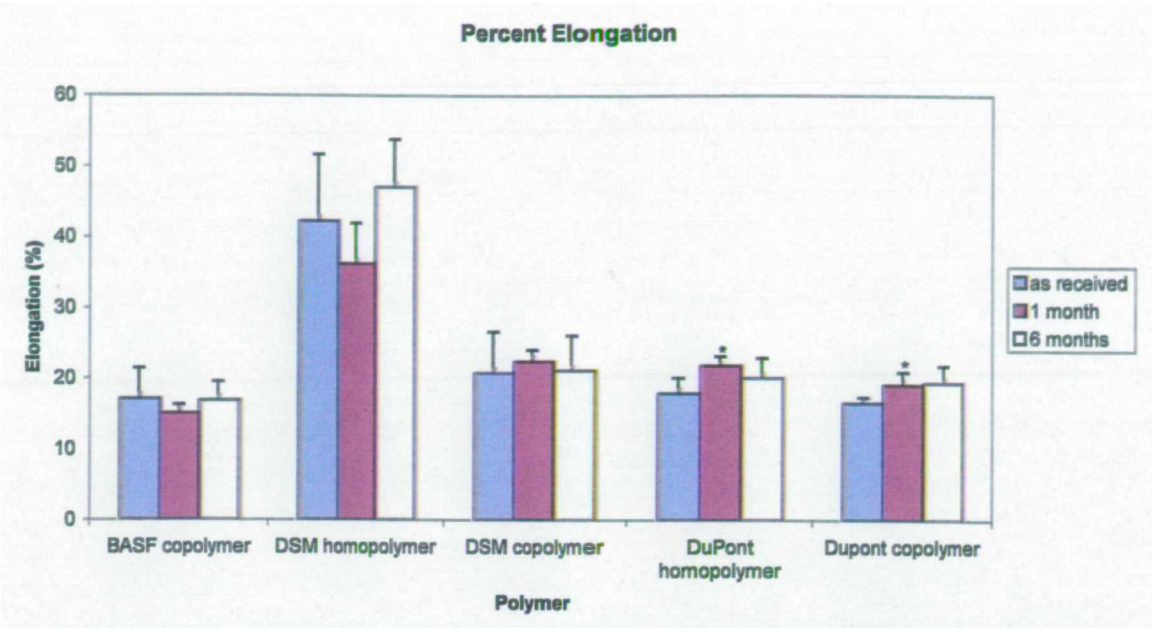

Figure 6.4.4 Percent elongation of polyacetal as received and after 1 and 6 months immersion in Ringer's solution. Significant differences with the as received group are indicated * $p < 0.05$ and ** $p < 0.01$. Error bars show one standard deviation.

The DSM homo-polymer showed very large (up to 56%) elongation at failure (Figure 6.4.4). There were significant increases in elongation in the two DuPont polymers ($p < 0.05$) after one month's immersion, but the same grades showed no significant changes after six months' immersion. There were no significant changes in elongation between one and six months' immersion and no clear increasing or decreasing trends.

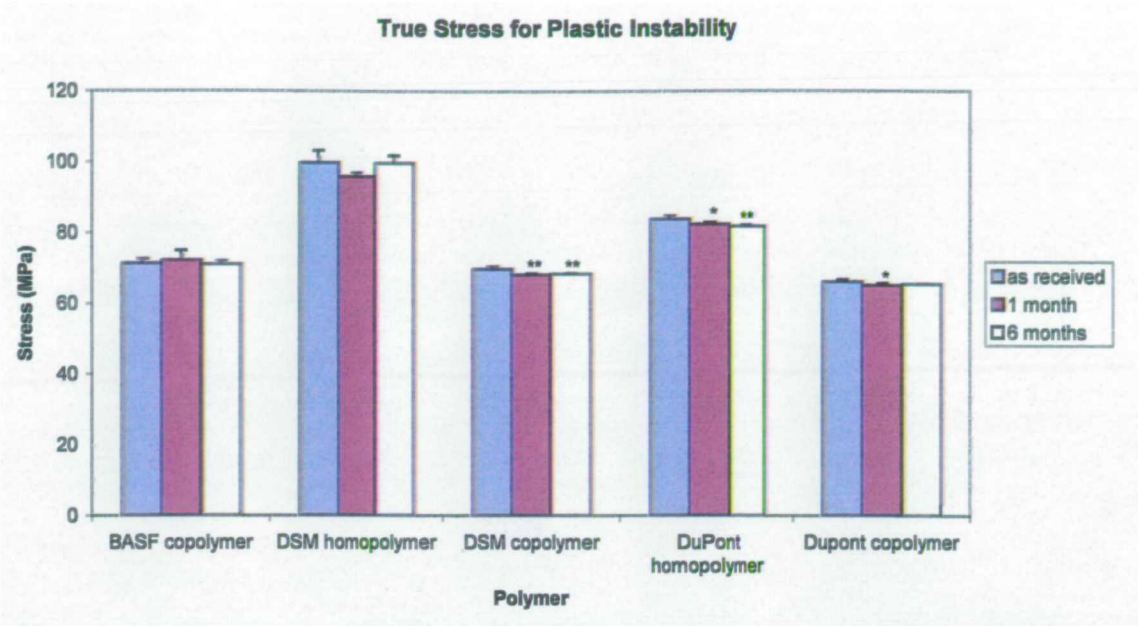

Figure 6.4.5 True stress for onset of plastic instability (Considère's criterion) of polyacetal as received and after 1 and 6 months immersion in Ringer's solution. Significant differences with the as received group are indicated * $p < 0.05$ and ** $p < 0.01$. Error bars show one standard deviation.

The homo-polymers showed the highest true stresses for onset of plastic instability (Figure 6.4.5). There were small, but significant, reductions after one month's immersion in the DuPont homo- and co-polymers ($p < 0.05$) and in the DSM co-polymer ($p < 0.01$) and after six months' in the DuPont homo-polymer and the DSM co-polymer ($p < 0.01$). There was a significant ($p < 0.05$) increase in the Considère stress in the DSM hompolymer between one and six months' immersion. All other grades showed slight reductions. Comparing the Considère stress with the maximum true stress showed greatest plastic instability in the DSM polymers, but all polymers demonstrated some instability before fracture. The plastic instability in the DuPont co-polymer increased from as received to one and six months' immersion.

The water uptake measurements are presented in Table 6.4.1. The water content increased significantly between one and six months in the DuPont co-polymer only. There were no correlations between water uptake and the changes in any of the measured mechanical properties. The homo-polymer specimens showed significantly greater water uptake than the co-polymer specimens at one and six months ($p < 0.01$).

Table 6.4.1 Water uptake (mean ± SD) following one and six months' soak in Ringer's solution. * indicates significant difference $p < 0.05$.

Polyacetal	Water uptake / wt%	
	1 month	6 month
BASF co-polymer	0.69 ± 0.04	0.65 ± 0.03
DSM homo-polymer	0.78 ± 0.06	0.86 ± 0.11
DSM co-polymer	0.63 ± 0.04	0 67 ± 0.03
DuPont homo-polymer	0.72 ± 0.02	0.75 ± 0.03
DuPont co-polymer	0.68 ± 0.02	0.74 ± 0.04*

6.5 Discussion

The mechanical properties of the as received polymer tested at 37°C in saline are not markedly lower than those reported for tests at 23°C in air (section 2.6.3). As expected the co-polymers have lower stiffnesses and strengths than the homo-polymers. The variability of the percentage elongation at failure is characteristic of a semi-crystalline polymer which fails in a brittle rather than ductile mode. The rough fracture surfaces confirm this behaviour. The increased opacity around the fracture surfaces is evidence of strain-induced crystallisation.

The water absorbed into the polyacetal may be expected to have two separate effects on its mechanical properties. The first effect is as fast as the diffusion of the water into the polymer. The diffusion coefficient of water in polyacetal, measured in a preliminary experiment, was found to be approximately $D = 8 \times 10^{-12}$ m^2s^{-1}. For a specimen of thickness 6.5 mm this gives a characteristic time of $(3.25\ mm)^2/D = 15$ days. Therefore water uptake by diffusion will be at equilibrium in specimens immersed for one month. The water molecules in the amorphous regions within the polymer will acts a plasticisers, increasing the free volume per polymer molecule and leading to a reduction in stiffness. The uptake of water appears to produce significant, but small, immediate reductions in the strength of some of the polymers. The reduced stiffnesses produce a larger strain at the same stress.

The second effect expected following water uptake is the degradation of the polymer by the water itself and by solutes in the water. These processes produced no significant reductions in mechanical properties between one and six months. However, there were significant increases in the stiffness of three polymers and a significant increase in the Considère stress for another polymer. The increase in stiffness may be due to a secondary process of crystallisation facilitated by the

increase in free volume per molecule. The increase in stress for plastic instability is interesting and may benefit from further investigation.

The differences observed between polymer grades in the reduction of stiffness following immersion may be due to differences in crystallinity. A polymer with more amorphous material will show a greater effect of water uptake on stiffness. However the polymer with the highest stiffness (DuPont homo-polymer), which might be expected to have the highest crystallinity, also shows the largest percentage reduction in stiffness. The effect of water uptake on stiffness is confounded by the presence of different additives (e.g. plasticisers) in the polymer, which may themselves be water soluble.

6.6 Conclusions

The lack of significant reductions in the mechanical properties between one and six months after immersion in Ringer's solution demonstrates that polyacetal may be used in the physiological environment. The small differences between properties measured at 37°C in physiological saline and those reported at 23°C in air also encourage the use of the polymer.

The stiffness of all polyacetals is significantly decreased following immersion due to the plasticising action of the absorbed water. Effects other than those due to the increase in free volume per molecule appear to produce increases in stiffness and Considère stress in some polyacetals.

The mechanical tests showed that homo-polymers had higher stiffnesses and strengths than the co-polymers. The lack of significant differences between one and six months' immersion prevents differentiation between polymer grades on the basis of their lack of degradation in the physiological environment. On the basis of high strength, stiffness and strain to failure the DSM homo-polymer appears to be the most suitable grade for the resurfacing application.

7. Design Proposal

The preceding chapters form a basis from which to make a series of design choices. This chapter draws these studies and three years' experience of work in biomechanics together in a discussion of resurfacing design. The proposed design is presented and the reasons for particular choices discussed. These reasons go beyond the immediate function of the implant to encompass ease of implantation and design for manufacture.

This chapter is divided into seven sections. In the first the principles that have guided the design process are stated and discussed. The next section gives a physical description of the proposed implant in its simplest form. The functional implications of these physical characteristics are discussed in the next section, under the subheadings used previously in the review of literature on THR (load bearing, load distribution, range of motion). Section 7.4 discusses aspects of the fixation of the design and section 7.5 briefly reviews the choice of materials. The final two sections consider the design in the context of its use by surgeons in an operating theatre environment and in clinical follow-up, and in the context of its production and manufacture.

7.1 Design principles

The fundamental principle of the design is the conservation of bone. Acetabular bone is in shorter supply and so must be conserved at the cost of femoral bone. It is this principle which informs the first section on physical shape.

A second principle is to maximise the theoretical Range of Motion (ROM). The theoretical ROM is defined by the subtended angle of the prosthetic or natural acetabulum and the femoral neck to head ratio:

$$ROM = 2*\cos^{-1}(neck/head) + 180° - \text{subtended angle}$$

This is the limit of motion before the femoral neck impinges upon the acetabular rim. Impingement is a cause of resurfacing and conventional THR failure (Freeman and Bradley, 1983; Wiadrowski *et al.,* 1991). Impingement also occurs in slightly dysplastic intact hips, causing pain and possibly osteoathrosis (Reynolds *et al.,* 1999). Therefore in all patients the theoretical ROM must be larger than the ROM required in every day use. Due to dependence of the actual ROM on relative orientation of

implant components, the theoretical ROM may have to be larger than the required ROM to allow a margin of error in implant insertion. The required ROM for the younger, more active patients for whom this implant is intended will be larger than that for older patients.

It is important to note that ROM relates directly only to femoral neck motion. It is smaller than angles measured for leg flexion-extension, abduction-adduction and internal-external rotation because these motions involve a substantial component of rotation about the femoral neck axis.

The final principle stems from the experience of the surgeons implanting early resurfacing prostheses. The neck cortex must not be damaged; fracture of the femoral neck has been reported frequently following notching or other damage to the cortical bone (section 3.4).

7.2 Physical shape

7.2.1 Femoral component

The femoral component will consist of a truncated sphere of polyacetal with a tapered, chamfered concentric cylinder cut into its plane surface (Figure 7.2.1). The ratio of the diameter of this cylinder to the spherical surface diameter is an important design parameter. This ratio and the subtended angle of the acetabular component determine the ROM of the implant.

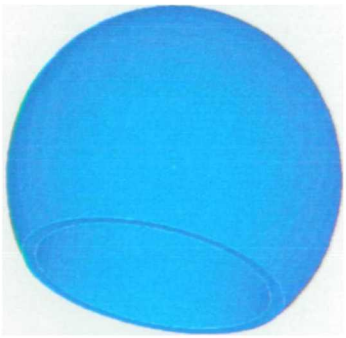

Figure 7.2.1 Basic shape of the femoral component

Amstutz *et al.* (1975) measured the neck-head ratios of various THRs and found a range of values from 0.33 (Trapezoidal 28) to 0.57 (Charnley). Data from Sugano (2000) give neck-head ratios for 32 dry cadaveric femora with a range of 0.60 – 0.75, a mean of 0.69 and 0.04 standard deviation. Replacement and intact hip neck-head ratios have different implications for ROM however, because THR acetabular cups,

with some exceptions, have subtended angles of 180°, unlike intact acetabula. The ROM must not be reduced significantly by the operation, nor the implant components impinge on bone. Bone removal from the neck cortices must not occur, so the neck width has to be maintained. Therefore the bearing surface diameter may not be significantly smaller than the original femoral head diameter in order to maintain a constant neck-head diameter ratio.

In addition to this constraint on the diameter of the spherical surface, there is also a constraint upon the internal diameter of the femoral implant. At the mouth of the implant this must exceed the largest dimension of the femoral neck in the plane perpendicular to its axis.

The angle of the taper and of the chamfer on the internal cylindrical surface may have implications for the pressurisation of bone cement. The depth of the component at its pole is also negotiable. The range of bearing surface diameters should be capable of accommodating 38 – 54 mm diameter femoral heads (Sugano *et al.*, 1999). Figure 7.2.2 shows a 48 mm diameter femoral component.

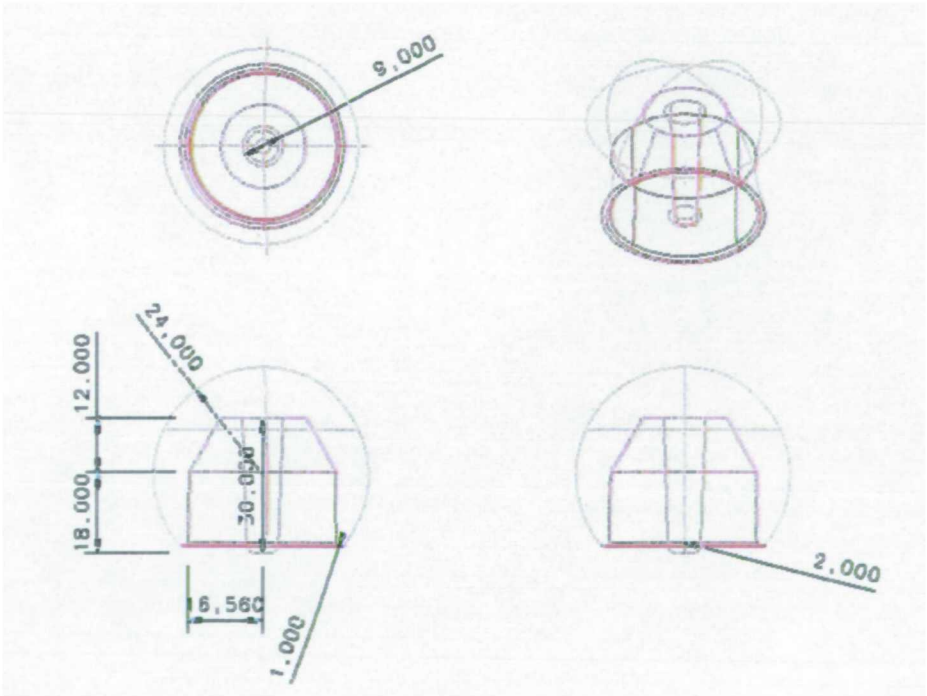

Figure 7.2.2 Femoral component drawing (dimensions in mm).

7.2.2 Acetabular component

The acetabular component will consist of an UHMWPE cup defined by portions of two concentric spherical surfaces. The internal surface will subtend an angle less than

180°. The precise value of subtended angle may be varied according to direction and may be modified by the surgeon intra-operatively with the use of trimmable components. The angle subtended by the basic shape presented here is 160° (section 4.4).

To maximise the thickness of a bone conserving acetabular replacement the bearing surface diameter must not exceed that of the original femoral head. The bearing surface diameter is already constrained, by consideration of the femoral component, to be at least that of the original femoral head.

The lower limit of thickness of the acetabular component is determined by the compliance of the cup as a whole. The thinner and more compliant a cup, the larger the tensile stresses set up at the bone – implant interface (Morscher, 1992; Dalstra, 1993). Large tensile stresses make fixation by bone ingrowth less likely and are likely to cause cement failure depending on the method of fixation. Past experience of UHMWPE resurfacing acetabular components suggests that 6 mm thickness will provide sufficient stiffness to avoid this problem. FE analysis (section 5.7) showed that if tangential motion at the bone-implant interface were restricted the motions normal to the interface of a press-fit 6 mm thick UHMWPE acetabular cup would not prevent ingrowth. Thicker components risk removing more acetabular bone than is necessary. Dalstra (1993) and New (1997) both showed the radical effects of removal of the subchondral bone plate on the load transfer in the pelvis. Figures 7.2.3 and 7.2.4 show the proposed 48 mm internal diameter acetabular component.

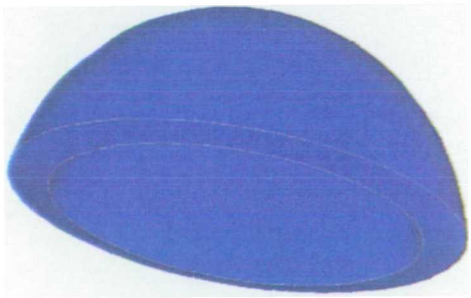

Figure 7.2.3 Basic shape of the acetabular component.

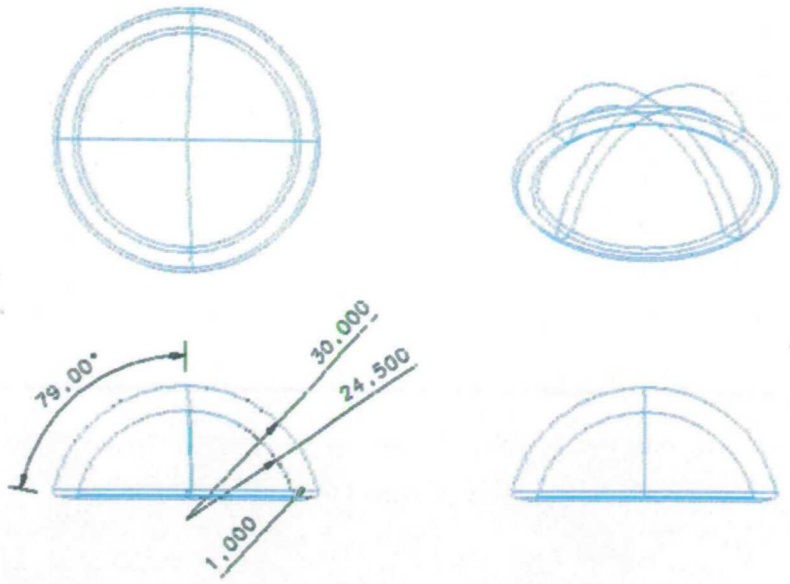

Figure 7.2.4 Acetabular component drawing (dimensions in mm).

7.3 Function

7.3.1 Load bearing

The stresses set up within these implant components during normal use are well within the range of static and fatigue limits of the materials (sections 2.6 and 5.7). The stresses in the acetabular cup are no higher than those reported in conventional acetabular cups (Dalstra, 1993; Mantell *et al.*, 1998).

One important issue not investigated in this thesis is the role of bone cement (PMMA) underneath the femoral component of resurfacing. Designs in current use allow clearance of less than 1 mm between the reshaped femoral head and neck and the femoral component. The cement penetrates into the trabecular bone several millimetres forming a cement-bone construct (McMinn, 2000). As stated previously (section 2.5.6) there are correlations between cement thickness around THR acetabular components (Joshi *et al.*, 1998) and implant loosening due to cement failure. While the bone in the acetabulum may not provide such an extensive area of porous surface for cement interdigitation the mechanical environment (predominantly compressive stress) is similar. The mechanical behaviour of this "cement-bone" construct should be characterised more fully.

7.3.2 Load distribution

The elastic mismatch at the implant-bone interface is minimised by the use of materials with moduli closer to those of bone. The shape of the interface is also

important in determining the way load is transferred to the bone. Although the joint force is applied normal to the implant surface and articulating surface frictional forces are negligible (section 2.5.6) shearing and tensile stresses develop at the bone-implant interface. Cement fixation is vulnerable to tensile forces and bone ingrowth fixation is prevented by large tangential motions (section 5.8). Therefore both femoral and acetabular components must present fixation surface features that resist these forces.

The femoral components of both BHR and Cormet 2000 resurfacing prostheses have stems that project down the femoral neck several centimetres beyond the end of the spherical surface. Revision of the femoral component of these resurfacings has been undertaken subsequent to X-ray findings of implant stem fracture (Krikler, 2000). A simple bending moment calculation shows the potential for this fracture:

$$BM_{max} = \sigma_y I_{section}/\text{depth}.$$

where BM_{max} is the maximum bending moment, σ_y is the yield stress and $I_{section}$ is the second moment of area of the stem section ($\pi r^4/4$). With a stem diameter of 8 mm and a yield stress of 240 MPa for CoCr this gives BM_{max} = 12 Nm. In the worst case with only the distal end of the stem providing support this represents a maximum perpendicular load of 170 N (stem 70mm long). The fatigue limit for CoCr is lower than the yield stress and hip joint loads of up to 2000 N (3×BW) are encountered in every gait cycle. While this loading is not perpendicular to the stem axis, it need only be 6° off-axis for the perpendicular component to exceed 200 N. Holographic interferometry used to study the surface strains in a femur implanted with a McMinn surface replacement showed stress concentrations in the cortical bone near the end of the stem (Shelton, 1999). Three dimensional FEA of the proximal femur implanted with an prosthesis resembling the BHR found stress concentrations at the stem tip (Watanabe *et al.*, 2000). However the stem does have a role in preventing the component from rotating and sliding on the femoral head remnant and also in positioning the component correctly during surgery. Therefore a reduced length stem has been included in the design.

The conclusion of the FE study (section 5.9) that the CoCr acetabular cup is likely to show lower migration than an UHMWPE cup appears to contradict the suggestion that implant materials with lower elastic mismatch to bone will perform better. The stiffer Co-Cr acetabular cup seems to be capable of transferring more load directly to

cortical bone regardless of the fixation conditions. However, load transfer to acetabular cancellous bone may be beneficial in retaining suitable quality bone for cemented revision. Further investigation into the complex interaction between acetabular bone and implant deformation is required.

7.3.3 Motion

The tribology and wear of polyacetal is not well characterised and only one paper exists recording its behaviour against UHMWPE. McKellop *et al.* (1993) used polyacetal – UHWMPE clearances of 0.51 – 0.66 mm with bearing diameters of 41.0 mm. They measured UHMWPE wear rates of 61 mm^3 per million cycles against polyacetal and 98 mm^3 per million cycles against CoCr. The polyacetal itself wore at a rate of 19 mm^3 per million cycles. Conventional THR produces approximately 30 mm^3 wear debris per million cycles in hip simulator tests (McKellop *et al.*, 1999) and *in vivo* wear volumes may exceed 130 mm^3 per year with large diameter femoral heads (Hall *et al.*, 1998). The resurfacing has a longer wear distance over which wear may occur.

The wear patches on the UHMWPE component against polyacetal and CoCr appeared similarly smooth under SEM examination indicating similar wear processes (McKellop *et al.*, 1993). While the mean frictional torque recorded for the polyacetal on UHMWPE bearings was lower than that for the CoCr on UHMWPE bearings, the temperature of the serum bath around the former rose to 50°C and the around the latter to 44°C. This temperature rise gives some cause for concern since heat generation at prosthetic joints has been suggested as a cause of implant loosening (Bergmann *et al.*, 2000). A temperature of 45°C is sufficient to kill bone tissue. While polyacetal has a much lower thermal conductivity than Co-Cr of which the conventional THR instrumented by Bergmann *et al.* was made, the bone in a resurfacing is much nearer to the articulating surfaces where the heat is generated and so may be at greater risk.

The FEA study of resurfacing (chapter 5) found that the rim of the acetabular component is significantly involved in the contact behaviour of the implant. This suggests that further simulation or experimental work should be carried out to determine the shape of edge that optimises the lubrication conditions in the bearing.

7.4 Fixation

The polyacetal on UHMWPE implant will use the hybrid fixation favoured by McMinn *et al.* (1996). The UHMWPE acetabular cup may be coated with a thin layer of HA, or a thin layer of HAPEX™ may be incorporated onto its fixation surface. Compression moulding has produced a good junction between PE and HAPEX™ (Tanner, 2001).

The FE study of press-fit acetabular components showed that fixation by bony ingrowth would be prevented by excessive tangential motion at the implant-bone interface. This motion was highest in the infero-posterior quadrant of the acetabulum. Therefore an initial press-fit must be supplemented if bone ingrowth fixation is to be achieved. The areas where such additional fixation should be applied are not only determined by the location of the largest motions to be resisted, but also by the quality and quantity of bone available. In the inferior part of the acetabulum the bone on the anterior and posterior horns of the lunate surface is suitable, with the ischium or pubis providing sufficient depth of bone for a secure anchorage. The supplementary fixation may take the form of pegs or fins. One implant that opted for pegs was the acetabular cup of the RM Isoelastic Hip Prosthesis. These pegs were anchored in the superior part of the acetabulum. The holes for the pegs were drilled at a slightly larger angle to the bone surface than the pegs themselves. This placed a small pre-stress on the pegs, pulling the implant into the socket. The RM Isoelastic cementless acetabular cup is coated with a layer of HA. At six year follow-up the rate of acetabular loosening reported by Olivier *et al.* (1998) was 3.5%.

The femoral component of the proposed design will be fixed with PMMA bone cement. The internal surface of the femoral component will be grooved and textured to provide a mechanical interlock for the bone cement.

7.5 Materials

The femoral component will be made from polyacetal, also known as Polyoxymethylene (POM). In the mechanical tests reported in chapter 6 the homo-polymers were stiffest and strongest and the DSM homo-polymer showed outstanding elongation at failure which was unaffected by long-term immersion in Ringer's solution. Although its properties are inferior the BASF co-polymer is already in routine use in operating theatres so lot controlled material for medical applications is

available. However, while mechanical properties provide a guide, there has been no investigation into the comparative wear resistance of these grades.

The results of McKellop *et al.* (1993) and the FE study in chapter 5 suggest that the wear mechanisms of polyacetal on UHMWPE will be similar to those of CoCr on UHMWPE. Lewis (2001) recently surveyed the properties of cross-linked UHMWPE (XLPE) and the clinical outcome of acetabular cups made from this material. The wear rates of XLPE in hip simulator trials are reduced to as low as 0.12 mm^3 per million cycles with high (28 Mrad) gamma radiation doses (McKellop *et al.*, 1999). Chemical cross-linking can achieve similar reductions in wear rate without the deleterious effects on the ultimate and fracture properties of the material of exposure to radiation. Clinical reports of XLPE are encouraging (Wroblewski *et al.*, 1999).

The fixation surface of the acetabular cup may be coated with HA or a layer of HAPEX™. HAPEX has a fully reversed axial fatigue limit of 4.4 MPa at 1 million cycles in physiological conditions (Ton That *et al.*, 2000a & b). While the peak stresses predicted by the FE model of the acetabular component are larger than this they will be mainly compressive in the fixation surface providing a less favourable regime for crack propagation. Ton That (2000) showed that compression-only fully-reversed torsion fatigue did not cause failure after 1.5×10^6 cycles.

7.6 Design for clinical use

The outcome of hip replacement is strongly affected by decisions made and actions taken by the surgeon at the initial operation. However good the science and theoretical work supporting an orthopaedic implant its clinical success depends upon the ability of the implanting surgeon to use it to make a good reconstruction of the hip joint.

A finding of the review of resurfacing outcomes (section 3.5) was that the most successful resurfacings were available in a large number of sizes. Clearly in the restricted space available for a resurfacing implant, the correct size of components is more important than for conventional THR. However one problem with providing a range of implant sizes is that even with careful pre-operative planning surgeons will require a choice of several component sizes for every operation. This entails sophisticated management of stocks of expensive implants (all with limited shelf lives) at a hospital and in practice hospitals will opt for implants with as few sizes as possible.

The proportions of the dimensions in the implant proposed here are based upon mean values of head-to-neck ratios. Any one component size is able to accommodate variations by up to one standard deviation from the mean ratio. This means that the femoral component bearing surface-to-neck opening ratio is larger than the ratio measured by Sugano (2000). The angle subtended by the femoral bearing surface is therefore smaller than that subtended by an intact femoral head with a mean head-to-neck ratio.

One aim of conventional THR is the restoration of function of the hip joint. Unfavourable biomechanics caused by developmental dysplasia often underlie joint disease and secondly destruction of the normal shape of the joint is a feature of many disease processes. Therefore the restoration of function requires the reconstruction of the joint, placing the bones and centre of rotation in the optimal relative positions. Contracted muscles may be released, but adequate muscle tension must be provided across the joint to prevent dislocation. The contralateral hip can sometimes provide a guide to the geometry of an optimal reconstruction. However the potential for altering the relative positions of the femur and the acetabulum is much lower in resurfacing than in THR. Therefore the indications for resurfacing must include relatively normal shapes of the hip joint.

The instrumentation must enable accurate and repeatable bone cuts to be made. The orientation of the femoral component on the femoral neck was reported to be highly important in early resurfacing designs, although there was no consensus on the optimum position. The currently used metal-on-metal resurfacings all employ sophisticated instrumentation to align and position components on the bone.

Both components of a polyacetal on UHMWPE resurfacing will be radiolucent. To enable accurate measurements of component migration both components need to be fitted with radiographic markers.

One of the potential advantages of resurfacing is the ease with which a loose resurfacing may be converted to a conventional THR. Both components of the all-polymer resurfacing, even if well fixed by bone ingrowth, will always be susceptible to being cut, drilled or otherwise removed. The removal of well-fixed CoCr acetabular components can be very destructive of bone and so their manufacturers produce large diameter modular heads for stemmed revision of femoral resurfacing components.

The sterilisation of a polyacetal component may be problematic. Polyacetal is degraded quickly when exposed to gamma radiation (Skiens and Williams, 1983) and doses high enough for sterilisation will cause deterioration of mechanical properties. The instrument handles made from polyacetal in current use are sterilised by autoclave. However this may not be suitable for high tolerance components which may suffer dimensional change. The polyacetal femoral components in the Freeman all polymer knee were sterilised with ethylene oxide (Moore *et al.*, 1998), but concerns exist about the possible carcinogenic effects of the residue.

7.7 Manufacturability and commercialisation

Polyacetal components can be formed using injection moulding. The large initial costs involved in setting up injection moulding machines and preparing dies make this a practicable option only if large volumes of each component size are to be produced (Pickard, 2000). One benefit of injection moulding is the lower surface roughness achieved on the finished components.

However, the proposed implant is still experimental and the time until full-scale introduction onto the market may be as long as ten years. Therefore despite the wastage of offcut material the cheaper option is to machine components directly from bar stock. This is also the only option for the production of prototype components.

There are two major patents granted in the field of resurfacing prostheses. The first (Swanson and Freeman, 1975) claims an "endoprosthetic hip joint device". This is a metal-on-polymer double cup hip replacement with concentric spherical surfaces and the patent covers similar devices made from different materials. The second patent (Clarke and Amstutz, 1978) claims a method for replacing the hip using a conservative surface replacement. Clarke and Amstutz also claim their resurfacing prosthesis (THARIES) which has eccentric spherical surfaces.

These two patents limit the protection that can be obtained for a new design of resurfacing and make it less viable for commercialisation.

8. Conclusions

The concept of resurfacing has been thoroughly investigated and discussed. A literature review of resurfacing showed that past attempts at the operation failed to produce clinical results equal to those of conventional hip replacement and drew attention to the problem of conservation of acetabular bone. However, early results of the most recent generation of metal-on-metal resurfacings are encouraging.

A survey of the morphology of the acetabulum demonstrated that the bony surface, while approximately spherical, had mean subtended angles of approximately 160°. This survey also showed large variability in acetabular shape which a conservative acetabular component would need to accommodate.

FEA of the resurfacing concept showed that the all-polymer design reduced stress shielding and concentrations on the femoral head and transferred more load to the acetabular cancellous bone than a metal-on-metal implant. The increased loading of the acetabular cancellous bone may lead to increased migration but the corresponding stress shielding found with the metal-on-metal implant may present problems at revision. The use of bone-ingrowth fixation was not ruled out by the FEA study of micromotion at the implant bone interface as long as the design provided adequate resistance to tangential motion.

Mechanical testing of polyacetal following immersion in Ringer's solution showed that it was not subject to degradation and that its properties were adequate for use in the proposed implant.

Other reservations raised about a polyacetal on UHMWPE resurfacing include the generation of heat at the bearing surface and the problem of sterilising a polyacetal femoral component. Further the production of polymer wear debris which is suggested to be one of the major causes of hip implant loosening may be increased by the use of large diameter polymer bearings. The lack of possible intellectual property protection reduces the attraction of the idea for commercialisation.

In conclusion the concept of an all-polymer resurfacing is an interesting one and has provoked some useful research into the engineering of hip replacement. However this research has not shown that an all-polymer resurfacing is likely to perform any better than other currently available resurfacings or conventional THRs and several important concerns about its use have been highlighted.

9. Future Work

9.1 Wear Tests

The polyacetal on UHMWPE hip prosthesis bearing concept discussed in chapter 7 is reported to have a lower volumetric wear rate than a similar hip prosthesis bearing using Co-Cr on UHMWPE (McKellop *et al.,* 1993). This difference was found using a multi-station hip wear simulator with soak controls. There are several reasons for needing to replicate this result. McKellop reports "erratic" wear of polyacetal. Even after subtraction of the soak control difference some measurements recorded a net weight gain of the polyacetal component. The temperature and speed of the tests was variable: at first the machine was run at 68 rpm, but this resulted in a serum bath temperature of up to 50°C and discoloration of the polyacetal so the speed was reduced to 45 rpm for the remainder of the test. The acetabular components were mounted below the femoral components in the inverted position which produces lower wear rates than components mounted in the physiological position with the femoral component uppermost. The tests were only continued to one million cycles with measuring intervals of 200,000 cycles. Finally the UHMWPE acetabular components were sterilised in air with gamma radiation, a technique which has been shown to result in higher wear rates (Lewis, 1997).

Therefore wear tests are planned on an MTS 8 station hip wear simulator to compare a 48 mm diameter polyacetal on UHMWPE with a 48 mm Co-Cr on UHMWPE bearing couple. The UHMWPE will be processed and sterilised according to current best practice implant protocols. The components will be mounted in the physiological configuration. Of the eight wear test stations, four will contain Co-Cr and UHMWPE pairings and four will contain polyacetal and UHMWPE pairings. One polyacetal and one Co-Cr station will not articulate to provide loaded soak controls.

The wear tests will require the design of specific wear testing prototype implants and fixtures to hold the prototypes in the wear testing machine. The components need to be stiff to maintain the alignment of the bearing surfaces with the axes of loading and rotation of the machine otherwise non-physiological wear patterns will be produced. The test components reported by McKellop *et al.* (1993) may not have been sufficiently stiff. The solutions to the prototype design problem will also depend upon manufacturing methods and will involve collaboration with Corin Medical. The

fixtures on the MTS machine at QMW for conventional hip replacements were designed and built here, so a modified design will be simple to produce.

The water uptake of polyacetal may be a problem. The soak controls in gravimetric wear rate measurements allow compensation for water uptake. However the equilibrium water uptake of the polyacetal specimens used in the study reported in chapter 6 was 0.67 – 0.78 wt% and the standard deviations in those results were 0.02 – 0.06 wt%, with a sample size of five. A variability of 0.06 wt% in water uptake between the material in soak and wear test components of approximate mass given by $4/3\pi r^3\rho$ (where r = 24 mm, ρ = 1.4 Mgm^{-3}) = 81 g would result in an uncertainty of 0.049 g. The polyacetal wear rate reported by McKellop *et al.* (1993) of 18.8 mm^3 per million cycles is equivalent to 0.026 g per million cycles. This comparison suggests that water uptake variability was the cause of the negative wear rates measured by McKellop. Wear testing must be continued well beyond one million cycles for the change in mass due to wear to be distinguished from water uptake variability. Also metal-on-PE wear studies show two distinct wear rates, the first up to 1 million cycles and the second thereafter, so wear tests should be performed for a minimum of 2 or 3 million cycles. In addition further investigation of the variability of the water uptake characteristics of the chose polyacetal with larger sample sizes should be undertaken before wear tests are carried out.

9.2 Biological Reaction to Wear Debris

The reports by Mathiesen *et al.* (1983; 1986) of the clinical outcomes of the Christiansen prosthesis have prejudiced the orthopaedic world against polyacetal. Before any implant made of the polymer could be commercialised the effects of polyacetal wear debris, upon which the Christiansen failures were blamed, would have to be quantified and shown to be no more damaging than UHMWPE debris. Systems for quantifying the relative bio-reactivity of wear debris from different THR bearing material combinations have been reported (Ingham and Fisher, 2000). Wear debris from hip simulator studies of the polyacetal on UHMWPE and CoCr on UHMWPE would be collected and used to challenge cells. The cells' production of inflammatory cytokines and other inflammatory markers would then be used to determine the particles relative bio-reactivity.

9.3 FEA of the Femoral Component and Mechanical Validation

Although there are published FEA studies of femoral resurfacing components (Strens, 1986; Fyhrie *et al.*, 1988; Watanabe *et al.*, 2000) only the most recent of these is three dimensional. Watanabe *et al.* applied joint reaction force and muscle loading consistent with three instants close to the peak reaction force loading during the gait cycle to their model. While their results provide a useful guide to the positions of the peak stresses and strains in sections across the femoral neck their model fails to take into account the high variability in cancellous bone density in the proximal femur. Also recent work (Latour and Brattain, 2000) shows that the proximal femur experiences significantly higher strains during toe-off and heel strike than at mid-stance.

FEA of the femoral component of resurfacing would develop a model using the standardised femur (Viceconti *et al.*, 1996) to allow proper comparison with other studies and validation with an identical polymeric femur. Muscle loading and joint reaction forces would be applied to simulate instants throughout the gait cycle from heel strike to toe-off.

The mechanical testing of a prototype implant is an important step in satisfying the guidelines for novel medical devices laid down by the Medical Devices Agency (MDA) in the UK and the Food and Drug Administration (FDA) in the USA. FEA studies alone are not acceptable and experimental validation is required.

In order to validate the implanted hemi-pelvis and femur FEA models, prototype components could be implanted in polymeric model hemi-pelves and femora and then loaded using similar schemes to those applied in the FEA study. Strain gauges, linear displacement transducers or holographic laser interferometry may be used to measure the effect of the implant upon bone loading. In addition, fatigue tests, similar to the THR femoral stem bending test, may be required, although this test is not yet part of any standards system.

9.4 Contact Behaviour of Polyacetal on UHMWPE Bearings

The tribological behaviour of polyacetal on UHMWPE bearings is not reported. Jin *et al.* (1999) reported the effect of the clearance gap upon contact area and stress in metal on UHWMPE bearings using a simple axisymmetric FEA model of contacting spherical surfaces. A similar model along with data on the achievable surface

roughness of the polymer implant components could be used to predict the lubrication regime which would operate in a polyacetal on UHMWPE hip resurfacing.

9.5 Clinical Trials

Before a novel implant can achieve widespread application its performance must be studied in a limited number of patients. Also, in order to obtain CE marking, which is essential for the marketing of a medical device within the EC, the implant must be subject to a clinical investigation (Yamac *et al.,* 1999). The aim of a clinical trial would be to prove that the novel implant was safe and that its performance was better than or no worse than other currently available implants.

The first objective, of showing an implant's safety and basic efficacy, may be carried out with a small series of patients at a specialist hospital, probably by the team involved in its invention. However, the task of showing that the implant's performance is as good or better than another requires a larger, multi-centre trial in which the inventors and others with an interest in the implant's success are not directly involved. Orthopaedic clinical trials fall below the high standards of proof found in clinical trials for drugs where prospective, randomised, double-blind trials are required. This is due to practical difficulties, including the fact that an operating surgeon cannot be "blinded".

Standard hip scores would be used to assess the function and the relief of pain of patients with the new implant. In addition Radio Stereometric Analysis (RSA) would be used to follow the migration of both components. In conjunction with survivorship the migration of the novel hip replacement would be used to compare its performance with other implants.

10. References

Abrahamsson S, Ahlgren S, Stigsson L. Wagner Surface Replacement of the Hip. *Acta Orthopaedica Scandinavica* 1987; 58:93-96.

Adler E, Stuchin SA, Kummer FJ. Stability of Press Fit Acetabular Cups. *Journal of Arthroplasty* 1992; 7:295-301.

Ahnfelt L, Herberts P, Malchau H, Andersson GBJ. Prognosis of Total Hip Replacement - A Swedish Multicenter Study of 4,664 Revisions. *Acta Orthopaedica Scandinavica* 1990; 61:1-26.

Aiello L, Dean C. *An Introduction to Human Evolutionary Anatomy*, London: Academic Press, Harcourt Brace, 1990; 429-482.

Albrektsson T, Carlsson LV, Jacobsson M, Macdonald W. Gothenburg Osseointegrated Hip Arthroplasty: Experience With a Novel Type of Hip Design. *Clinical Orthopaedics and Related Research* 1998; 352:81-94.

Alexander RM, Vernon A. The Mechanics of Hopping by Kangaroos (Macropodidae). *Journal of Zoology: Proceedings of the Zoological Society of London* 1975; 177:265-303.

American Academy of Orthopedic Sugeons. *The Clinical Measurement of Joint Motion*. American Academy of Orthopedic Surgeons, 1994; 102.

Amstutz HC, Dorey F, O'Carroll PF. THARIES Resurfacing Arthroplasty Evolution and Long Term Results. *Clinical Orthopaedics and Related Research* 1986; 213:92-114.

Amstutz HC, Graff-Radford A, Gruen TA, Clarke IC. THARIES Surface Replacements: A Review of the First 100 Cases. *Clinical Orthopaedics and Related Research* 1978; 134:87-101.

Amstutz HC, Graff-Radford A, Mai LL, Thomas BJ. Surface Replacement of the Hip with the THARIES System: Two to Five Year Results. *Journal of Bone and Joint Surgery* 1981; 63-A:1069-1077.

Amstutz HC, Grigoris P, Dorey FJ. Evolution and Future of Surface Replacement of the Hip. *Journal of Orthopaedic Science* 1998a; 3:169-186.

Amstutz HC, Grigoris P. Metal on Metal Bearings in Hip Arthroplasty. *Clinical Orthopaedics and Related Research* 1996; 329s:S11-S34.

Amstutz HC, Kilgus D, Kabo M, Dorey F. Porous Surface Replacement of the Hip with Chamfered-Cylinder Component. *Archives of Orthopaedic and Traumatic Surgery* 1988; 107:73-85.

Amstutz HC, Lodwig RM, Schurman DJ, Hodgson AG. Range of Motion Studies for Total Hip Replacments: A Comparative Study with a New Experimental Apparatus. *Clinical Orthopaedics and Related Research* 1975; 111:124-130.

Amstutz HC, Sparling EA, Grigoris P, Campbell PA, Dorey FJ. Surface Replacement: The Hip Replacement of the Future? *Hip International* 1998b; 8:187-207.

Amstutz HC, Thomas BJ, Jinnah RH, Kim WC, Grogan T, Yale C. Treatment of Primary Osteoarthritis of the Hip: A Comparison of Total Joint and Surface Replacement Arthroplasty. *Journal of Bone and Joint Surgery* 1984; 66-A:228-241.

Amstutz HC, Thomas BJ, Mai LL. Total Hip Articular Replacement by Internal Eccentric Shells. *Orthopaedic Transactions* 1981; 5:374

Amstutz HC. Recent Advances in Total-Hip Resurfacing. In: McKibbin B, ed. *Recent Advances in Orthopaedics*. Edinburgh, Churchill-Livingstone, 1983; 155-177.

Arajärvi E, Santavirta S. Revision Arthroplasty of the Hip Joint. *Archives of Orthopaedic and Traumatic Surgery* 1987; 106:152-156.

Aspenberg P, van der Vis H. Migration, Particles, and Fluid Pressure: A Discussion of the Causes of Prosthetic Loosening. *Clinical Orthopaedics and Related Research* 1998a; 352:75-80.

Aspenberg P, van der Vis H. Fluid Pressure May Cause Periprosthetic Osteolysis: Particles are Not the Only Thing. *Acta Orthopaedica Scandinavica* 1998b; 69(1):1-4

Avai A, Bombelli M. Is the RM- Uncemented Coated Acetabular Cup a Reliable Component in Total Hip Replacement? *Hip International* 1993; 3:75-83.

Barbour PSM, Barton DC, Fisher J. The Influence of Stress Conditions on the Wear of Total Joint Replacements. *Journal of Materials Science: Materials in Medicine.* 1997; 8:603-611.

Bassett LW, Gold RH, Hedley AK. Radiology of Failed Surface Replacement Total-Hip Arthroplasty. *American Journal of Roentgenology* 1982; 139:1083-1088.

Bell RS, Schatzker J, Fornasier VL, Goodman SB. A Study of Implant Failure in the Wagner Resurfacing Arthroplasty. *Journal of Bone and Joint Surgery* 1985; 67-A:1165-1175.

Bereiter H, Huggler AH, Jacob HAC, Seemann P. The Thrust Plate Prosthesis (TPP) A New Concept in Hip Prosthesis Design Eight Years of Clinical Experience. *Orthopaedics and Related Sciences* 1991; 2:191-202.

Bergmann G, Graichen F, Rohlmann A. Hip Joint Loading Measured During Walking and Running, Measured in Two Patients. *Journal of Biomechanics* 1993; 26:969-990.

Bergmann G, Graichen F, Rohlmann A. Is Staircase Walking a Risk for the Fixation of Hip Implants? *Journal of Biomechanics* 1995; 28:535-553.

Bergmann G, Graichen F, Rohlmann A, Verdonschot N, van Lenthe GH. Frictional Heating In and Around Total Hip Implants. *Proceedings of the 12th Conference of the European Society of Biomechanics,* Dublin, 2000; 142.

Besong AA, Tipper JL, Mathews BJ, Ingham E, Stone MH, Fisher J. The Influence of Lubricant on the Morphology of Ultra-High Molecular Weight Polyethylene Wear Debris Generated in Laboratory Tests. *Proceedings of the Insitution of Mechanical Engineers, part H* 1999; 213:155-158.

Beuchel FF, Drucker D, Jasty M, Jiranek W, Harris WH. Osteolysis Around Uncemented Acetabular Components of Cobalt Chrome Surface Replacement Hip Arthroplasty. *Clinical Orthopaedics and Related Research* 1994; 298:202-211.

Bigsby RJA, Auger DD, Jin ZM, Dowson D, Hardaker CS, Fisher J. A Comparative Tribological Study of the Wear of Composite Cushion Cups in a Physiological Hip Joint Simulator. *Journal of Biomechanics* 1998; 31:363-369.

Bigsby RJ, Hardaker CS, Fisher J. Wear of Ultra-High Molecular Weight Polyethylene Acetabular Cups in a Physiological Hip Joint Simulator in the Anatomical Position Using Bovine Serum as a Lubricant. *Proceedings of the Insitution of Mechanical Engineers, part H* 1997; 211(3):265-269.

Birkinshaw C, Buggy M, Daly S. Mechanism of Ageing in Irradiated Polymers. *Polymer Degradation and Stability* 1988; 22:285-294.

Black J, Sholtes V. Biomaterial Aspects of Surface Replacement Arthroplasty of the Hip. *Orthopedic Clinics of North America* 1982; 13:709-728.

Black J. Polymers. In: *Orthopaedic Biomaterials in Research and Practice.* New York, Churchill Livingstone, 1988; 133-162.

Blamey J, Rajan S, Unsworth A, Dawber R. Soft Layered Prostheses for Arthritic Hip Joints - A Study of Materials Degradation. *Journal of Biomedical Engineering* 1991; 13(3):180-184.

Boettcher WG, Krengel WF, Toomey HE. Surface Replacement of the Hip: A Community Experience. In: Philip-Nelson J, ed. *The Hip.* St. Louis, C.V.Mosby, 1982; 146-155.

Bogoch ER, Fornasier VL, Capello WN. The Femoral Head Remnant in Resurfacing Arthroplasty. *Clinical Orthopaedics and Related Research* 1982; 162:92-105.

Bonfield W, Bowman J, Grynpas MD. Composite Materials for Use in Orthopaedics. UK patent no. GB2085461B; 1980.

Bonfield W, Coombs RRH, Doyle C, Sharp DJ, Tanner KE. Mechanical Properties of Subchondral Bone from Normal and Osteoarthrotic Human Femoral Heads. In: Bergmann G, Kölbel R, Rohlmann A, eds. *Biomechanics: Basic and Applied Research.* Dordrecht, Martinus Nijoff, 1987; 213-218.

Bonfield W, Grynpas MD. Anisotropy of the Young's Modulus of Bone. *Nature* 1977; 270:453-454.

Boone DC, Azen SP. Normal Range of Motion of Joints in Male Subjects. *Journal of Bone and Joint Surgery* 1979; 61-A:756-759.

Borzacchiello A, Ambrosio L, Nicolais L, Harper EJ, Tanner KE, Bonfield W. Isothermal and Non-isothermal Polymerization of a New Bone Cement. *Journal of Materials Science: Materials in Medicine* 1998; 9:317-324.

Bourne GH. *The Biochemistry and Physiology of Bone.* 2nd ed. New York: Academic Press, 1972.

Bradley GW, Freeman MAR, Revell PA. Resurfacing Arthroplasty. *Clinical Orthopaedics and Related Research* 1987; 220:137-141.

Bradley GW, Freeman MAR, Tuke MA, Elias SG, McKellop HA. All-Polymer Total Knee Replacement. *American Journal of Knee Surgery* 1992; 5:3-8.

Bradley GW, Freeman MAR. Revision of Failed Hip Resurfacing. *Clinical Orthopaedics and Related Research* 1983; 178:236-240.

Bradley GW, Freeman MAR, Tuke MA, McKellop HA. Evaluation of Wear in an All-Polymer Total Knee Replacement. Part 2: Clinical Evaluation of Wear in a Polyethylene on Polyacetal Total Knee. *Clinical Materials* 1993; 14:127-132.

Brand RA, Pedersen DR, Davy DT, Kotzar GM, Heiple KG, Goldberg VM. Comparison of Hip Force Calculations and Measurements in the Same Patient. *Journal of Arthroplasty* 1994; 45-51.

Bryant MJ, Mollan RA, Nixon JR. Survivorship analysis of the Ring hip arthroplasty. *Journal of Arthroplasty* 1991; 6 Suppl:S5-S10.

Brydson JA. Polyacetals and Related Materials. In *Plastic Materials*, Butterworth Heinemann, Oxford, 1993. 19, 497-512.

Buckwalter JA, Mankin HJ. Articular Cartilage Part II: Degeneration and Osteoarthrosis, Repair, Regneration, and Transplantation. *Journal of Bone and Joint Surgery* 1997; 79-A:612-632.

Byers PD, Contemponi CA, Farkas TA. A Post Mortem Study of the Hip Joint. *Annals of the Rheumatic Diseases* 1970; 29:15-31.

Capello WN, Ireland PH, Trammell TR, Eicher P. Conservative Total Hip Arthroplasty. *Clinical Orthopaedics and Related Research* 1978; 134:59-74.

Capello WN, Misamore GW, Trancik TM. Conservative Total Hip Arthroplasty. *Orthopedic Clinics of North America* 1982a; 13:833-842.

Capello WN, Misamore GW, Trancik TM. The Indiana Conservative (Surface-Replacement) Hip Arthroplasty. *Journal of Bone and Joint Surgery* 1984; 66-A:518-527.

Capello WN, Trancik TM, Misamore GW, Eaton R. Analysis of Revision Surgery of Resurfacing Hip Arthroplasty. *Clinical Orthopaedics and Related Research* 1982b; 170:50-55.

Capello WN, Trancik TM. Indiana Conservative Hip - Results, 2-4.5 Years. *Orthopaedic Transactions* 1981; 5:375.

Carter DR, Hayes WC. Bone Compressive Strength: the Influence of Density and Strain Rate. *Science* 1976; 194(4270):1174-1176.

Chan FW, Bobyn JD, Medley JB, Krygier JJ, Tanzer M. Wear and Lubrication of Metal-on-Metal Hip Implants. *Clinical Orthopaedics and Related Research* 1999; 369:10-24.

Chan FW, Bobyn JD, Medley JB, Krygier JJ, Yue S, Tanzer M. Engineering Issues and Wear Performance of Metal on Metal Hip Implants. *Clinical Orthopaedics and Related Research* 1996; 333:96-107.

Chanda M, Roy SK. Polyacetal. In: *Plastics Technology Handbook.* New York, Dekker, 1998; 675-679.

Chang WCW, Christensen TM, Pinilla TP, Keaveny TM. Uniaxial Yield Strains for Bovine Trabecular Bone are Isotropic and Asymmetric. *Journal of Orthopaedic Research* 1999; 17:582-585.

Charnley J. Arthroplasty of the Hip: A New Operation. *The Lancet* 1961; 1129-1132.

Charnley J. Tissue Reactions to Polytetrafluorethylene. *The Lancet* 1963; 1379.

Clarke HJ, Jinnah RH, Warden KE, Cox QGN, Curtis MJ. Evaluation of Acetabular Stability in Uncemented Prostheses. *Journal of Arthroplasty* 1991; 6:335-340.

Clarke IC, Amstutz HC. Human hip joint geometry and hemiarthroplasty selection. In: *The Hip.* St. Louis, C.V.Mosby, 1975; 63-89.

Clarke IC, Amstutz HC. Total Hip Joint Replacement. US Patent Number: US19770764184 19770131. 1978.

Clarke IC, Good V, Williams P, Schroeder D, Anissian L, Stark A, Oonishi H, Schuldies J, Gustafson G. Ultra-Low Wear Rates for Rigid-on-Rigid Bearings in

Total Hip Replacements. *Proceedings of the Insitution of Mechanical Engineers, part H* 2000; 214:331-347.

Clarke IC, Phillips W, McKellop H, Coster IR, Hedley A, Amstutz HC. Development of a Ceramic Surface Replacement for the Hip. An Experimental Sialon Model. *Biomaterials, Medical Devices and Artificial Organs* 1979; 7:111-126.

Clark JM, Freeman MAR, Witham D. The Relationship of Neck Orientation to the Shape of the Proximal Femur. *Journal of Arthroplasty* 1987; 2:99-109.

Collier JP, Bargmann LS, Currier BH, Mayor MB, Currier JH, Bargmann BC. An Analysis of Hylamer and Polyethylene Bearings From Retrieved Acetabular Components. *Orthopedics* 1998; 21:865-871.

Corin. *Corin Technical Data Sheet: Cormet 2000 Metal/Metal Resurfacing Hip.* 1998

Cotella L, Railton GT, Nunn D, Freeman MAR, Revell PA. ICLH Double-Cup Arthroplasty, 1980-1987. *Journal of Arthroplasty* 1990; 5:349-357.

Cristofolini L. Muscular Activity and the Biomechanics of the Hip. *Hip International* 1997; 7:39-41.

Crowninshield RD, Brand RA. A Physiologically Based Criterion of Muscle Force Prediction in Locomotion. *Journal of Biomechanics* 1981; 14(11):793-801.

Curtis MJ, Jinnah RH, Wilson VD, Hungerford DS. The Initial Stability of Uncemented Acetabular Components. *Journal of Bone and Joint Surgery* 1992; 74-B:372-376.

Currey JD. Mechanical Properties of Vertebrate Hard Tissues. *Proceedings of the Institution of Mechanical Engineers Part H* 1998; 212:399-411

Dalstra M. Biomechanical Aspects of the Pelvic Bone and Design Criteria for Acetabular Prostheses. PhD Thesis. University of Nijmegen, 1993.

Dobrev R. A Method for Evaluation of the Supportive Muscle Activity in the Human Hip. Personal Communication, 2000.

Dornhoffer JL. Hearing Results with the Dornhoffer Ossicular Replacement Prostheses. *Laryngoscope* 1998; 108(4):531-536.

Dostal WF, Andrews JG. A Three-Dimensional Biomechanical Model of Hip Musculature. *Journal of Biomechanics* 1981; 14(11):803-812.

Dowson D. Friction and Wear of Medical Implants and Prosthetic Devices. In: *Friction, Lubrication and Wear Technology.* Ohio, American Society for Metals, 1992; 656-664.

D'Souza SR, Sadiq S, New AMR, Northmore-Ball MD. Proximal Femoral Osteotomy as the Primary Operation for Young Adults Who Have Osteoarthrosis of the Hip. *Journal of Bone and Joint Surgery* 1998; 80-A:1428-1438.

Duda GN, Heller M, Albinger J, Schulz O, Schneider E, Claes L. Influence of Muscle Forces on Femoral Strain Distribution. *Journal of Biomechanics* 1998; 31:841-846.

Eckstein F, Eisenhart-Rothe Rv, Landgraf J, Adam C, Loehe F, Müller-Gerbl M, Putz R. Quantitative Analysis of Incongruity, Contact Areas and Cartilage Thickness in the Human Hip Joint. *Acta Anatomica* 1997; 158:192-204.

Eckstein F. Morphology of the Acetabulum. Personal Communication. 1998.

Eftekhar NS. A Historical Note on the Development of Hip Arthroplasty. In: *Principles of Total Hip Arthroplasty.* Saint Louis, C.V. Mosby, 1978; 1-8.

Eftekhar NS. *Total Hip Arthroplasty.* St Louis, C.V. Mosby, 1993, Vol. I; 6-7.

Eisenhart-Rothe Rv, Eckstein F, Müller-Gerbl M, Landgraf J, Rock C, Putz R. Direct Comparison of Contact Areas, Contact Stress and Subchondral Mineralization in Human Hip Joint Specimens. *Anatomy and Embryology* 1997; 195:279-288.

Fisher J. Tribology of Natural and Artificial Joints. In: Hughes SPF, McCarthy ID, eds. *Sciences Basic to Orthopaedics.* London, W.B.Saunders, 1997(16); 240-249.

Fisher J, Dowson D. Tribology of Total Artificial Joints. *Proceedings of the Insitution of Mechanical Engineers, part H* 1991; 205:73-79.

Forester AJ, Draper EC. Applied Biomechanics of Prosthetic Joint Replacement. In: Hughes SPF, McCarthy ID, eds. *Sciences Basic to Orthopaedics.* London, W.B.Saunders, 1997.

Fraker AC. Corrosion of Metallic Implants and Prosthetic Devices. In: Ohio, Amercian Society for Metals, 1992; 1324-1335.

Franzén H, Mjöberg B, Rydholm U. Metal Backing Improves the Survival of Surface Replacement of the Hip. *Archives of Orthopaedic and Traumatic Surgery* 1993; 112:257-259.

Freeman MAR, Bradley GW. Experience With the ICLH Surface Replacement Hip Prosthesis. *Orthopaedic Transactions* 1981; 5:375-376.

Freeman MAR, Bradley GW. ICLH Double Cup Arthroplasty. *Orthopedic Clinics of North America* 1982; 13:799-811.

Freeman MAR, Bradley GW. ICLH Surface Replacement of the Hip: An Analysis of the First 10 Years. *Journal of Bone and Joint Surgery* 1983; 65-B:405-411.

Freeman MAR, Brown GC. ICLH Cemented Double Cup Replacement. *Archives of Orthopaedic and Traumatic Surgery* 1978; 92:191-198.

Freeman MAR, Cameron HU, Brown GC. Cemented Double Cup Arthroplasty of the Hip: A 5 Year Experience with the ICLH Prosthesis. *Clinical Orthopaedics and Related Research* 1978; 134:45-52.

Freeman MAR, Plante-Bordeneuve P. Early Migration and Late Aseptic Failure of Proximal Femoral Prostheses. *Journal of Bone and Joint Surgery* 1994; 76-B:432-438.

Freeman MAR, Swanson SAV, Day WH, Thomas RJ. Conservative Total Replacement of the Hip. *Journal of Bone and Joint Surgery* 1975; 57-B:114.

Freeman MAR. Some Anatomical and Mechanical Considerations Relevant to the Surface Replacement of the Hip. *Clinical Orthopaedics and Related Research* 1978b; 134:19-24.

Freeman MAR. Subtended Angle of Reamed Acetabulum. Personal Communication. 1998.

Freeman MAR. Total Surface Replacement Hip Arthroplasty. *Clinical Orthopaedics and Related Research* 1978a; 134:2-4.

Freeman MAR. Why Resect the Neck? *Journal of Bone and Joint Surgery* 1986; 68-B:346-349.

Früh HJ, Willmann G, Pfaff HG. Wear Characteristics of Ceramic-on-Ceramic for Hip Endoprostheses. *Biomaterials* 1997; 18:873-876.

Furlong R. Experience of Wagner Resurfacing. Personal Communication. 1998.

Furuya K, Tsuchiya M, Kawachi S. Socket-Cup Arthroplasty. *Clinical Orthopaedics and Related Research* 1978; 134:41-44.

Fyhrie DP, Carter DR, Schurman DJ. Effects of Ingrowth, Geometry, and Material on Stress Transfer Under Porous-Coated Hip Surface Replacements. *Journal of Orthopaedic Research* 1988; 6(3):425-433.

Gander W, Golub GH, Strebel R. Fitting of Circles and Ellipses: Least Squares Solution. Techreport, Departement Informatik, ETH Zürich. 1994. (ftp.inf.ethz.ch/doc/tech-reports/1994/217.ps)

Gerard Y. Hip Arthroplasty by Matching Cups. *Clinical Orthopaedics and Related Research* 1978; 134:25-35.

Gibson LJ. The Mechanical Behaviour of Cancellous Bone. *Journal of Biomechanics* 1985; 18:317-328.

Graeter JH, Nevins R. Early Osteolysis With Hylamer Acetabular Liners. *Journal of Arthroplasty* 1998; 13:464-466.

Gray's Anatomy. 37th ed. Edinburgh: Churchill Livingstone, 1989.

Greenwald AS, O'Connor JJ. The Transmission of Load Through the Human Hip Joint. *Journal of Biomechanics* 1971; 4:507-528.

Grujic H, Olerud S, Soreff J. Wagner Resurfacing Hip Arthroplasty Preliminary Results. *Acta Orthopaedica Scandinavica* 1982; 53:785-789.

Guild FJ, Bonfield W. Predictive Modelling of the Mechanical Properties and Failure Processes in Hydroxyapatite-Polyethylene (Hapex(TM)) Composite. *Journal of Materials Science: Materials in Medicine* 1998; 9:497-502.

Hall RM, Siney P, Unsworth A, Wroblewski BM. The Association Between Rates of Wear in Retrieved Acetabular Components and the Radius of the Femoral Head. *Proceedings of the Insitution of Mechanical Engineers, part H* 1998; 212:321-326.

Harman MK, Banks SA, Hodge WA. Wear Analysis of a Retrieved Hip Implant with Titanium Nitride Coating. *Journal of Arthroplasty* 1997; 12:938-945.

Head WC. The Wagner Surface Replacement Arthroplasty. *Orthopedic Clinics of North America* 1982; 13:789-797.

Head WC. Total Articular Resurfacing Arthroplasty. *Journal of Bone and Joint Surgery* 1984; 66-A:28-34.

Head WC. Wagner Surface Replacement Arthroplasty of the Hip. *Journal of Bone and Joint Surgery* 1981a; 63-A:420-427.

Head WC. Wagner vs. TARA: Comparison of Early Results with Two Types of Conservative Total Hip Replacement Procedures. *Orthopaedic Transactions* 1981b; 5:387-388.

Herberts P, Lansinger O, Romanus B. Surface Replacement Arthroplasty of the Hip: Experience with the ICLH Method. *Acta Orthopaedica Scandinavica* 1983; 54:884-890.

Hodge WA, Carlson KL, Fijan RS, Burgess RG, Riley PO, Harris WH, Mann RW. Contact Pressures from an Instrumented Hip Endoprosthesis. *Journal of Bone and Joint Surgery* 1989; 71-A:1378-1385.

Howatson AM, Lund PG, Todd JD. *Engineering Tables and Data.* 2nd edition. London: Chapman & Hall, 1994.

Howie DW, Campbell D, McGee M, Cornish B. Wagner Resurfacing Hip Arthroplasty. *Journal of Bone and Joint Surgery* 1990a; 72-A:708-714.

Howie DW, Campbell D, McGee MA, Cornish BL. Eight to 13-Year Survival Analysis of 270 Resurfacing Hip Arthroplasties with 100 Percent Long-Term Follow-Up. *Journal of Bone and Joint Surgery* 1992; 74-B:274-275.

Howie DW, Cornish BL, Vernon-Roberts B. Resurfacing Hip Arthroplasty: Classification of Loosening and Role of Prosthesis Wear Particles. *Clinical Orthopaedics and Related Research* 1990b; 255:144-159.

Howie DW, Cornish BL, Vernon-Roberts B. The Viability of the Femoral Head After Resurfacing Hip Arthroplasty in Humans. *Clinical Orthopaedics and Related Research* 1993; 291:171-184.

Huang J, Di Silvio L, Wang M, Tanner KE, Bonfield W. *In Vitro* Mechanical and Biological Assessment of Hydroxyapatite-Reinforced Polyethylene Composite. *Journal of Materials Science: Materials in Medicine* 1997; 8:775-779.

Huiskes R, Ruimerman R, van Lenthe GH, Janssen JD. Effects of Mechanical Forces on Maintenance and Adaptation of Form in Trabecular Bone. *Nature* 2000; 405:704-706.

Huiskes R, Strens PHGE, Vroemen W, Slooff TJ. Post-Loosening Mechanical Behaviour of Femoral Resurfacing Prostheses. *Clinical Materials* 1990; 6:37-55.

Husmann O, Rubin PJ, Leyvraz PF, Roguin Bd, Argenson JN. Three-dimensional Morphology of the Proximal Femur. *Journal of Arthroplasty* 1997; 12:444-450.

Ingham E, Fisher J. Biological Reactions to Wear Debris in Total Joint Replacement. *Proceedings of the Insitution of Mechanical Engineers, part H* 2000; 214(1):21-37.

Jin ZM, Dowson, D, Fisher J. Analysis of Fluid Film Lubrication in Artificial Hip Joint Replacements with Surfaces of High Elastic Modulus. *Proceedings of the Insitution of Mechanical Engineers, part H* 1997; 211(3):247-256.

Jin ZM, Heng SM, Ng HW, Auger DD. An Axisymmetric Contact Model of Ultra High Molecular Weight Polyethylene Cups Against Metallic Femoral Heads for Artificial Hip Joint Replacements. *Proceedings of the Insitution of Mechanical Engineers, part H* 1999; 213(4):317-327.

Jolley MN, Salvati EA, Brown GC. Early Results and Complications of Surface Replacement of the Hip. *Journal of Bone and Joint Surgery* 1982; 64-A:366-377.

Joshi RP, Eftekhar NS, McMahon DJ, Nercessian OA. Osteolysis after Charnley Primary Low-Friction Arthroplasty - A Comparison of Two Matched Paired Groups. *Journal of Bone and Joint Surgery* 1998; 80-B:585-590.

Joshi MG, Santare MH, Advani SG. Survey of Stress Analyses of the Femoral Hip Prosthesis. *Applied Mechanics Reviews* 2000; 53(1):1-18.

Judet J, Judet R. The Use of an Artificial Femoral Head for Arthroplasty of the Hip Joint. *Journal of Bone and Joint Surgery* 1950; 32-B:166-173.

Kärrholm J, Borssen B, Löwenhielm G, Snorrason F. Does Early Micromotion of Femoral Stem Prostheses Matter? 4-7-Year Stereoradiographic Follow-Up of 84 Cemented Prostheses. *Journal of Bone and Joint Surgery* 1994; 76-B:912-917.

Katz DM, Blatcher S, Shelton JC. Quantification of Holographic Fringe Data: Comparison of Intact and Implanted Femurs. *Medical Engineering and Physics* 1998; 20:114-123.

Kawalec JS, Brown SA, Payer JH, Merritt K. Mixed-Metal Fretting Corrosion of Ti6Al4V and Wrought Cobalt Alloy. *Journal of Biomedical Materials Research* 1995; 29:867-873.

Keaveny TM, Niebur GL, Yeh OC, Morgan EF. Micromechanics and Trabecular Bone Strength. *Proceedings of the 12th Conference of the European Society of Biomechanics,* Dublin 2000; 5-6.

Keyak JH, Rossi SA. Prediction of Femoral Fracture Load Using Finite Element Models: An Examination of Stress- and Strain-Based Failure Theories. *Journal of Biomechanics* 2000; 33(2):209-214.

Kim WC, Grogan T, Amstutz HC, Dorey F. Survivorship Comparison of THARIES and Conventional Hip Arthroplasty in Patients Younger than 40 Years Old. *Clinical Orthopaedics and Related Research* 1987; 214:269-277.

Kobayashi A, Donnelly WJ, Scott G, Freeman MAR. Early Radiological Observations May Predict the Long-Term Survival of Femoral Hip Prostheses. *Journal of Bone and Joint Surgery* 1997a; 79-B:583-589.

Kobayashi A, Freeman MAR, Bonfield W, Kadoya Y, Yamac T, Al-Saffar N, Scott G, Revell PA. Number of Polyethylene Particles and Osteolysis in Total Joint Replacements. *Journal of Bone and Joint Surgery* 1997b; 79-B:844-848.

Kohn DH, Ducheyne P. Materials for Bone and Joint Replacement. In: Williams DF, ed. *Medical and Dental Materials*. Weinheim, VCH, 1992:33-109.

Krikler S. BHR and Cormet 2000 Outcomes. Personal Communication. 1999.

Krismer M, Stöckl B, Fischer M, Bauer R, Mayrhofer P, Ogon M. Early Migration Predicts Late Aseptic Failure of Hip Sockets. *Journal of Bone and Joint Surgery* 1996; 78-B:422-426.

Krzypow DJ, Rimnac CM. Cyclic Steady State Stress-Strain Behaviour of UHMW Polyethylene. *Biomaterials* 2000; 21:2081-2087.

Kuiper J. Numerical Optimization of Artificial Hip Joint Designs. PhD Thesis. University of Nijmegen, 1993.

Kurrat HJ, Oberländer W. The Thickness of the Cartilage in the Hip Joint. *Journal of Anatomy* 1978; 126(1):145-155.

Lanyon LE. Osteocytes, Strain Detection, Bone Modeling and Remodeling. *Calcified Tissue International* 1993; 53:S102-S107.

Latour RA, Brattain MA. Femoral Strain Profiles Under Simulated 3-D Muscle and Joint Loads for Heel Strike, Midstance, and Toe Off. *Critical Reviews in Biomedical Engineering* 2000; 28(1-2):109-113.

Lazennac JY, Laudet CG, Guérin-Surville H, Roy-Camille R, Saillant G. Dynamic Anatomy of the Acetabulum: An Experimental Approach and Surgical Implications. *Surgical and Radiologic Anatomy* 1997; 19:23-30.

Lewis G. Properties of Crosslinked Ultra-High-Molecular-Weight Polyethylene. *Biomaterials* 2001; 22:371-401.

Lewis G. Polyethylene Wear in Total Hip and Knee Arthroplasties. *Journal of Biomedical Materials Research* 1997; 38:55-75.

Lewold S, Olsson H, Gustafson P, Rydholm A, Lidgren L. Overall Cancer Incidence Not Increased after Prosthetic Knee Replacement: 14,551 Patients Followed for 66,622 Person-Years. *International Journal of Cancer* 1996; 68:30-33.

Li J, Liao H, Hermansson L. Sintering of Partially-Stabilized Zirconia and Partially-Stabilized Zirconia-Hydroxyapatite Composites by Hot Isostatic Pressing and Pressureless Sintering. *Biomaterials* 1996; 17:1787-1790.

Li S, Burstein AH. Current Concepts Review: Ultra-High Molecular Weight Polyethylene. *Journal of Bone and Joint Surgery* 1994; 76-A:1080-1090.

Linde F, Nørgaard P, Hvid I, Odgaard A, Søballe K. Mechanical Properties of Trabecular Bone. Dependency on Strain Rate. *Journal of Biomechanics* 1991; 24(9):803-809.

Linde F, Hvid I, Madsen F. The Effect of Specimen Geometry on the Mechanical Behaviour of Trabecular Bone Specimens. *Journal of Biomechanics* 1992; 25(4):359-368.

Ling RSM, O'Connor JJ, Tung-Wu L, Lee AJC. Muscular Activity and the Biomechanics of the Hip. *Hip International* 1996; 6:91-105.

Loupasis G, Birtwistle SJ, Hyde ID. Hydroxyapatite-coated Threaded Acetabular Prostheses. A Five Year Follow-up Radiographic Study. *Hip International* 1997; 7:11-16.

Ma SA, Kabo JM, Amstutz HC. Frictional Torque in Surface and Conventional Hip Replacement. *Journal of Bone and Joint Surgery* 1983; 65-A:366-370.

Mai MT, Schmalzried TP, Dorey F, Campbell PA, Amstutz HC. The Contribution of Frictional Torque to Loosening at the Cement-Bone Interface in THARIES Hip Replacements. *Journal of Bone and Joint Surgery* 1996; 78-A:505-511.

Makiyama AM, Platts MJ. Topology Design for Composite Components of Minimum Weight. *Applied Composite Materials* 1996; 3:29-41.

Malchau H, Herberts P. *Prognosis of Total Hip Replacement.* University of Gothenburg, Swedish National Hip Arthroplasty Register, 1998.

Malchau H, Herberts P, Ahnfelt L. Prognosis of Total Hip Replacement in Sweden - Follow Up of 92,675 Operations Performed 1978-1990. *Acta Orthopaedica Scandinavica* 1993; 64:497-506.

Malchau H, Herberts P, Söderman P, Odén A. *Prognosis of Total Hip Replacement: Update and Validation of Results from the Swedish National Registry 1979-1998.* University of Gothenburg, Swedish National Hip Arthroplasty Register, 2000.

Mallory TH, Ballas S, Atta Gv. Total Articular Replacement Arthroplasty: A Clinical Review. *Clinical Orthopaedics and Related Research* 1984; 185:131-136.

Mantell SC, Chanda H, Bechtold JE, Kyle RF. A Parametric Study of Acetabular Cup Design Variables Using Finite Element Analysis and Statistical Design of Experiments. *Journal of Biomechanical Engineering* 1998; 120:667-675.

Martini FH. *Fundamentals of Anatomy and Physiology.* 3rd edition. London: Prentice Hall, 1995.

Massoud SN, Hunter JB, Holdsworth BJ, Wallace WA, Juliusson R. Early Femoral Loosening in One Design of Cemented Hip Replacement. *Journal of Bone and Joint Surgery* 1997; 79-B:603-608.

Mathiesen EB, Sudmann E, Lindgren U, Reinholt F. Tissue Reaction to Wear Products from Delrin(R) and UHMW-Polyethylene. *Acta Orthopaedica Scandinavica* 1983; 54:485.

Mathiesen EB, Lindgren U, Reinholt F, Sudmann E. Wear of the Acetabular Socket: Comparison of Polyacetal and Polyethylene. *Acta Orthopaedica Scandinavica* 1986; 57:193-196.

Maxian TA, Brown TD, Pedersen DR, McKellop HA, Lu B, Callaghan JJ. Finite Element Analysis of Acetabular Wear. Validation, and Backing and Fixation Effects. *Clinical Orthopaedics and Related Research* 1997; 344:111-117.

McGee MA, Howie DW, Neale SD, Haynes DR, Pearcy MJ. The Role of Polyethylene Wear in Joint Replacement Failure. *Proceedings of the Insitution of Mechanical Engineers, part H* 1997; 211(1):65-72.

McKellop HA. All Polymer Hip Replacement. Personal Communication. 1998.

McKellop H, Clarke I, Markolf K, Amstutz H. Friction and Wear Properties of Polymer, Metal, and Ceramic Prosthetic Joint Materials Evaluated on a Multichannel Screening Device. *Journal of Biomedical Materials Research* 1981; 15:619-653.

McKellop HA, Milligan HL, Röstlund T. Long Term Biostability of Polyacetal (Delrin) Implants. *Journal of Heart Valve Disease* 1996; 5:S238-S242.

McKellop HA, Röstlund T, Bradley G. Evaluation of Wear in an All-Polymer Total Knee Replacement. Part 1: Laboratory Testing of Polyethylene on Polyacetal Bearing Surfaces. *Clinical Materials* 1993; 14:117-126.

McKellop H, Shen FW, Lu B, Campbell P, Salovey R. Development of an Extremely Wear-Resistant Ultra High Molecular Weight Polyethylene for Total Hip Replacements. *Journal of Orthopaedic Research* 1999; 17:157-167.

McMinn DJW. Co-Cr on Co-Cr Wear Mechanisms in the McMinn Resurfacing. Personal Communication. 1997.

McMinn DJW. Cement Thickness Under Femoral Component of Resurfacing. Personal Communication. 2000.

McMinn D, Treacy R, Lin K, Pynsent P. Metal on Metal Surface Replacement of the Hip. Experience of the McMinn Prosthesis. *Clinical Orthopaedics and Related Research* 1996; 329s:S89-S98.

McMinn DJW, Pynsent PB, DeCock CAEM, Isbister ES, Treacy RBC. Results of Metal on Metal Hip Resurfacing. *Proceedings of the British Hip Society,* Oxford, 2000; 19.

McNie C, Barton DC, Stone MH, Fisher J. Prediction of Plastic Strains in Ultra-High Molecular Weight Polyethylene Due to Microscopic Asperity Interactions During Sliding Wear. *Proceedings of the Insitution of Mechanical Engineers, part H* 1998; 212:49-56.

Merritt K, Brown SA. Distribution of Cobalt Chromium Wear and Corrosion Products and Biologic Reactions. *Clinical Orthopaedics and Related Research* 1996; 329s:S233-S243.

Mesko WJ, Goodman FG, Stanescu S. Total Articular Replacement Arthroplasty: A Three- to Ten-Year Case-Controlled Study. *Clinical Orthopaedics and Related Research* 1994; 300:168-177.

Mjöberg B. Theories of Wear and Loosening in Hip Prostheses: Wear-induced Loosening vs Loosening-induced Wear - A Review. *Acta Orthopaedica Scandinavica* 1994; 65:361-371.

Moore DJ, Freeman MAR, Revell PA, Bradley GW, Tuke M. Can a Total Knee Replacement Prosthesis be made entirely of Polymers? *Journal of Arthroplasty* 1998; 13:388-395.

Morscher EW, Dick W. Cementless Fixation of "Isoelastic" Hip Endoprosthesis Manufactured from Plastic Materials. *Clinical Orthopaedics and Related Research* 1983; 176:77-87.

Morscher EW. Current Status of Acetabular Fixation in Primary Total Hip Arthroplasty. *Clinical Orthopaedics and Related Research* 1992; 274:172-193.

Munting E, Smitz P, Sante Nv, Nagant de Deuxchaisnes C, Vincent A, Devogelaer J. Effect of a Stemless Femoral Implant for Total Hip Arthroplasty on the

Bone Mineral Density of the Proximal Femur. *Journal of Arthroplasty* 1997; 12:373-379.

Munting E, Verhelpen M. Fixation and Effect on Bone Strain Pattern of Stemless Hip Prosthesis. *Journal of Biomechanics* 1995; 28:949-961.

Murphy LA, Prendergast PJ, Christie R, Resch H. Finite Element Analysis of an Offset Keeled Glenoid Prosthesis Compared to a Centre Keeled Design. *Proceedings of the 12th Conference of the European Society of Biomechanics,* Dublin. 2000; 161.

Murray DW. The Definition and Measurement of Acetabular Orientation. *Journal of Bone and Joint Surgery* 1993; 75-B:228-232.

Murray M. (Morgan Matroc Limited). Personal Communication, 1998.

Murray WR, Meter JWV. Surface Replacement Hip Arthroplasty: Results of the First Seventy-Four Consecutive Cases at the University of California, San Francisco. In: Philip-Nelson J, ed. *The Hip.* St. Louis, C.V.Mosby, 1982:156-166.

Nevelos J, Ingham E, Doyle C, Nevelos A, Walter W, Fisher J. Micro-Separation of the Centres of Alumina-Alumina Artificial Hip Joints During Simulator Testing Produces Clinically Relevant Wear Rates and Patterns. *Proceedings of the 12th Conference of the European Society of Biomechanics,* Dublin 2000; 197.

New AMR. Experimental and Finite Element Studies of Acetabular Cement Pressurisation and Socket Fixation in Total Hip Replacement. PhD Thesis. London University, 1997.

Niebur GL, Feldstein MJ, Yuen JC, Chen TJ, Keaveny TM. High-Resolution Finite Element Models with Tissue Strength Asymmetry Accurately Predict Failure of Trabecular Bone. *Journal of Biomechanics* 2000; 33:1575-1583.

Niininmaki T, Puranen J, Jalovaara P. Total Hip Arthroplasty Using Isoelastic Femoral Stems. A Seven- to Nine- Year Follow-up in 108 Patients. *Journal of Bone and Joint Surgery* 1994; 76-B:413-418.

Nishio A, Eguchi M, Kaibara N. Socket and Cup Surface Replacement of the Hip. *Clinical Orthopaedics and Related Research* 1978; 134:53-58.

Noble PC, Alexander JW, Lindahl LJ, Yew DT, Granberry WM, Tullos HS. The Anatomic Basis of Femoral Component Design. *Clinical Orthopaedics and Related Research* 1988; 235:148-165.

Northmore-Ball MD. Conservative Reaming of the Acetabulum. Personal Communication. 1998.

Olivier LC, Neudeck F, Hippel C, Kaiser S, Schmit-Neuerburg KP. [Results of Cement-Free Implanted, Robert Mathys Isoelastic Acetabular Cup]. *Unfallchirurgie* 1998; 24(2):49-54.

Paavolainen P, Pukkala E, Pulkkinen P, Visuri T. Cancer Incidence in Finnish Hip Replacement Patients From 1980 to 1995. *Journal of Arthroplasty* 1999; 14:272-280.

Pappas MJ, Makris G, Beuchel FF. Titanium Nitride Ceramic Film Against Polyethylene. A 48 Million Cycle Wear Test. *Clinical Orthopaedics and Related Research* 1995; 317:64-70.

Parkin I. Morphology of the Hip. Personal Communication. 1998.

Paul JP. Techniques of Gait Analysis. *Proceedings of the Royal Society of Medicine* 1974; 67:401-404.

Pauwels F. *Biomechanics of the Locomotor Apparatus.* Chapter 19. Berlin: Springer-Verlag, 1980.

Peterson L, Minas T, Brittberg M, Nilsson A, Sjogren-Jansson E, Lindahl A. Two- to 9-Year Outcome After Autologous Chondrocyte Transplantation of the Knee. *Clinical Orthopaedics and Related Research* 374:212-234, 2000.

Pedersen, DR, Brand, RA, Davy, DT. Pelvic Muscle and Acetabular Contact Forces During Gait. *Journal of Biomechanics* 1997; 30(9):959-965.

Pickard,JE. All-Polymer Resurfacing: Design for Manufacture. Personal Communication. 2000.

Pidaparti RMV, Turner CH. Cancellous Bone Architecture: Advantages of Nonorthogonal Trabecular Alignment Under Multidirectional Joint Loading. *Journal of Biomechanics* 1997; 30:979-983

Pilliar RM, Lee JM, Maniatopoulos C. Observations on the Effect of Movement on Bone Ingrowth into Porous-Surfaced Implants. *Clinical Orthopaedics and Related Research.* 1986; 208:108-113.

Pilliar RM, Weatherly GC. Developments in Implant Alloys. In: Williams DF, ed. *CRC Critical Reviews in Biocompatibility.* 1986:371-403.

Plath J, Schuhr T, Fethke K, Zacharias T, Johnson M, Mach J. Loosening Pattern in a Cementless Custom-Made Hip Stem: X-ray Analysis, Finite-Elements and Photoelasticity Measurements. *Archives of Orthopaedic and Traumatic Surgery.* 2000; 120:103-107.

van Raay JJAM, Rozing PM, Eulderink F. Tissue response to the failed Gerard double-cup. *Acta Orthopaedica Scandinavica* 1993; 64:268-272.

Reigstad A, Brandt M, Hetland KR. Total Hip Replacement with Müller Prosthesis and ICLH Double Cup: 2- to 6- Year Results of a Prospective Comparative Study. *Acta Orthopaedica Scandinavica* 1986; 105:175-182.

Reikerås O, Bjerkreim I, Kolbenstvedt A. Anteversion of the Acetabulum and Femoral Neck in Normals and in Patients with Osteoarthritis of the Hip. *Acta Orthopaedica Scandinavica* 1983; 54:18-23.

Reilly DT, Burstein AH. The Elastic and Ultimate Properties of Compact Bone Tissue. *Journal of Biomechanics* 1975; 8:393-405.

Reilly DT, Burstein AH, Frankel VH. The Elastic Modulus for Bone. *Journal of Biomechanics* 1974; 7:271-275.

Reynolds D, Lucas J, Klaue K. Retroversion of the Acetabulum: A Cause of Hip Pain. *Journal of Bone and Joint Surgery* 1999; 81-B(2):281-288.

Ritter MA, Gioe TJ. Conventional Versus Resurfacing Total Hip Arthroplasty. *Journal of Bone and Joint Surgery* 1986; 68-A:216-225.

Roach KE, Miles TP. Normal Hip and Knee Active Range of Motion: The Relationship to Age. *Physical Therapy* 1991; 71:656-665.

Roass A, Andersson GB. Normal Range of Motion of the Hip and Knee and Ankle Joints in Male Subjects 30-40 Years of Age. *Acta Orthopaedica Scandinavica* 1982; 53:205-208.

Roberts SNJ, Wallace WA, Coughlan DP. The Geometry of the Humeral Head and the Design of Prostheses. *Journal of Bone and Joint Surgery* 1991; 73-B:647-650.

Rubin PJ, Leyvraz PF, Aubaniac JM, Argenson JN, Estève P, Roguin Bd. The Morphology of the Proximal Femur. *Journal of Bone and Joint Surgery* 1992; 74-B:28-32.

Rushfeldt PD, Mann RW, Harris WH. Improved Techniques for Measuring *In Vitro* the Geometry and Pressure Distribution in the Human Acetabulum - 1. Ultrasonic Measurement of Acetabular Surfaces, Sphericity and Cartilage Thickness. *Journal of Biomechanics* 1981; 14:253-260.

Rushton N, Rae T. The Intra-Articular Response to Particulate Carbon Fibre Reinforced High Density Polyethylene and its Constituents: an Experimental Study in Mice. *Biomaterials* 1984; 5:352-356.

Ryd L, Albrektsson BEJ, Carlsson L, Dansgård F, Herberts P, Lindstrand A, Regner L, Toksvig-Larsen S. Roentgen Stereophotogrammetric Analysis as a Predictor of Mechanical Loosening of Knee Prostheses. *Journal of Bone and Joint Surgery* 1995; 77-B(3):377-383.

Rydell NW. Forces Acting on the Femoral Head-Prosthesis. A Study on Strain Guage Supplied Prostheses in Living Persons. *Acta Orthopaedica Scandinavica* 1966; 37:1-132.

Salzer M, Knahr K, Locke H, Stärk N. Cement-Free Bioceramic Double-Cup Endoprosthesis of the Hip-Joint. *Clinical Orthopaedics and Related Research* 1978; 134:80-86.

Scheller G, Schwarz M, Fruh HJ, Jani L. Simulator Trials to Determine the Wear of the Combination Aluminium Oxide Ceramic-Carbon Fibre Reinforced Plastic (CFRP) Used as an Insert in a Hip Socket. *Archives of Orthopaedic and Traumatic Surgery* 1999; 119:13-17.

Schmalzried TP, Fowble VA, Ure KJ, Amstutz HC. Metal on Metal Surface Replacement of the Hip: Technique, Fixation and Early Results. *Clinical Orthopaedics and Related Research* 1996; 329s:S106-S114.

Sedel L, Kerboull L, Christel P, Meunier A, Witvoet J. Alumina-on-Alumina Hip Replacement: Results and Survivorship in Young Patients. *Journal of Bone and Joint Surgery* 1990; 72-B:658-663.

Sedel L, Nizard RS, Kerboull L, Witvoet J. Alumina-Alumina Hip Replacement in Patients Younger than 50 Years Old. *Clinical Orthopaedics and Related Research* 1994; 298:175-183.

Sedel L. Ceramic Hips. *Journal of Bone and Joint Surgery* 1992; 74-B:331-332.

Semlitsch M, Streicher RM, Weber H. Long-Term Results with Metal/Metal Pairing in Artificial Hip Joints. In: Buchhorn, G.H., Willert, H. eds. *Technical Principles, Design and Safety of Joint Implants.* Göttingen, Hogrefe and Huber, 1994:62-67.

Sevostianov I, Kachanov M. Impact of Porous Microstructure on the Overall Elastic Properties of the Osteonal Cortical Bone. *Journal of Biomechanics* 2000; 33:881-888.

Shelton JC. Holographic Interferometry of the McMinn Resurfacing. Personal Communication. 1999.

Simank H, Brocal DRC, Reiser D, Thomsen M, Sabo D, Lukoschek M. Middle-Term Results of Threaded Acetabular Cups: High Failure Rates Five Years After Surgery. *Journal of Bone and Joint Surgery* 1997; 79-B:366-370.

Skiens WE, Williams JL. Ionizing Radiation's Effects on Selected Biomedical Polymers. In: Szycher,M. ed. *Biocompatible Polymers, Metals and Composites.* Lancaster (PA), Society of Plastics Engineers, 1983; 44:1001-1018.

Skittides P, Ioannides T, Vandersloten J, Marsh R. Design principles of hip prostheses based on the endosteal and periosteal geometry of the hip. 1994:356-360.

Smith GDW. Stainless Steels. *Lecture Course: Engineering Alloys,* Oxford, 1995.

Smith SL, Ash HE, Unsworth A. A Tribological Study of UHMWPE Acetabular Cups and Polyurethane Compliant Layer Acetabular Cups. *Journal of Biomedical Materials Research* 2000; 53:710-716.

Smith-Petersen MN. Evolution of Mould Arthroplasty of the Hip Joint. *Journal of Bone and Joint Surgery* 1948; 30-B:59-75.

Spears IR, Pfleiderer M, Schneider E, Hille E, Bergmann G, Morlock MM. Interfacial Conditions Between a Press-Fit Acetabular Cup and Bone During Daily Activities: Implications for Achieving Bone In-Growth. *Journal of Biomechanics* 2000; 33:1471-1477.

Stansfield B. Joint Force in a Pelvic Co-ordinate System. Personal Communication. 2000.

Streicher RM, Schön R, Semlitsch M. Investigation of the Tribological Behaviour of Metal on Metal Combinations for Artificial Hip Joints. *Biomedizinische Technik* 1990; 35:3-7.

Strens PHGE. Analysis of Implant Failure in Wagner Resurfacing Arthroplasty. PhD Thesis. St Radboud Hospital, Nijmegen, the Netherlands, 1986.

Sugano N, Noble PC, Kamaric MS. Predicting the Position of the Femoral Head Center. *Journal of Arthroplasty* 1999; 14:102-107.

Sugano N. Femoral Head to Neck Diameter Ratio. Personal Communication. 2000.

Sullivan CP, Donachie MJ, Morral FR. *Cobalt-base Superalloys - 1970.* Brussels: Centre d'Information du Cobalt, 1970.

Swanson SAV, Freeman MAR. Endoprosthetic Bone Joint Devices. UK Patent Number: GB19720052945 19721116. 1975.

Sychterz CJ, Shah N, Engh CA. Examination of Wear in Duraloc Acetabular Components: Two- to Five-Year Evaluation of Hylamer and Enduron Liners. *Journal of Arthroplasty* 1998; 13:508-514.

Täger KH. Aspects of Loosening in McKee-Farrar Endoprostheses. In: Buchhorn GH, Willert H, eds. *Technical Principles, Design and Safety of Joint Implants.* Göttingen, Hogrefe + Huber, 1994:72-81.

Tanaka S. Surface Replacement of the Hip Joint. *Clinical Orthopaedics and Related Research* 1978; 134:75-79.

Tanner KE. Compression Moulding of HAPEX™ and PE. Personal Communication. 2001.

Tanner KE, Downes RN, Bonfield W. Clinical Application of Hydroxyapatite-Reinforced Polyethylene. *British Ceramic Transactions* 1994; 93:104-107.

Tanner KE, Sharp DJ, Doyle C, Coombs RRH, Bonfield W. Osteoarthrosis and the Mechanical Behaviour of Trabecular Bone in the Human Femoral Head. *Implant Materials in Biofunction.* Eds. de Putter C, de Lange GL, de Groot K, Lee AJC. In *Advances in Biomaterials, vol. 8.* Elsevier, Amsterdam. 1988; 423-428.

Taylor M, Tanner KE, Freeman MAR, Yettram AL. Finite Element Modelling - Predictor of Implant Survival? *Journal of Materials Science: Materials in Medicine* 1995; 6:808-812.

Taylor M, Tanner KE, Freeman MAR, Yettram AL. Stress and Strain Distribution Within the Intact Femur: Compression or Bending? *Medical Engineering and Physics* 1996; 18:122-131.

Taylor M, Tanner KE. Fatigue Failure of Cancellous Bone: A Mechanism of Implant Migration and Loosening? Gisela Sturm Prize Essay, 1996.

Taylor M, Tanner KE. Fatigue Failure of Cancellous Bone: A Possible Cause of Implant Migration and Loosening. *Journal of Bone and Joint Surgery* 1997; 79-B:181-182.

Taylor M. Finite Element Analysis of Cancellous Bone Stresses Within an Implanted Femur and Their Relationship to Implant Migration. PhD Thesis. University of London, 1997.

Thompson DW. *On Growth and Form*, Cambridge: Cambridge University Press, 1961.

Toksvig-Larsen S, Franzén H, Ryd L. Cement interface temperature in hip arthroplasty. *Acta Orthopaedica Scandinavica* 1991; 62(2):102-105.

Ton That PT. Fatigue Characterisation of HAPEX™ Bioactive Composite. PhD Thesis. University of London, 2000.

Ton That PT, Tanner KE, Bonfield W. Fatigue Characterization of a Hydroxyapatite-Reinforced Polyethylene Composite. I. Uniaxial Fatigue. *Journal of Biomedical Materials Research* 2000a; 51:453-460.

Ton That PT, Tanner KE, Bonfield W. Fatigue Characterization of a Hydroxyapatite-Reinforced Polyethylene Composite. II. Biaxial Fatigue. *Journal of Biomedical Materials Research* 2000b; 51:461-468.

Townley CO. Complications in Total Hip Replacement: Etiology, Prevention and The Role of a Ceramic Articulation. *Ceramic Transactions* 1995; 48:23-34.

Townley CO. Hemi and Total Articular Replacement of the Hip with Fixed Femoral Cup. *Orthopedic Clinics of North America* 1982; 13:869-894.

Townley CO. Conservative Total Articular Replacement Arthroplasty (The TARA Procedure) With the Fixed Femoral Cup. *Orthopaedic Transactions* 1981; 5(3):388.

Trentani C, Vaccarino F. Italian Experience: Resurfacing Arthroplasty utilizing the Paltrinieri-Trentani Resurfacing Arthroplasty, 8 Year Assessment. *Orthopaedic Transactions* 1981; 5:374.

Trentani C, Vaccarino F. Long Term Assessment of the Paltrinieri-Trentani Resurfacing Arthroplasty of the Hip - 8 Year Study. *Orthopaedic Transactions* 1981; 5:387.

Trentani C, Vaccarino F. The Paltrinieri-Trentani Hip Joint Resurface Arthroplasty. *Clinical Orthopaedics and Related Research* 1978; 134:36-40.

Trentani C, Vaccarino F. The Paltrinieri-Trentani Hip Joint Resurface Arthroplasty. *Orthopedic Clinics of North America* 1982; 13:857-867.

Trotter M, Peterson RR. Weight of the Skeleton During Postnatal Development. *American Journal of Physical Anthropology* 33(3):313-323, 1970.

Unsworth A. Tribology of Human and Artificial Joints. *Proceedings of the Insitution of Mechanical Engineers, part H* 1991; 205:163-172.

Vaughan JM. *The Physiology of Bone.* 2nd ed. Oxford: Clarendon Press, 1975.

Viceconti M, Casali M, Massari B, Cristofolini L, Bassini S, Toni A. The "Standardized Femur Program" Proposal for a Reference Geometry to be Used for the Creation of Finite Element Models of the Femur. *Journal of Biomechanics* 1996; 29(9):1241.

Visuri T, Pukkala E, Paavolainen P, Pulkkinen P, Riska EN. Cancer Risk After Metal on Metal and Polyethylene on Metal Total Hip Arthroplasty. *Clinical Orthopaedics and Related Research* 1996; 329s:S280-S289.

de Waal Malefijt MC, Huiskes R. A Clinical, Radiological and Biomechanical Study of the TARA Hip Prosthesis. *Archives of Orthopaedic and Traumatic Surgery* 1993; 112:220-225.

Wagner H. Cemented Surface Replacement of the Hip Joint. *Orthopaedic Transactions* 1981; 5:374-375.

Wagner H. Surface Replacement Arthroplasty of the Hip. *Clinical Orthopaedics and Related Research* 1978; 134:102-130.

Wagner M, Wagner H. Preliminary Results of Uncemented Metal on Metal Stemmed and Resurfacing Hip Replacement Arthroplasty. *Clinical Orthopaedics and Related Research* 1996; 329s:S78-S88.

Wallbridge N, Dowson D. The Walking Activity of Patients with Artificial Hip Joints. *Engineering in Medicine* 1982; 11:95-96.

Wang A, Sun DC, Yau S-S, Edwards B, Sokol M, Essner A, Polineni VK, Stark C, Dumbleton JH. Orientation softening in the deformation and wear of ultra-high molecular weight polyethylene. *Wear* 1997; 203:230-241.

Wang M, Joseph R, Bonfield W. Hydroxyapatite-Polyethylene Composites for Bone Substitution: Effects of Ceramic Particle Size and Morphology. *Biomaterials* 1998a; 19(24):2357-2366.

Wang M, Berry C, Braden M, Bonfield W. Young's and Shear Moduli of Ceramic Particle Filled Polyethylene. *Journal of Materials Science: Materials in Medicine* 1998b; 9(11):621-624.

Watanabe Y, Shiba N, Matsuo S, Higuchi F, Tagawa Y, Inoue A. Biomechanical Study of the Resurfacing Hip Arthroplasty. *Journal of Arthroplasty* 2000; 15(4):505-511.

Weiner S, Price PA. Disaggregation of Bone into Crystals. *Calcified Tissue International* 1986; 39:365-375.

Weiner S, Traub W. Bone Structure: From Ångstroms to Microns. *FASEB Journal* 1992; 6:879-885.

Weiner S, Traub W, Wagner HD. Lamellar Bone: Structure-Function Relations. *Journal of Structure Biology* 1999; 126:241-255.

Weiner S, Wagner HD. The Material Bone: Structure-Mechanical Function Relations. *Annual Review of Materials Science* 1998; 28:271-298.

Whittle MW. *Gait Analysis: An Introduction.* Butterworth Heinemann, 1991.

Wiadrowski TP, McGee M, Cornish BL, Howie DW. Peripheral Wear of Wagner Resurfacing Hip Arthroplasty Acetabular Components. *Journal of Arthroplasty* 1991; 6:103-107.

Williams DF. Biofunctionality and Biocompatibility. In: Williams DF, ed. *Medical and Dental Materials*. Weinheim, VCH, 1992:2-27.

Willmann G. Ceramics For Total Hip Replacement - What a Surgeon Should Know. *Orthopedics* 1998; 21:173-177.

Willmann G. Oxide Ceramics for Articulating Components of Total Hip Replacements. In: Sedel L, Rey C, eds. *Bioceramics*. Elsevier Science, 1997:123-126.

Wilson LF, Nolan JF, Heywood-Waddington MB. Fracture of the Femoral Stem of the Ring TCH Hip Prosthesis. *Journal of Bone and Joint Surgery* 1992; 74-B(5):725-728.

Witte H. Joint Forces in a Pelvic Co-ordinate System. Personal Communication. 2000.

Witte H, Eckstein F, Recknagel S. A Calculation of the Forces Acting on the Human Acetabulum during Walking. *Acta Anatomica* 1997:160(4):269-280.

Wroblewski BM, Fleming PA, Siney PD. Charnley Low-Friction Torque Arthroplasty of the Hip: 20- to 30-Year Results. *Journal of Bone and Joint Surgery* 1999a; 81-B(3):427-430.

Wroblewski BM, Siney PD, Fleming PA. Low-Friction Arthroplasty of the Hip Using Alumina Ceramic and Cross-Linked Polyethylene: A Ten-Year Follow-Up Report. *Journal of Bone and Joint Surgery* 1999b; 81-B(1):54-55.

Yamac T, Tanner KE, Best S. *Medical Devices - Materials for Human Contact: A Design Guide.* London: The Institute of Materials, 1999.

Yamac T. The Extraction and Characterisation of Wear Particles from Tissues Around Failed Orthopaedic Implants of Different Designs. PhD Thesis. University of London, 1999.

Yamamuro T, Shikata J, Kakutani Y, Yoshii S, Kitsugi T, Ono K. Novel Methods for Clinical Applications of Bioactive Ceramics. In: Ducheyne P, Lemons JE, eds. *Bioceramics: Material Characteristics Versus In Vivo* Behaviour. New York, Annals of New York Academy of Sciences, 1988:107.

Yuan X. Accuracy Analysis of RSA and Development of Roentgen Single-Plane Photogrammetric Analysis. PhD Thesis. Department of Orthopaedics, University Hospital, Lund, 1999.

Appendix A: MATLAB Sphere Fitting Routine

Adapted from Gander *et al.* (1994).

```
function [z, r, max, ave, sdev] = sphere (X, z, r);

%sphere   Geometric sphere fit

%

% [z,r] = sphere (X, z, r);

% fits the best sphere by nonlinear least squares

% for true geometric distance

%

% X: given points <X(i,1), X(i,2), X(i,3)>

% z, r: starting values for sphere solution

%

% z, r: parameters for sphere found


u = [z(1), z(2), z(3), r]';   %starting values

h = u;

while norm(h)>norm(u)*1e-6,

     a = u(1)-X(:,1); b = u(2)-X(:,2); c = u(3)-X(:,3);

     fak = sqrt(a.*a + b.*b + c.*c);

     J = [a./fak b./fak c./fak -ones(size(a))];

     f = fak -u(4);

     h = -J\f;

     u = u + h;

end;

z = u(1:3); r= u(4);
```

```
max = norm(f, inf); ave = mean(abs(f)); sdev =
std(abs(f));


end % sphere
```

Data points saved as MATLAB executable file.

```
function [z, r, max, ave, std] = fitdat %
% MARC exported data with call to sphere fitting
algorithm
% no inputs
% outputs are z, r: centre and radius of sphere
% ensure MATLAB is in correct dir
A = [
A11, A12, A13;            % matrix of co-ordinate data
A21, A22, A23;
…
An1, An2, An3;
];


si = size(A);
su = sum(A);
z1 = su./si(1);                % starting value for
position vector
r1 = sqrt(z1*z1');        % starting value for radius
[z, r, max, ave, std] = sphere(A, z1, r1 ;    %call
"sphere"
end % fitdat
```

Appendix B: Geometric Correction Factor

The specimen strain, ε_{sp}, measured by cross head displacement, δ_{total} for a specimen of length L is given:

$$\varepsilon_{sp} = \delta_{total}/L \tag{B.1}$$

The strain that occurs in the gauge section, ε, is related to the measured strain by a shape factor, r.

$$\varepsilon = r\varepsilon_{sp} \tag{B.2}$$

The total displacement is the sum of the displacements that occur due to strain in the gauge section, δ_{gauge}, in the shouldered sections, δ_{sh}, and in the end sections which protrude from under the grips, δ_{end}.

The displacement occurring in the shoulder sections can be determined as follows:

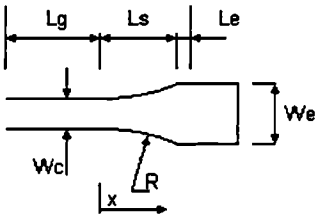

Figure B.1 Test specimen defining variables and co-ordinate system.

The equation describing the width, w, of the specimen for $0 < x < L_s$ (Figure B.1) is:

$$w = 2\,[R + W_c/2 - (R^2 + x^2)^{1/2}\,] \tag{B.3}$$

Therefore the displacement occurring as a result of applied force P in the shoulder section, thickness t and Young's modulus E is:

$$\delta_{sh} = \int_0^{Ls} \frac{P}{Ewt} = \frac{P}{2Et}\int_o^{Ls} [R + W_C/2 - (R^2 + x^2)^{1/2}]^{-1}\,dx \tag{B.4}$$

This expression may be integrated numerically using Simpson's rule. The other displacements are easily calculated as:

$$\delta_{gauge} = 2L_gP/(EtW_c) \tag{B.5}$$

$$\delta_{end} = L_eP/(EtW_e) \tag{B.6}$$

Therefore

$$r = \frac{\varepsilon_{sp}}{\varepsilon} = \frac{\delta_{gauge} + 2\delta_{sh} + 2\delta_e}{(2L_s + 2L_g + 2L_e)}\left[\frac{2L_g}{\delta_{gauge}}\right] \tag{B.7}$$

Using R = 60 mm, L_g = 30 mm, W_c = 10 mm, W_e = 20 mm, L_e = 3 mm, t = 6.5 mm, and by trigonometry:

$$L_s = R\sin(\arccos[1-(W_e-W_c)/2R]) \tag{B.8}$$

Gives $r \approx 1.13$.

Appendix C: Considère's Criterion

Consider a tensile bar of plastic material, with instantaneous cross sectional area S, and length L. A strain, ε, is applied giving rise to a load, P. Assume that the material deforms with constant volume, V_0 such that $SL = V_0$ throughout.

The nominal stress is $\sigma_n = P/S_0$, where S_0 is the cross sectional area of the unloaded bar. This is related to the true stress, $\sigma = P/S$:

$$\sigma = P/S = P(1 + \varepsilon)/S_0 = \sigma_n(1 + \varepsilon) \tag{C.1}$$

Since

$$S = V_0/L = V_0/L_0(1 + \varepsilon) = S_0/(1 + \varepsilon) \tag{C.2}$$

Instability occurs when an increase in ε does not bring about a corresponding increase in P, i.e.:

$$dP/d\varepsilon = 0 \tag{C.3}$$

$$P = \sigma S \tag{C.4}$$

Therefore

$$dP/d\varepsilon = Sd\sigma/d\varepsilon + \sigma dS/d\varepsilon \tag{C.5}$$

But

$$dS/d\varepsilon = d[S_0/(1+\varepsilon)]/d\varepsilon = -S_0/(1 + \varepsilon)^2 = -S/(1 + \varepsilon) \tag{C.6}$$

So

$$dP/d\varepsilon = S(d\sigma/d\varepsilon - \sigma/(1 + \varepsilon))$$

$$= S(d\sigma/d\varepsilon - \sigma_n) \tag{C.7}$$

So for instability to occur:

$$d\sigma\, d\varepsilon = \sigma_n \tag{C.8}$$

Appendix D: Glossary

Acetabulum	The socket of the hip joint.
Aetiology	The cause of a disease.
Arthrodesis	The immobilisation of a joint allowing the bones to fuse.
Arthritis	Inflammatory disease of the joints.
Arthropathy	Disease of the joints.
Arthrosis	Degenerative, non-inflammatory, disease of the joints.
Biomaterials	Materials used in devices having intimate contact with living tissue.
Biomechanics	The study of the mechanical behaviour and properties of living systems.
Chondrocyte	Cells found in cartilage responsible for synthesis of matrix.
Contra-indication	A set of patient characteristics that rule out a particular treatment.
Dysplastic hip	A hip joint with a developmental abnormality.
FEA – Finite Element Analysis	Computer based numerical solution of stress states in complex structures by their discretisation into simply shaped elements.
Femur	The long bone of the thigh.
Indication	A particular course of treatment is indicated by a set of patient characteristics.
Orthopaedic	The restoration of function and relief of pain arising from (childhood) musculoskeletal disease or injury.
Osteoblast, osteoclast, osteocyte	Cells that respectively deposit, resorb and regulate bone material.
Osteophyte	Abnormal bony growths frequently found on the periphery of articular surfaces in osteoarthrosis.
Osteotomy	The rotation and relative displacement of cut sections of bone.

Primary, idiopathic osteoarthrosis	Osteoarthrosis that is not caused by another condition or disease process.
RSA – Radio Stereometric Analysis	A technique using X-ray pictures taken from two viewpoints to determine the relative three-dimensional positions of implants and bones (formerly Röntgen Stereophotogrammetric Analysis).
Subchondral bone	The bone underlying cartilage surfaces in synovial joints.

Anatomical Frame of Reference

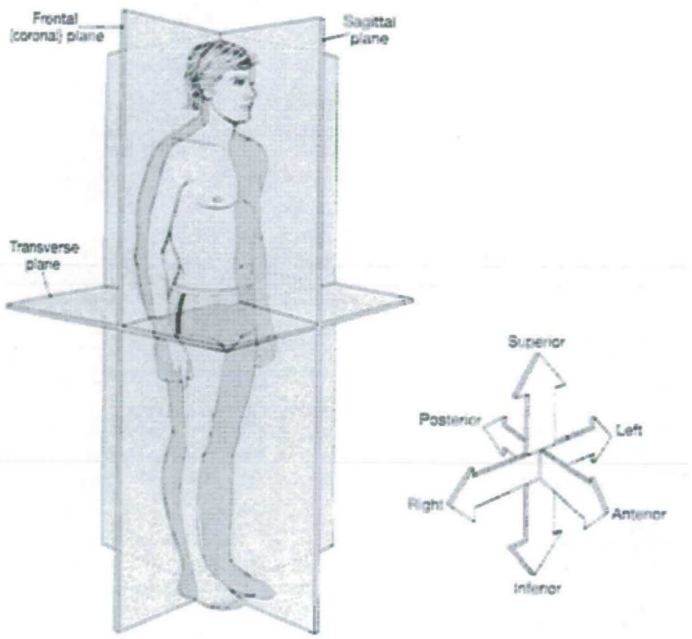

Figure D.1 Anatomical planes and directions (Martini, 1995).

In addition to the terms defined in Figure D.1, the following are often required:

Proximal	A direction on a limb: closer to or towards the body.
Distal	A direction on a limb: further away from the body.
Medial	Towards the central sagittal plane.
Lateral	Away from the central sagittal plane.

Appendix E: Publications and Abstracts

Thompson MS, Dawson T, Northmore-Ball MD, Tanner KE.
A survey of the morphology of the bony surface of the acetabulum.
Presented at: Measurements & Simulations in Musculoskeletal Biomechanics, Institute of Physics and Engineering in Medicine, London. 11th June 1999.

Thompson MS, Dawson T, Northmore-Ball MD, Tanner KE.
Anthropometric Studies of the Human Acetabulum and Resurfacing Design.
Presented at: The British Hip Society, Oxford, 24th – 25th March 2000.

Thompson MS, Patel M, Northmore-Ball MD, Tanner KE.
The use of polyacetal as an orthopaedic implant material.
Presented at: Materials Congress 2000, Cirencester. 13th – 14th April 2000.

Thompson MS, Northmore-Ball MD, Tanner KE.
Finite element analysis in the design of a novel hip resurfacing prosthesis
Presented at: The European Society of Biomechanics, Dublin. 28th – 30th August 2000.

Thompson MS, Dawson T, Kuiper JH, Northmore-Ball MD, Tanner KE.
Acetabular morphology and resurfacing design.
Journal of Biomechanics 33 (12) 1645-1653 (2000)

A SURVEY OF THE MORPHOLOGY OF THE BONY SURFACE OF THE ACETABULUM

M.S. Thompson[1,3], T. Dawson[2], M.D. Northmore-Ball[3], K.E. Tanner[1]

[1]. IRC in Biomedical Materials, QMW College, London
[2]. Department of Human Anatomy, University of Liverpool
[3]. Robert Jones and Agnes Hunt Orthopaedic Hospital, Oswestry

The bony surfaces of 20 pelves were scanned using a 3D laser surface scanner and CyDir software on a Silicon Graphics workstation. The acetabular area was selected and point data from the approximately spherical bone surface saved to a text file. This file was input to a Matlab routine that calculated the radius and centre of the best-fit sphere. The goodness of fit was estimated using the mean and standard deviation of the distance of the bone surface points from the sphere surface. Eight points at approximately equal distances around the acetabular rim were selected with reference to bony landmarks. A plane containing three of these points served as an orientation reference. Vectors between the eight rim points and the centre point of the best-fit sphere were calculated. These angles characterise the extent of the surface of a sphere that the articular surface of the acetabulum comprises by defining the angle subtended by the acetabular rim at the centre of rotation of the hip. This angle, along with the ratio of articular surface diameter to femoral neck diameter, sets an upper limit on the range of motion at the human hip joint. These angles are important parameters in the design of the acetabular component of a hip replacement, and in particular for the design of a resurfacing hip replacement for which the volume available is tightly constrained.

Anthropometric studies of the human acetabulum and resurfacing design

M.S. Thompson [1,2], T. Dawson [2], M.D. Northmore-Ball [2], K.E. Tanner [1]

1. IRC in Biomedical Materials, QMW College, London
2. Robert Jones and Agnes Hunt Orthopaedic Hospital, Oswestry

A conservative resurfacing hip replacement must be shaped to fit the existing bony surfaces to enable optimal use of implant material and minimal removal of bone. Early resurfacing designs did not conserve acetabular bone and many failed through impingement of the femoral neck on the acetabular component. This study characterised the extent of the acetabular articular surface using the angles subtended by the acetabular rim at eight equispaced points. The maximum range of motion at the human hip joint is determined by these angles and the femoral head neck ratio. A Matlab routine was used to calculate the best-fit sphere to the laser surface scans of 18 acetabula. The goodness of fit of the bone surface to the sphere was estimated. The overall mean angle was 158° (range of mean angles 145° - 173°). The mean angle in the anterior-posterior direction (i.e. that controlling flexion-extension) was 152° and the largest individual angles, some exceeding 180°, were in the superior-inferior direction. Males had larger subtended angles than females, although the difference was not statistically significant. A simulated conservative reaming operation increased all angles by approximately 10°. Current resurfacing designs subtend between 160° and 180°. In addition to determining the proper subtended angle of a conservative acetabular resurfacing component, these data provide constraints on the acetabular fixation system since a component significantly less than hemispherical cannot be secured with an interference fit.

THE USE OF POLYACETAL AS AN ORTHOPAEDIC IMPLANT MATERIAL

M. S. Thompson[1,2], M. Patel[1], M. D. Northmore-Ball[2], K. E. Tanner[1]

1. IRC in Biomedical Materials, Queen Mary and Westfield College, London UK

2. Unit for Joint Reconstruction, Robert Jones and Agnes Hunt Orthopaedic Hospital, Oswestry, Shropshire UK

Introduction: The engineering plastic polyoxymethylene, also known as polyacetal, has a thirty year history as an implant material. Applications include heart valve occluder disks and finger joint prostheses. In joint replacement it has been used for the acetabular component in the Christiansen hip replacement, in the composite femoral stem of the Isoelastic Hip and as the femoral component in the Freeman all-polymer knee replacement. The large quantities of polyacetal wear debris generated by the Christiansen hip provoked bone resorption giving poor clinical results [1]. The poor results of the Freeman all-polymer knee replacement and of the Isoelastic hip were attributable to sterilisation and cementless fixation issues rather than to the use of polyacetal [2].

Polyacetal has a stiffness of 2.5-3 GPa, lying between that of cortical (17 – 25 GPa) and cancellous bone (100 – 500 MPa). Therefore a polyacetal orthopaedic implant will eliminate the problem of stress shielding caused by the use of much stiffer metals Co-Cr (240 GPa), stainless steel (210 GPa) and Ti (120 GPa). A hip wear simulator study showed a reduction of 23% in total wear volume with a UHMWPE counterface when using a polyacetal replacement compared with a similar Co-Cr replacement [3]. Characterisation of polyacetal in hip and heart valve implants retrieved after up to 20 years using FTIR, viscometry and chromatography indicated that no systematic degradation had taken place under exposure to body fluids [4], although mechanical testing was not carried out. The present study was undertaken to characterise the effects of fluid uptake on the mechanical properties of polyacetal obtained from different manufacturers.

Materials and methods:

A preliminary study measured the change in mass with time of 1 mm thick polyacetal homo- and co-polymer samples immersed in pure distilled water at 37°C. Once equilibrium was reached the samples were dried again at 37°C and the change of mass followed. Plotting the mass uptake at time t (M_t) divided by the equilibrium mass uptake (M_{eq}) against time$^{1/2}$ allowed the calculation of the diffusion coefficients for water absorption and desorption according to the following equation:

$$\frac{M_t}{M_{eq}} = 2\left[\frac{Dt}{\pi l^2}\right]^{1/2}$$

where l is the thickness of the sample.

Results: The diffusion coefficients measured in the preliminary study were as follows: absorption: 4.7×10^{-12} m^2s^{-1} (SD 3.7×10^{-13}), desorption: 8.0×10^{-12} m^2s^{-1} (SD 5.7×10^{-13}). The mean equilibrium water uptake was 0.65 wt% (SD 0.017).

Discussion and conclusions: The water absorption and desorption diffusion coefficients for many polymers differ, but not usually by as much as a factor of two. This may be due to differences in the mechanisms for water desorption and absorption. The polyacetal diffusion coefficients are of the same order as those of PMMA [5]. An important property of an orthopaedic implant material is resistance to degradation from long term exposure to body fluid. The equilibrium water uptake of UHMWPE is much smaller (<0.01 wt%) than that of polyacetal. However long term retrieval studies show good resistance to chemical degradation. Future work will evaluate the changes in polyacetal tensile stiffness and yield stress following immersion in Ringer's solution.

References

[1] Mathiesen, E.B., Sudmann, E., Lindgren, U., Reinholt, F. (1983) Acta Orth Scand 54: 485

[2] Bradley, G.W., Freeman, M.A.R., Tuke, M.A., McKellop, H.A. (1993) Clin Mat 14: 127-132

[3] McKellop, H.A., Röstlund, T., Bradley, G. (1993) Clin Mat 14: 117-126

[4] McKellop, H.A., Milligan, H.L., Röstlund, T. (1996) J Heart Valve Disease 5(suppl. II): S238-S242

[5] Patel, M.P. (1984) PhD Thesis, University of London.

FEA in the design of a novel hip resurfacing prosthesis

M. S. Thompson[1,2], M. D. Northmore-Ball[2] and K. E. Tanner[1]

[1]IRC in Biomedical Materials, Queen Mary and Westfield College, London E1 4NS, UK. [2]Unit for Joint Reconstruction, Robert Jones and Agnes Hunt Orthopaedic Hospital, Oswestry, Shropshire SY10 7AG, UK.

Introduction

Resurfacing hip replacements are a bone conserving alternative to conventional stemmed hip replacements intended for the younger, more active patient. The surface layer of diseased cartilage and bone is removed and the head reshaped to accept a cup prosthesis. A smaller amount of natural material is replaced by artificial material, the loading of the proximal femur is nearer physiological and the revision options are similar to those available at primary hip replacement.

Recently there has been a renewal of interest in the concept, largely abandoned in the mid 1980s, and now there are at least three metal-on-metal designs in clinical use [1]. These designs have not been supported by finite element studies of their effects on the stresses in the supporting bone, which have been shown to be predictive of early implant migration and loosening [2]. This work compares these devices with those of a novel all polymer design using three dimensional finite element analysis and determines the optimal fixation system for the novel acetabular component.

Materials and methods

A preliminary study using a simple axisymmetric model of the resurfacing concept demonstrated its feasibility and highlighted regions of interest.

The three dimensional models of the femur [2] and the pelvis [3] had been developed previously from CT data by other authors. The pelvic model included variable cancellous bone stiffness and variable cortical shell thickness. The resurfacing FE model was developed, meshed and combined with the bone models using IDEAS™ and Hypermesh™ on a Silicon Graphics workstation. The resurfacing geometry was partly determined from anatomical parameters measured previously. Analysis was performed using ABAQUS™ 5.8, and post processing using ABAQUS/Post™.

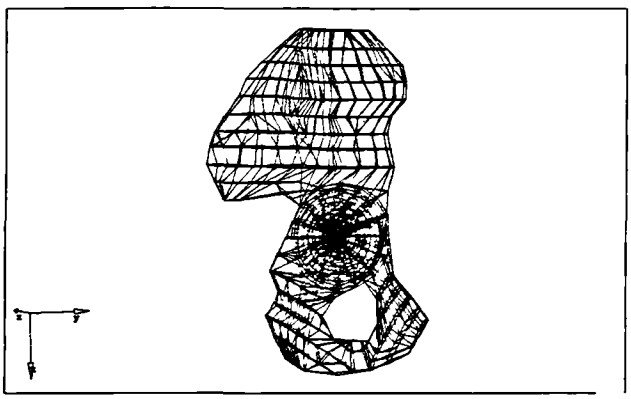

Fig. 1: The pelvis model developed by Dalstra [3].

Material models

All implant materials (UHMWPE, POM, PMMA, Co-Cr) and cortical bone were modelled as isotropic elastic materials. Cancellous bone was modelled as an isotropic elastic-perfect-plastic material. The yield stress is related to the stiffness by the following equation [4]:

$$\sigma_y = 0.015E + 0.193 \quad (1)$$

Loading and Boundary conditions

26 muscles crossing the hip joint were included in the model. Eight load steps modelled muscle forces at eight points during the gait cycle. The distal end of the femur and the sacro-iliac joint surface were built in and symmetrical boundary conditions applied to the symphysis pubis.

Analyses performed

The pelvic and femoral meshes were "implanted" with prostheses with materials combinations as defined below and the results compared with those of the intact bones.

Table 1. Prosthesis material combinations

analysis	femoral material	acetabular material
1	POM (+PMMA)	UHMWPE
2	Co-Cr (+PMMA)	Co-Cr
3	Co-Cr (+PMMA)	UHMWPE

All these simulations assumed fully bonded bone-implant interfaces. A second set of simulations were performed selectively releasing areas on the acetabular component-bone interface. Pinned areas of interface represent fixed parts of the implant, e.g. by pegs, and the relative motion at released nodes was determined. The positions and shapes of the fixed areas represented three fixation systems: two supero-lateral fins, central peg with radial splines and infero-medial pegs.

Results

The preliminary axisymmetric analysis showed that compared to the POM on UHMWPE implants, the Co-Cr on Co-Cr implants resulted in stress shielding of the cancellous bone in the pelvis and femur. This was combined with stress concentration in the bone supporting the edge of the femoral component, the von Mises stresses here exceeded 26 MPa.

Discussion and conclusions

These results demonstrate the improved physiological loading of the proximal femur obtained with a polymer-on-polymer resurfacing. The relative motions at the implant-bone interface must be below 100 μm for fixation by bony ingrowth. A future study using holographic interferometry of implanted cadaveric femora should provide appropriate validation.

References

[1] H.C. Amstutz, E.A. Sparling, P. Grigoris, P.A. Campbell, and F.J. Dorey (1998) Hip Int. 8: 187-207. [2] M. Taylor, K.E. Tanner, M.A.R. Freeman and A.L. Yettram (1996) In: 2nd International Symposium on Computer Methods in Biomechanics and Biomedical Engineering, (ed. J. Middleton) Gordon and Breach, pp. 47-55. [3] M. Dalstra (1993) PhD Thesis, University of Nijmegen. [4] F. Linde, P. Nørgaard, I. Hvid, A. Odgaard and K. Søballe (1991) J Biomech 24: 803-809.

Acknowledgements

The Engineering and Physical Sciences Research Council is gratefully acknowledged for the core programme grant of the IRC in Biomedical Materials and for the provision of a research studentship (MST). Dr Mark Taylor and Dr Michel Dalstra are thanked for access to their FE models.

ELSEVIER

Journal of Biomechanics 33 (2000) 1645–1653

JOURNAL OF BIOMECHANICS

www.elsevier.com/locate/jbiomech

Acetabular morphology and resurfacing design

M.S. Thompson[a,b,*], T. Dawson[c], J.H. Kuiper[b], M.D. Northmore-Ball[b], K.E. Tanner[a]

[a]*IRC in Biomedical Materials, Queen Mary and Westfield College, Mile End Road, London E1 4NS, UK*
[b]*Unit for Joint Reconstruction, Robert Jones and Agnes Hunt Orthopaedic Hospital, Oswestry, UK*
[c]*ORLAU, Robert Jones and Agnes Hunt Orthopaedic Hospital, Oswestry, UK*

Accepted 5 May 2000

bstract

The bony surfaces of 18 archaeological hemipelves were scanned using a 3D laser surface scanner and CyDir™ software on Silicon Graphics workstation. The acetabular area was selected and point data from the approximately spherical bone surface saved. hese data were input to a MATLAB routine that calculated the radius and centre of the best-fit sphere. The goodness of fit was timated using the mean and standard deviation of the distance of the bone surface points from the sphere surface. Eight points, at proximately equal distances around the acetabular rim, were selected with reference to bony landmarks. A plane containing three of ese points served as an orientation reference plane. The vectors joining the eight rim points to the centre of the best-fit sphere were und. The angles between these vectors and the normal to the reference plane were calculated. Paired angles were summed to give the gle subtended by the acetabular rim in four directions. The overall mean angle was 158° (range of mean angles 145°–173°). The rgest individual angles, some exceeding 180°, were in the superior–inferior direction, while the mean angle in the anterior–posterior rection, i.e. that controlling flexion-extension, was 152°. Males had larger subtended angles than females, although the difference was t statistically significant. Simulated reaming increased all angles by approximately 10°. The subtended angles are important rameters in the design of the acetabular component of a hip replacement and particularly important in resurfacing hip replacement hen the volume available is tightly constrained. © 2000 Elsevier Science Ltd. All rights reserved.

ywords: Acetabular morphology; Implant design; Sphericity; Subtended angles

Introduction

The long-term fixation of the acetabular socket has come one of the most important problems in total hip placement (THR) today (Harris, 1995; Paavolainen et , 1995; Wroblewski et al., 1999). Loosening of the etabular component alone, while the femoral compon- t remained well fixed, accounted for over 30% of all visions in Finland from 1990 to 1994 (Paavolainen et , 1995). In particular, higher activity levels and higher idence of RA, with poor-quality acetabular bone ck, lead to lowered acetabular survivorship in young tients (Sharp and Porter, 1985; Kobayashi et al., 1997). ne stock is destroyed by the loosening process result- g in more difficult revision procedures and poorer tcomes (Wroblewski et al., 1999).

A bone-stock-preserving prosthesis, intended for use in young patients, is the resurfacing replacement. A resurfacing operation leaves the femoral neck and head intact, replacing only the diseased surfaces of the femoral head and acetabulum. Many resurfacing designs have been documented, but the concept was largely abandoned in the 1980s due to high early failure rates (Freeman et al., 1975; Amstutz et al., 1978; Capello et al., 1978; Wagner, 1978; Townley, 1981). One problem is the relatively small volume into which the components must fit. This was not appreciated by some early designers and the femoral head and neck were preserved at the expense of acetabular bone stock (Amstutz, 1983). In order to design a bone-conserving resurfacing replacement it is necessary to know the detailed shape of the bony surfaces of the hip joint.

While the morphology of the proximal femur is well characterised (Clark et al., 1987; Noble et al., 1988; Husmann et al., 1997; Sugano et al., 1999) the shape of the acetabulum has received less attention. It is generally agreed that the cartilage surface of the acetabulum is

* Corresponding author. IRC in Biomedical Materials, QMW, Mile d Road, London E1 4NS, UK. Tel.: + 44-20-7882-3316, fax: + 44-8983-1799.
E-mail address: m.s.thompson@qmw.ac.uk (M.S. Thompson).

1-9290 00/$ - see front matter
: S0021-9290(00)00115-9

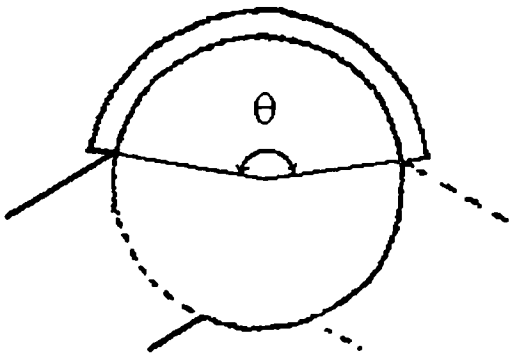

Fig. 1. Subtended angle (θ) and its effect on range of motion.

ightly ellipsoidal with its major axis in the superior - inferior direction (Greenwald and O'Connor, 1971; ckstein et al., 1997). The bony surface of the acetabulum as been studied (Rushfeldt et al., 1981), but only in two bjects, both of whom showed signs of osteoarthrosis. he study concentrated on mapping local surface devi- ions from the spherical. There are conflicting defini- ons of such fundamental parameters as the orientation the acetabulum (Murray, 1993).

Consideration of the effect of an acetabular implant on range of motion (Fig. 1) shows the importance of e subtended angle. This angle (together with the head- -neck ratio) defines the angle through which an im- anted hip can move. A set of subtended angles is quired to characterise the irregular shape of the natural etabulum. Before the subtended angle can be mea- red, it is necessary to know the position of the centre of tation of the acetabulum.

Given the prevalence of acetabular loosening, the need conserve acetabular bone in young patients, for whom e large diameter resurfacing hip is intended, and the ck of detailed morphological knowledge the present udy set out to characterise the shape of the human etabulum. This aim was achieved by measuring four gles subtended at the centre of hip rotation by the etabular rim. Further, the acetabular reaming operation rried out during hip replacement was simulated and llowing this the subtended angles were re-calculated.

Materials and methods

The analysis was carried out on the digitised 3D laser rface scans of 18 hemipelves. This technique uses the flected light from a laser line scanned across the solid rface to build up a 3D computer image. The scans were anipulated using CyDir™ software on a Silicon raphics workstation. Eight were female, nine male and e was of undetermined gender. The most common timated age range at death was 25–35 years, with the dest range 41–67 and the youngest 16 + .

The bones came from two archaeological sites in Gloucester (periods 43–410 AD and 1066–1500 AD) and one came from the pathology laboratory in the Robert Jones and Agnes Hunt hospital. Heights estimated from the length of the femur (Trotter and Peterson, 1970) ranged from 1.49 to 1.81 m with a mean of 1.62 m. There were 12 right and six left hemipelves, including one right and left pair. None of the hemipelves showed signs of degenerative joint disease, although many were broken, the most common sites being the pubic ramus and the anterior horn of the lunate surface. Biographical details and the condition of each hemipelvis are listed in Table 1. The scanned hemipelvis data files were in ASCII format and consisted of a list of nodal co-ordinates and a list of element connectivities.

The files were converted to an ASCII format that MENTAT, the solid modeller pre-processor for MARC (MARC Analysis Corporation, Palo Alto, CA, USA), could read using a QuickBasic routine. Once loaded and displayed in the solid modeller the nodes and elements on the acetabular articular surface were chosen and output as a separate file. The co-ordinate data from this file were extracted using QuickBasic and saved as a MATLAB executable file. A short MATLAB routine (see the appendix 1) was implemented to fit a sphere to the nodal co-ordinate data in the acetabular shell. The mean position vector of the set of nodal co-ordinates and its magnitude were used as first approximations for the centre co-ordinates and radius. The routine then used an iterative Newtonian method to reach a better approximation, minimising the square of the distance from the sphere's surface to the data set nodes. The best-fit sphere centre co-ordinates, radius and maximum, mean and standard deviation of the error were output.

Eight approximately equidistant points around the acetabular rim were picked at anterior, posterior, superior and inferior locations and the quarter points between these (Fig. 2). Four distant bony landmarks (anterior superior iliac spine, posterior superior iliac spine, ischial tuberosity and pubic symphysis) and two peri-acetabular landmarks (anterior and posterior horns of the acetabular rim) were used to orient the specimens. In five hemipelves the anterior horn of the acetabular rim was broken so no point was picked in this region. The superior, posterior and inferior (points 3, 5 and 7) points were used to define the acetabular opening plane except in three pelves where the rim was damaged at the inferior position (point 7). The angles between the rim-centre vectors and the opening plane normal were calculated. The subtended angle in any plane through the centre of rotation is the sum of two of these angles. Therefore, four different subtended angles were calculated. Table 2 shows the relationship between the rim points, bony landmarks, the directions in which the subtended angles were measured and anatomical directions. The error introduced by the manual placement of the rim points was

able 1
iographical data and condition of hemipelves. PS pubic symphysis, IT ischial tuberosity, ASIS anterior superior iliac spine, PSIS posterior superior iac spine, AH anterior horn of acetabular rim

eriod	Subject	Side	Estimated			Condition
			Sex	Age at death	Height	
3–410 AD	1	R	F	17–25	1.54	Complete
	2	R	M	41–67	1.81	PS, IT and AH missing
	3	L	F	17–25	—	PS missing
	4	R	F	25–35	1.49	Complete
	5a	R	F	25–35	1.61	PS and AH missing
	5b	L		Pair of 5a		ASIS and PSIS missing
	6	L	M	17–25	1.60	Complete
	7	L	?M	< 16	—	Complete
	8	R	M	17–25	1.72	Complete
	9	R	?M	17–25	—	ASIS and PS missing
	10	R	M	25–35	1.65	Complete
	11	R	F	25–35	1.58	Complete
066–1500 AD	12	R	?F	25–35	1.57	Complete
	13	R	?M	35–45	1.65	PS and AH missing
	14	L	F	25–35	1.52	Complete
	15	R	M	25–35	1.77	PS and AH missing
	16	R	M	25–35	1.60	Complete
Modern	17	L	—	—	—	Complete

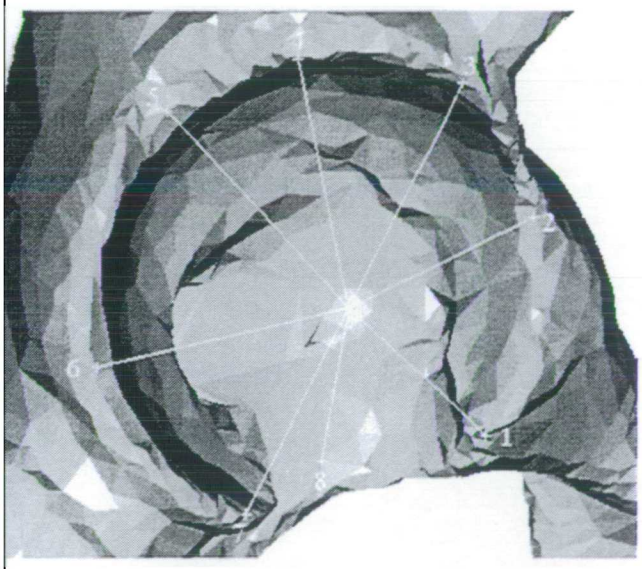

g. 2. Locations of points on acetabular rim, showing rim-centre ctors (1 = anterior, 3 = superior, 5 = posterior, 7 = inferior).

ssessed by picking new positions for a point 5 mm on ther side of the original and recalculating the subtended ngle.

The conservative reaming of an acetabulum was mulated and then the subtended angles re-calculated. conservative reaming operation was defined as follows: The acetabulum is first deepened medially to the "true oor", increasing the reamer size until the anterior and osterior rim are just grazed. The reamer is then pushed periorly until the most lateral portion of the rim is just azed.

Table 2
Subtended angle directions

Rim points	Landmarks	Approximate anatomical direction
1 and 5	Anterior horn of lunate surface	Anterior–posterior
2 and 6	—	Supero-anterior–infero posterior
3 and 7	Anterior iliac crest and posterior horn of lunate surface	Superior–inferior
4 and 8	Acetabular notch	Infero-anterior–supero-posterior

This operation was simulated by selecting one node on the floor and one on the rim and moving the best-fit sphere centre medially and superiorly until its surface contained these points.

The angles between rim-centre vectors and the opening plane normal were then re-calculated for the reamed acetabulum and a theoretical maximum removed bone volume calculated. This simulation was not performed on three of the hemipelves which did not have complete acetabular floors.

Significant differences between groups of diameters and groups of subtended angles were assessed using a two-tailed t-test assuming unequal variances.

3. Results

The diameters of the spheres fitted to the acetabula ranged from 43.7 to 58.2 mm. The overall mean diameter was 50.9 mm, with a standard deviation (S.D.) of 3.6 mm.

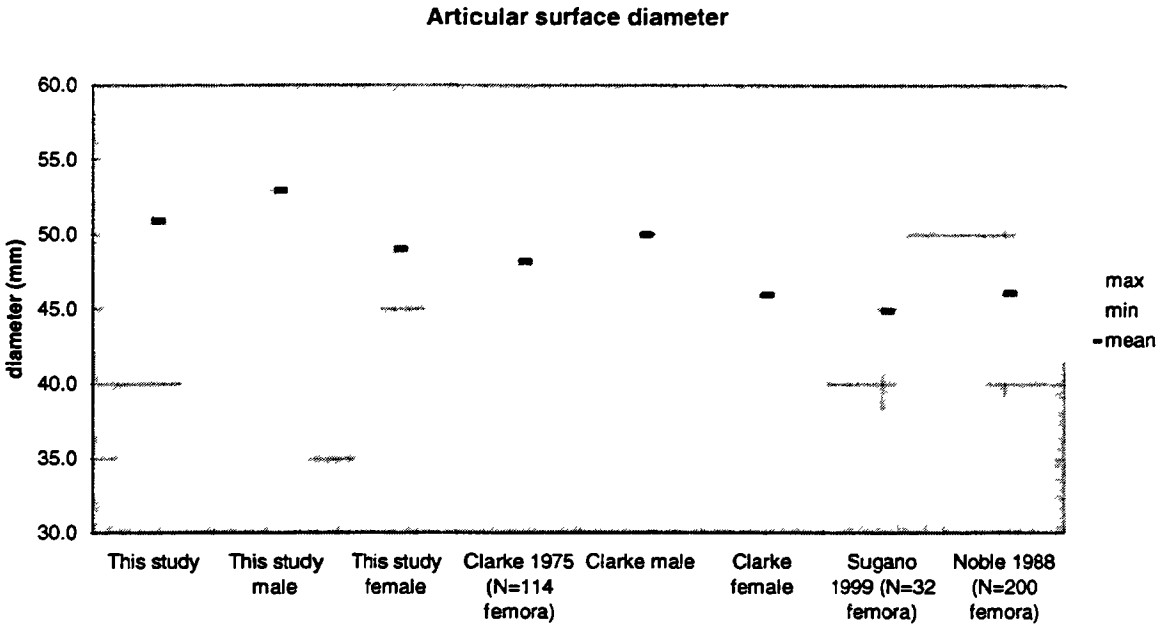

Fig. 3. Acetabula diameters and gender differences compared with the literature.

The mean diameter of the male acetabula was 52.9 mm (S.D. 1.7 mm), of the female 49.0 mm (S.D. 1.45 mm) and this difference was significant ($p = 0.02$). These figures are compared with published values of femoral head diameters in Fig. 3 (Clarke and Amstutz, 1975; Noble et al., 1988; Sugano et al., 1999). The mean acetabular diameter in this study was 3–6 mm larger than the reported mean femoral head diameters. The data from Clarke and Amstutz show a similar difference between male and female diameters of c. 4 mm.

There was a c. 2 mm difference in diameter between the left and right acetabula of the only paired bones, but there was no significant difference between right and left acetabula groups ($p = 0.58$). The mean diameter of the Norman period (1066–1500 AD) acetabula was 3 mm larger than that of the Roman period (43–410 AD), however the difference was not significant ($p = 0.20$). The group mean of the mean deviation from each fitted sphere was 0.6 mm and the group mean of the maximum deviation was 3 mm, while the maximum deviation for any acetabulum was 6 mm. Visualising the set of nodes to which the sphere was fitted together with the best-fit sphere allowed qualitative assessment of the size and region of the deviations. In general, the anterior and posterior regions of the articular surface lay just within the sphere, while the superior part of the surface lay outside.

The acetabular diameter plotted against the estimated height (Fig. 4) shows a strong correlation ($R^2 = 0.5994$). The estimated height is calculated from the maximum length of long bones using the regression formula reported by Trotter and Peterson (1970).

When male and female diameters were plotted separately against height a stronger relation between male diameter and height than female diameter or combined diameter and height was seen. However, the small size of the sample groups (seven in each group) prevents any firm conclusions from being drawn.

3.1. Subtended angles

The mean subtended angles in each of four directions — anterior to posterior, supero-anterior to infero-posterior, superior to inferior and infero-anterior to supero–posterior — are shown in Fig. 5. The error bars represent one standard deviation. The only subtended angles larger than 180° were in the superior - inferior direction, the maximum being 188°. One acetabulum had a supero-anterior - infero-posterior angle of 180°, but the remaining acetabula had substantially smaller angles in this direction. The minimum subtended angle, 128°, was in the infero-anterior – supero-posterior direction of the acetabula of a male subject of above average height. The mean subtended angle for each acetabulum, a measure of its depth, ranged from 145 to 173°, with a mean of 158°. The estimated error in a subtended angle introduced by manual picking was less than 1°.

Also shown in Fig. 5 are the differences between the male and female groups. Males had slightly larger subtended angles, and hence deeper acetabula, than females although the difference was not significant ($p = 0.19$). In males the acetabular notch was slightly deeper and hence the inferior–superior angle was smaller. The gender difference was largest in the superior–inferior direction

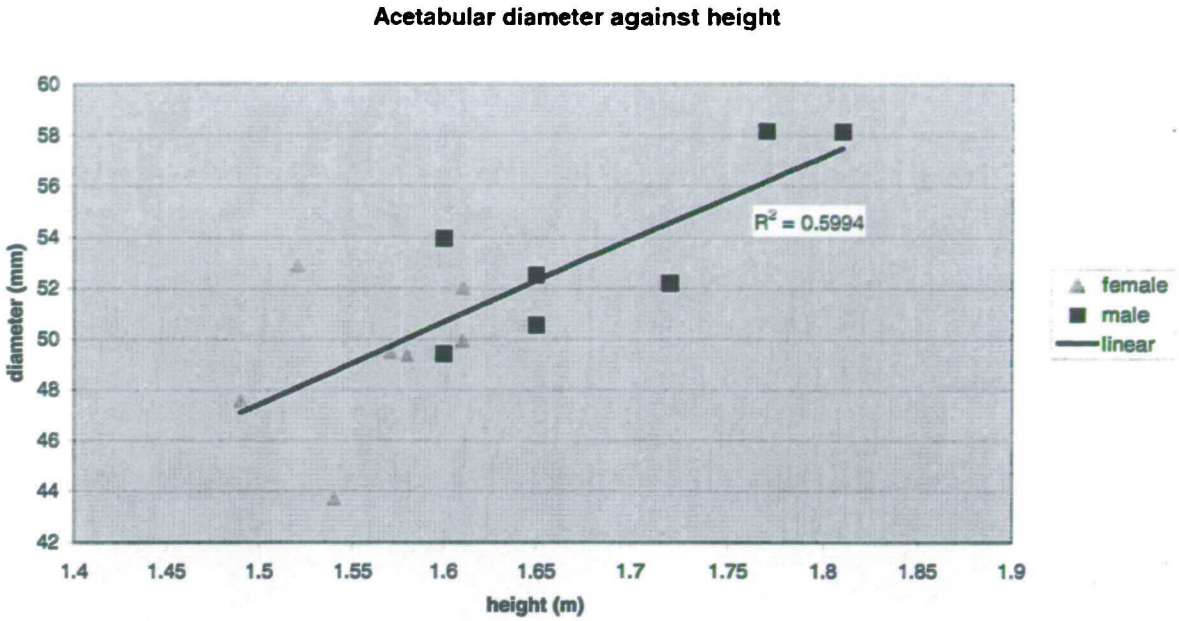

Fig. 4. Estimated height plotted against acetabular diameter showing least square fit.

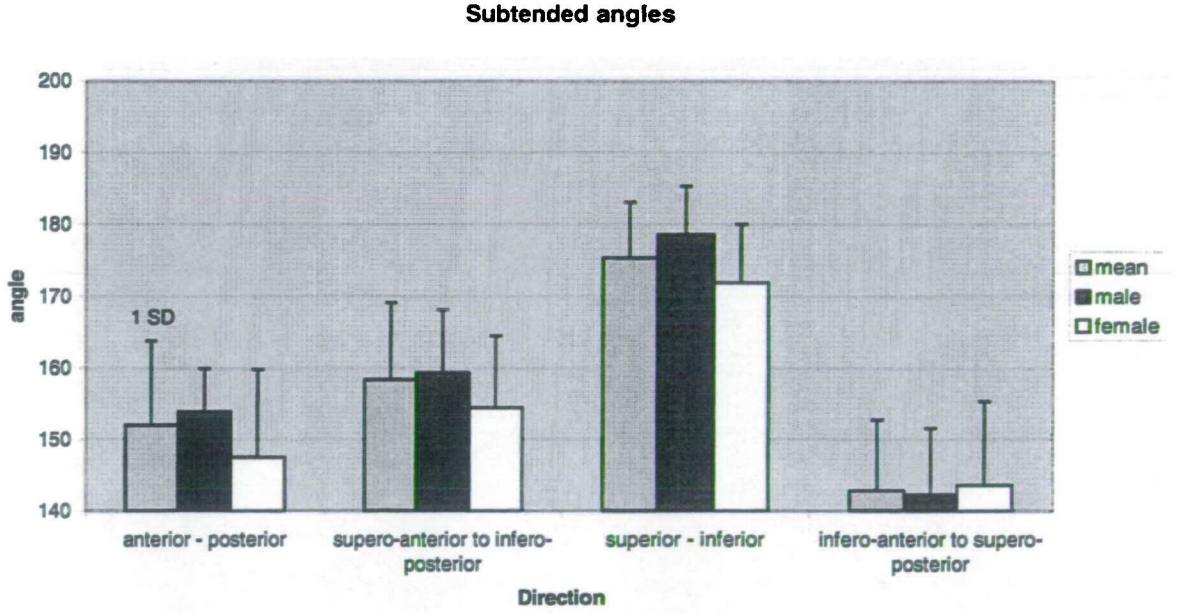

g. 5. Acetabular subtended angles in four directions. Overall mean and mean male and female compared. Error bars show one standard deviation.

ifference of 6.7°), but below one standard deviation .7°). The mean subtended angle showed no correlation ith the estimated height, or with estimated age at death.

2. *Reaming simulation*

The mean distance moved medially and superiorly by e centre of the sphere during the simulated reaming eration was 3.6 mm (1.2–5.4 mm). Fig. 6 shows that the btended angles in each direction were increased by approximately 10°. The mean estimated bone volume removed was 7400 mm^3 (2200–14,400 mm^3). The gender differences for the reamed acetabula were similar to those for unreamed acetabula.

4. Discussion

The sphere fitting results show that the lunate surface of the acetabulum lies on a good approximation to the

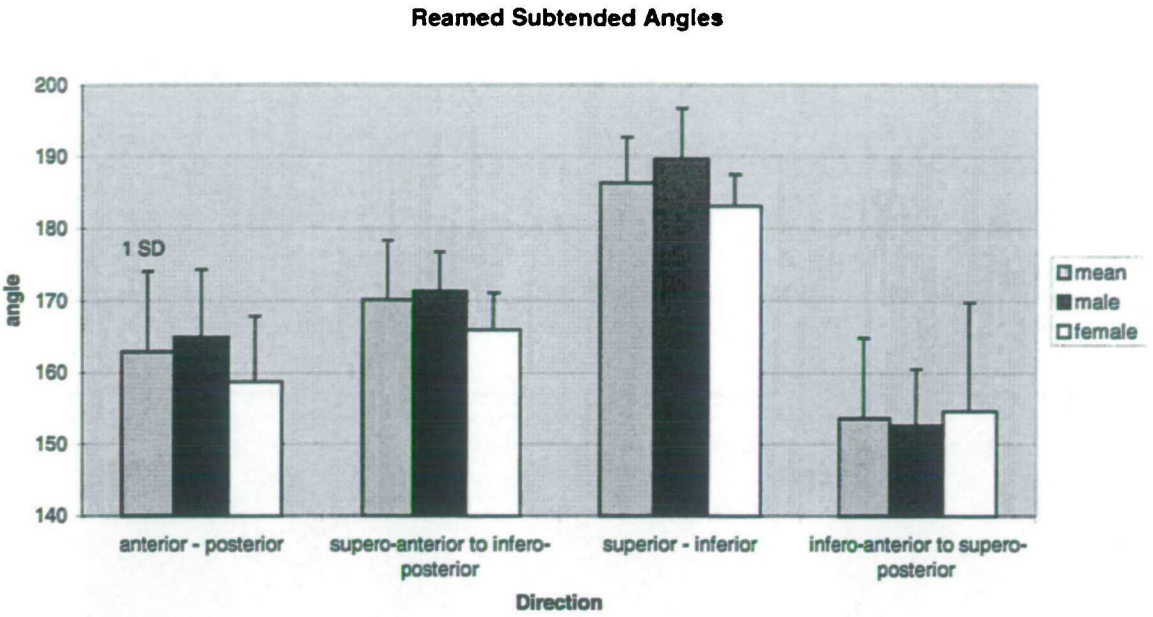

Fig. 6. Acetabular subtended angles in four directions after simulated reaming. Error bars show one standard deviation.

rface of a sphere. Rushfeldt et al. (1981) reported 0.5 mm maximum deviation from spherical of the acetbular subchondral bone. The locations of these deviions were idiosyncratic. They only measured two ecimens, aged 62 and 49 years, both of which showed gns of degenerative joint disease. It has been shown that ips become more spherical with age (Bullough et al., 968) and congruency is associated with joint disease on Eisenhart-Rothe et al., 1997), so larger deviations in e younger healthy population presented here are to be pected. However the largest deviations are due to the istaken inclusion of nodes peripheral to the articular rface.

The acetabulum has been reported previously to be llipsoid (Greenwald and O'Connor, 1971; Eckstein et al., 997; von Eisenhart-Rothe et al., 1997). These studies ave all considered the contact between femoral head nd acetabular articular surfaces and shown that there is n area in the dome (superior sector between points and 5) of the acetabulum which is not load bearing cept at high joint loads. This is consistent with the llipsoidal acetabulum with reduced anterior–posterior nd increased inferior–superior axes described in the esent paper. The bony surface may be even less spheril than the cartilage surfaces studied previously since e mean deviation from spherical of 0.6 mm measured re implies a far larger gap in the dome than the mean of 31 mm (0.06–0.75 mm) measured by Eckstein et al. 997).

The range of sizes and difference between the genders rresponds well with the literature on femoral head sizes an intervening 2–3 mm thickness of cartilage on each rface is included. This correspondence also helps to confirm the sexing of the hemipelves, which in archaeological remains is subject to some uncertainty. Lack of significance in the differences between groups of acetabula such as that between the Norman and Roman groups may only reflect the small sizes of the sample groups.

The hemipelves studied here are those of modern homo sapiens (Aiello and Dean, 1990) and although differences in lifestyle may have an impact on their morphology the hemipelves are comparable with present day populations. It is important to note that hip replacement candidates include people with a wide diversity of lifestyles. The correspondence between measured acetabular diameter and published values of femoral head diameter helps to confirm the validity of this comparison.

The main sites of damage to the hemipelves were the pubic ramus and the anterior horn of the acetabular rim. Three bony landmarks were always available to provide adequate orientation. In five cases the anterior horn of the rim was absent and no rim point 1 could be assigned therefore no anterior–posterior subtended angle was calculated, increasing the uncertainty in the value of this angle.

These subtended angles provide new information on the morphology of the acetabulum. The first point to note is the large variation in acetabular depth. The mean acetabular subtended angle is 158° with a range of 28°. This variation may be seen as part of a spectrum that begins with acetabula so shallow that the hip is unstable (congenital dislocation of the hip). A second point is that some subtended angles are greater than 180°. These largest angles are exclusively in the superior–inferior direction, limiting the ad- and abductive motion of the femur.

ıe rim points were chosen to lie near maxima on the ɛtabular rim, ensuring that the subtended angles mea-ɾed are the maximum for the acetabulum. The small terior–posterior subtended angle reflects the large ıge of motion in the flexion–extension plane. The ɯest subtended angle, that measured between the pero–posterior quadrant and the acetabular notch, ɔuld effectively be larger in vivo due to the presence of ɛ transverse acetabular ligament.

It is interesting that Rushfeldt et al. (1981) suggest that ɛ best-fit sphere to the acetabular cartilage surface lies ɛdially and anteriorly to that of the best fit sphere to ɛ subchondral bone. The consequence of this and of the ger subtended angles would appear to be curtailment the range of motion of the femur. However, it is portant to note that the largest angular motions pos-ɔle include a large component of rotation about the is of the femoral neck which is limited solely by the ɛtabular ligaments and musculature.

No measure of the portion of a sphere that the acet-ular surface occupies has been documented previously. ıe measure proposed here, the subtended angles, are perfect. Firstly they are discrete measurements, taken four directions between eight points across the acet-ular rim. The points were chosen carefully to reflect nilar positioning with respect to landmarks such as the ıc crest and the anterior and posterior horns of the ıate surface, while the smoothness of the rim ensures ıt the error from variation in relative position is less ın 1°. Secondly, the opening plane normal is defined by ɾee of the rim points and is, therefore, an arbitrary ɾection. However, by using subtended angles as neasure, rather than the individual rim-centre vector to rmal angles, the variation introduced by the choice of ɛ opening plane normal should be eliminated.

The simulated reaming operation may be taken as guide to the change of shape that the acetabulum dergoes at hip replacement. The points in the floor and the rim that define the simulated reaming operation ɛ arbitrarily chosen. The simulation is unrepeatable d unreproducible. However, the uniform increase of ɛ mean subtended angles in all directions by 10°, leav-ɛ a cavity that is still less than hemispherical, is an portant result.

The observation made by Townley (1981) that males ve thicker acetabular walls and smaller head-to-neck ios and females have thinner acetabular walls and ger head-to-neck ratios is interesting when related to ɛ gender differences reported in this study. Small head-neck ratios in males will further reduce the range of ɔtion already limited by large subtended angles, while ge head-to-neck ratios will further increase range of ɔtion in females. The different orientations of the acet-ulum and femoral neck in males and females, not nsidered in this study, may account for these apparent ɾepancies, although Reikerås et al. (1983), in a CT study, found no gender difference for anteversion of the femoral neck and acetabulum.

5. Implications for resurfacing design

The parameters measured in this survey affect the shape and thickness of a conservative resurfacing both directly and indirectly. First the acetabular subtended angle has a direct effect upon the subtended angle of the acetabular component. Acetabular cups which overhang the acetabular rim are associated with impingement, early loosening and increased wear (Cotella et al., 1990; Wiadrowski et al., 1991). The fixation surface of the resurfacing acetabular cup therefore must conform to the subtended angles of the reamed acetabular rim.

The subtended angle of the bearing surface of the acetabular component should reflect the subtended angles of the unreamed acetabulum if the component is not to restrict range of motion, or give rise to impingement. Several resurfacing designers reduced the subtended angle of the acetabular component following early experience with their implants (Amstutz et al., 1986; Capello and Trancik, 1981). The ICLH resurfacing acetabular component was first reduced from 180 to 168° and then to 140° (Cotella et al., 1990). While a reduced angle will reduce the possibility of impingement, some authors report the importance of covering all exposed cancellous bone with implant material to prevent ingress of wear debris and joint fluid (Schmalzried et al., 1994) which has been shown to initiate bone resorption and implant loosening (Aspenberg and Van der Vis, 1998).

The diameter of the bearing surface of the resurfacing prosthesis must not exceed that of the original cartilage bearing surface. If it were larger then more acetabular bone would have to be reamed than necessary to insert the implant. An increased bearing surface diameter would also decrease the thickness available for the acetabular component, leading to material strength and fatigue problems. The lower limit on the bearing surface diameter is determined by the thickness of the femoral neck. If the ratio of the bearing surface to the femoral neck diameter is reduced too far, the range of motion of the hip will again be restricted and impingement will occur.

Thus the subtended angles of the reamed and unreamed acetabulum lie at the top of a long chain of related design decisions. The challenge of designing a new conservative resurfacing hip prosthesis will be to address the problem of the large variability in shape of the acetabulum.

Acknowledgements

The Engineering and Physical Sciences Research Council is gratefully acknowledged for the core

rogramme grant of the IRC in Biomedical Materials nd for the provision of a research studentship (MST).

ppendix 1

MATLAB sphere fitting routine adapted from Gander al. (1994).

```
function[z, r, max, ave, sdev] = sphere (X, z, r);
%sphere Geometric sphere fit
%
%[z,r] = sphere (X, z, r);
% fits the best sphere by nonlinear least squares
% for true geometric distance
%
% X: given points <X(i,1), X(i,2), X(i,3)>
% z, r: starting values for sphere solution
%
% z, r: parameters for sphere found
u = [z(1), z(2), z(3), r]';      %starting values
h = u;
while norm(h) > norm(u)*1e-6,
    a = u(1) - X(:,1); b = u(2) - X(:,2);
    c = u(3) - X(:,3);
    fak = sqrt(a.*a + b.*b + c.*c);
    J = [a./fak b./fak c./fak -ones(size(a))];
    f = fak - u(4);
    h = -J\f;
    u = u + h;
end;
z = u(1:3); r = u(4);
max = norm(f, inf); ave = mean(abs(f));
sdev = std(abs(f));
end % sphere
```

Data points saved as MATLAB executable file.

```
function[z, r, max, ave, std] = fitdat %
% MARC exported data with call to sphere fitting
algorithm
% no inputs
% outputs are z, r: centre and radius of sphere
% ensure MATLAB is in correct dir
A = [
A11, A12, A13;     % matrix of co-ordinate data
A21, A22, A23;
...
An1, An2, An3;
];
si = size(A);
su = sum(A);
z1 = su./si(1);     % starting value for position vector
r1 = sqrt(z1*z1');     % starting value for radius
[z, r, max, ave, std] = sphere(A, z1, r1);     %call
"sphere"
end % fitdat
```

References

Aiello, L., Dean, C., 1990. The hominoid pelvis and the hominoid femur. In: Aiello, L., Dean, C. (Eds.), An Introduction to Human Evolutionary Anatomy. Academic Press, Harcourt Brace, London, pp. 429–482.

Amstutz, H.C., 1983. Recent advances in total-hip resurfacing. In: McKibbin, B. (Ed.), Recent Advances in Orthopaedics. Churchill-Livingstone, Edinburgh, pp. 155–177.

Amstutz, H.C., Graff-Radford, A., Gruen, T.A., Clarke, I.C., 1978. THARIES surface replacements: a review of the first 100 cases. Clinical Orthopaedics and Related Research 134, 87–101.

Amstutz, H.C., Dorey, F., O'Carroll, P.F., 1986. THARIES resurfacing arthtoplasty: evolution and long-term results. Clinical Orthopaedics and Related Research 213, 92–114.

Aspenberg, P., Van der Vis, H., 1998. Migration, particles, and fluid pressure: a discussion of causes of prosthetic loosening. Clinical Orthopaedics and Related Research 352, 75–80.

Bullough, P., Goodfellow, J., Greenwald, A.S., O'Connor, J., 1968. Incongruent surfaces in the human hip joint. Nature 217, 1290.

Capello, W.N., Ireland, P.H., Trammell, T.R., Eicher, P., 1978. Conservative total hip arthroplasty. Clinical Orthopaedics and Related Research. 134, 59–74.

Capello, W.N., Trancik, T.M., 1981. Indiana conservative hip — results 2–4.5 years. Orthopaedic Transactions 5, 375.

Clarke, I.C., Amstutz, H.C., 1975. Human hip joint geometry and hemiarthroplasty selection. In: The Hip. St. Louis, C.V.Mosby, pp. 63–89.

Clark, J.M., Freeman, M.A.R., Witham, D., 1987. The relationship of neck orientation to the shape of the proximal femur. Journal of Arthroplasty 2, 99–109.

Cotella, L., Railton, G.T., Nunn, D., Freeman, M.A.R., Revell, P.A., 1990. ICLH double-cup arthroplasty, 1980-1987. Journal of Arthroplasty. 5, 349–357.

Eckstein, F., von Eisenhart-Rothe, R., Landgraf, J., Adam, C., Loehe, F., Müller-Gerbl, M., Putz, R., 1997. Quantitative analysis of incongruity, contact areas and cartilage thickness in the human hip joint. Acta Anatomica. 158, 192–204.

von Eisenhart-Rothe, R., Eckstein, F., Müller-Gerbl, M., Landgraf, J., Rock, C., Putz, R., 1997. Direct comparison of contact areas, contact stress and subchondral mineralization in human hip joint specimens. Anatomy and Embryology. 195, 279–288.

Freeman, M.A.R., Swanson, S.A.V., Day, W.H., Thomas, R.J., 1975. Conservative total replacement of the hip. Journal of Bone and Joint Surgery. 57-B, 114.

Gander, W., Golub, G.H., Strebel, R., 1994. Fitting of Circles and Ellipses: Least Squares Solution. Techreport from Departement Informatik, ETH Zürich. (ftp.inf.ethz.ch/doc/tech-reports/1994/217.ps)

Greenwald, A.S., O'Connor, J.J., 1971. The transmission of load through the human hip joint. Journal of Biomechanics. 4, 507–528.

Harris, W.H., 1995. The problems is osteolysis. Clinical Orthopaedics and Related Research 311, 46–53.

Husmann, O., Rubin, P.J., Leyvraz, P.F., Roguin, Bd., Argenson, J.N., 1997. Three-dimensional morphology of the proximal femur. Journal of Arthroplasty. 12, 444–450.

Kobayashi, S., Eftekhar, N.S., Terayama, K., Joshi, R.P., 1997. Comparative study of total hip arthroplasty between younger and older patients. Clinical Orthopaedics and Related Research 339, 140–151.

Murray, D.W., 1993. The definition and measurement of acetabular orientation. Journal of Bone and Joint Surgery. 75-B (2), 228–232.

Noble, P.C., Alexander, J.W., Lindahl, L.J., Yew, D.T., Granberry, W.M., Tullos, H.S., 1988. The anatomic basis of femoral component design. Clinical Orthopaedics and Related Research. 235, 148–165.

avolainen, P., Slätis, P., Hämäläinen, M., Visuri, T., Pulkkinen, P., 1995. Long-Term Results of Total Joint Arthroplasty: Results of a 15-year Follow-Up on a Nationwide Registration Programme in Finland with 67,714 TJAs. National Agency for Medicines, Helsinki.

eikerås, O., Bjerkreim, I., Kolbenstvedt, A., 1983. Anteversion of the acetabulum and femoral neck in normals and in patients with osteoarthritis of the hip. Acta Orthopaedica Scandinavica 54, 18–23.

ushfeldt, P.D., Mann, R.W., Harris, W.H., 1981. Improved techniques for measuring in vitro the geometry and pressure distribution in the human acetabulum – 1. ultrasonic measurement of acetabular surfaces sphericity and cartilage thickness. Journal of Biomechanics. 14 (4), 253–260.

hmalzried, T.P., Guttman, D., Grecula, M., Amstutz, H.C., 1994. The relationship between the design, position and articular wear of acetabular components inserted without cement and the development of pelvic osteolysis. Journal of Bone and Joint Surgery. 76-A, 677–688.

Sharp, D.J., Porter, K.M., 1985. The charnley total hip arthroplasty in patients under age 40. Clinical Orthopaedics and Related Research. 201, 51–56.

Sugano, N., Noble, .P.C., Kamaric, .M.S., 1999. Predicting the position of the femoral head center. Journal of Arthroplasty. 14, 102–107.

Townley, C.O., 1981. Conservative total articular replacement arthroplasty (The TARA Procedure) with the fixed femoral cup. Orthopaedic Transactions. 5 (3), 388.

Trotter, M., Peterson, R.R., 1970. Weight of the skeleton during postnatal development. American Journal of Physical Anthropology. 33 (3), 313–323.

Wagner, H., 1978. Surface replacement arthroplasty of the hip. Clinical Orthopaedics and Related Research. 134, 102–130.

Wiadrowski, T.P., McGee, M., Cornish, B.L., Howie, D.W., 1991. Peripheral wear of wagner resurfacing hip arthroplasty acetabular components. Journal of Arthroplasty. 6, 103–107.

Wroblewski, B.M., Fleming, P.A., Siney, P.D., 1999. Charnley low-friction torque arthroplasty of the hip, 20- to 30-year results. Journal of Bone and Joint Surgery. 81-B (3), 427–430.